# Origine et modification des cycles stratigraphiques à haute-fréquence (10's à 100's ka). Rôle des déformations courte longueur et modélisation du comportement des systèmes fluviatiles

Sébastien Castelltort

N° Ordre : 2822

**THÈSE**

Présentée

**DEVANT L'UNIVERSITÉ DE RENNES 1**

pour obtenir

Le grade de : ***DOCTEUR DE L'UNIVERSITÉ DE RENNES 1***

*Mention Sciences de la Terre*

PAR

**Sébastien Castelltort**

Équipe d'accueil : Géosciences Rennes, Université de Rennes 1

École doctorale : Sciences de la Matière

Composante universitaire : UFR Structure et Propriétés de la Matière

Titre de la thèse :

# Origine et modification des cycles stratigraphiques à haute-fréquence (10's à 100's ka)

## Rôle des déformations courte longueur d'onde et modélisation du comportement des systèmes fluviatiles

SOUTENUE LE 13 JUIN 2003 devant la commission d'Examen

COMPOSITION DU JURY

| | |
|---|---|
| Mr Philip Allen | rapporteur |
| Mr François Métivier | rapporteur |
| Mr Jacques Malavieille | examinateur |
| Mr Philippe Davy | examinateur |
| Mr Jean-Pierre Brun | examinateur |
| Mr François Guillocheau | directeur de thèse |

## Résumé

Dans les séries terrigènes, les cycles stratigraphiques sont présents sur une large gamme de périodes (0.01-100 Ma), et sont dus aux variations du rapport entre l'espace disponible à l'accummulation des sédiments et le flux sédimentaire. Quelle est la responsabilité de chacun de ces paramètres dans l'origine et l'expression des cycles stratigraphiques, en particulier à haute-fréquence (10-100 ka) où tous interviennent ?
Si les variations d'espace disponible d'échelle régionale ou globale (tectonique et climat) existent à ces fréquences et sont une origine fréquement admise, on connaît mal (1) l'influence de la croissance des structures tectoniques intra-bassin (plis et failles) sur leur expression, et (2) les contrôles du flux sédimentaire à haute-fréquence. Ce travail examine ces deux aspects à travers l'étude sédimentologique d'un anticlinal de croissance, et la modélisation numérique de l'effet de la zone de transfert (rivières) des sédiments sur la variabilité du flux sédimentaire.

## Abstract

Detrital accummulations are always composed of stratigraphic cycles at a large range of time scales (0.01-100 Ma), linked to variations of the ratio between available space to sedimentation (accommodation) and sediment supply due to tectonics and climate. What are the respective contributions of each of these factors in the origin and expression of the cycles, in particular at high-frequency (10-100 ka) where they can all play a role?
If regional and global accommodation variations (tectonics and climate) at these frequencies are largely admitted as a dominant origin, (1) the influence of intra-basin tectonic structures (folds and faults) on the expression of stratigraphic cycles, and (2) the controls on high-frequency sediment supply, are less well constrained. This work adresses both aspects through the sedimentological study of a growth anticline, and the numerical modelling of rivers and their control on sediment supply variations at the entrance of sedimentary basins.

# TABLE DES MATIÈRES

# 1. INTRODUCTION

Les mouvements verticaux de la lithosphère induits par la tectonique des plaques, créent un gradient de masse entre des zones en relief et des zones en dépression. En raison de la gravité, ce gradient de masse constitue un deséquilibre : les zones en relief ont un potentiel d'érosion, et les zones en dépression un potentiel d'accommodation (hébergement des sédiments). Le reéquilibrage est réalisé principalement par l'eau, et par le climat au sens large, qui érodent et transportent les sédiments depuis les reliefs jusqu'aux bassins sédimentaires.

Les accumulations sédimentaires sont le résultat de cette dynamique, et elles contiennent ainsi un enregistrement à toutes les échelles de temps des processus qui interviennent tour à tour lors de l'extraction des sédiments, pendant leur transport et lorsqu'ils arrivent dans la zone de dépôt.

L'objectif de la sédimentologie et de la stratigraphie est de mettre à jour cette histoire à partir de l'analyse des accumulations sédimentaires.

Le language écrit dans les sédiments qui apparaît au premier ordre est celui des cycles stratigraphiques. Dans les successions terrigènes, ces cycles sont reconnaissables grâce au suivi de la position au cours du temps d'indicateurs tels que la ligne de rivage ou la transition sable-graviers dans les dépôts marins ou continentaux respectivement (Marr et al., 2000; Paola et al., 1992; Swenson et al., 2000). On observe ainsi que sur des échelles de temps allant de la dizaine de milliers d'années à plusieurs million d'années, la sédimentation enregistre des cycles de mouvement de l'ensemble du paysage sédimentaire (à l'échelle du bassin). Ceux-ci correspondent à des changements de forme de la zone en dépôt dans son ensemble, dans le but de trouver un équilibre avec des conditions aux limites qui varient.

Une des questions fondamentales qui se pose est *l'origine de ces cycles*.

Depuis Sloss (1962) et les avancées de la stratigraphie séquentielle en général (Blum and Törnqvist, 2000; Cross, 1988; Cross and Lessenger, 1998; Galloway, 1989; Helland-Hansen, 1995; Jervey, 1988; Muto and Steel, 2000; Posamentier et al., 1988; Schlager, 1993; Shanley and McCabe, 1994; Swift et al., 1991; Guillocheau, 1995), il est maintenant largement admis que les changements de forme de la zone en dépôt, les cycles stratigraphiques, sont gouvernés par les variations du rapport entre l'espace disponible pour la sédimentation (accommodation A) et le flux sédimentaire (S).

*Il existe une différence fondamentale entre ces deux paramètres : l'accommodation A varie sous l'influence de facteurs qui s'appliquent uniquement à la zone de dépôt, alors que le*

*flux sédimentaire S est une fonction de facteurs qui s'appliquent à la zone en amont de la zone en dépôt c'est à dire aux domaines de production et de transport des sédiments.*

C'est l'analyse de cette distinction qui nous a conduit aux problèmes abordés dans ce travail.

**L'accommodation**

L'espace disponible pour la sédimentation (accommodation) à un instant donné est défini entre la surface de la terre qui constitue sa limite inférieure à cet instant, et une limite supérieure qui est un niveau d'équilibre (niveau de base) au dessus duquel les sédiments sont érodés, et au dessous duquel ils peuvent se déposer. Ainsi tous les facteurs qui sont suceptibles d'affecter ces deux limites peuvent engendrer des variations d'accommodation. On en distingue deux principaux : (1) la tectonique au sens large qui déforme la surface de la terre (limite inférieure de l'accommodation, et (2) les mouvements absolus (i.e., par rapport à un point fixe du substratum, et non par rapport à la surface de la terre) du niveau d'équilibre (limite supérieure de l'accommodation), liés aux variations eustatiques dans le domaine marin, ou lacustre ou d'un autre niveau de base dans le domaine continental.

La viscosité du manteau lui permet de répondre à une déformation du type charge/décharge sur des échelles de temps de l'ordre de $10^3$-$10^4$ ans (Turcotte and Schubert, 1982). *En conséquence on peut s'attendre à ce que la vitesse de subsidence des bassins puisse varier au cours du temps depuis les hautes (10's à 100's ka) jusqu'aux basses fréquences (> 1 Ma)*.

Les mécanismes invoqués pour supporter des variations de la subsidence au cours du temps sont nombreux comme par exemple l'épisodicité des phases tectoniques en compression et extension (à partir de < 1 Ma) à l'échelle globale (e.g., Lister et al., 2001), les variations de contraintes intraplaques pour les marges passives (> 1 Ma, e.g., Cloetingh and Kooi, 1989; Cloetingh et al., 1985), l'influence de l'hétérogénéité de la lithosphère (Waschbusch and Royden, 1992), ou les alternances de charge tectonique/décharge par érosion (e.g., Burns et al., 1997). Cependant, de nombreux travaux considèrent qu'il est également probable que les déformations à l'échelle de la lithosphère aussi bien dans les zones de collision que dans les zones d'extension soient continus, à l'image des déplacements de plaques (e.g., Molnar and Lyon-Caen, 1988; Tapponnier et al., 2001; Van der Woerd et al., 2000). *Finalement, la vitesse de subsidence des bassins peut être théoriquement variable aux échelles de temps appropriées pour la création de cycles stratigraphiques, mais le débat reste*

*ouvert sur la validité de ces variations, et sur les mécanismes possibles et les échelles de temps des variations des mouvements tectoniques.*

Un certain nombre de processus ont été invoqués pour rendre compte des oscillations du niveau de base. Au premier ordre, en domaine océanique ou continental, elles sont liées à la variabilité du climat *s.l.*, qui est connue à toutes les fréquences depuis les saisons, les cycles de glaciation/déglaciation de Milankovitch (10's à 100's ka), jusqu'aux grandes périodes géologiques (> 10's Ma). Les variations de vitesse d'accrétion aux rides océaniques permettent également de rendre compte des cycles eustatiques avec des périodes >1Ma.

En conclusion, les variations d'accommodation qu'elles soient liées à la déformation de la lithosphère ou au climat, peuvent être à l'origine des cycles stratigraphiques.

En revanche, au contraire des variations du niveau d'équilibre, la déformation du substratum peut être spatialement variable au sein même d'un bassin. L'enregistrement cyclique des bassins dû au forcage externe s'appliquant depuis l'échelle bassin jusqu'à l'échelle globale, peut donc être localement modifié par les déformations intra-bassin comme les plis, les failles, les diapirs, etc… *Ainsi, les sédiments syntectoniques déposés pendant la croissance de ces structures enregistrent la superposition d'un signal régional voire global et du signal correspondant à la déformation locale.*

Les strates syntectoniques sont largement utilisées pour reconstruire et comprendre la cinématique de ces structures (plis, failles de croissance), en faisant généralement l'hypothèse d'une sédimentation constante et uniforme. *Il est donc important d'explorer les effets et les implications de la superposition dans l'enregistrement sédimentaires de cycles stratigraphiques sur la croissance des structures tectonique de courte longueur d'onde.*

C'est l'objet de la première partie de ce travail.

**Le flux sédimentaire**

L'importance du flux sédimentaire dans le contrôle de l'enregistrement stratigraphique est aujourd'hui reconnue (Galloway, 1989; Lawrence, 1993; Schlager, 1993). Le débat se situe sur les échelles de temps auxquelles le flux sédimentaire est variable. La quantification des flux sédimentaires anciens est un exercice difficile à cause de problèmes de corrélation, de datations, de compaction et de diagénèse, et d'un enregistrement sédimentaire souvent incomplet. Quelques études ont pu montrer que le flux sédimentaire pouvait varier sur des échelles de temps de l'ordre de quelques millions d'années ou plus (e.g., Galloway and Williams, 1991; Liu and Galloway, 1997; Peizhen et al., 2001; Sloss, 1978). Récemment,

d'autres ont suggéré que le flux sédimentaire aux bassins pouvait varier sur des échelles de temps de l'ordre de 10's à 100's ka en réponse à des cycles climatiques ou tectoniques dans l'aire source (Burns et al., 1997; Lopez-Blanco et al., 2000; Marzo and Steel, 2000; Perlmutter and Matthews, 1989; Perlmutter et al., 1998; Van der Zwan, 2002; Weltje and de Boer, 1993; Weltje et al., 1996), et puisse ainsi avoir un contrôle direct sur l'enregistrement stratigraphique à haute fréquence. Ces travaux considèrent implicitement que le flux sédimentaire peut varier directement, comme l'accommodation, en réponse à la tectonique et au climat. En fait, les stratigraphes négligent le plus souvent de prendre en compte le *système sédimentaire dans son ensemble*, c'est-à-dire comme constitué d'une *zone de production des sédiments, d'une zone de transfert des sédiments, et d'une zone de dépôt* (Schumm, 1977). Or, chacune de ces zones possède un *temps de réponse propre* aux sollicitations extérieures. Ce temps demande à être déterminé avant d'envisager une possible relation directe entre les variations des facteurs externes et le flux sédimentaire résultant.

*Le problème est donc de savoir à quelles échelles de temps les variations climatiques et tectoniques produisent des variations du flux sédimentaire à partir de la zone en érosion, et si ces variations peuvent être effectivement transmises par les systèmes fluviatiles jusqu'aux bassins.*

Nous traitons ce problème dans la deuxième partie de ce travail.

Ce mémoire est constitué d'un ensemble d'articles parus, soumis et en préparation regroupés en deux parties.

La première partie concerne dans un premier temps l'analyse sédimentologique et stratigraphique d'un anticlinal de croissance (anticlinal d'Arguis, Pyrénées espagnoles). Cet exemple montre l'influence des variations locales d'espace disponible sur les cycles stratigraphiques. Les modifications de l'enregistrement sédimentaire ainsi mises en évidence nous conduisent ensuite à analyser certaines implications pour l'étude de la cinématique des structures de croissance, et en particulier dans le cas des failles normales. Ceci nous permet également de développer une méthode de détermination des lithologies à partir des données de sismique pétrolière.

La deuxième partie tente de déterminer dans quelle mesure il peut exister des variations de flux sédimentaire à haute fréquence (10's à 100's ka), à travers (1) une approche diffusive des systèmes alluviaux, et (2) une modélisation numérique des systèmes fluviatiles grâce au logiciel EROS développé par P. Davy et A. Crave à Rennes.

**Références**


Blum, M.D., and Törnqvist, T.E., 2000, Fluvial responses to climate and sea-level change: a review and look forward: Sedimentology, v. 47 (Suppl. 1), p. 2-48.

Burns, B.A., Heller, P.L., Marzo, M., and Paola, C., 1997, Fluvial response in a sequence stratigraphic framework: example from the Montserrat fan delta, Spain: J. Sed. Res., v. 67, p. 311-321.

Cloetingh, S., and Kooi, H., 1989, intraplate stresses: a new perspective on QDS and Vail's third-order cycles, *in* Cross, T.A., ed., Quantitative Dynamic Stratigraphy: Englewood Cliffs, Prentice Hall, p. 127-148.

Cloetingh, S., McQueen, H., and Lambeck, K., 1985, On a tectonic mechanism for regional sea level variations: Earth Planet. Sci. Lett., v. 75, p. 157-166.

Cross, T.A., 1988, Controls on coal distribution in transgressive-regressive cycles. Upper Cretaceous, Western Interior, USA, *in* Wilgus, C.K., Hastings, B.S., Kendall, C.G., Posamentier, H.W., Ross, C.A., and Van Wagoner, J.C., eds., Sea-level changes: an integrated approach, Volume 42: vol.42: Boulder, Soc. Econ. Paleontol. Mineral. Spec. Publ., p. 47-70.

Cross, T.A., and Lessenger, M.A., 1998, Sediment volume partitioning: rationale for stratigraphic model evaluation and high-resolution stratigraphic correlation, *in* Gradstein, F.M., Sandvik, K.O., and Milton, N.J., eds., Sequence Stratigraphy - Concepts and Applications, Volume 8: Norwegian Petroleum Society (NPF) Special Publications, Elsevier, p. 171-195.

Galloway, W.E., 1989, Genetic stratigraphic sequences in basin analysis I: architecture and genesis of flooding-surface bounded depositional systems: Am. Assoc. Petr. Geol. Bull., v. 73, p. 125-142.

Galloway, W.E., and Williams, T.A., 1991, Sediment accumulation rates in time and space: Paleogene genetic stratigraphic sequences of the northwestern Gulf of Mexico basin: Geology, v. 19, p. 986-989.

Guillocheau, F., 1995, Nature, rank and origin of Phanerozoic sedimentary cycles: C. R. Acad. Sci. Paris, v. 320, p. 1141-1157.

Helland-Hansen, W., 1995, Sequence stratigraphy theory: remarks and recommendations, *in* Steel, R.J., Felt, V.L., Johannessen, E.P., and Mathieu, C., eds., Sequence Stratigraphy on the Northwest European Margin: Amsterdam, NPF Special Publications 5, Elsevier, p. 13-21.

Jervey, M.T., 1988, Quantitative geological modeling of siliciclastic rock sequences and their seismic expression, *in* Wilgus, C.K., Hastings, B.S., Kendall, C.G.S.C., Posamentier, H.W., Ross, C.A., and Van Wagoner, J.C., eds., Sea-Level Changes: An Integrated Approach, Volume 42: Spec. Publ. Soc. Econ. Palaeont. Miner.: Tulsa, SEPM, p. 47-69.

Lawrence, D.T., 1993, Evaluation of eustasy, subsidence, and sediment input as controls on depositional sequence geometries and the synchroneity of sequence boundaries, *in* Weimer, P., and Posamentier, H., eds., Siliciclastic Sequence Stratigraphy: Recent Developments and Applications, Volume 58: American Association of Petroleum Geologists Memoir, p. 337-367.

Lister, G.S., Forster, M.A., and Rawling, T.J., 2001, Episodicity during orogenesis, *in* Miller, J.A., Holdsworth, R.E., Buick, I.S., and Hand, M., eds., Continental Reactivation and Reworking, Volume 184, Geological Society, London, Special Publications, p. 89-113.

Liu, X., and Galloway, W.E., 1997, Quantitative determination of Tertiary sediment supply to the North Sea basin: Am. Ass. Petr. Geol. Bull., v. 81, p. 1482-1509.

Lopez-Blanco, M., Marzo, M., and Piña, J., 2000, Transgressive-regressive sequence hierarchy of foreland, fan-delta clastic wedges (Montserrat and Sant Llorenç del Munt, Middle Eocene, Ebro Basin, NE Spain): Sediment. Geol., v. 138, p. 41-69.

Marr, J.G., Swenson, J.B., Paola, C., and Voller, V.R., 2000, A two-diffusion model of fluvial stratigraphy in closed depositional basins: Basin Res., v. 12, p. 381-398.

Marzo, M., and Steel, R.J., 2000, Unusual features of sediment supply-dominated, transgressive-regressive sequences: Paleogene clastic wedges, SE Pyrenean foreland basin, Spain: Sediment. Geol., v. 138, p. 3-15.

Molnar, P., and Lyon-Caen, H., 1988, Some simple physical aspects of the support, structure, and evolution of mountain belts: Geological Society of America, Special Paper, v. 218, p. 179-207.

Muto, T., and Steel, R.J., 2000, The accommodation concept in sequence stratigraphy: some dimensional problems and possible redefintion: Sediment. Geol., v. 130, p. 1-10.

Paola, C., Heller, P.L., and Angevine, C.L., 1992, The large-scale dynamics of grain-size variation in alluvial basins. I : Theory: Basin Res., v. 4, p. 73-90.

Peizhen, Z., Molnar, P., and Downs, W.R., 2001, Increased sedimentation rates and grain sizes 2-4 Myr ago due to the influence of climate change on erosion rates: Nature, v. 410, p. 891-897.

Perlmutter, M.A., and Matthews, M.D., 1989, Global cyclostratigraphy-A model, *in* Cross, T.A., ed., Quantitative Dynamic Stratigraphy: Englewood Cliffs, Prentice Hall, p. 233-260.

Perlmutter, M.A., Radovic, B.J., Matthews, M.D., and Kendall, M.D., 1998, The impact of high-frequency sedimentation cycles on stratigraphic interpretation, *in* Gradstein, F.M., Sandvick, K.O., and Milton, N.Y., eds., Sequence Stratigraphy, Concepts and Applications, Volume 8, NPF Special Publications, p. 141-170.

Posamentier, H.W., Jervey, M.T., and Vail, P.R., 1988, Eustatic control on clastic deposition I: Conceptual framework, *in* Wilgus, C.K., Hastings, B.S., Kendall, C.G., Posamentier, H.W., Ross, C.A., and Van Wagoner, J.C., eds., Sea-level change: an integrated approach, Volume 42: vol.42: Boulder, Soc. Econ. Paleont. Min. Spec. Publ., p. 109-124.

Schlager, W., 1993, Accommodation and supply - a dual control on stratigraphic sequences: Sediment. Geol., v. 86, p. 111-136.

Schumm, 1977, The Fluvial System, John Wiley & Sons, 338 p.

Shanley, K.W., and McCabe, P.J., 1994, Perspectives on the Sequence Stratigraphy of Continental Strata: Am. Ass. Petrol. Geol. Bull., v. 78, p. 544-568.

Sloss, L.L., 1962, Stratigraphic Models in Exploration: Am. Ass. Petr. Geol. Bull., v. 46, p. 1050-1057.

—, 1978, Global Sea Level Changes: A view from the Craton: Am. Ass. Petr. Geol. Bull., p. 461-467.

Swenson, J.B., Voller, V.R., Paola, C., Parker, G., and Marr, J.G., 2000, Fluvio-deltaic sedimentation: a generalized Stefan problem: European Journal of Applied Mathematics, v. 11, p. 1-20.

Swift, D.J.P., Oertel, G.F., Tillman, R.W., and Thorne, J.A., 1991, Shelf Sand and Sandstone Bodies, IAS Special Publications, Volume 14, Blackwell.

Tapponnier, P., Ryerson, F.J., VanDerWoerd, J., Meriaux, A.-S., and Lasserre, C., 2001, Long-term slip rates and characteristic slip: keys to active fault behaviour and earthquake hazard: C. R. Acad. Sci. Paris, Sciences de la Terre, v. 333, p. 483-494.

Turcotte, D.L., and Schubert, G., 1982, Geodynamics, John Wiley & Sons.

Van der Woerd, J., Ryerson, F.J., Tapponnier, P., Meriaux, A.-S., Gaudemer, Y., Meyer, B., Finkel, R.C., Caffee, M.W., Guoguang, Z., and Zhiqin, X., 2000, Uniform Slip-Rate along the Kunlun Fault: Implications for seismic behaviour and large-scale tectonics: Geophys. Res. Lett., v. 27, p. 2353-2356.

Van der Zwan, C.J., 2002, The impact of Milankovitch-scale climatic forcing on sediment supply: Sediment. Geol., v. 147, p. 271-294.

Waschbusch, P.J., and Royden, L.H., 1992, Episodicity in foredeep basins: Geology, v. 20, p. 915-918.

Weltje, G.J., and de Boer, P.L., 1993, Astronomically induced paleoclimatic oscillations reflected in Pliocene turbidite deposits on Corfu (Greece): implications for the interpretation of higher order cyclicity in ancient turbidite systems: Geology, v. 21, p. 307-310.

Weltje, G.J., VanAnsenwoude, S.O.K.J., and DeBoer, P.L., 1996, High-frequency detrital signals in eocene fan-delta sandstones of mixed parentage (south-central Pyrenees, Spain): a reconstruction of chemical weathering in transit: J. Sed. Res., v. 66, p. 119-131.

# 2. MODIFICATION DES CYCLES STRATIGRAPHIQUES PAR LES STRUCTURES TECTONIQUES COURTE LONGUEUR D'ONDE (KM)

# Etude de terrain et implications

## 2.1. Exemple de l'anticlinal d'Arguis, Pyrénées espagnoles

Les cycles stratigraphiques sont controllés par les variations du rapport entre accommodation (espace disponible pour l'accumulation des sédiments) et flux sédimentaire. S'il est acquis grâce à la stratigraphie séquentielle que les variations d'accommodation, qu'elles soient liées à la tectonique (subsidence) ou au niveau de base (eustatisme ou un autre niveau en domaine continental) et qu'elles soient d'échelle régionale ou globale, sont une origine possible de ces cycles, on connaît moins bien l'influence des variations locales d'accommodation. Dans les bassins sédimentaires, les déformations courte longueur d'onde (km) comme les failles normales ou les plis induisent des variations locales d'accommodation. Les points principaux qui ont attiré l'attention des études existantes (voir Gawthorpe & Leeder 2000 pour une revue), portent principalement sur l'influence de la croissance des structures sur (1) la distribution des faciès sédimentaires, et (2) la nature des surfaces stratigraphiques clés, leur expression et leur position temporelle.

Pour comprendre l'influence de ces déformations locales sur l'enregistrement sédimentaire, nous examinons les dépôts deltaïques syntectoniques de l'anticlinal d'Arguis (Pico del Aguila anticline), un pli de croissance qui s'est formé pendant le Bartonien dans le bassin d'avant-pays sud-pyrénéen.

A partir d'une analyse sédimentologique et paléontologique détaillée, et de la corrélations des surfaces stratigraphiques clés sur le terrain, nous proposons un nouveau cadre stratigraphique pour ces dépôts, composé de trois ordres de cycles. Nous quantifions aussi les variations d'accommodation, l'uplift de l'anticlinal, les taux d'accumulation grâce aux paléobathymétries et aux datations des surfaces à l'aide des données paléontologiques et magnétostratigraphiques existantes. Nos conclusions montrent que *la signature de la déformation dans les cycles stratigraphiques est une fonction de leur durée par rapport à la vitesse d'uplift du pli qui peut être considérée comme constante sur de courtes périodes de*

*temps (<100ka) mais varie au cours de l'évolution du pli. La réponse stratigraphique n'est pas linéaire en raison des différences de sédimentation entre les différentes périodes des cycles stratigraphiques, i.e. progradation ou rétrogradation*. Ceci doit être pris en compte lors de la restauration des déformation à partir des strates de croissance.

### 2.1.1. Contrôle tectonique de l'enregistrement sédimentaire : stratigraphie séquentielle des dépôts syntectoniques de l'anticlinal d'Arguis dans les Pyrénées Espagnoles

---

Article :

## Fold control on the stratigraphic record: a quantified sequence stratigraphic study of the Pico del Aguila anticline in the South-western Pyrenees (Spain)

Sébastien Castelltort[1], François Guillocheau[1], Cécile Robin[2], Delphine Rouby[1], Thierry Nalpas[1], Fançois Lafont[3] and Rémi Eschard[4]

[1] Géosciences Rennes, Campus de Beaulieu, 35042 Rennes cedex - France

[2] Université Pierre et Marie Curie, 75252, Paris – France

[3] Total Fina Elf, Avenue Larribeau, 64018 Pau – France

[4] IFP, 92852 Rueil Malmaison - France

*Accepted at Basin Research, revised version*

---

## ABSTRACT

**The aim of this paper is to test a new approach combining field study and sequence stratigraphic analysis to gain insights into the influence of local deformation upon the sequence stratigraphic architecture of syndeformation deposits. To do so, we investigated the influence of the growth of the Pico del Aguila anticline, a kilometric compressive fold located in the Jaca basin, at the southwestern border of the Pyrenean foreland basin, upon coeval deltaic sedimentation.**

**We analysed six stratigraphic sections located along the structure, identified facies associations, palaeoenvironments and proposed a new sequence stratigraphic framework taking into account three orders of depositional cycles (genetic units, minor cycles and major cycles) and their stacking pattern. We quantified the rates of accommodation variations, sediment accumulation and relative uplift of the anticline, and showed that minor cycles were driven by accommodation variations of regional scale (rather than sediment supply variations), and that the uplift rate of the anticline axis was continuously decreasing through time. We determined four different controls of the growth of the anticline on the sedimentary record: the distribution of sedimentary thickness, the depositional profile (shallower facies are preserved on the hinge of the anticline), the thickness ratio of progradational and retrogradational sub-cycle (P/R ratio) of depositional sequences (most of the thickness difference takes place during the prograding trend) and locally the alteration of the time of occurrence of the inversion from progradation to retrogradation trend between the hinge and the synclines. The growth of the anticline consistently distorted the geometry of the three scales of depositional cycles with an intensity depending upon the difference in subsidence rate between the hinge and the synclines (i.e. the uplift rate).**

**Finally, we propose that these distortions of the P/R ratio (thickness ratio of progradational and retrogradational sub-cycle) and the alteration of the timing of trend can be explain by the simple superimposition of a continuous uplift of the anticline (local deformation) and regional variations of relative sea level (eustasy and/or foreland basin subsidence).**

## INTRODUCTION

The stratigraphic infill of sedimentary basins provides a high-resolution record of the history and kinematics of deformation combined with external forcing factors such as sea-level changes and climate fluctuations. However, as noted in Gupta and Cowie (2000), how this combination of factors comes to be preserved is still not well understood as it results from a complex interaction of processes acting at different time- and space-scales.

The sedimentary record is characterized by depositional sequences of multiple orders corresponding to cycles of shoreline progradation and retrogradation that are controlled by variations of sediment supply, eustasy and deformation of the basin basement. These have been formalized as variations of the ratio between two independent parameters: the accommodation A (i.e. the space available for sedimentation; Jervey, 1988) and sediment supply S (e.g. Cross, 1988; Homewood *et al.*, 1992; Schlager, 1993; Shanley & McCabe,

1994; Muto & Steel, 1997; Cross & Lessenger, 1998; Homewood *et al.*, 2000; Muto & Steel, 2000). The accommodation itself is controlled by variations of the sea level (or lake-level in lacustrine basins) and by vertical displacements of the basement in response to local and regional deformation.

At basin scale, numerous studies demonstrated the strong link between regional deformation and the sequence stratigraphic architecture (Posamentier & Allen, 1993a) in either extensional (e.g. Gupta *et al.*, 1998; Gawthorpe & Leeder, 2000) or compressional settings (e.g. Jordan & Flemings, 1991; Posamentier & Allen, 1993b; Catuneanu *et al.*, 1997a; Catuneanu *et al.*, 1997b). At local scale, however, less studies addressed the relationships between kilometric deformation and the sequence stratigraphic architecture (for normal growth faults: Gawthorpe *et al.,* 1994; Gawthorpe *et al.,* 1997ab; Hardy & Gawthorpe, 1998; or compressional growth folds Gawthorpe *et al.,* 2000). Paradoxically, the geometry of syntectonic strata is widely used to restore the kinematics and growth mode of local deformations like faults and folds (e.g. McClay & Ellis, 1987; Suppe *et al.*, 1992; Poblet & Hardy, 1995; Storti & Poblet, 1997; Ford *et al.*, 1997; Poblet *et al.*, 1998), generally assuming that sedimentary layers can be considered as passive markers recording only tectonics. There is therefore a need to understand how these local deformations can modify the sequence stratigraphic architecture of syndeformation deposits, and as a consequence, how vertical displacements due to these deformations can be extracted from the stratigraphic record.

The aim of this paper is to combine field study and sequence stratigraphic analysis to gain insights in these issues. To do so, we investigated the influence of the growth of a kilometric compressive fold upon the sequence stratigraphic architecture of syndeformation deposits. The case studied is the Pico del Aguila anticline, located in the Jaca basin, at the southwestern border of the Pyrenean foreland basin (Fig. 1). Strong thickness variations of the syndeformation deposits between the hinge and the synclines of the growth fold (Fig. 2) suggest potential modifications of the stratigraphic architecture due to the growth of the anticline. Excellent field exposure permit detailed mapping of depositional sequences of the upper Eocene at various scales. We present a new sedimentary facies analysis and sequence stratigraphic framework for the syndeformation infill of the Pico del Aguila anticline. From this, we quantified the accommodation variations across the anticline, the rate of relative uplift of its axis and sediment accumulation. We discuss regional and local controls on stratigraphic architecture that is to say, the influence of the growth of the anticline on geometry of depositional cycles in term of thickness ratio of progradational/retrogradational hemicycles.

## GEOLOGICAL SETTING AND PREVIOUS WORK

### Basin setting and stratigraphic framework

The Jaca piggyback basin is located along the southern border of the Pyrenees, to the west of the South Central Pyrenean Unit (SCPU), and to the south of the Axial Zone (Fig. 1). Its southern border corresponds to the South Pyrenean Frontal Thrust ramp (SPFT) lying over the undeformed molasse sediments of the Ebro basin (Millán *et al.*, 1994). This border shows a series of N-S trending folds (each a few km wide), forming a relief called the "Sierras Marginales". The Pico del Aguila anticline is one of these folds (Fig. 2).

The sedimentary cover ranges from Triassic to Lower Miocene ages (Fig. 1). The thick evaporites series of the Keuper (Triassic) are directly overlained by a thin series of alternating Cretaceous to Palaeocene marls and carbonates (Seguret, 1972; Puigdefàbregas, 1975; Puigdefàbregas & Souquet, 1975; Millán *et al.*, 1994) and by the Guara limestones (Lutetian) which correspond to a thick carbonate platform. This platform developed in a retreating pattern over the forebulge of the Palaeocene to Eocene foreland basin that formed at that time (Barnolas & Teixell, 1994). From late Lutetian to Bartonian/Priabonian boundary, a sharp transition to glauconitic offshore marls (Pamplona Marls formation) marks a sudden deepening of the basin, which has been interpreted as resulting from the southward migration of the basin axis (Puigdefàbregas & Souquet, 1986). The growth of the Pico del Aguila and the associated anticlines (Fig. 1) initiated during this period and was coeval with the filling of the basin by a delta prograding from east to west (Arguis and Belsué-Atarès formations, e.g. Millán *et al.*, 1994; Lafont, 1994). During the Oligocene and Miocene, the basin evolved from continental alluvial sedimentation (Campodarbe formation) as it was progressively filled, to an erosional uplifted basin (late Oligocene to early Miocene; Friend et al., 1996; i.e. late stage foreland basin of Puigdefàbregas & Souquet, 1986). This was contemporaneous of the further development of the SPFT, carrying the Jaca basin over the Ebro area as a “piggyback” basin (Ori & Friend, 1984).

### Structural evolution of the Pico del Aguila anticline

The Pico del Aguila anticline is one of the folds of the western « Sierras Marginales » (Fig. 1), deforming the Guara carbonates over a décollement layer (made up of the Triassic to Palaeocene incompetent units) during the upper Eocene. These folds result from an E-W shortening related to the southward displacement of the SCPU (Seguret, 1972; Millán *et al.*,

1994). Their finite geometry (fold axes trending N-S and dipping 30° to the north, on average) cut by the current topography results in a pseudo-2D section of the folds on maps (Fig. 1) and aerial photographs (Fig. 2). This geometry resulted from both (1) a clockwise rotation of 10° to 50° of the axes of the folds induced by the progressive translation to the south of the SCPU (Pueyo-Morer *et al.*, 2002) and (2) a tilting to the north of these axes resulting from the location of the folds above the south-verging ramp of the SPFT (Millán *et al.*, 1994). Millán *et al.* (1994) showed that deformation propagated from east to west (younger folds are located to the west). The Pico del Aguila anticline has been interpreted as a detachment fold, that is, not associated with an emergent thrust ramp (Millán *et al.*, 1994; Poblet & Hardy, 1995). Using the geometry of syndeformation strata, Poblet & Hardy (1995) showed that the uplift rate of the fold decreased through time. They show that the growth of the fold was accommodated by limb rotation (Poblet & Hardy, 1995; Poblet *et al.*, 1998) combined with kink-band migration (Novoa *et al.* 2000).

**Interaction between deformation and sedimentation processes**

The syndeformation strata (from late Lutetian to lower Priabonian) show (1) significant thickening between the hinge and the eastern (Belsué) and western (Arguis) synclines, and (2) progressive onlap geometries at the base of both limbs (Fig. 2). Syndeformation deposits correspond to a mixed delta-carbonate ramp system prograding to the west during the Bartonian to Priabonian. They have been largely documented in Puigdefàbregas (1975), Medjadj (1985), Nuñez del Prado (1986), Millán *et al.* (1994), Lafont (1994), and Millán *et al.* (2000).

Using a sequence stratigraphic approach, Millán *et al.* (1994, 2000) identified four depositional sequences (hundreds of metres thick, about 1 Ma duration) within these syndeformation strata. Each sequence is composed of a thick marly trangressive systems tract (TST) and a thin shallow carbonates and siliciclastics highstand systems tract (HST). Also, they observed that the thickness of the HST was systematically more homogeneously distributed in space than the thickness of the TST (i.e. for the same depositional cycle, the thickness ratio of the progradational and retrogradational sub-cycles was different on the hinge and in the synclines). From this, they proposed a tectonic origin for these sequences and systems tracts : the HST formed during periods of deformation quiescence (and spatially homogeneous distribution of accommodation). By contrast, the TST formed during periods of growth of the anticline (increased regional accommodation, but less homogeneously

distributed). In contrast, Lafont (1994) suggested, without further explanation, that the different progradation/retrogradation thickness ratio between the hinge and the synclines was not necessarily related to a discontinuous deformation process. These contrasting conclusions result in part from the fact that these authors did actually not used the same sequence stratigraphic framework and do not discuss the same scale of depositional sequences.

Consequently, in the present paper, we propose an new sequence stratigraphic framework, taking into account a whole range of scales of depositional cycles (three orders of sequences) and their stacking pattern. We quantified accommodation variations and vertical displacements related to local deformation in order to confront the component of the accommodation signal related to deformation to the stratigraphic record and discuss the influence of the growth of the anticline upon the geometry of depositional cycles.

## FACIES MODEL

### General presentation

Six stratigraphic sections located along the structure (Fig. 2) were constructed: in synclines (S1 in the Arguis syncline, S5 and S6 in the Belsué syncline), on the flanks (S2 to the west and S4 to the east), and on the crest of the anticline (S3). They cover the interval ranging from the top of the Guara limestones to the Ralla de las Tinas bed (Fig. 2) corresponding to the base of the fourth sequence of Millán *et al.* (1994).

Sedimentologic description of each section includes lithology, granulometry, sedimentary structures, fossils and trace fossils, lateral variations and geometries. Six facies associations are identified (Table 1): *FA1 blue marlstones and siltstones, FA2 siltstones to fine sandstones, FA3 cross-stratified sandstones, FA4 mud-draped sigmoidal cross-stratified sandstones, FA5 well-sorted siltstones to medium sandstones, and FA6 bioclastics*. These facies associations have been interpreted in terms of palaeoenvironments and integrated into a depositional model (Fig. 3).

### Reconstructed depositional profile and palaeobathymetry

The sedimentary facies and facies associations (Table 1) indicate that the depositional system for this area between the top of the Guara limestones and the Ralla de las Tinas bed (Fig. 2) correspond to a shallow marine mixed siliciclastic/carbonate setting (Fig. 3). However, the deltaic component largely predominates. It was dominated by fluvial-influenced sedimentation, but showed also the influence of storms and tides. The deltaic systems at that

time were sourced south-east of the study area (Puigdefàbregas & Souquet, 1986; Lafont, 1994; Millán *et al.*, 1994, 2000). At the same time, as noted in Puigdefàbregas & Souquet (1986), carbonates developed as nummulite bars and patch reefs (the carbonate platform typical of the preceding Guara period did not further exist). In this study area, this led to the deposition of bioclastics in a storm ramp setting, preserved during retrogradation times when the delta retreated and siliciclastics were trapped landward (Puigdefàbregas & Souquet, 1986; Lafont, 1994; Millán *et al.*, 1994, 2000).

Facies can be positioned on a depositional profile that includes the fluvial-, tide-, and storm-influenced deltaic settings along with the storm carbonate ramp (Fig. 3). Palaeobathymetries are estimated from foraminifera and bibliographic data (Fig. 3). The storm wave-base is estimated at 60 metres +/- 30 metres, and the fair-weather wave-base at 5 metres +/- 5 metres.

## SEQUENCE STRATIGRAPHY

### Methodology and sequence hierarchy

Depositional sequences are defined on the basis of vertical variations of facies and according to the principles of sequence stratigraphy (Van Wagoner *et al.*, 1988; Van Wagoner *et al.*, 1990; Homewood *et al.*, 1992; Cross *et al.*, 1993). A depositional sequence records a progradation/retrogradation cycle of the shoreline. The smallest correlatable sequences are called “parasequences” when bounded by the two shallowest facies (flooding surface FS, Van Wagoner *et al.*, 1988, 1990), or “genetic units” when bounded by the two deepest facies (maximum flooding surfaces MFS, Homewood *et al.*, 1992). The unconformity (UN) or downward shift, is defined as a sharp decrease of the depth in a shallowing-upward trend, i.e. during progradation.

Three orders of sequences have been defined (Figs. 4 and 5). Genetic units are several decimetres to 30 m thick. Their vertical stacking defines six progradational / retrogradational cycles (5 m to 450 m thick), called here “minor cycles” themselves stacked in one and a half large progradational / retrogradational cycle (300 m to 1100 m thick) called here “major cycle”. Sequence geometries (Figs. 4 and 5) have been constructed using time lines correlated across the studied area using both physical correlations in the field and on aerial photographs (Fig. 2). In some case, the lack of outcrop does not allow direct correlations, we then used the stacking pattern of genetic units to correlate maximum 500 m distant outcrops (stacking pattern method; Van Wagoner *et al.*, 1988; Van Wagoner *et al.*, 1990; Homewood *et al.*,

1992). The time lines correspond to turnaround surfaces (FS and MFS) at the scale of minor cycles defined along section S6.

**Genetic units**

The basic stratigraphic units (genetic units) are generally asymmetric with a thicker progradational half cycle (Figs. 4 and 6) and retrogradational trend almost as thick on the flanks than on the hinge of the anticline.

Within the retrogradational half-cycle of minor cycle 5, field exposure between sections S2 and S3 allowed us to correlate physically some genetic units between the hinge and the flanks of the anticline (Fig. 6). The genetic units are well representative of the general characteristics of these units across the system. On the anticline hinge (S3), the genetic units are composed of (1) a maximum flooding surfaces (MFS) composed of blue marls and silts facies (facies FA1) overlained by a progradational trend recorded by prodelta facies (FA1 and FA2) sharply overlained by (2) a by pass surface and an aggrading trend recorded by storm deposits (FA4), and finally (3) a retrogradational trend recorded by carbonate ramp deposits overlying a ravinement surface (FA6 and locally FA1 and FA2). On the west flank (S2), the genetic units are composed of (1) a maximum flooding surfaces (MFS) composed of blue marls and silts facies (facies FA1) overlained by a progradational trend recorded by prodelta to delta front facies (FA 1 to FA 3) overlained by (2) an aggrading trend recorded by mouth-bar and subtidal facies (FA3 and FA4) topped by a ravinement surface and (3) a retrogradational trend recorded by carbonate ramp deposits (FA 6 and locally FA1 and FA2).

The most distal facies (storm deposits) are better preserved on the hinge even though the latter lies on a more proximal location than the western flanks (deltaic systems were sourced to the south-east). The geometry and the facies of the progradational and aggradational trends of genetic units therefore depend on their position across the studied area suggesting an influence of the growth of the anticline upon their geometry.

**Minor cycles**

The geometry and the lithologic expression of minor cycles is variable both in space and in time (Figs. 4 and 5).

*Initial retrogradational half-cycle*

The initial retrogradational half-cycle is composed of mixed siliciclastic-carbonate

backstepping genetic units lying over the Guara limestones by a wave ravinement surface that marks a sudden deepening. On the hinge of the anticline, it is only recorded by a glauconitic hard-ground.

*Cycle 1*

The minor cycle 1 is highly asymmetric dominated by the progradational sub-cycle (few hundreds of metres thick) whereas the retrogradational phase is only few tens of metres thick. It shows progressive onlap geometries on the flanks of the anticline and was therefore condensed on the hinge. Foraminifera indicate that the MFS ending this cycle (MFS2) corresponds to the deepest palaeobathymetry encountered in the studied section (Stràkos and Castelltort, 2001). Facies indicate deeper environments on sections located west of the anticline (S1 and S2). Palaeocurrents directions are nearly parallel to the anticline axis (N-S).

*Cycle 2*

Minor cycle 2 is symmetric in the western syncline (section S1) and asymmetric dominated the progradational sub-cycle in the eastern syncline (sections S6 and S5). This asymmetry is accentuated on the hinge of the anticline (section S3). The flooding surface of minor cycle 2 (FS2) is marked by shallowest facies (mouth-bars) than the turnaround surface of minor cycle (FS1). Facies deepen to the west (distal delta-front at the FS2 on section S1, and mouth-bars at the FS2 on S6). Palaeocurrents directions are mainly directed northwards in the Belsué syncline, and westwards on S6.

Minor cycle 2 show a specific feature. The surface identified as the flooding surface in the synclines (FS2 on S1, S5 and S6) can be physically traced and appears not to correspond to the surface identified as the flooding surface on the anticline hinge (FS2' on S3). This suggests that the trend inversion from progradation to retrogradation of minor cycle 2 is diachronous, i.e. it occurs earlier in the synclines (FS2) than on the hinge of the anticline (FS2').

*Cycle 3*

Minor cycle 3 is the thinnest minor cycle (5 to 40 m) and marks the first proximal deltaic facies recorded in the western syncline. It is generally asymmetric, dominated by its retrogradational sub-cycle and the erosional surface of unconformity is merged with the

flooding surface (FS3). This erosive surface (and associated bypass facies) form a clear marker bed that can be physically correlated across the studied area (the Arguis bed of Millán *et al.*, 2000). Palaeocurrents directions measured locally in scours are nearly parallel to the anticline axis (N-S).

*Cycle 4*

Minor cycle 4 is highly asymmetric dominated by the progradational sub-cycle. The flooding surface (FS4) is marked by tide-dominated mouth-bar facies i.e. shallowest facies than the flooding surface of minor cycle 3 (FS3). Facies generally indicate deeper bathymetries to the west. Palaeoflows are mainly directed to the northwest, except on the hinge of the anticline where the tidal influence may have caused the observed variability in flow directions.

*Cycle 5*

Minor cycle 5 is dominated by the retrogradational sub-cycle, this asymmetry being enhanced to the west. This cycle records the shallowest facies encountered in the studied sections. The flooding surface (FS5) is better marked towards the hinge of the anticline (i.e. showing more small-scale erosive scours). Facies are only slightly deeper towards the west. Palaeocurrents are directed to the northwest on average.

*Cycle 6*

Minor cycle 6 is only recorded on sections S4, S5 and S6 and is asymmetric dominated by the retrogradational sub-cycle. The facies significantly deepen to the west. Palaeoflows measured in the eastern syncline were directed northwestwards.

The following stratigraphic record corresponds the beginning of a new progradational phase corresponding to sequence 4 of Millán *et al.* (1994) and Millán *et al.* (2000).

*Summary*

Like genetic units, the retrogradational trends of minor cycles (carbonates, mixed siliciclastics-carbonates and distal deltaics deposits) always show a more homogeneous thickness distribution than progradational trends (delta-front deposits), which are very reduced on the anticline hinge.

**Major cycles**

The stacking pattern of the minor cycles defines (Fig. 5): (1) a major retrogradational hemicycle (composed of the initial retrogradational minor sub-cycle and minor cycle 1) topped by MFS2 (i.e. the deepest facies encountered in the section; Stràkos and Castelltort, 2001) and not recorded on the anticlinal hinge, (2) a progradational sub-cycle (composed of minor cycles 2, 3, 4 and the progradational trend of minor cycle 5) with an unconformity merged with FS3 (unconformity of minor cycle 3) and bounded by FS5 (i.e. the shallowest facies encountered in the section) and, finally (3) a retrogradational sub-cycle (composed of the retrogradational sub-cycle of minor cycle 5 and minor cycle 6).

The complete major cycle is asymmetric dominated by the progradational trend, and like the lower orders of depositional sequences, most of the thickness variation of the major cycle between the anticlinal hinge and the synclines is taking place during the major progradational sub-cycle.

**Paleocurrents**

As already pointed out by several authors deltaic sediment supply is sourced to the south-east (e.g. Puigdefabregas, 1975; Lafont, 1994; Millán *et al.*, 1994; Millán *et al.*, 2000). We here analyse data only measured along a 2-D transect and therefore cannot fully discuss the influence of the growth of the anticline upon paleocurrent direction since it is obviously a three-dimensional problem. However, we observe that before the major unconformity (merged with FS3), palaeocurrents are directed northward (i.e. parallel to the anticline present-day axis) whereas they display northwest directions (i.e. oblique to the anticline axis) after (Fig. 5).

**Calibration of time lines on absolute ages**

We propose a calibration on absolute ages of the time lines bounding the minor cycles (FS and MFS) using a diagram compiling magnetostratigraphic and biostratigraphic data (Fig. 7). Stràkos and Castelltort (2001) calibrated the section of the western syncline (S1) to biostratigraphic timescale of calcareous nannofossils (NP, column 4 on Figure 7) and planktonic foraminifera (P, column 5 on Fig. 7).

We positioned the magnetostratigraphic samples of Hogan and Burbank (1996) measured in western syncline along our own section (S1; see column 1 on Fig. 7). From these,

we calibrated the reverse and normal periods of Hogan and Burbank (1996) to the MPTS (magnetic polarity time scale) of Cande and Kent (1995) or the MPTS of Wei (1995) following two hypothesis: in one case we took biostratigraphic data into account (column 2 on Fig. 7), in the other not (column 3 on Fig. 7). We used these two different hypotheses because, according to Berggren *et al.* (1995), the absolute dating of the boundary between NP14 and NP15 is problematic (with a potential error several 100 Ka). We then extrapolated the age of our time lines assuming a constant accumulation rate between the data points. Taking into account two MPTS and two hypotheses (with or without biostratigraphic data), we obtain 4 different dating models for the time lines that we use to assess their influence on our results.

Whatever the dating model, the duration of the genetic units is less than 100 ka, the duration of minor cycles range between 100 ka and 1,8 Ma and the major cycle (and the major retrogradational hemicycle) last about 4 Ma.

In the following, for simplicity, we show the values obtained for the first model (taking into account biostratigraphic data and the MPTS of Cande and Kent, 1995) unless specified. We discuss the influence of the dating model on the results below.

## ACCOMMODATION, SEDIMENT ACCUMULATION, AND UPLIFT RATES

### Methodology

Accommodation variations reflect eustatic sea level changes and vertical movements of the basin substratum related to deformation and this, independently of the sediment supply, filling or not this space available for sedimentation. On a vertical section, the accommodation variation for a given time interval can be quantified by summing the decompacted thickness of deposited sediments and the variation of palaeobathymetries/palaeoaltitudes (Jervey, 1988). Positive accommodation values represent accommodation creation during the given time step, whereas negative values represent accommodation reduction. Cross *et al.* (1993) used the definition of accommodation to define depositional sequences as the record of variations of the ratio of accommodation and sedimentation (A/S ratio): the A/S ratio is lower than 1 during progradational trend (or negative when erosion occurs), equal to 1 during aggradation around the FS, larger then 1 during retrogradation and again equal to 1 around the MFS.

The measure of accommodation variations requires (Fig 8): (1) time-lines defined across the section, (2) lithological data and (3) estimations of palaeobathymetry along each

time line (e.g. Robin *et al.*, 1996, 1998).

(1) The time-lines used are the surfaces bounding minor cycles on section S1.

(2) The averaged lithology of each interval (i.e. percentages of carbonate, shale and sand) is obtained from the sedimentological analysis of the sections (Fig 3 and Table 2). Thickness are then corrected for compaction according to laws established by Sclater & Christie (1980) taking into account the estimated thickness of the eroded Priabonian to Oligocene palaeocover (about 2000 metres; Puigdefabregas, 1975; Lafont, 1994).

(3) Bathymetric boundaries of the depositional environments are estimated from facies analysis (see palaeodepth synthesis on Table): – 5 m (+/-5 m) for the fair-weather wave-base; – 60 m (+/-30 m) for the storm wave-base and -150 m (+/- 50m) for the deepest facies encountered. Between these boundaries, we determined the bathymetry assuming a linear gradient, taking into account foraminifera fauna and local variations of this gradient indicated by sedimentary facies. The error intervals defined for bathymetric boundaries are intended to provide an evaluation of the variability of the results depending upon the chosen depositional profile.

Accommodation variations are measured along sections S1, S3, S5 and S6 (Fig. 9). Also, since we could not correlate the time line corresponding to the turnaround surfaces of minor cycle 6 (FS6 and MFS7) between S1, S2 and S3, they were not used in these calculations. We then estimated the rates of accommodation variations using the dating models discussed above (Fig. 9). In the same way, we measured the sediment accumulation rates from the (decompacted) thickness of sediment deposited during each time step (Fig. 9). These values do not give the sediment supply at the boundaries of the studied system, only an evaluation of the amount of sediments preserved.

We measure the uplift of the anticline hinge with respect to synclines by subtracting the accommodation measured on section S3 to the one measured in the synclines (i.e. S1, S5 or S6; Figs. 8 and 10). Also, we measure the uplift with respect to the surface marking the top of the Guara sandstones (FS1). However, it should be pointed out that early syntectonic geometries have been found within the Guara formation (Millán *et al.*, 1994, 2000) suggesting the uplift initiated during their deposition and Poblet & Hardy (1995) suggested that they are associated with an uplift of about 60 m.

**Accommodation**

At the scale of minor cycles, accommodation variation rates range from -1500 m/Ma to

+2500 m/Ma and correspond to alternating periods of rapid and slow accommodation variation (Fig. 9). Accommodation variation rates are mostly positive, even on the hinge of the anticline, except in two cases. On all sections, the progradational phase of cycle 3 corresponds to an accommodation reduction (-950 m/Ma on average). Also, on the anticlinal hinge only (S3), an accommodation reduction is recorded at FS5 (-40 m/Ma). All sections show a highly consistent behaviour in terms of cycles of rate of variation of space available for sedimentation: minimum and maximum of accommodation variations are contemporaneous and show similar amplitude. Also, retrogradational minor sub-cycles correspond to rapid accommodation creation whereas progradational ones correspond to slow accommodation creation (or reduction).

At the scale of major cycles, accommodation variation rates range from –10 m/Ma to 360 m/Ma (Fig. 9). In the synclines, the initial retrogradational sub-cycle correspond to a rapid increase accommodation creation (up to 350 m/Ma), the progradational sub-cycle to an equivalent or slightly lower accommodation creation and the retrogradational sub-cycle to a decrease in accommodation creation (down to 110 m/Ma). On the hinge, the progradational trend occurs during a moderate accommodation creation (up to 150 m/Ma) and the retrogradational trend during a slowing accommodation creation.

**Sediment accumulation**

Sediment accumulation rates range from 0 to 800 m/Ma. At the scale of the minor cycles, sediment accumulation rates generally increase when accommodation variation rates decrease and vice-versa, i.e. sediment accumulation and accommodation variations are out-of-phase (Fig. 9). At the scale of the major cycles, sediment accumulation rates are correlated with accommodation variations (Fig. 9).

**Uplift of the anticline**

The measured uplift rate of the anticline with respect to both synclines is continuously decreasing: from about 750 m/Ma during minor cycles 1, 2 and 3 to below 200 m/Ma during minor cycles 4, 5 and 6 (Fig. 10). These results are consistent with the uplift curve proposed by Poblet & Hardy (1995) with respect to the western syncline only. Uplift rates measured with respect to the section located to the west are higher than the ones measured for sections located to the east (compare uplift measured with respect to S1, S5 and S6 on Fig. 10).

### Variability of accommodation variations measurements

The variability of our results is due to three sources of errors, namely: (1) lithology, (2) paleobathymetry, and (3) age of time lines.

(1) In order to estimate the effect of errors of lithologies interpreted on well logs on the calculated accommodation evolution, we performed four sets of calculations. For each section, we calculated accommodation variations using (1) the lithologies determined from sections, (2) an equivalent section composed entirely of clay, (3) of sand, or (4) of carbonates. These calculations give an estimation of the maximum errors related to decompaction, i.e. about 1% on average of the uplift values. Also, the effects of errors on the thickness of the post-Eocene palaeocover were estimated by measuring accommodation variations with a palaeocover ranging between 0 and 2000 m: the maximum associated error is also about 1%.

(2) The error brackets shown on Figures 9 and 10 reflect the variability of the accommodation variation and uplift rates related to the errors on the bathymetric boundaries defined along the depositional profile (+/- 5m for the fair-weather wave-base and +/- 30 m for the storm wave-base). However, if the depositional profile gradient sign is preserved, the sign of the accommodation gradient will also be preserved between given locations. Thus, even if errors on the slope of the depositional profile may produce significant uncertainties in the absolute values of accommodation variation, the relative variations are preserved from one section to the other (Robin, 1997).

(3) To evaluate the influence of the age model on the calculated accommodation variation rates, we compared the results obtained with the 4 dating models (Fig. 11). Whatever the dating model, nor the pattern of alternating phases of rapid and slow increase of accommodation variations nor their relative magnitude (accept for the two values around MFS2) are altered.

The influence of these various sources of errors is to modify the duration of the cycles and the absolute values of the rate of accommodation variations, however, none of these source of errors does alter the general tendencies and the relative behaviour of the different sections.

## INTERPRETATION OF THE RESULTS

### Stratigraphic framework

The stratigraphic framework we define is different from the one proposed by Millán *et al.* (1994, 2000) based on the study of all the anticlines of the western Sierras Marginales (*i.e.*

a wider area). There are three differences.

(1) We defined depositional sequences between the two deepest facies (MFS) whereas they used Vail-type sequence boundaries (SB).

(2) Also, they defined depositional sequences composed of two units: a marly interval interpreted as a transgressive system tract (TST) followed by mixed deltaics/bioclastic intervals interpreted as highstand system tracts (HST). We, on the other hand, define minor cycles composed of (i) a shallowing-upward trend from blue marls to front-deltaic facies interpreted as a progradation (early to late highstand system tracts HST) followed by (ii) a mixed deltaics/bioclastic interval interpreted as vertically stacked and backstepping successions of genetic units that is to say corresponding to an aggradation (equivalent to low stand system tracts LST) and a retrogradation (TST).

(3) Consequently, we identified six minor cycles over the period during which they defined three sequences (sequences 1 to 3).

**Accommodation variations**

Three observations can be drawn from the quantification of accommodation variations.

(1) Even if amplitudes of accommodation variation rates are lower on the hinge (S3) than in the synclines (S1, S5 and S6), they remain mostly positive (even on the hinge of the anticline; Fig. 9). This implies a constant creation of space available for sedimentation over the studied period (about 4 Ma). Since this accommodation creation is recorded throughout the system (hinge and synclines), it should be related to a process effective at a larger scale than the studied area i.e. larger than 10 km (such as a general subsidence of the basin or a global sea-level rise for example).

(2) At the scale of minor cycles, all sections (hinge and synclines) show a highly consistent behaviour in terms of cycles of rate of variation of space available for sedimentation (Fig. 9). Also, retrogradational minor sub-cycles correspond to rapid accommodation creation whereas progradational ones correspond to slow accommodation creation (or reduction). Since depositional sequences correspond to cycles of variations of the ratio of accommodation variation versus sediment supply (A/S ratio), this observation implies that minor cycles are essentially driven by accommodation variations (A) rather than sediment supply (S). Indeed, sediment accumulation rates generally decrease when accommodation variation rate increase and vice-versa, however progradation/retrogradation cycles do occur even when sediment accumulation rate is constant (see for example minor

cycle 2 on S1 or minor cycles 5 and 6 on S5; Fig. 9).

Since accommodation variations at the scale of minor cycles are driven by a process effective at a larger scale than the studied area, this suggests that minor cycles are driven by this process effective at a larger scale than the studied system.

(3) The only period of strong accommodation reduction on all sections is taking place during the progradational phase of minor cycle 3 whose erosional surface of unconformity is merged with the flooding surface (FS3; Figs. 4 and 9). This suggest that, at that time, the negative accommodation variation across the system (i.e. driven at a larger scale than the studied area) is strong enough to prevent the preservation of the late progradational phase of minor cycle 3, i.e. the period between the unconformity and the turnaround surface.

### Uplift

Two observations can be drawn from the quantification of uplift rate.

(1) We pointed out earlier that uplift rates measured with respect to the section located in the western syncline are higher than the ones measured for sections located in the eastern syncline (Fig. 10). This could be related to the position of the eastern syncline neighbouring a contemporaneous anticline of the Sierras Marginales (the Gabardiella-Lusera anticline; Fig. 1). The growth of the latter might have limited the subsidence of this western syncline, as it progressively involved section S6 (and S5 on a lesser extent) into its limb.

(2) We do not observe a systematic relationship between the timing of minor cycles and the variations of uplift rates (Fig. 10). For example, progradational trends can be coeval to either accelerations or decelerations of uplift. Furthermore, even during periods of continuous uplift, minor cycles are recorded (for example during minor cycles 2 to 6 on S5).

## INFLUENCE OF THE ANTICLINE GROWTH UPON THE STRATIGRAPHIC RECORD

We observe three different controls of the growth of the anticline on the sedimentary record: (1) the distribution of sedimentary thickness, (2) the facies of sediments deposited (i.e. the depositional profile) and (3) the geometry of depositional sequences.

### Thickness distribution

The most obvious influence of the anticline growth is the variation of the thickness of the syndeformation infill between the hinge and the synclines resulting from the spatial

variation in subsidence rate.

All scale of sequences (genetic units minor and major cycles) are generally thinner on the hinge. In detail, however, the thickness variation of minor cycles is evolving into three successive steps (Fig. 5b). During step 1 (up to the early progradation of minor cycle 2), sedimentary deposits show onlap geometries onto the flanks of the anticline and are not recorded on the hinge. During step 2 (end of minor cycle 2 and progradation of minor cycle 3), sediments are preserved on the hinge but are much thicker in the synclines. During step 3 (end of minor cycle 3 to minor cycle 6), the relative thickening of deposits in the synclines with respect to the hinge is lower than before. This can be interpreted as the record of the overall decrease of the uplift rate of the anticline over the studied period, progressively reducing the subsidence difference between the hinge and the synclines. At the scale of the major cycles, this evolution results in the absence of the initial retrogradational hemicycle on the hinge and the lateral pinch out of the major cycle.

**Depositional profile**

When the sediment supply is low enough with respect to the deformation rate, growth structures might modify the topography of the basin floor and in doing so, influence the depositional profile. In the studied area, the growth of the anticline is recorded in two ways: (1) a lateral variation of sediment facies and (2) a local deflection of paleocurrent directions.

*Genetic unit*

Lateral variation of facies resulting from a topography associated with the anticline growth can be observed at the scale of genetic units. The beginning of the progradation trend is recorded by distal deltaics (blue marls facies) across the whole system (Fig. 6). However, during the progradational trend, the hinge records a surface of erosion/bypass whereas the syncline records prograding deltaic facies. During late progradation, the aggradation trend is recorded by wave-dominated facies (high energy condensed deposits) on the hinge and tide-dominated facies (low energy accumulating deposits) in the synclines. The retrogradation is marked by a wave ravinement surface increasingly erosive towards the anticline hinge overlain by bioclastic deposits that drape the whole structure with shallower facies on the hinge.

*Minor cycles*

Lateral variation of facies resulting from a topography associated to the anticline growth can also be observed at the scale of the minor cycles (Fig. 5).

As pointed out earlier, during step 1 (up to the early progradation of minor cycle 2), siliciclastic deltaic deposits recorded in the synclines show onlap geometries onto the flanks of the anticline and are by passed or condensed on the hinge. During step 2, the bathymetric gradients along time lines FS2 and FS2' indicate an accentuation of the topography of the anticline. Indeed, along FS2, the facies preserved on the hinge are shallower than the facies preserved in the synclines and, along FS2', the facies become even more shallower on the hinge and deeper in the synclines, indicating an increase in the anticline slope during this time-step. During step 3, we do not observe any clear evidence of the influence of a topography related to the anticline on sedimentary facies. Also, carbonates facies, recorded throughout the studied, become more homogeneous with time, suggesting a decreasing influence of the anticline growth on the topography. These observations can be again be interpreted as the record of the overall decrease of the uplift rate of the anticline over the studied period, progressively reducing the topographic influence of the anticline.

Variations of paleocurrent directions observed during the studied period may also be interpreted as a reducing influence of the anticlinal hinge in the topography of the basin floor. Indeed, we observe an evolution in flow directions: during step 1 and 2 palaeocurrent directions are mainly parallel to the anticline axis (northward) and became progressively oblique during step 3 (northwestward). Also, the transition between step 2 and 3 (around the time line FS3) corresponds to the proximal deltaics being preserved on the anticlinal hinge in the studied section. These two observations can be interpreted as a transition between a period during which regional paleocurrents (e.g. Puygdefabregas, 1975) were locally deflected by the anticline and a period during which they do not seem to be altered.

**Depositional sequences geometry**

Beyond the variation of the thickness of syndeformation deposits and the alteration of the depositional profile, the growth of the anticline also altered the geometry of depositional sequences, that is to say distort them. The term distortion has been proposed by Cross (1988) and Guillocheau (1991, 1995) to describe the modification of the geometry of a cycle of a given duration involved in a cycle of lower frequency. For example, a high frequency cycle superimposed to the lower frequency prograding trend will display a thicker (Guillocheau, 1995) and longer (Granjeon, 1997) prograding sub-cycle than a cycle of the same duration

superimposed to the lower frequency retrograding trend. This temporal distortion is different from the spatial change in geometry of depositional sequences between the continental and marine domains due to volumetric partitioning (Cross and Lessenger, 1998).

As pointed out by Gawthorpe *et al.* (1994), the spatial variation of subsidence associated with growth structures, results in spatial alteration of the A/S variation curves (faster subsidence resulting in steeper A/S variation curves will favour the retrograding trend of resulting depositional sequences). For a given depositional sequence, spatial variation of subsidence rate associated with a growth structure (fold or faults) will therefore result in a spatial distortion by altering its thickness ratio of prograding and retrograding sub-cycles (P/R ratio).

In the studied area, we observed two types of distortion of depositional sequences: (1) the spatial distortion of the P/R ratio of given depositional sequences, but also (2) the alteration of the time of occurrence of the trend inversion between progradation and retrogradation across the system.

*Genetic units*

As already pointed out, genetic units are thinner on the hinge of the anticline. However, this thickness variation is accommodated differently during the prograding and the retrograding trends (Figs. 4 and 6). The progradational sub-cycles are significantly thicker in the synclines whereas the retrogradational sub-cycles display a more even thickness across the anticline.

The contrasting thicknesses of progradational sub-cycles and more even retrogradational sub-cycles could be interpreted as the result of the alternance of period of anticline growth (thickening) and quiescence (even thickness) and this, at the scale of the genetic units (i.e. less than 100 ka according to our model). However, having no clear evidence of a deformation mechanism systematically oscillating at such frequencies, we propose an alternating explanation for these observed spatial distorsion genetic units (Fig. 12). In this model, we suppose that, at the scale of genetic units, the anticline growth is continuous. Also, since they can be correlated across the system, we suppose that genetic units are driven by A/S variations controlled by a process effective at a larger scale than the studied system.

(1) At the beginning of the progradation, distal deltaics (blue marls facies) are homogeneously deposited across the system ($0< A/S <1$, decreasing). (2) As progradation rate

increases, the hinge records a surface of erosion/bypass (A/S≤0) whereas the syncline records a normal progradation of the delta-front (0< A/S <1). (3) During late progradation (up to the turnaround to retrogradation) sediments aggrade again throughout the system (A/S slightly lower than 1). Wave-dominated facies are preserved on the hinge and tide-dominated facies in the synclines, indicating a slightly larger A/S ratio on the hinge. However, the preserved thickness (S) is significantly thicker in the synclines (at least 5 folds) suggesting that to maintain a similar value of A/S, the accommodation variation (A) was significantly larger in the synclines. (4) The retrogradation is marked by a wave ravinement surface (increasingly erosive towards the anticline hinge) overlained by continuous bioclastic deposits of homogeneous thickness that drape the whole structure with shallower facies on the hinge than in the western syncline (A/S >1, increasing). This homogeneous carbonate deposits probably result from the retrogradation of the depositional profile, trapping terrigeneous sediments upslope, and favoring carbonate deposits, by nature, more homogeneously distributed across the structure.

This model offers an explanation for the spatial distortion of genetic units, simply by the superimposition of (1) a relative-sea-level variation of larger wavelength origin than the structure, and (2) a continuous local deformation.

*Minor cycles*

The distortion of the P/R ratio across the anticline is also visible at the scale of minor cycles (the progradational sub-cycles are thicker in the synclines whereas the retrogradational sub-cycles show a more even thickness). Nonetheless, like already observed for sedimentary thickness variations and depositional profiles alterations, the intensity of the distortion is attenuated with time probably recording the progressive decrease of the uplift rate. Indeed, during the rapid initial uplift > 750 m/Ma (Fig. 10), the initial retrogradational sub-cycle and minor cycle 1 are not recorded on the hinge, this strong distortion resulting from the absence of accommodation creation on the hinge at that time (S3 on Fig. 9). During the following slowing uplift (about 200 m/Ma), minor cycles 2, 3 and 4 are recorded on the hinge and display a distortion of the P/R ratio (thicker prograding phases in the synclines). During the final slow uplift period (< 200 m/Ma), the P/R ratio of cycles 5 and 6 is barely altered, indicating a light (to null) distortion as accommodation creation is more homogeneously distributed across the system.

The distortion of the P/R ratio of depositional sequences of the syndeformation infill of

Pico De Aguila anticline had already been observed by Millán *et al.* (1994). It has been interpreted as resulting from the alternance of periods of anticline growth (resulting in thickened TST across the structure) and quiescence (even thickness of HST), implying a tectonic origin for these cycles. Based on different stratigraphic framework, we propose an alternating explanation for these observed spatial distortions of minor cycles (Fig. 13).

In this model, and based on uplift measurement, we suppose that the anticline growth is a continuous process at the scale of minor cycles. Also, based on accommodation variations measurements, we assume that minor cycles are driven by accommodation variations (rather than sediment supply variations) controlled by a process effective at a larger scale than the studied system. Finally, we suppose a constant sediment supply filling up the system. Under these conditions, the variations of the P/R ratio may solely result from accommodation variations produced by the superimposition of (1) the continuous deformation component creating laterally differential subsidence between the hinge and the synclines, and (2) the cyclic variations of relative sea level of regional or global origin (Fig. 13). During periods of regional low accommodation creation rate (progradation), locally variable accommodation created by the anticline growth results in greater contrast of space available for sedimentation (and preserved thickness) between the hinge and the synclines (cases 2 and 3 on Fig. 16). In contrast, periods of regional high accommodation (retrogradation) tend to attenuate local contrasts created by the anticline growth resulting in the deposition of more even thickness of sediments (cases 1 and 4 on Fig. 13).

In this model, we assumed a constant preserved sediment supply filling up the system. However, in the studied case, this effect should be even amplified because, as pointed out earlier, the sediment supply preserved in the system is actually anti-correlated to accommodation variation (the larger the accommodation variation, the smaller the sediment thickness preserved).

We showed that for minor cycle 2, the distortion of the P/R ratio is associated with the alteration of the time of occurence of the trend inversion between progradation and retrogradation across the system: it occurs earlier in the synclines (FS2) than on the hinge of the anticline (FS2'). Such a distortion, at basin-scale (hectokilometric), of the timing of stratigraphic surfaces is implicit in the model of Catuneanu *et al.* (1997ab) for cycles of duration about 1 to 5 Ma and has been described for local deformation (kilometre scale) and high frequency cycles (Nishikawa & Ito, 2000). Here, we observe this distortion for cycle durations between 100 ka and 1,8 Ma by kilometric deformation structures. This specific

feature occurred during the period of moderate distortion, as uplift rate decreased enough to allow preservation of sediments on the hinge of the anticline. This specific distortion can be explained theoretically (Fig. 14) by adding a regional cyclic variation of relative sea level (represented by a sinusoidal curve on Fig. 14a) to a local linear subsidence (Fig. 14b) whose rate depends on the location with respect to the structure (Fig. 14c) i.e. higher in the synclines (location A) than on the hinge (location B). Assuming a constant rate of sediment input (S), the curve of rate of accommodation variation gives the timing of turnaround surface (Fig. 14d): the FS occurs when the A/S ratio equals 1 and increases (the MFS when the A/S ratio equals 1 and decreases). The comparison of the two locations shows that the FS will occur earlier (and MFS later) in areas of higher subsidence rate (location A). We therefore interpret the time shift of the trend inversion from progradation to retrogradation of minor cycle 2 as a consequence of the differential subsidence rate between the hinge and the synclines (i.e. the uplift rate). Again, we assumed a constant preserved sediment supply, however, in the studied case, this effect should be even amplified because the sediment supply preserved in the system is actually anti-correlated to accommodation.

*Major cycle*

We observe a distortion of the P/R ratio across the anticline at the scale of the major cycle (Fig. 5) which is consistent with the observations made for higher frequency cycles (i.e. reflecting the stacking pattern of genetic units and minor cycles) and whose intensity is attenuated with time as recording the progressive decrease of the uplift rate (the initial retrogradational major sub-cycle is not recorded on the hinge and the change in thickness of the complete major cycle is mainly accommodated during the progradational sub-cycle).

**Influence of sediment supply and origin of minor cycles**

During the studied period, major changes in the nature of sediment supply seems to follow the evolution of the anticline growth (Figs. 1 and 5). The rapid initial uplift (fold initiation) corresponds to the rapid flooding of the Guara carbonate platform and the installation of deltaic sedimentation. The following reducing uplift rate of the anticline is associated with the progressive progradation of deltaic sedimentation. The final phase of low uplift rate is associated with a larger proportion of carbonate deposits. After the end of the anticline growth, the system evolved into a continental alluvial sedimentation. This evolution in the nature of sediment supply reflects an evolution of depositional systems at regional scale

(larger than the studied area), i.e. either regional deformation or eustasy. Having no evidence of a process that could link eustasy to local deformation, we interpret this as a link between local and regional deformation (decreasing local deformation rate corresponds to a decreasing regional subsidence of the foreland basin).

We showed that minor cycles are mainly driven by variations of the accommodation rate (with out of phase sediment accumulation rates) and that these accommodation variations where not related to the evolution of the growth of the anticline. This suggests that both accommodation variations and sediment accumulation are driven by a process effective at regional scale (larger than the studied area). Because of the duration of minor cycles (< 1Ma), we would tend to favour the hypothesis of accommodation variation driven by eustasy, however we have no definitive arguments to exclude variations in the foreland basin subsidence at that scale.

## CONCLUSION

We investigated the influence of the growth of the Pico del Aguila anticline upon the sequence stratigraphic architecture of syndeformation deposits by combining field study and sequence stratigraphic analysis.

(1) We analysed six stratigraphic sections located along the structure including lithology, sedimentary figures and geometries, fossils and trace fossils. We identified six facies associations that we interpreted in terms of palaeoenvironments and integrated into a depositional model of a shallow marine mixed deltaic/carbonate ramp mostly flood-dominated (fluvial-influenced) with local storm and tide influence.

(2) From this we proposed a new sequence stratigraphic framework of the syndeformation deposits, taking into account three orders of depositional cycles (genetic units, minor cycles and major cycles) and their stacking pattern. Using a dating model integrating bio- and magneto- stratigraphic data, we proposed durations for each scale of sequences (less than 100 ka, 100 ka to 1,8 Ma and 4 Ma respectively).

(3) We then quantified the rates of accommodation variations, sediment accumulation and relative uplift of the anticline. We showed that accommodation variation rates correspond to alternating periods of rapid and slow accommodation creation, i.e. are mostly positive even on the hinge of the anticline. We showed that minor cycles were driven by accommodation variations of regional scale (rather than sediment supply variations) and that the uplift rate of the anticline axis was continuously decreasing through time.

(4) We observed four different controls of the growth of the anticline on the sedimentary record: the distribution of sedimentary thickness, the depositional profile (shallower facies are preserved on the hinge of the anticline), the P/R ratio of depositional sequences (most of the thickness difference takes place during the prograding trend) and locally the alteration of the time of occurrence of inversion from progradation to retrogradation trend between the hinge and the synclines. The growth of the anticline consistently distorted the geometry of the three scales of depositional cycles with an intensity depending upon the difference in subsidence rate between the hinge and the synclines (i.e. the uplift rate).

(5) We propose that the distortion of the P/R ratio (the thickness ratio between progradational et retrogradational sub-cycles) and the alteration of the timing of trend can be explain by a simple superimposition of a continuous uplift of the anticline (local deformation) and regional variations of relative sea level (eustasy and/or foreland basin subsidence). As a consequence, in our interpretation, depositional sequences are not driven by the anticline growth.

**Acknowledgements**

We acknowledge M. de Urreiztieta and Total Fina Elf for their support and the discussions. The ideas involved in this paper partly developed during long-term cooperation between Rennes University and the Institut Français du Pétrole. We are very grateful to editor H. Sinclair and reviewers S. Gupta, C. Puygdefabregas and M. Marzo for their detailed and extremely useful comments that helped us to sort out our arguments. The paper benefited largely from a lot of stimulating discussions with J. Van Den Driessche, I. Coutand, R. Bouroullec and S. Pochat. Thanks is also due to «El Parque de la Sierra y Cañones de Guara» that allowed us for sampling.

## References


BHATTACHARYA, J. P. & WALKER, R. G. (1992) Deltas. In: *Facies Models* (Ed. by R. G. Walker, and N. P. James), Geological Association of Canada, pp. 157-177.

BERGGREN, W.A., KENT, D.V., SWISHER, C.C. & AUBRY, M.P. (1995) A revised Cenozoic geochronology and chronostratigraphy. In: *Geochronology, time scales and global stratigraphic correlations* (Ed. by W. A. Berggren, D. V. Kent, M. P. Aubry and J. Hardenbol), *Soc. Econ. Palaeont. Miner. Spec. Publ*., **54**, pp. 129-212.

CANDE, S.C. & KENT, D.V. (1995) Revised calibrations of the geomagnetic polarity timescale for the late Cretaceous and Cenozoic. *J. Geophys. Res.,* **100**, 6093-6095.

CATUNEANU, O., SWEET, A.R. & MIALL, A.D. (1997a) Reciprocal architecture of Bearpaw T-R sequences, uppermost Cretaceous, Western Canada sedimentary basin. *Bull. Can. Petrol. Geol.,* **45**, 75-94.

CATUNEANU, O., BEAUMONT, C. & WASCHBUSCH, P. (1997b) Interplay of static loads and subduction dynamics in foreland basins: Reciprocal stratigraphies and the "missing" peripheral bulge. *Geology,* **25**, 1087-1090.

COLEMAN, J. M., & GAGLIANO, S. M. (1964) Cyclic sedimentation in the Mississippi River deltaic plain. *Gulf Coast Assoc. Geol. Soc. Trans*., **14**, 67-80.

COLEMAN, J. M., & PRIOR, D. (1982) Deltaic environments of deposition, In: *Sandstone Depositional environments* (Ed. by P. A. S. Sholle, D.), *Amer. Assoc. Petrol. Geol. Mem*, **31**, pp. 139-178.

CROSS, T.A. (1988) Controls on coal distribution in transgressive-regressive cycles. Upper Cretaceous, Western Interior, USA. In: *Sea-Level Changes: An Integrated Approach* (Ed. by C. K. Wilgus, B. S. Hastings, C. G. Kendall, H. W. Posamentier, C. A. Ross and J. C. Van Wagoner), *Soc. Econ. Palaeont. Miner. Spec. Publ.,* **42**, pp. 371-380.

CROSS, T.A., BAKER, M.R., CHAPIN, M.A., CLARK, M.S., GARDNER, M.H., HANSON, M.S., LESSENGER, M.A., LITTLE, L.D., MCDONOUGH, K.-J., SONNENFELD, M.D., VALASEK, D.W., WILLIAMS, M.R. & WITTER, D.N. (1993) Application of High-Resolution Sequence Stratigraphy to Reservoir Analysis. In: *Subsurface Reservoir Characterization from Outcrop Observations* (Ed. by R. Eschard and B. Doligez), IFP Exploration and Production Research Conferences, **51**, pp. 11-33. Editions Technip, Paris.

CROSS, T.A. & LESSENGER, M.A. (1998) Sediment volume partitioning: rationale for stratigraphic model evaluation and high-resolution stratigraphic correlation. In: *Sequence Stratigraphy - Concepts and Applications* (Ed. by F. M. Gradstein, K. O. Sandvik and N. J.

Milton), *Norwegian Petroleum Society (NPF) Spec. Publ.,* **8**, pp. 171-195. Elsevier, Amsterdam.

FORD, M., WILLIAMS, E.A., ARTONI, A., VERGÉS, J. & HARDY, S. (1997) Progressive evolution of a fault-related fold pair from growth strata geometries, Sant Llorenç de Morunys, SE Pyrenees. *J. Struct. Geol.,* **19**, 413-441.

FRIEND, P.F., LLOYD, M.J., MCELROY, R., TURNER, J., VAN GELDER, A. & VINCENT, S.J. (1996) Evolution of the central part of the northern Ebro basin, as indicated by its Tertiary fluvial sedimentary infill. In: *Tertiary basins of Spain* (Ed. by P. F. Friend and C. J. Dabrio), pp. 166-171. Cambridge Univ. Press, Cambridge.

GAWTHORPE, R.L., FRASER, A.J. & COLLIER, R.E.L.L. (1994) Sequence stratigraphy in active extensional basins: implications for the interpretation of ancient basin-fills. *Mar. Petrol. Geol.,* **11**, 642-658.

GAWTHORPE, R.L., HALL, M., SHARP, I. & DREYER, T. (2000) Tectonically enhanced forced regressions: examples from growth folds in extensional and compressional settings, the Miocene of the Suez rift and the Eocene of the Pyrenees. In: *Sedimentary Responses to Forced Regressions* (Ed. by D. Hunt and R. L. Gawthorpe), *Geol. Soc. London Spec. Publ.,* **172**, pp. 177-191.

GAWTHORPE, R.L. & LEEDER, M.R. (2000) Tectono-sedimentary evolution of active extensional basins. *Basin Res.,* **12,** 195-218.

GAWTHORPE, R.L., SHARP, I., MCMURRAY, L., UNDERHILL, J.R. & GUPTA, S. (1997a) Variability of Systems Tracts, Sequence Boundaries and Flooding Surfaces. In: *Sedimentary Events & Hydrocarbon Systems* (Ed. by B. Beauchamp), pp. 106. CSPG-SEPM, Calgary.

GAWTHORPE, R.L., SHARP, I., UNDERHILL, J.R. & GUPTA, S. (1997b) Linked sequence stratigraphic and structural evolution of propagating normal faults. *Geology,* **25**, 795-798.

GRANJEON, D. (1997) *Modélisation stratigraphique déterministe : conception et applications d'un modèle diffusif 3D multilithologique*. Mémoires Géosciences-Rennes, Géoscience Rennes, France, **78**, 197p.

GUILLOCHEAU, F., (1990) Stratigraphie séquentielle des bassins de plate-forme: l'exemple du Dévonien armoricain. Unpublished thesis, University of Strasbourg, France, 257 p.

GUILLOCHEAU, F. (1991) Modalités d'empilement des séquences génétiques dans un bassin de plate-forme (Dévonien armoricain): nature et distorsion des différents ordres de séquences de dépôts emboitées. *Bull. Centre Rech. Elf Explor. Prod.,* **15**, 383-410.

GUILLOCHEAU, F. (1995) Nature, rank and origin of Phanerozoic sedimentary cycles. *C. R. Acad. Sci. Paris,* **320**, 1141-1157.

GUPTA, S. & COWIE, P. (2000) Processes and controls in the stratigraphic development of extensional basins. *Basin Res.,* **12**, 185-194.

GUPTA, S., COWIE, P.A., DAWERS, N.H. & UNDERHILL, J.R. (1998) A mechanism to explain rift-basin subsidence and stratigraphic patterns through fault-array evolution. *Geology,* **26**, 7, 595-598.

HAQ, B.U., HARDENBOL, J. & VAIL, P.R. (1987) Chronology of fluctuating sea level since the Triassic. *Science,* **235**, 1156-1167.

HARDY, S. & GAWTHORPE, R.L. (1998) Effects of variations in fault slip rate on sequence stratigraphy in fan deltas: Insights from numerical modelling. *Geology,* **26**, 911-914.

HOGAN, P.J. & BURBANK, D.W. (1996) Evolution of the Jaca piggyback basin and emergence of the External Sierras, southern Pyrenees. In: *Tertiary Basins of Spain* (Ed. by P. F. Friend and C. J. Dabrio), pp. 153-160. Cambridge Univ. Press, Cambridge.

HOMEWOOD, P.W., GUILLOCHEAU, F., ESCHARD, R. & CROSS, T. (1992) Corrélations haute résolution et stratigraphie génétique: une démarche intégrée. *Bull. Centre Rech. Elf Explor. Prod.,* **16**, 375-381.

HOMEWOOD, P.W., MAURIAUD, P. & LAFONT, F. (2000) Best practices in Sequence Stratigraphy for explorationists and reservoir engineers. *Bull. Centre Rech. Elf Explor. Prod.*, Mem. **25**, 63p.

JERVEY, M.T. (1988) Quantitative geological modelling of siliciclastic rock sequences and their seismic expression. In: *Sea-Level Changes: An Integrated Approach* (Ed. by C. K. Wilgus, B. S. Hastings, C. G. S. C. Kendall, H. W. Posamentier, C. A. Ross and J. C. Van Wagoner), *Soc. Econ. Palaeont. Miner. Spec. Publ.,* **42**, pp. 47-69.

LAFONT, F. (1994) *Influences relatives de la subsidence et de l'eustatisme sur la localisation et la géométrie des réservoirs d'un système deltaïque. Exemple de l'Eocène du bassin de Jaca (Pyrénées espagnoles)*. Mémoires Géosciences-Rennes, Géosciences-Rennes, France, **54**, 270p.

MCCLAY, K.R. & ELLIS, P.G. (1987) Analogue models of extensional faults geometries. In: *Continental Extensional Tectonics* (Ed. by M. P. Dewey and P. L. Hancock), *Geol. Soc. London Spec. Publ.,* **28**, pp. 109-125.

MEDJADJ, F. (1985) *Une zone de confluence deltaïque en domaine compressif: le delta paléogène de Jaca dans le secteur de Sabiñanigo*. Unpublished PhD Thesis, Université de Pau, France.

MILLÁN, H., AURELL, M. & MELÉNDEZ, A. (1994) Synchronous detachment folds and coeval sedimentation in the Prepyrenean External Sierras (Spain): a case study for a tectonic origin of sequences and systems tracts. *Sedimentology,* **41**, 1001-1024.

MILLÁN, H., PUEYO, E.L., AURELL, M., LUZON, A., OLIVA, B., MARTINEZ, M.B. & POCOVI, A. (2000) Actividad tectonica registrada en los depositos terciarios del frente meridional del Pirineo central. *Rev. Soc. Geol. España,* **13**, 279-300.

MUTO, T. & STEEL, R.J. (1997) Principle of regression and transgression: the nature of the interplay between accommodation and sediment supply. *J. Sedim. Res.,* **67**, 994-1000.

MUTO, T. & STEEL, R.J. (2000) The accommodation concept in sequence stratigraphy: some dimensional problems and possible redefinition. *Sediment. Geol.,* **130**, 1-10.

NISHIKAWA, T. & ITO, M. (2000) Late Pleistocene barrier-island development reconstructed from genetic classification and timing of erosional surfaces, palaeo-Tokyo Bay, Japan. *Sediment. Geol.,* **137**, 25-42.

NOVOA, E., SUPPE, J. & SHAW, J.H. (2000) Inclined-shear Restoration of growth folds. *Am. Ass. Petrol. Geol. Bull.,* **84**, 6**,** 787-804.

NUÑEZ DEL PRADO, H. (1986) *Systèmes de dépôt et évolution sédimentaire des séries de transition marin-continental dans le synclinorium du Rio Guarga*. Unpublished PhD Thesis, Université de Pau, France.

ORI, G.G. & FRIEND, P.F. (1984) Sedimentary basins formed and carried piggyback on active thrust sheets. *Geology,* **12**, 475-478.

POBLET, J. & HARDY, S. (1995) Reverse modelling of detachment folds; application to the Pico del Aguila anticline in the South Central Pyrenees (Spain). *J. Struct. Geol.,* **17**, 12**,** 1707-1724.

POBLET, J., MUÑOZ, J.A., TRAVÉ, A. & SERRA-KIEL, J. (1998) Quantifying the kinematics of detachment folds using three-dimensional geometry: Application to the Mediano anticline (Pyrenees, Spain). *Geol. Soc. Am. Bull.,* **110**, 1**,** 111-125.

POSAMENTIER, H.W. & ALLEN, G.P. (1993a) Variability of the sequence stratigraphic model: effects of local basin factors. *Sediment. Geol.,* **86**, 91-109.

POSAMENTIER, H.W. & ALLEN, G.P. (1993b) Siliciclastic sequence stratigraphic patterns in foreland ramp-type basins. *Geology,* **21**, 455-458.

PUEYO-MORER, E.L MILLÁN-GARRIDO, H. & POCOVÍ JUAN, A. (2002) Rotation velocity of a thrust: a paleomagnetic study in the External Sierras (Southern Pyrenees). *Sediment. Geol.,* **146**, 191-208.

PUIGDEFABREGAS, C. (1975) La sedimentación molásica en la cuenca de Jaca. *Pirineos,* **104**, 1-188.

PUIGDEFÀBREGAS, C. & SOUQUET, P. (1986) Tecto-sedimentary cycles and depositional sequences of the Mesozoic and Tertiary from the Pyrenees. *Tectonophysics,* **129**, 173-203.

REINECK, H. E., & SINGH, I. B. (1980) *Depositional Sedimentary Environments*. Berlin, Springer-Verlag, 549 p.

ROBIN, C. (1997) *Mesure stratigraphique de la déformation : application à l'évolution jurassique du Bassin de Paris*, Mémoires Géosciences-Rennes, Géoscience Rennes, France, **77**, 293p.

ROBIN, C., GUILLOCHEAU, F. & GAULIER, J.M. (1996) Mesure des signaux eustatiques et tectoniques au sein de l'enregistrement sédimentaire d'un bassin intracratonique. Application au Lias du Bassin de Paris. *C. R. Acad. Sci. Paris,* **322**, 1079-1086.

ROBIN, C., GUILLOCHEAU, F. & GAULIER, J.M. (1998) Discriminating between tectonic and eustatic controls on the stratigraphic record in the Paris basin. *Terra Nova,* **10**, 323-329.

SCHLAGER, W. (1993) Accommodation and supply - a dual control on stratigraphic sequences. In: *Basin Analysis and Dynamics of Sedimentary Basin Evolution* (Ed. by S. Cloetingh, W. Sassi, P. Horvath and C. Puigdefabregas), *Sediment. Geol.*, **86**, pp. 111-136.

SCLATER, J.G. & CHRISTIE, P.A.F. (1980) Continental stretching: an explanation of the mid-Cretaceous subsidence of the Central North Sea Basin. *J. Geophys. Res.,* **85**, 3711-3739.

SEGURET, M. (1972) *Etude tectonique des nappes et séries décollées de la partie centrale du versant sud des Pyrénées. Caractère synsédimentaire, rôle de la compression et de la gravité,* Série Géol. Struct., Publ. Univ. Sci. Tech. Languedoc, Montpellier, France, **2**, 155p.

SHANLEY, K.W. & MCCABE, P.J. (1994) Perspectives on the Sequence Stratigraphy of Continental Strata. *Am. Ass. Petrol. Geol. Bull.,* **78**, 4**,** 544-568.

STORTI, F. & POBLET, J. (1997) Growth stratal architectures associated to décollement folds and fault-propagation folds. Inferences on fold kinematics. *Tectonophysics,* **282**, 353-373.

SUPPE, J., CHOU, C.T. & HOOK, S.C. (1992) Rates of folding and faulting determined from growth strata. In: *Thrust Tectonics* (Ed. by K. McClay), pp. 105-121. Chapman & Hall, London.

SZTRÀKOS, K. & CASTELLTORT, S. (2001) La sédimentologie et les foraminifères bartoniens et priaboniens des coupes d'Arguis (Prépyrénées aragonaises, Espagne). Incidence sur la corrélation des biozones à la limite Bartonien/Priabonien. *Rev. Micropaléont.,* **44**, 233-248.

VAN WAGONER, J.C., MITCHUM, R.M., CAMPION, K.M. & RAHMANIAN, V.D. (1990) Siliciclastic sequence stratigraphy in well logs, cores and outcrops: Concepts for high-resolution correlation of time and facies. *AAPG Methods in Exploration*, **7**, 55p.

VAN WAGONER, J.C., POSAMENTIER, H.W., MITCHUM, R.M., VAIL, P.R., SARG, J.F., LOUTIT, T.S. & HARDENBOL, J. (1988) An overview of the fundamentals of sequence stratigraphy and key definitions. In: *Sea-Level Change: An Integrated Approach* (Ed. by C. K. Wilgus, B. S. Hastings, C. G. S. C. Kendall, H. W. Posamentier, C. A. Ross and J. C. Van Wagoner), *Soc. Econ. Palaeont. Miner. Spec. Publ.,* **42**, pp. 39-45.

VERGÈS, J., MARZO, M., SANTAEULÀRIA, T., SERRA-KIEL, J., BURBANK, D.W., MUNOZ, J.A. & GIMÉNEZ-MONTSANT, J. (1998) Quantified vertical motions and tectonic evolution of the SE Pyrenean foreland basin. In: *Cenozoic Foreland Basins of Western Europe* (Ed. by A. Mascle, C. Puigdefàbregas, H. P. Luterbacher and M. Fernàndez), *Geol. Soc. London Spec. Publ.,* **134**, pp. 107-134.

WEI, W., (1995) Revised age calibration points for the geomagnetic polarity time scale. *Geophys. Res. Lett.*, **22**, 957-960.

**Table legend**

**Table 1.** Simplified description and interpretation of the sedimentary facies of the six facies associations found in this study.

**Table 2.** Values of the parameters used for the calculation of accommodation variation, sedimentation and uplift.

**Figures legends**

**Figure 1.** (a) Simplified geological map of the N-S trending anticlines of the western Sierras Marginales at the southern border of the Jaca piggyback basin, south-pyrenean foreland (modified after Seguret, 1972 and Puigdefabregas, 1975). This study focuses on the Pico del Aguila anticline and adjacent synclines (black box). (b) Synthetic stratigraphic column of the southern margin of the Jaca basin (modified after Millàn *et al.,* 1994). The studied series, i.e. Bartonian to early Priabonian sediments coeval with the growth of the Pico del Aguila anticline, are comprised between the top of Guara limestones and the base of Campodarbe conglomerates. (c, d) Cross-sections across the studied area (modified after Puygdefàbregas, 1975). The anticlines of the western Sierras Marginales are from east to west, the Sierra de Guara anticline, the Gabardiella-Lusera anticline, the Pico del Aguila anticline, the Bentué de Rasal anticline, and the Rasal anticline.

**Figure 2.** a) Aerial photograph of the Pico del Aguila anticline. b) Line drawing of the photograph. The fold exposure in a cross-section like attitude is due to its 30° dip towards the north. The Guara limestones (dashed line) form the pre-deformation layer of the anticline. The studied sedimentary series range from the top of the Guara limestones to the Ralla de las Tinas bed. Stratigraphic markers (FSi to S7) refer to time lines determine from the stratigraphic architecture (see Fig. 4). Note the onlaps on both flanks of the anticline and the strong thickness variation between the hinge and the synclines.

**Figure 3.** Schematic depositional model for the studied series. It includes the dominant setting of flood-dominated delta, along with substitutions by the tide- and storm-influenced deltas, and storm carbonated ramp components. Bathymetries and depositional slopes are indicated from foraminifera: (1) Sztràkos & Castelltort, 2001; and bibliographic data: (2) Bhattacharya & Walker, 1992; (3) Coleman & Gagliano, 1964; (4) Coleman & Prior, 1982; (5) Guillocheau, 1990; (6): Millán *et al.*, 1994 and Millán *et al.*, 2000; (7) Reineck & Singh, 1980.

**Figure 4.** Sedimentological sections with the interpretation of stacking pattern of the 3 orders of depositional sequences (genetic units, minor and major cycles).

**Figure 5.** (a) Cross-section of the Pico del Aguila anticline showing the sedimentologic and sequence stratigraphic framework of the syndeformation deposits at the scale of the minor

cycles. (b) Simplified cross-section of the anticline showing the three steps of evolution of the fold growth.

**Figure 6.** Comparison of genetic units between the west flank and the hinge of the anticline (the represented genetic unit is located in the retrogradational sub-cycle of minor cycle 5). Palaeoenvironments abbreviations: LO: Lower Offshore, dUO: distal Upper Offshore, mUO: median Upper Offshore, pUO: proximal Upper Offshore, Sh: Shoreface.

**Figure 7.** Calibration on absolute ages of the time lines. (a) Diagram compiling magnetostratigraphic and biostratigraphic data for section S1. Column 1 shows magnetostratigraphic normal and reverse periods of Hogan and Burbank (1996) measured in western syncline and positioned along our own section. Column 4 is the calibration (by Stràkos and Castelltort, 2001) of our section to biostratigraphic timescale of calcareous nannofossils (NP, Berggren *et al*,. 1995) and column 4 to biostratigraphic timescale of planktonic foraminifera (P, Berggren *et al*,. 1995). Column 2 is the calibration of reverse and normal periods to the MPTS (magnetic polarity time scale) of Cande and Kent (1995) taking into account biostratigraphic data and column 3 without taking into account biostratigraphic data. Stars are data points corresponding to reverse and normal periods (from Hogan and Burbank, 1996) and diamonds are biostratigraphic data points (from Stràkos and Castelltort, 2001). The ages of our time lines are extrapolated assuming a constant accumulation rate between those data points. (b) Simplified diagram showing the calibration of our time lines (circles) to absolute ages using two different MPTS (stars; Cande and Kent, 1995; Wei, 1995) taking into account biostratigraphic data (stars, Stràkos and Castelltort, 2001). (c) Simplied diagram showing the calibration of our time lines (circles) to absolute ages using two different MPTS (stars; Cande and Kent, 1995; Wei, 1995) without taking into account biostratigraphic data.

**Figure 8.** Method used to measure accommodation variations and uplift (differential subsidence) of the hinge of the anticline (location B) with respect to the adjacent syncline (location A).

**Figure 9.** Accommodation variation and sediment accumulation rates calculated for sections S1, S3, S5 and S6 at the scale of minor cycles (left column) and major cycle (right column). The accommodation variation rates (thin line) and sediment accumulation rates (grey surface)

are calculated between two time lines. The value is then affected to the top of the corresponding time interval. Bold lines represent error bars on accommodation due to palaeobathymetry uncertainties. Note that the last interval of the major cycle is calculated between FS5 and S7 (instead of MFS7).

**Figure 10.** Uplift of the anticline hinge measured with respect to the Arguis syncline (S1-S3) and the Belsué syncline (S5-S1 and S6-S1).

**Figure 11.** Influence of the 4 dating models upon the calculated rates of accommodation variation. (a) Calculations with biostratigraphic constraints and the magnetic time scale of Cande and Kent (1995). (b) Calculations with biostratigraphic constraints and the magnetic time scale of Wei (1995). (c) Calculations with the magnetic time scale of Cande and Kent (1995) and without biostratigraphic constraints and. (d) Calculations with the magnetic time scale of Wei (1995) and without biostratigraphic constraints.

**Figure 12.** Model for the distortion of the genetic units due to the superimposition of a regional relative-sea-level variation and a continuous fold growth. Example of a genetic unit of the retrogradational sub-cycle of minor cycle 5. See text for explanations.

**Figure 13.** Model for the distortion of the minor cycles by the superimposition of a regional relative-sea-level variation and a continuous fold growth. See text for explanations.

**Figure 14.** Theoretical model for the distortion of the time of occurrence of the inversion between progradation and retrogradation trend at the scale of the minor cycles by the superimposition of a constant sediment supply, a regional relative-sea-level variation and a different subsidence rate according to the considered location. See text for explanations.

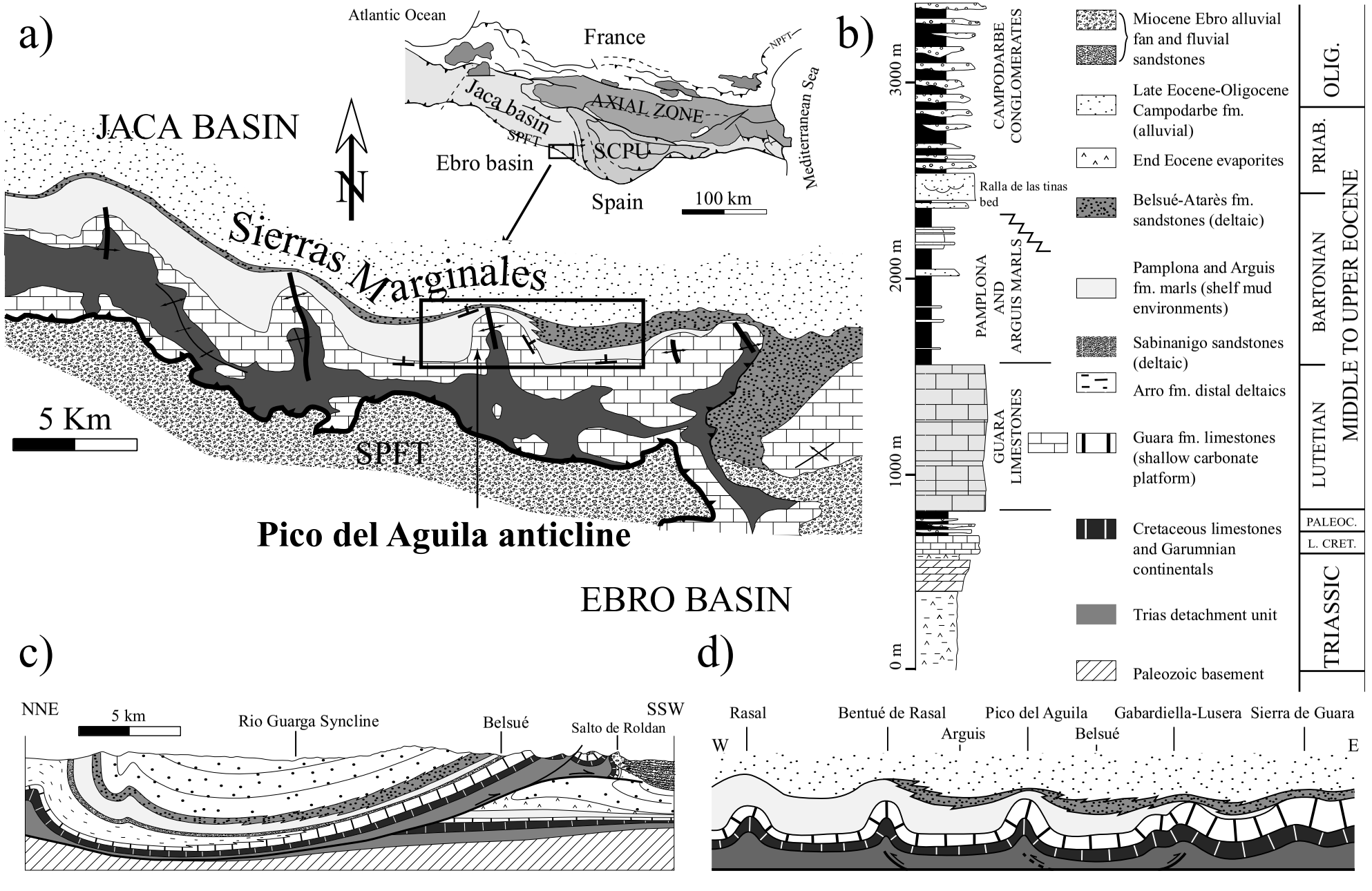
a)
Atlantic Ocean
France
NPFT
Jaca basin
SPFT
AXIAL ZONE
SCPU
Ebro basin
Spain
100 km
Mediterranean Sea
JACA BASIN
N
Sierras Marginales
5 Km
SPFT
Pico del Aguila anticline
EBRO BASIN
b)
3000 m
2000 m
1000 m
0 m
CAMPODARBE CONGLOMERATES
Ralla de las tinas bed
PAMPLONA AND ARGUIS MARLS
GUARA LIMESTONES
Miocene Ebro alluvial fan and fluvial sandstones
Late Eocene-Oligocene Campodarbe fm. (alluvial)
End Eocene evaporites
Belsué-Atarès fm. sandstones (deltaic)
Pamplona and Arguis fm. marls (shelf mud environments)
Sabinanigo sandstones (deltaic)
Arro fm. distal deltaics
Guara fm. limestones (shallow carbonate platform)
Cretaceous limestones and Garumnian continentals
Trias detachment unit
Paleozoic basement
OLIG.
PRIAB.
BARTONIAN
LUTETIAN
MIDDLE TO UPPER EOCENE
PALEOC.
L. CRET.
TRIASSIC
c)
NNE
5 km
Rio Guarga Syncline
Belsué
Salto de Roldan
SSW
d)
Rasal
Bentué de Rasal
Pico del Aguila
Gabardiella-Lusera
Sierra de Guara
Arguis
Belsué
W
E

Figure 1

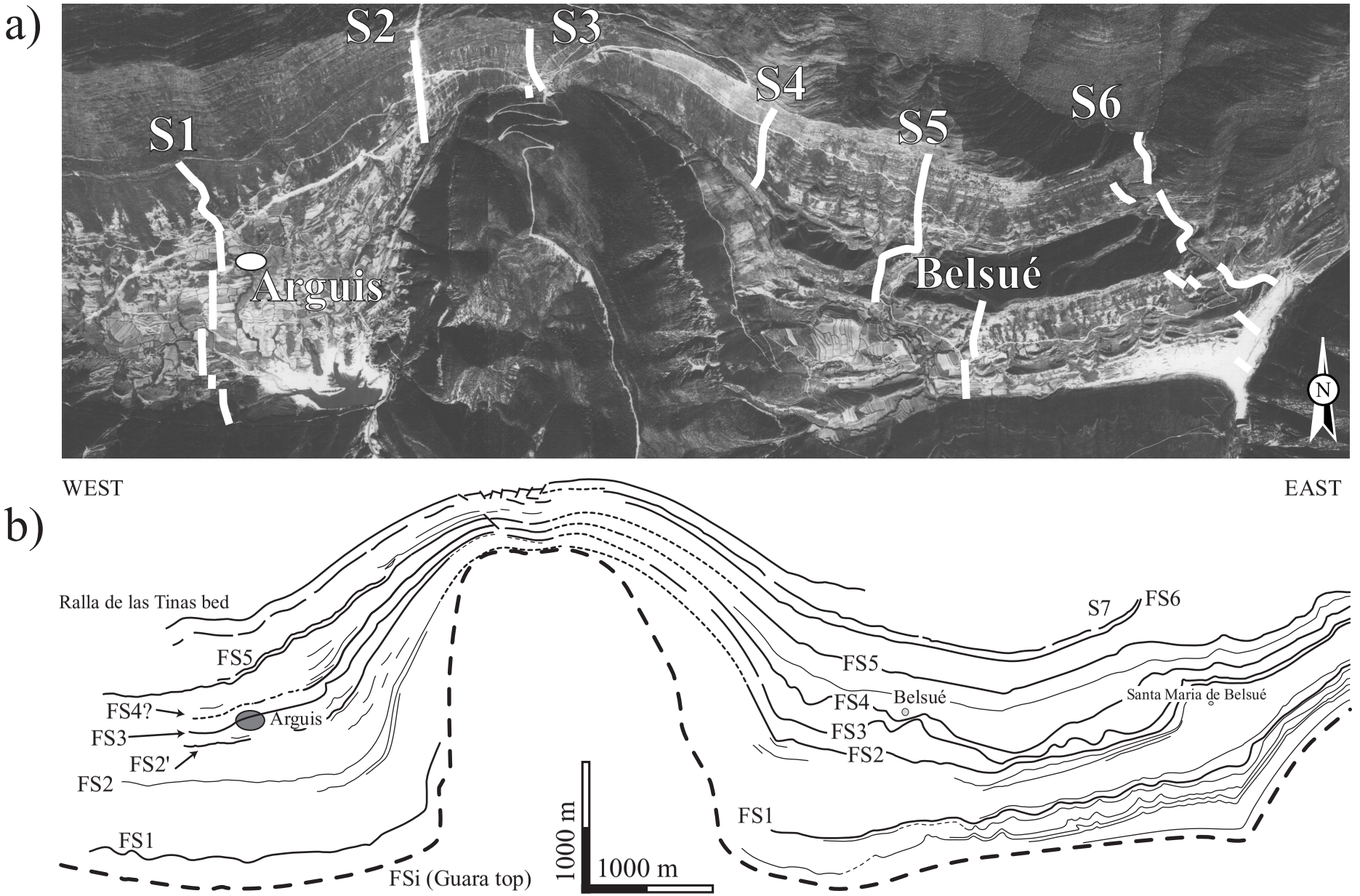
a)
S1
S2
S3
S4
S5
S6
Arguis
Belsué
N
WEST
EAST
b)
Ralla de las Tinas bed
FS5
FS4?
FS3
FS2'
FS2
FS1
Arguis
FSi (Guara top)
1000 m
1000 m
S7
FS6
FS5
FS4
FS3
FS2
FS1
Belsué
Santa Maria de Belsué

Figure 2

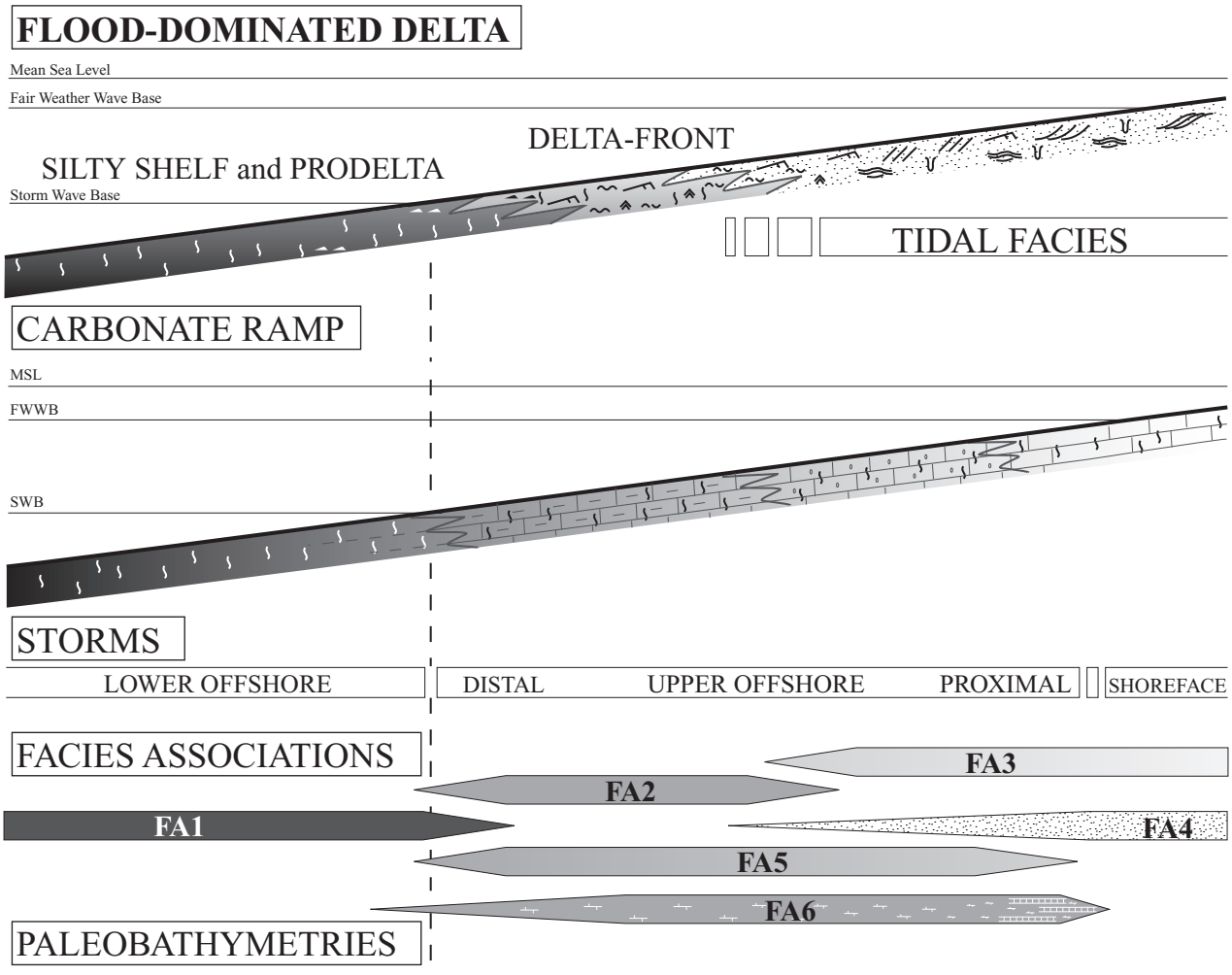


| | | | | | |
|---|---|---|---|---|---|
| (1) | -150 m | ~ -100 m / 60 m | -30 / -80 m | 0 / -50 m | |
| (2) | | ~ -60 m | 0.1°/ 1° | ~ -15 m | |
| (3) | | | -70 m | -10 / -50 ± 20 m | 0 / -10 m |
| (4) | | | 1° | ~ 0.5° | |
| (5) | | ~ -90 / -100 m | ~ -80 m | ~ -40 m | |
| (6) | | | 5° | | |
| (7) | | | | -20 m | |

sigmoidal cross-stratifications
3D cross-stratifications
2D cross-stratifications
small-scale current ripples
HCS
small-scale symetric wave ripples

flaser bedding
wavy bedding
lenticular bedding
ophiomorpha burrows
undifferentiated bioturbations

sand
sand/silt
silt/mud
grainstone to packstone
packstone to wackstone
wackstone to mudstone

**Figure 3**

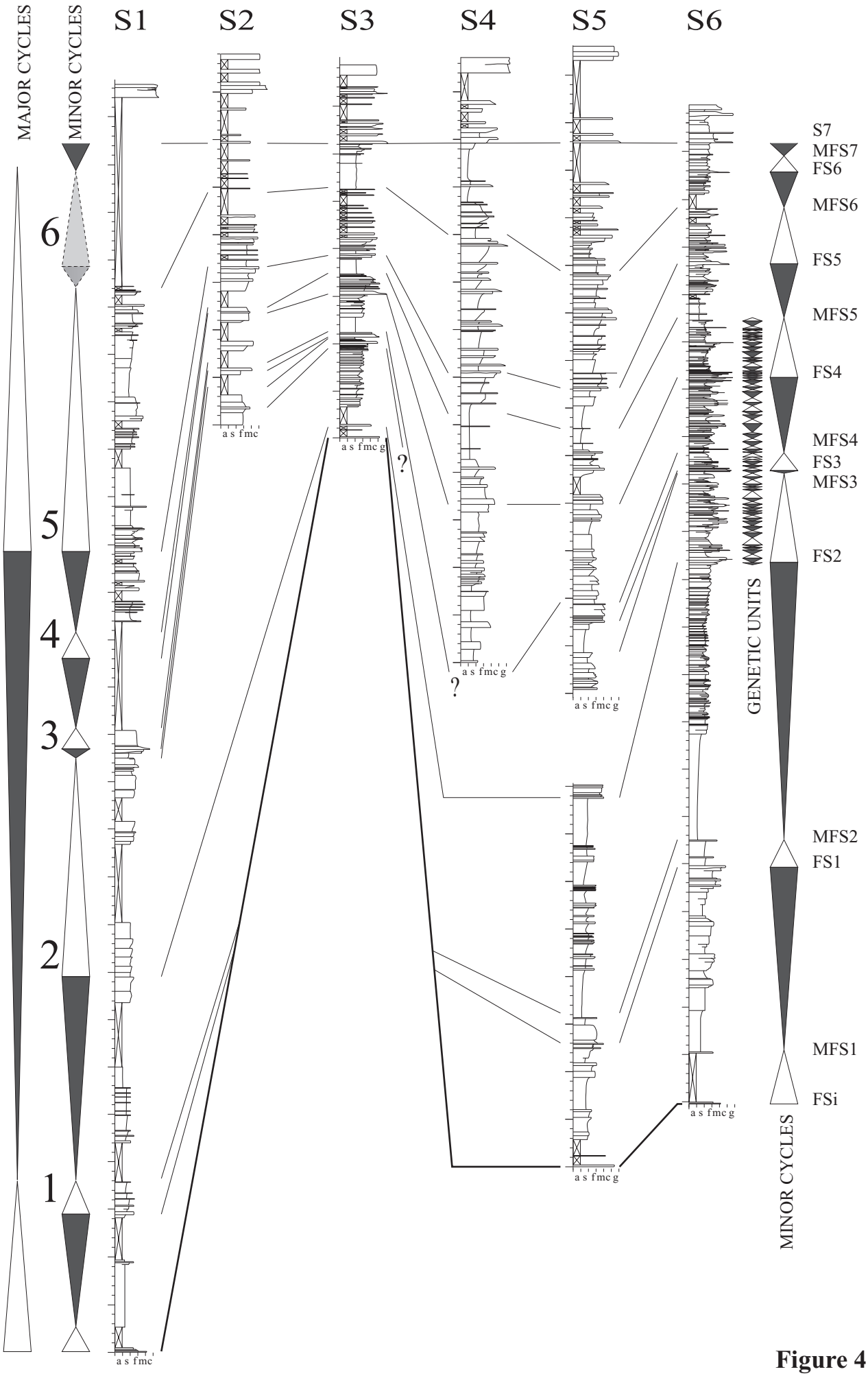
MAJOR CYCLES
MINOR CYCLES
S1
S2
S3
S4
S5
S6
6
5
4
3
2
1
a s fmc
a s fmc g
?
?
S7
MFS7
FS6
MFS6
FS5
MFS5
FS4
MFS4
FS3
MFS3
FS2
MFS2
FS1
MFS1
FSi
GENETIC UNITS
MINOR CYCLES

**Figure 4**

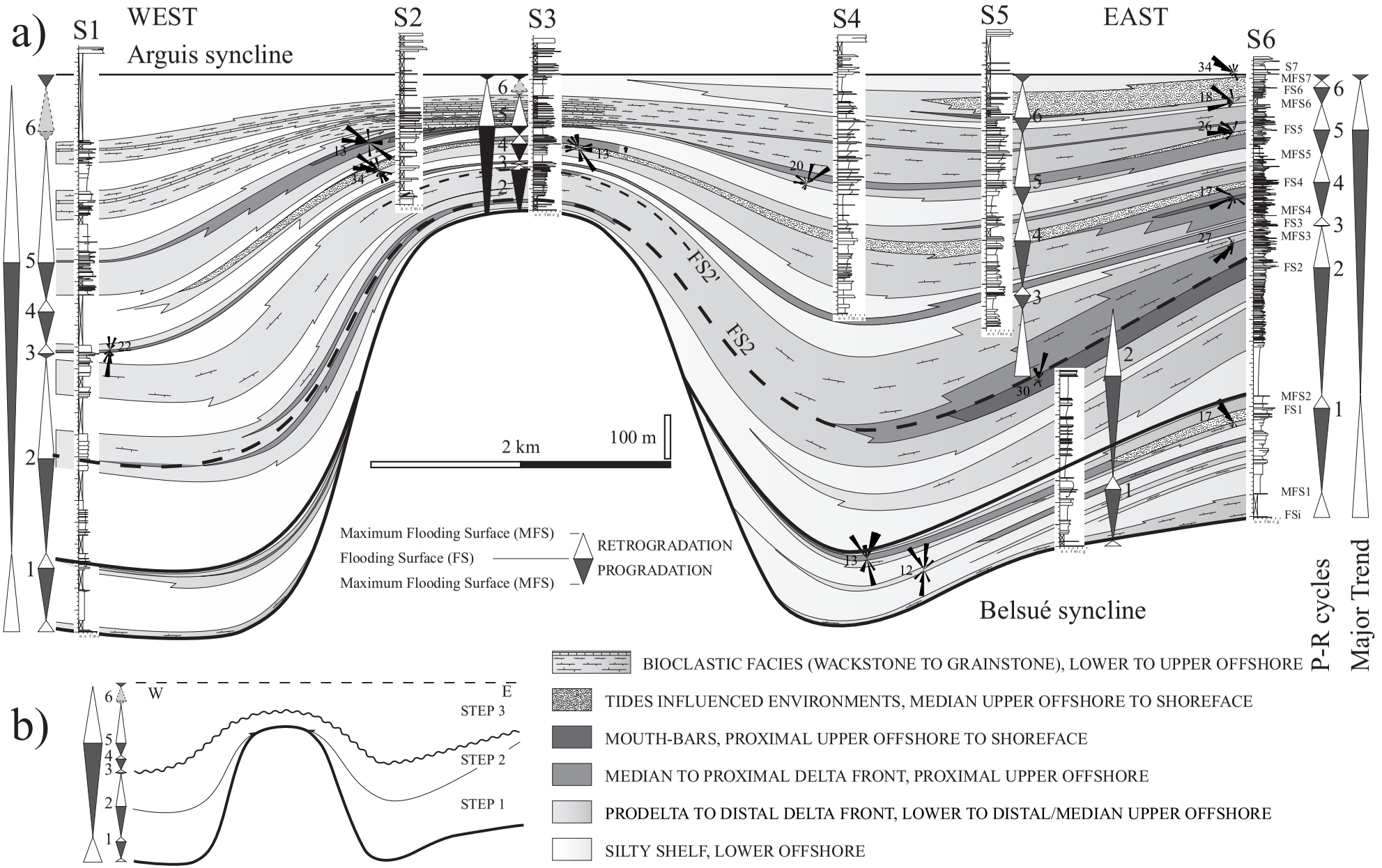
a)
WEST
Arguis syncline
S1
S2
S3
S4
S5
EAST
S6
FS2'
FS2
2 km
100 m
Maximum Flooding Surface (MFS)
Flooding Surface (FS)
Maximum Flooding Surface (MFS)
RETROGRADATION
PROGRADATION
Belsué syncline
S7
MFS7
FS6
MFS6
FS5
MFS5
FS4
MFS4
FS3
MFS3
FS2
MFS2
FS1
MFS1
FSi
P-R cycles
Major Trend
b)
W
E
STEP 3
STEP 2
STEP 1
BIOCLASTIC FACIES (WACKSTONE TO GRAINSTONE), LOWER TO UPPER OFFSHORE
TIDES INFLUENCED ENVIRONMENTS, MEDIAN UPPER OFFSHORE TO SHOREFACE
MOUTH-BARS, PROXIMAL UPPER OFFSHORE TO SHOREFACE
MEDIAN TO PROXIMAL DELTA FRONT, PROXIMAL UPPER OFFSHORE
PRODELTA TO DISTAL DELTA FRONT, LOWER TO DISTAL/MEDIAN UPPER OFFSHORE
SILTY SHELF, LOWER OFFSHORE

Figure 5

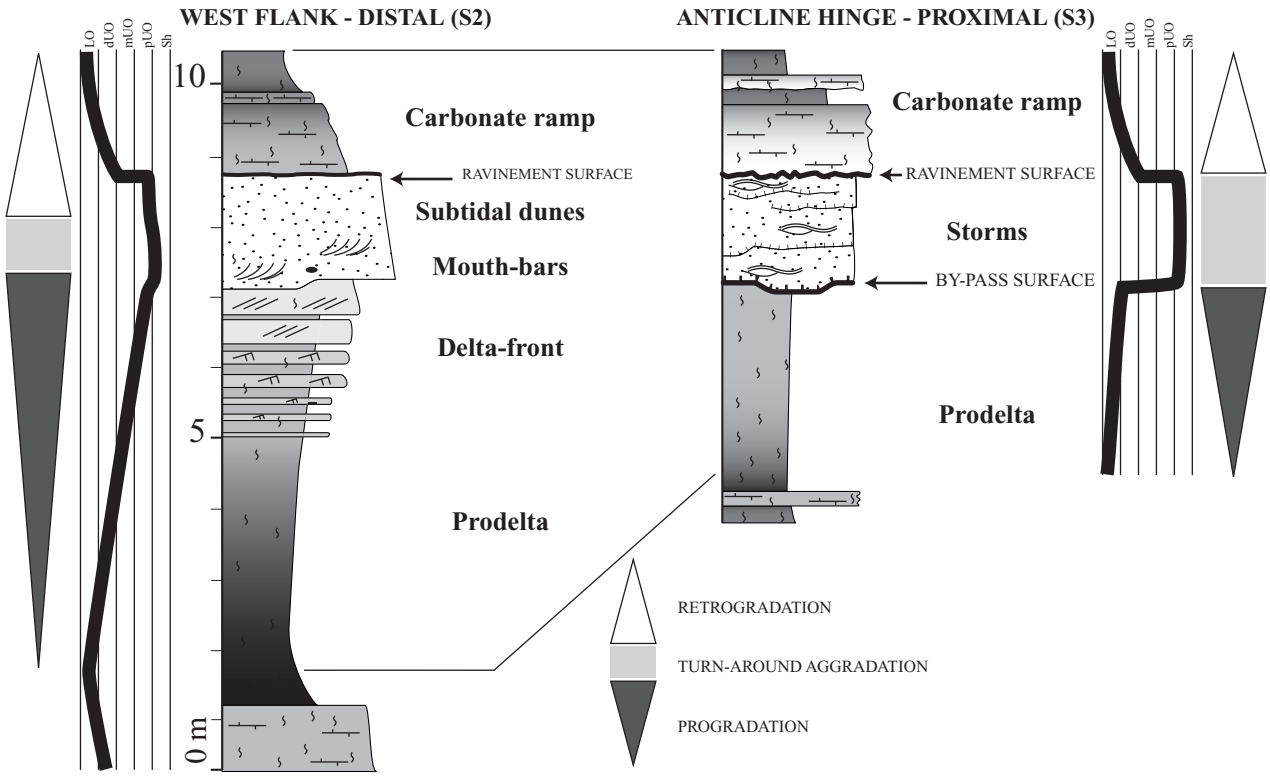
WEST FLANK - DISTAL (S2)
ANTICLINE HINGE - PROXIMAL (S3)
LO
dUO
mUO
pUO
Sh
10
5
0 m
Carbonate ramp
RAVINEMENT SURFACE
Subtidal dunes
Mouth-bars
Delta-front
Prodelta
Carbonate ramp
RAVINEMENT SURFACE
Storms
BY-PASS SURFACE
Prodelta
RETROGRADATION
TURN-AROUND AGGRADATION
PROGRADATION

**Figure 6**

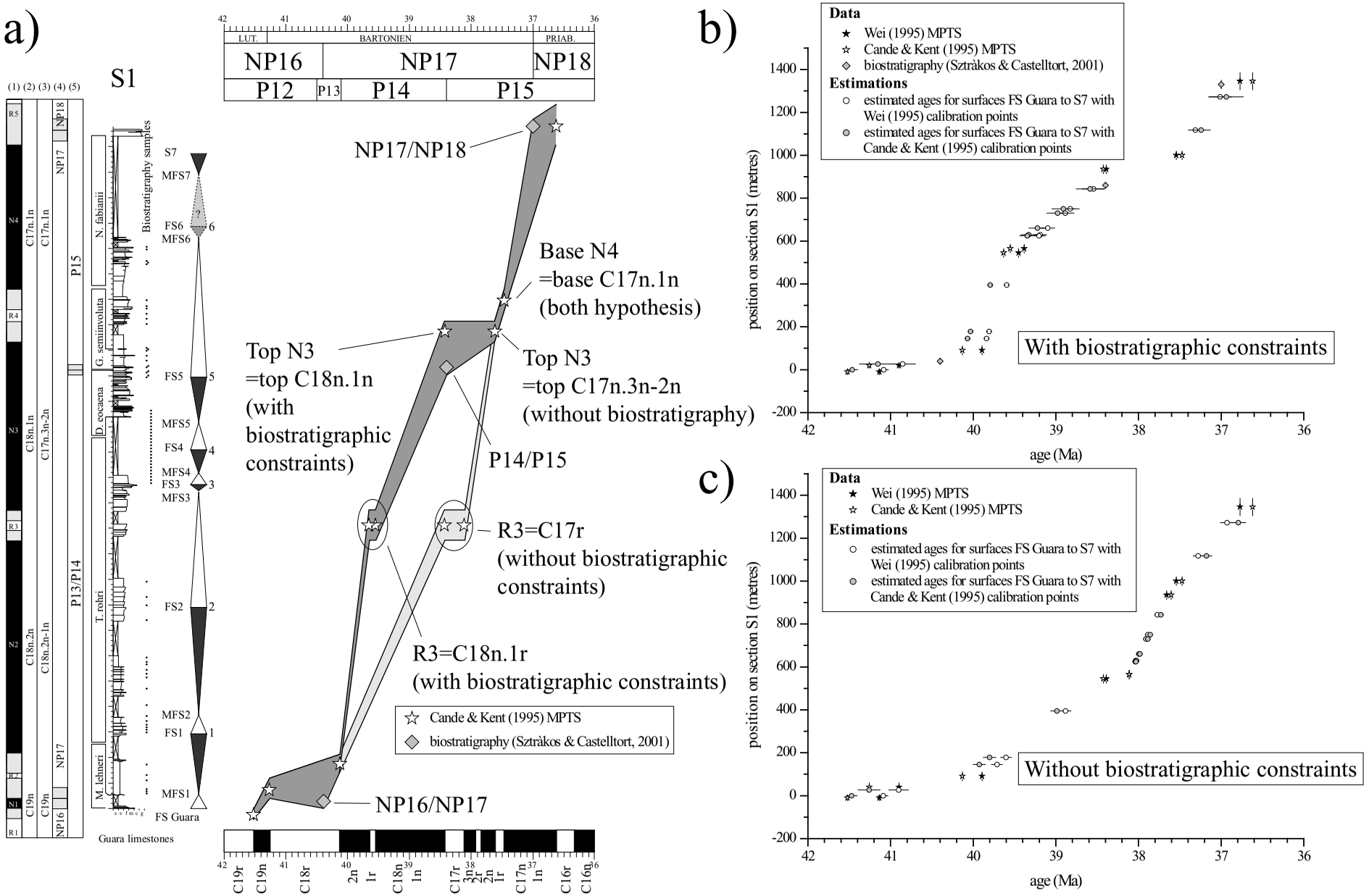
a)
S1
LUT.
BARTONIEN
PRIAB.
NP16
NP17
NP18
P12
P13
P14
P15
(1) (2) (3) (4) (5)
R5
N4
R4
N3
R3
N2
R2
N1
R1
C19n
C18n.2n
C18n.1n
C17n.3n-2n
C18n.2n-1n
C17n.1n
P15
P13/P14
N. fabiani
G. seminvoluta
D. eocaena
T. rohri
M. lehneri
Biostratigraphy samples
S7
MFS7
FS6
MFS6
FS5
MFS5
FS4
MFS4
FS3
MFS3
FS2
MFS2
FS1
MFS1
FS Guara
Guara limestones
NP17/NP18
Base N4
=base C17n.1n
(both hypothesis)
Top N3
=top C18n.1n
(with
biostratigraphic
constraints)
Top N3
=top C17n.3n-2n
(without biostratigraphy)
P14/P15
R3=C17r
(without biostratigraphic
constraints)
R3=C18n.1r
(with biostratigraphic constraints)
NP16/NP17
Cande & Kent (1995) MPTS
biostratigraphy (Sztràkos & Castelltort, 2001)
C19r
C19n
C18r
C18n
C17r
C17n
C16r
C16n
b)
Data
Wei (1995) MPTS
Cande & Kent (1995) MPTS
biostratigraphy (Sztràkos & Castelltort, 2001)
Estimations
estimated ages for surfaces FS Guara to S7 with Wei (1995) calibration points
estimated ages for surfaces FS Guara to S7 with Cande & Kent (1995) calibration points
With biostratigraphic constraints
position on section S1 (metres)
age (Ma)
c)
Data
Wei (1995) MPTS
Cande & Kent (1995) MPTS
Estimations
estimated ages for surfaces FS Guara to S7 with Wei (1995) calibration points
estimated ages for surfaces FS Guara to S7 with Cande & Kent (1995) calibration points
Without biostratigraphic constraints
position on section S1 (metres)
age (Ma)

**Figure 7**

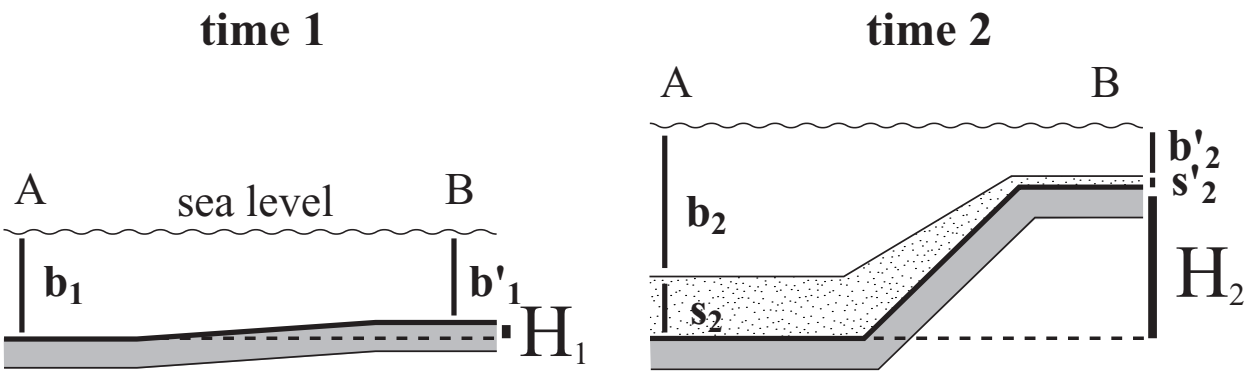


Location A: syncline

Location B: hinge of the anticline

b: bathymetry in the syncline at time t

b': bathymetry on the hinge of the anticline at time t

H: uplift of the hinge of the anticline with respect to the syncline floor at time t

s: deposited sedimentary thickness in the syncline between $t_1$ and $t_2$

s': deposited sedimentary thickness on the hinge of the anticline between $t_1$ and $t_2$

D(A): accommodation variation between $t_1$ and $t_2$ in the syncline

D(B): accommodation variation between $t_1$ and $t_2$ on the hinge of the anticline

dH: uplift variation (of the hinge of the anticline with respect to the syncline) between $t_1$ and $t_2$

$D(A) = s_2+(b_2-b_1)$ = space created between $t_1$ and $t_2$ in the syncline (1)

$D(B) = s'_2+(b'_2-b'_1)$ = space created between $t_1$ and $t_2$ on the hinge of the anticline (2)

at time 1: $b_1 = H_1+b'_1$ (3)

at time 2: $b_2+s_2 = H_2+b'_2+s'_2$ (4)

$\Rightarrow D(A) = (H_2+b'_2+s'_2) - (H_1+b'_1) = (H_2-H_1) + s'_2 + (b'_2-b'_1) = dH + D(B)$ (5)

$$\boxed{\Rightarrow dH = D(A)-D(B)}$$

**Figure 8**

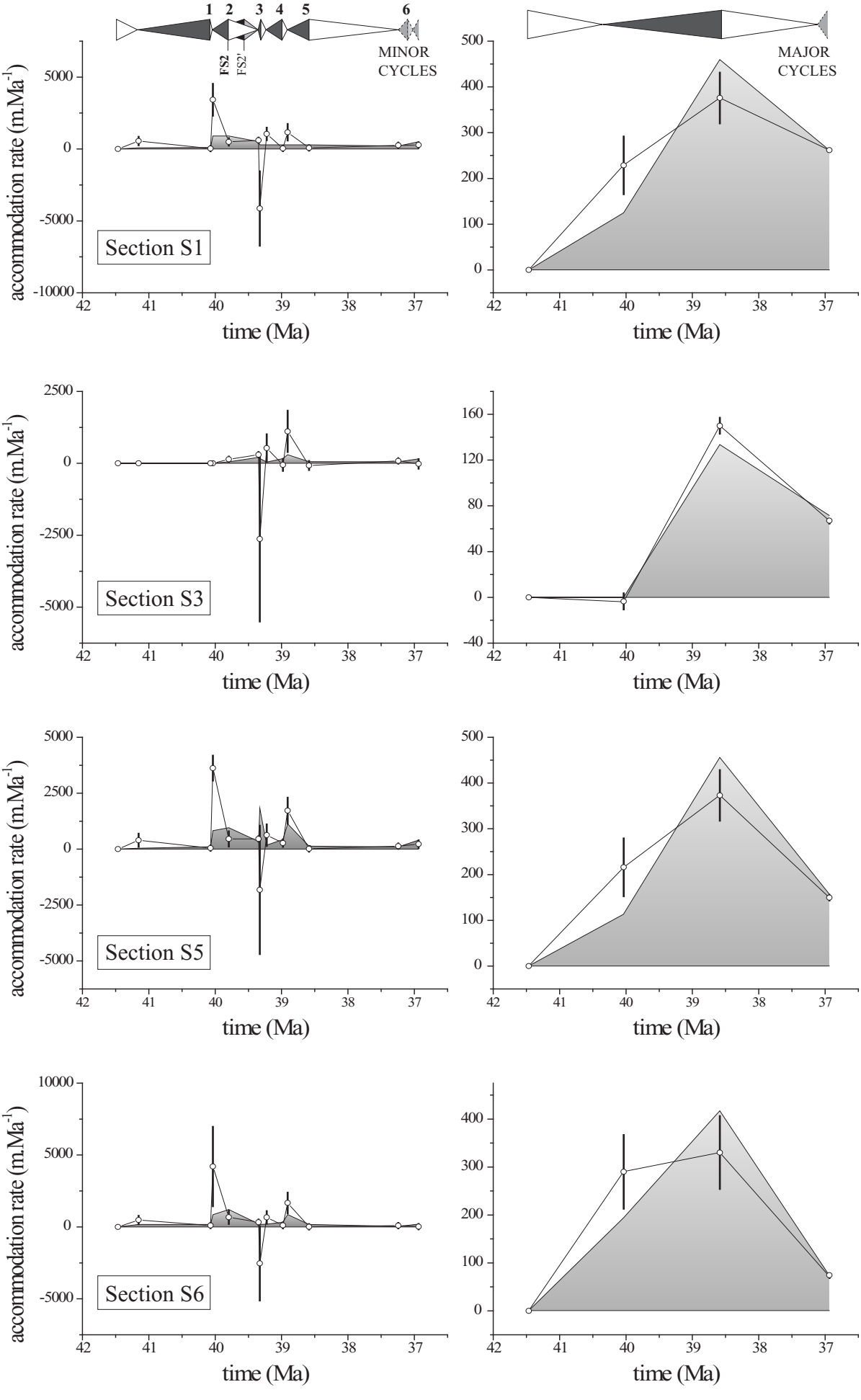
1
2
3
4
5
6
FS2
FS2'
MINOR CYCLES
MAJOR CYCLES
Section S1
Section S3
Section S5
Section S6
accommodation rate (m.Ma-1)
time (Ma)

**Figure 9**

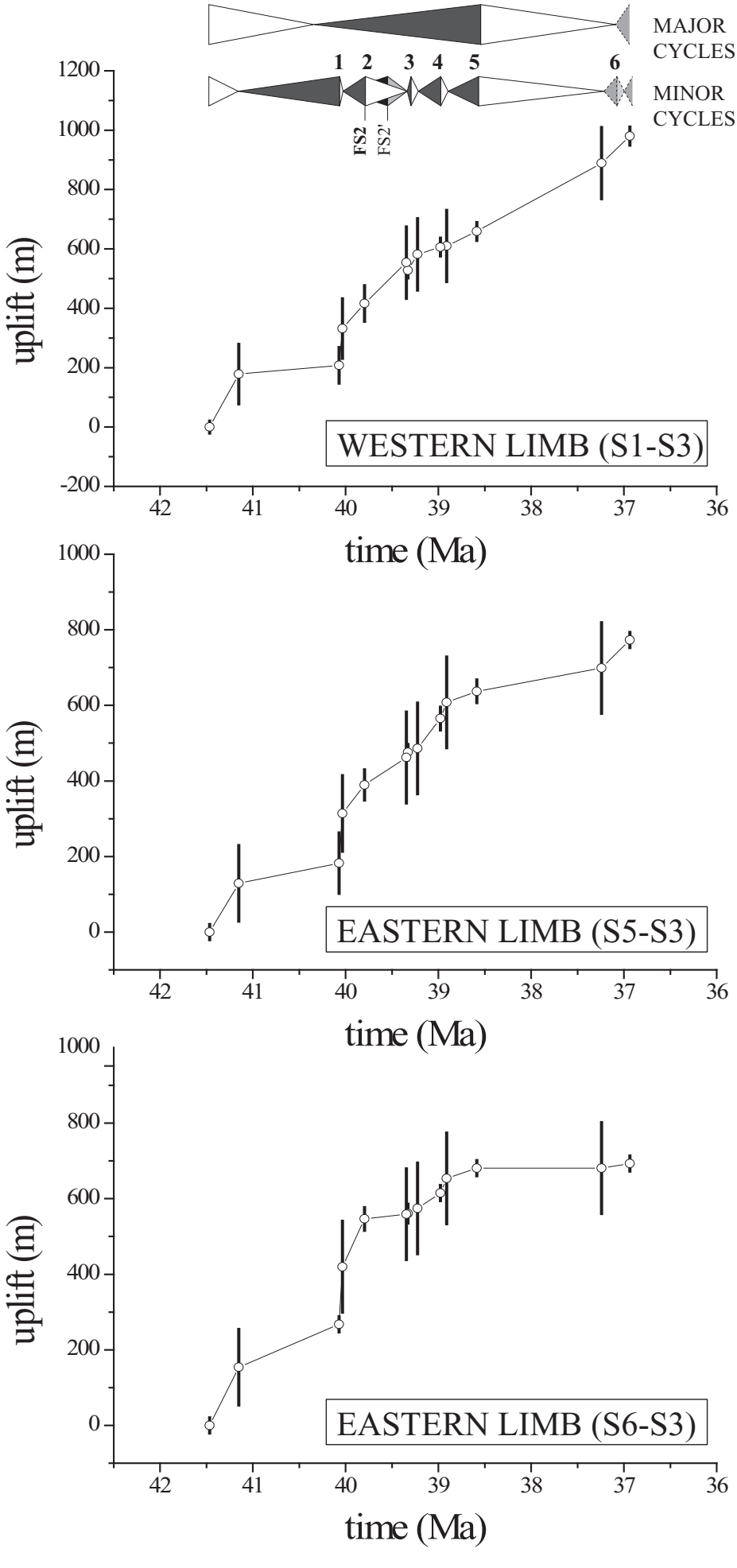
MAJOR CYCLES
1 2 3 4 5 6
MINOR CYCLES
FS2
FS2'
uplift (m)
1200
1000
800
600
400
200
0
-200
42 41 40 39 38 37 36
time (Ma)
WESTERN LIMB (S1-S3)
uplift (m)
1000
800
600
400
200
0
42 41 40 39 38 37 36
time (Ma)
EASTERN LIMB (S5-S3)
uplift (m)
1000
800
600
400
200
0
42 41 40 39 38 37 36
time (Ma)
EASTERN LIMB (S6-S3)

**Figure 10**

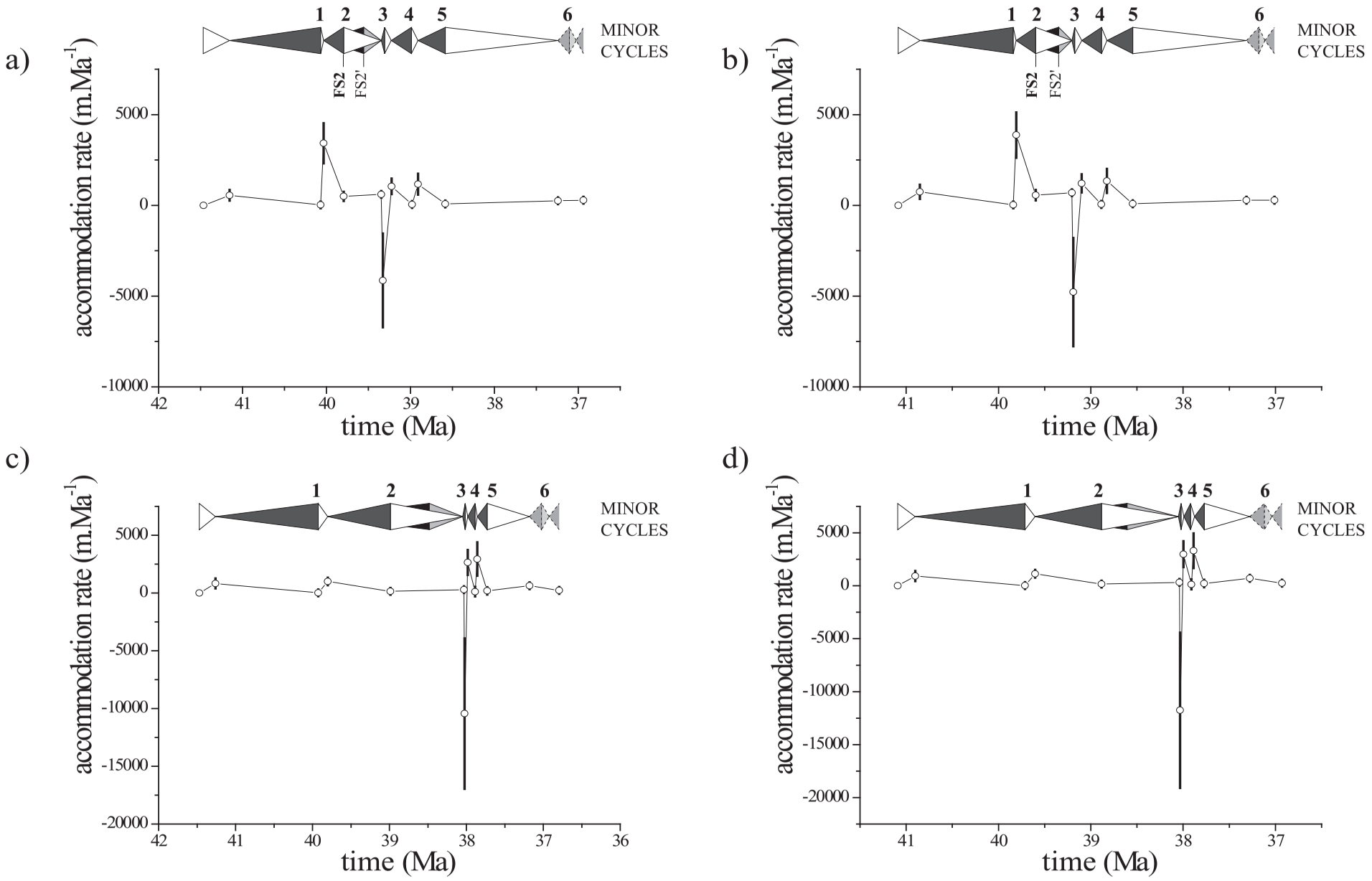
a)
b)
c)
d)
1
2
3
4
5
6
MINOR CYCLES
FS2
FS2'
accommodation rate (m.Ma-1)
time (Ma)

Figure 11

1. EARLY PROGRADATION


2. MAXIMUM PROGRADATION

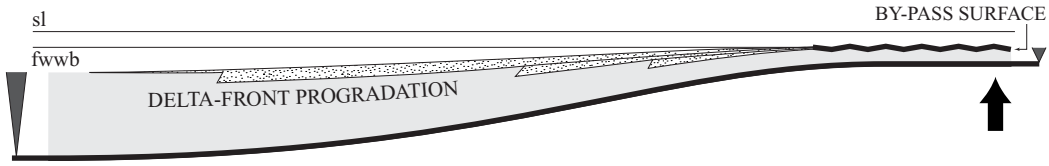


3. END PROGRADATION / EARLY RETROGRADATION

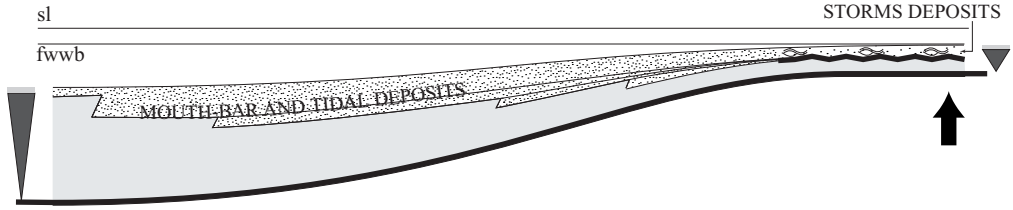


4. RETROGRADATION

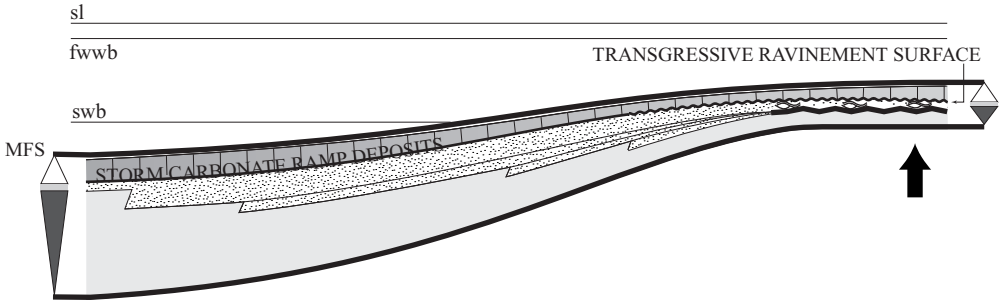


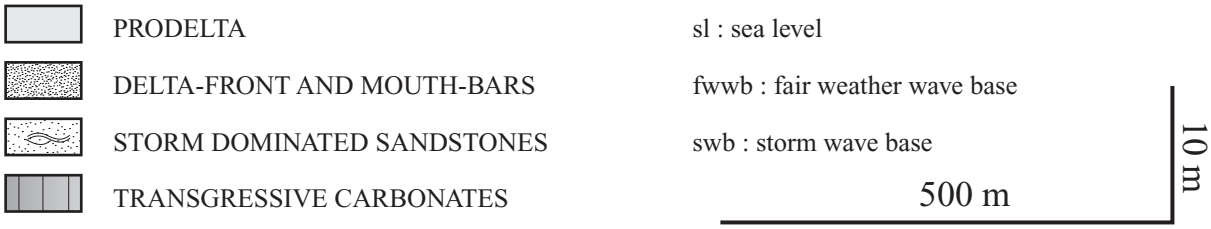


**Figure 12**

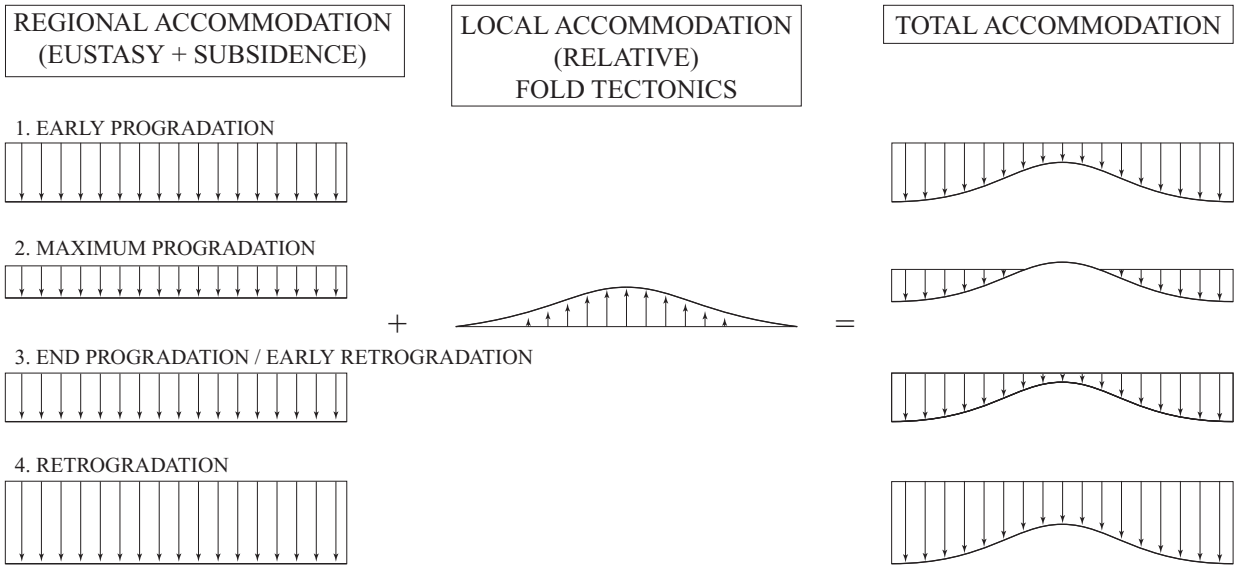
REGIONAL ACCOMMODATION
(EUSTASY + SUBSIDENCE)
LOCAL ACCOMMODATION
(RELATIVE)
FOLD TECTONICS
TOTAL ACCOMMODATION
1. EARLY PROGRADATION
2. MAXIMUM PROGRADATION
+
=
3. END PROGRADATION / EARLY RETROGRADATION
4. RETROGRADATION

**Figure 13**

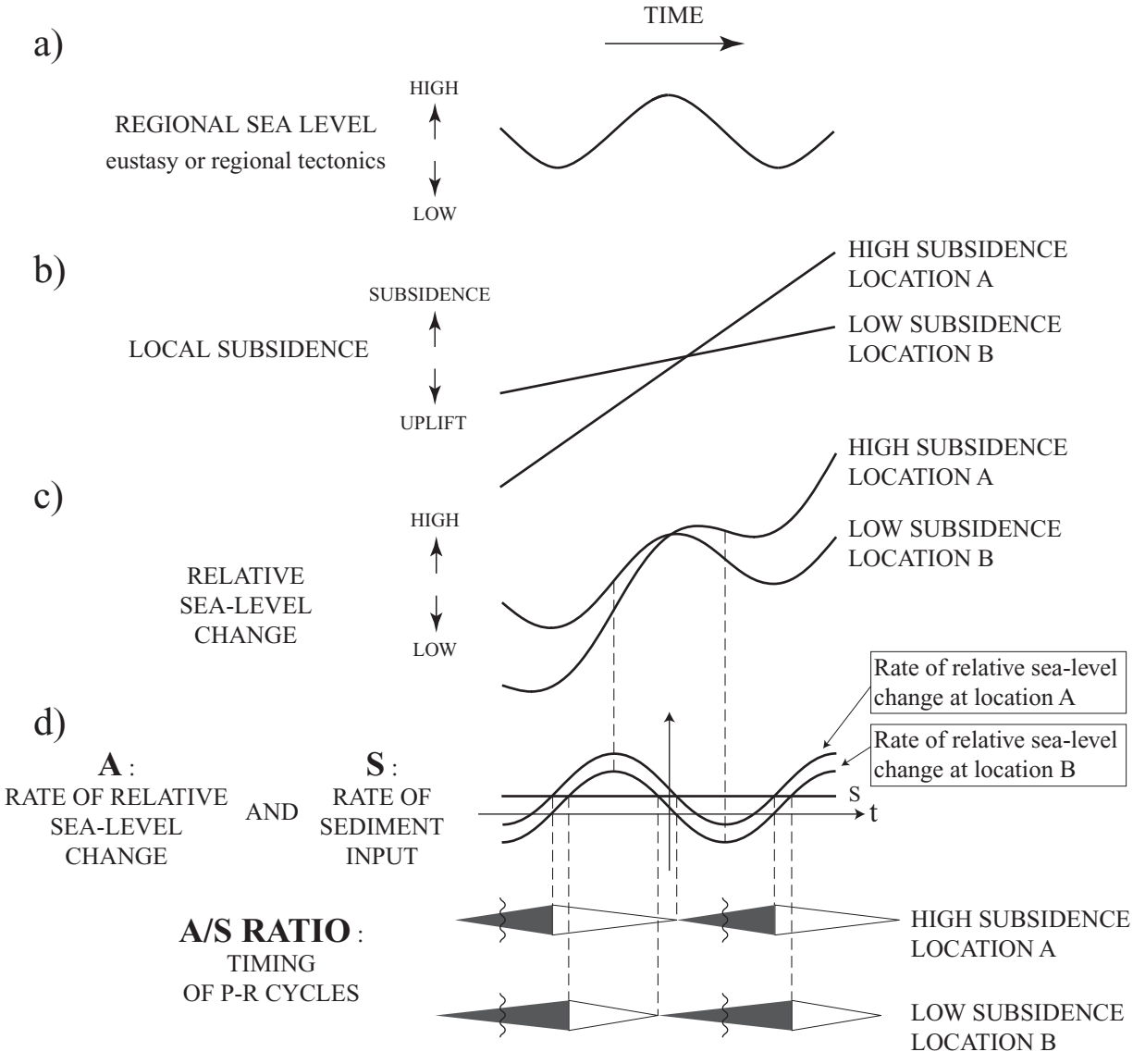
a)
TIME
HIGH
REGIONAL SEA LEVEL
eustasy or regional tectonics
LOW
b)
HIGH SUBSIDENCE
LOCATION A
SUBSIDENCE
LOCAL SUBSIDENCE
LOW SUBSIDENCE
LOCATION B
UPLIFT
c)
HIGH SUBSIDENCE
LOCATION A
HIGH
LOW SUBSIDENCE
LOCATION B
RELATIVE
SEA-LEVEL
CHANGE
LOW
Rate of relative sea-level
change at location A
Rate of relative sea-level
change at location B
d)
A :
RATE OF RELATIVE
SEA-LEVEL
CHANGE
AND
S :
RATE OF
SEDIMENT
INPUT
S
t
A/S RATIO :
TIMING
OF P-R CYCLES
HIGH SUBSIDENCE
LOCATION A
LOW SUBSIDENCE
LOCATION B

**Figure 14**

| Facies code | Lithology and Content | Structures | Bioturbation | Interpretation |
|---|---|---|---|---|
| **Blue Marls and Silts facies association, FA1** | | | | |
| 1 | Bioturbated silty blue marls, sparsely fossiliferous (foraminifera, echinids, lamellibranchs, bryozoans). Wood debris, pyrite and glauconite grains | Rare small scale current ripples | planolites, thalassinoides, teichichnus Ichnofacies: Cruziana | lower offshore silty shelf |
| 1' | Bioturbated marly siltstones to very fine sandstones, sparsely fossiliferous (idem 1). Wood debris, pyrite and glauconite grains | | | lower to distal upper offshore silty shelf |
| **Siltstones to Fine Sandstones facies association, FA2** | | | | |
| 2s | Barren to sparsely fossiliferous (idem 1), bioturbated very fine sandstones and siltstones. Wood debris, pyrite and glauconite grains | Lenticular to wavy bedding, small scale current (dominant) and wave (rare) ripples. | | upper offshore prodelta |
| 2f | Barren to sparsely fossiliferous (idem 1), bioturbated very fine to fine sandstones. Wood debris, pyrite and glauconite grains | Wavy to flaser bedding, small scale current (dominant) and wave (rare) ripples, some larger-scale 2D cross-stratifications in the coarsest beds | planolites, thalassinoides, teichichnus, and diplocraterion | upper offshore prodelta/distal delta-front |
| 2Bs | Sparsely to moderately fossiliferous (idem 1), completely bioturbated very fine sandstones and siltstones. Wood debris, pyrite and glauconite grains | | Ichnofacies: Cruziana to Skolithos | upper offshore prodelta |
| 2Bf | Sparsely to moderately fossiliferous, completely bioturbated, very fine to fine sandstones. Wood debris, pyrite and glauconite grains | No observable sedimentary structures due to the intense bioturbation | | upper offshore prodelta/distal delta-front |
| 2Bg | Sparsely to moderately fossiliferous, completely bioturbated, glauconious siltstones to fine sandstones. Wood debris, pyrite and glauconite grains | | | upper offshore prodelta/distal delta-front |
| 2Bc | Foraminifera, lamellibranchs, bryozoans and echinids, within completely bioturbated massive siltstones to medium sandstones; matrix (sand) dominated | | | upper offshore distal to median delta-front |
| **Cross-stratified Sandstones facies association, FA3** | | | | |
| 3Bm | Sparsely fossiliferous (idem 1), bioturbated, fine to medium sandstones. Wood debris | small-scale current ripples and 2D larger-scale cross-stratifications | | upper offshore distal/median delta-front |
| 3m | Barren to sparsely fossiliferous (idem 1), slightly bioturbated, fine to medium sandstones. Wood debris | small-scale current ripples, 2D and 3D larger-scale (up to meter-scale) cross-stratifications occurence of some wave ripples and HCS | thalassinoides and planolites in 3Bm and 3m, with increasing occurence of skolithos, diplocraterion, and ophiomorpha with increasing grain size. Only ophiomorpha in the coarsest facies. | upper offshore distal/median delta-front |
| 3c | Barren to sparsely fossiliferous (dominated by rare lamellibranchs), slightly bioturbated, medium to coarse sandstones. Wood debris | | | upper offshore median/proximal delta-front |
| 3g | Barren to sparsely fossiliferous (idem 3c), slightly bioturbated, medium to gravel sandstones. Wood debris | | | upper offshore to lower shoreface / proximal delta-front to mouth-bars |
| 3bp | Bioclastic, very poorly sorted, slightly bioturbated, fine to gravel sandstones, with numerous wood debris and mud clasts | small-scale current ripples and large-scale 2D and 3D cross-stratifications Numerous erosive features at bed boundaries and intra-beds (amalgamation surfaces) | | upper offshore to lower shoreface / bypass in delta-front environment |
| **Mud-draped Sigmoidal Cross-stratified Sandstones facies association, FA4** | | | | |
| 4fm | Bioturbated very fine to medium sandstones | Small-scale current ripples and 2D sigmoids, wavy to flaser bedding. | Thalassinoides and planolites | upper offshore distal/median delta front |
| 4g | Slightly bioturbated, medium to gravel sandstones with mud clasts and oysters debris | Up to metre scale, bidirectionnal mud-draped sigmoidal cross-stratifications. Normal grading. | Limited to sparse ophiomorpha burrows | upper offshore to lower shoreface subtidal dunes |
| **Well-sorted Siltstones to Medium Sandstones facies association, FA5** | | | | |
| 5f | Barren to sparsely fossiliferous, slightly bioturbated well-sorted siltstones to very fine sandstones | Low regime planar, and small-scale wave ripples. Good lateral continuity of beds. Sometimes observed normal grading. | Mostly small planolites and thalassinoides | distal upper offshore |
| 5m | Barren to sparsely fossiliferous, slightly bioturbated, well-sorted fine to medium sandstones | Small-scale wave ripples, and HCS. Amalgamation surfaces and erosive bases with gutter-casts and furrows. | | median upper offshore |
| 5dm | Barren to sparsely fossiliferous, slightly bioturbated, well-sorted fine to medium sandstones | Mainly HCS. Laterally discontinuous beds. Sometimes observed normal grading. | | proximal upper offshore |
| **Bioclastics facies association, FA6** | | | | |
| 6w | Foraminifera, lamellibranchs, bryozoans and echinids, within siltstones to very fine sandstones; completely bioturbated mudstones to wackestones; shell dominated | No sedimentary structures. Sometimes normal grading. | Intense bioturbation mainly due to thalassinoides | upper offshore distal ramp |
| 6p | Foraminifera, lamellibranchs, bryozoans and echinids, within siltstones to fine sandstones; completely bioturbated wackestones to packstones; shell dominated | | | upper offshore median ramp |
| 6g | Foraminifera, lamellibranchs, bryozoans and echinids, within siltstones to medium sandstones; completely bioturbated packstones to grainstones; shell dominated | | | upper offshore proximal ramp |
| 6ps | Foraminifera, lamellibranchs, bryozoans and echinids, within marly to gravelly grained very poorly sorted matrix, completely bioturbated; shell dominated | | | lower to upper offshore transgressive sheet |

**Table 1**

**Stratigraphic surfaces**

| | Fsi | MFS1 | FS1 | MFS2 | FS2 | MFS3 | FS3 | MFS 4 | FS4 | MFS5 | FS5 | MFS6 | S7 |
|---|---|---|---|---|---|---|---|---|---|---|---|---|---|

**Estimated ages of surfaces**

| | | | | | | | | | | | | | |
|---|---|---|---|---|---|---|---|---|---|---|---|---|---|
| With biostratigraphic constraints | | | | | | | | | | | | | |
| Cande & Kent (1995) | 41,46512 | 41,1536 | 40,07027 | 40,03397 | 39,79524 | 39,34604 | 39,32859 | 39,22388 | 38,97955 | 38,90974 | 38,58513 | 37,2416 | 36,93711 |
| *error* | *0,066* | *0,22257* | *0,02193* | *0,02193* | *0,02193* | *0,09022* | *0,09205* | *0,10306* | *0,12874* | *0,13608* | *0,1702* | *0,11129* | *0,20349* |
| Wei (1995) | 41,08483 | 40,85266 | 39,83921 | 39,80713 | 39,59615 | 39,20377 | 39,18867 | 39,09806 | 38,88663 | 38,82623 | 38,54533 | 37,31339 | 37,01125 |
| *error* | *0,05925* | *0,15233* | *0,01938* | *0,01938* | *0,01938* | *0,07511* | *0,07645* | *0,08449* | *0,10325* | *0,1086* | *0,13352* | *0,08327* | *0,13948* |
| Without biostratigraphic constraints | | | | | | | | | | | | | |
| Cande & Kent (1995) | 41,47084 | 41,26058 | 39,92603 | 39,80206 | 38,98685 | 38,03127 | 38,02436 | 37,9829 | 37,88614 | 37,8585 | 37,72996 | 37,17892 | 36,792 |
| *error* | *0,066* | *0,13334* | *0,0749* | *0,0749* | *0,0749* | *0,02751* | *0,02751* | *0,02751* | *0,02751* | *0,02751* | *0,02751* | *0,06674* | *0,08894* |
| Wei (1995) | 41,08997 | 40,90146 | 39,71209 | 39,60275 | 38,8837 | 38,03943 | 38,03329 | 37,99647 | 37,91055 | 37,886 | 37,77185 | 37,27747 | 36,92811 |
| *error* | *0,05925* | *0,1193* | *0,06607* | *0,06607* | *0,06607* | *0,02443* | *0,02443* | *0,02443* | *0,02443* | *0,02443* | *0,02443* | *0,06026* | *0,08031* |

**Data used to calculate accommodation on each interval (between two surfaces)**

| | | | | | | | | | | | | | |
|---|---|---|---|---|---|---|---|---|---|---|---|---|---|
| Section S1 | | | | | | | | | | | | | |
| depth | 3272 | 3245 | 3127 | 3094 | 2877 | 2647 | 2642 | 2612 | 2542 | 2522 | 2429 | 2154 | 2000 |
| bathy min/med/max | 0/5/10 | 100/150/200 | 30/60/90 | 100/150/200 | 30/50/70 | 30/60/90 | 5/10/20 | 60/90/120 | 20/30/40 | 60/90/120 | 10/20/30 | 60/90/120 | 10/20/30 |
| % carb/sand/shale | | 20/40/40 | 10/50/40 | 20/40/40 | 10/50/40 | 10/50/40 | 10/30/60 | 20/70/10 | 0/40/60 | 0/20/80 | 35/30/35 | 40/20/40 | 0/20/80 |
| Section S3 | | | | | | | | | | | | | |
| depth | 2311 | 2311 | 2311 | 2308,5 | 2298,5 | 2205 | 2203 | 2198,5 | 2158 | 2137 | 2118 | 2048 | 2000 |
| bathy min/med/max | 0/5/10 | 0/0/0 | 0/0/0 | 100/120/140 | 10/20/30 | 30/60/90 | 5/10/15 | 30/60/90 | 0/5/10 | 30/60/90 | 10/15/20 | 30/60/90 | 0/5/10 |
| % carb/sand/shale | | 0/0/0 | 0/0/0 | 0/0/100 | 0/30/70 | 20/60/20 | 0/10/90 | 30/60/10 | 10/60/30 | 10/80/10 | 0/30/70 | 50/20/30 | 0/20/80 |
| Section S5 | | | | | | | | | | | | | |
| depth | 3080 | 3067,5 | 2950 | 2920 | 2692 | 2537 | 2505 | 2486 | 2381 | 2302 | 2259 | 2122 | 2000 |
| bathy min/med/max | | 65/115/165 | 10/50/90 | 100/150/200 | 20/30/40 | 40/80/120 | 10/15/20 | 30/60/90 | 10/20/30 | 30/60/90 | 10/20/30 | 30/60/90 | 0/5/10 |
| % carb/sand/shale | | 40/30/30 | 20/40/40 | 5/60/35 | 20/60/20 | 20/60/20 | 0/20/80 | 20/75/5 | 20/60/20 | 20/30/50 | 10/40/50 | 40/40/20 | 10/50/40 |
| Section S6 | | | | | | | | | | | | | |
| depth | 3000 | 2947 | 2755 | 2724 | 2435 | 2340 | 2337 | 2317 | 2236 | 2176 | 2120 | 2060 | 2000 |
| bathy min/med/max | | 50/100/150 | 10/20/30 | 80/140/200 | 5/10/15 | 30/60/90 | 5/10/20 | 30/60/90 | 0/5/10 | 30/60/90 | 0/5/10 | 30/60/90 | 0/5/10 |
| % carb/sand/shale | | 30/30/40 | 20/40/40 | 0/60/40 | 20/60/20 | 20/70/10 | 0/40/60 | 30/50/20 | 10/70/20 | 20/40/40 | 10/60/30 | 40/40/20 | 10/60/30 |

**Table 2**

## 2.1.2. Distorsion tectonique des cycles stratigraphiques dans l'exemple de l'anticlinal d'Arguis

---

Article :

## Tectonically induced distorsion of stratigraphic cycles. Example of the Arguis anticline in the South Central Pyrenees (Spain)

Sébastien Castelltort[1], François Guillocheau[1], Thierry Nalpas[1], Delphine Rouby[1], Cécile Robin[2], Marc de Urreiztieta[3] & Isabelle Coutand[1]

[1] Géosciences Rennes, Campus de Beaulieu, 35042 Rennes cedex - France

[2] Université Pierre et Marie Curie, 75252, Paris – France

[3] Total Fina Elf, Avenue Larribeau, 64018 Pau – France

*Geotemas (2000)*

---

# Tectonically induced distorsion of stratigraphic cycles Example of the Arguis anticline in the South Central Pyrenees (Spain)

**S. Castelltort[1], F. Guillocheau[1], T. Nalpas[1],D. Rouby[1], C. Robin[2], M. de Urreiztieta[3] & I. Coutand[1]**

1 Géosciences Rennes, Campus de Beaulieu 35042 Rennes. sebastien.castelltort@univ-rennes1.fr
2 Université Paris VI, 4 Place Jussieu 75252 Paris
3 Elf EP, Avenue Larribeau 64018 Pau

**ABSTRACT**

*The distorsion of stratigraphic cycles refers to a variation in the symetry of the cycles, i.e. a variation of the ratio between progradation and retrogradation. Short wave-lenght growth tectonic structures, like growth folds, generate local variations in the subsidence field, and therefore potential perturbations of the stratigraphic signal. The influence of such tectonic structures on the sequential architecture of syntectonic deposits has not yet been studied. We present here the conceptual basis for a tectonic induced distorsion of stratigraphic cycles, and examine the field example of the Eocene deltaic syntectonic deposits of the Arguis anticline (South Central Pyrennees, Spain). The good correspondence between the theoric predictions and the field case studied, allows us to propose this type of distorsion as an additionnal tool for predictive sequence stratigraphy in syntectonic sedimentation settings. For structural investigations, our approach also shows that non-uniform variations of the thickness of growth strata can record a constant rate of development of the structure, taking in account the cyclic nature of the sedimentary record.*

***Keywords:*** *sequence-stratigraphy, growth structures, distorsion, Eocene*

## INTRODUCTION

Adressing the problem of interactions between tectonic and sedimentary processes, lots of works have focalised on reconstructing the kinematics of growth structures using the geometries of syntectonic strata (Riba, 1976 ; Suppe *et al*, 1992; Poblet & Hardy, 1995 ; among others). Also, numerous studies have intended to make the link between sequence stratigraphy and tectonic processes. Such approaches were principally seeking for a possible tectonic origin for depositional sequences and stratigraphic boundaries (Rey, 1995; Millán *et al* 1994).

The problem which remained was: what are the relationships between a growing short wave-lenght tectonic structure (x10 km), like a fold, and the sequence stratigraphic architecture we can observe in the contemporaneous syntectonic deposits ?

These structures can't generate depositional sequences as long as they are of shorter wave-lenght than the basin sedimentary depositional system. However, they induce local variations of subsidence and a potential perturbation of the sedimentary record.

The term distorsion has been used to describe such perturbations of the stratigraphic signal, expressed in the stratigraphic succession by a variation in thickness of the ratio between progradation and retrogradation periods (i.e. a variation of the symetry of the cycles). Cross (1988) and Guillocheau (1995) distinguished two types of distorsion: (1) the " volumetric partitionning " of sediments, which is linked to the position on the depositional profile, and (2) a more temporal distorsion which results from the superposition of several orders of cyclicity.

In this study we show how a growth structure can induce an other type of spatial distorsion of the contemporaneous sedimentary cycles.

Our results can be used as a predictive tool for sequence stratigraphic interpretation in tectonic settings, together with the two other types of distorsion. They also have implications for the reverse modelling of the development of growth structures (Poblet, 1995).

We begin by presenting the conceptual basis of the tectonic distorsion of sedimentary cycles. Then we compare our predictions with the stratigraphic architecture of the Eocene syntectonic deposits of the Arguis anticline, a very well documented growth fold in the southern Pyrenees foreland basin.

## CONCEPTUAL BASIS FOR A TECTONICALLY INDUCED DISTORSION OF STRATIGRAPHIC CYCLES

It is now widely accepted that sequences record the progradation, aggradation and retrogradation cycles of sedimentary depositional systems (Posamentier et al, 1988). Those general tendencies are controlled by the ratio between accommodation (relative changes of sea level) and sediment supply (Schlager, 1993), and can be read on any vertical section in the basin.

In this study, we assume that short-wave-lenght tectonic structures cannot generate stratigraphic cycles at the scale of the basin depositional system. Their influence is limited to a local variation of subsidence and though to spatial variations of the preservation potential of sedimentary successions.

The figure 1 represents the influence of a growing structure on relative sea level changes and on the differential preservation potential of progradation and retrogradation phases with regard to the location of the section. In order to simplify, we assume a constant rate of sediment influx, and a basic sinusoïdal signal A (Fig. 1) which controls the timing of general progradation and retrogradation periods of the sedimentary depositional system. In this study we do not assume any particular temporal scale for those signals.

The two other curves B and C (Fig. 1) represent the relative sea level changes at two near locations in the basin, affected by different rates of subsidence (i.e. for example the crest and adjacent syncline of a growth fold). They are the sum of the basic signal A and a linear subsidence in B, which is the third of the subsidence in C. In this extreme simplifying model, the constant sediment influx is high enough to fill-in all the space created during relative rises of sea level. All the space suppressed during relative falls is assumed to be eroded. The triangles on the right of the curves represent the thickness of the preserved progradation and retrogadation times for theoric sections recorded at B and C locations (Fig. 1).

It can be observed that: (1) the thickness of the progradation preserved at the low subsidence location B, is less than a half the thickness of the progradation recorded at the higher subsiding location C, (2) concerning the retrogradation time, the thickness in B is more than a half the thickness in C, (3) during progradation periods, the times of relative rise are longer and more rapid at the high subsidence area, whereas relative fall time is longer and more rapid at low subsidence location and (4) in contrast, while retrogradation takes place in the basin, slightly differing relative rises occur at both locations.

Therefore, this simple conceptual approach show that the symetry of sedimentary cycles can be disturbed by a local short-wave lenght variation in the subsidence field.

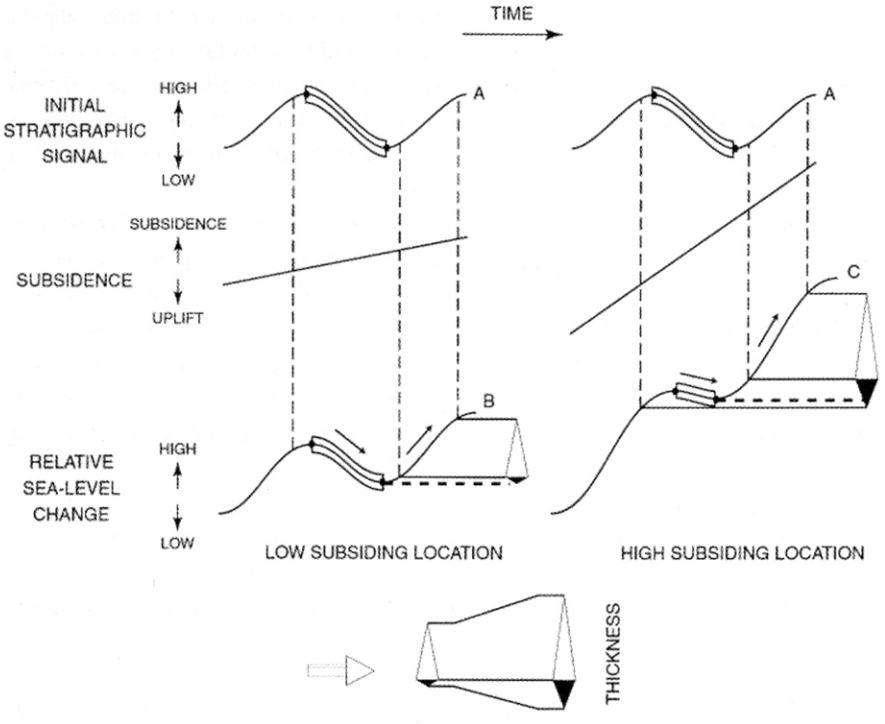


FIGURA 1.- *Response of the sedimentary record to a local variation of subsidence (as induced by the development of a fold for example).*

The prediction resulting, is that the variations of thickness between close zones undergoing differing rates of subsidence, will be of a greater factor during progradation than retrogradation periods.

## FIELD EXAMPLE: THE ARGUIS ANTICLINE

In order to test our predictions we choosed to analyse the well documented late Eocene deltaic syntectonic deposits of the Arguis Anticline in the southern Pyrenees. The aim of this field study, is to compare the vertical stacking pattern of syntectonic deposits at different locations with regard to the fold. Those comparisons have to be made at the higher order as possible (i.e. at the scale of the shortest correlatable stratigraphic units as possible), in order to set free of variations in the rate of uplift of the fold with time. In this way, we applied the classic method of stratigrahic correlations which comprises two stages (Homewood, 1992). After a detailed facies analysis and depositional environments interpretation, we established a hierarchised genetic sequence stacking pattern for each vertical section (major and minor regressive/transgressive cycles, and genetic units sets-parasequences). Then we correlated the sections using (1) the mapping of stratigraphic cycles from aerial photographs, (2) the following-up of stratigraphic surfaces on the field, and (3) the stacking pattern information.

The results are synthesised on the figure 2 which is a East-West cross section representing the stratigraphic geometries and gross depositionnal environments of the syntectonic deposits of the Arguis anticline, as well as stacking patterns of the various vertical sections (at a higher resolution in the eastern syncline and on the crest of the anticline because of a higher variety of facies and a better outcropping quality).

In this deltaic environment, most of the cycles are strongly asymetric in favour of the progradation period. The main observation is that the ratio progradation/-retrogradation (in thickness) of correlated cycles do not varies significantly between both synclines, whereas a strong decrease of this ratio occurs on the crest of the anticline. Indeed, on the hinge of the anticline, the decrease of the thickness of the progradation period with regard to the adjacent syncline is of a higher factor than for the retrogradation period.

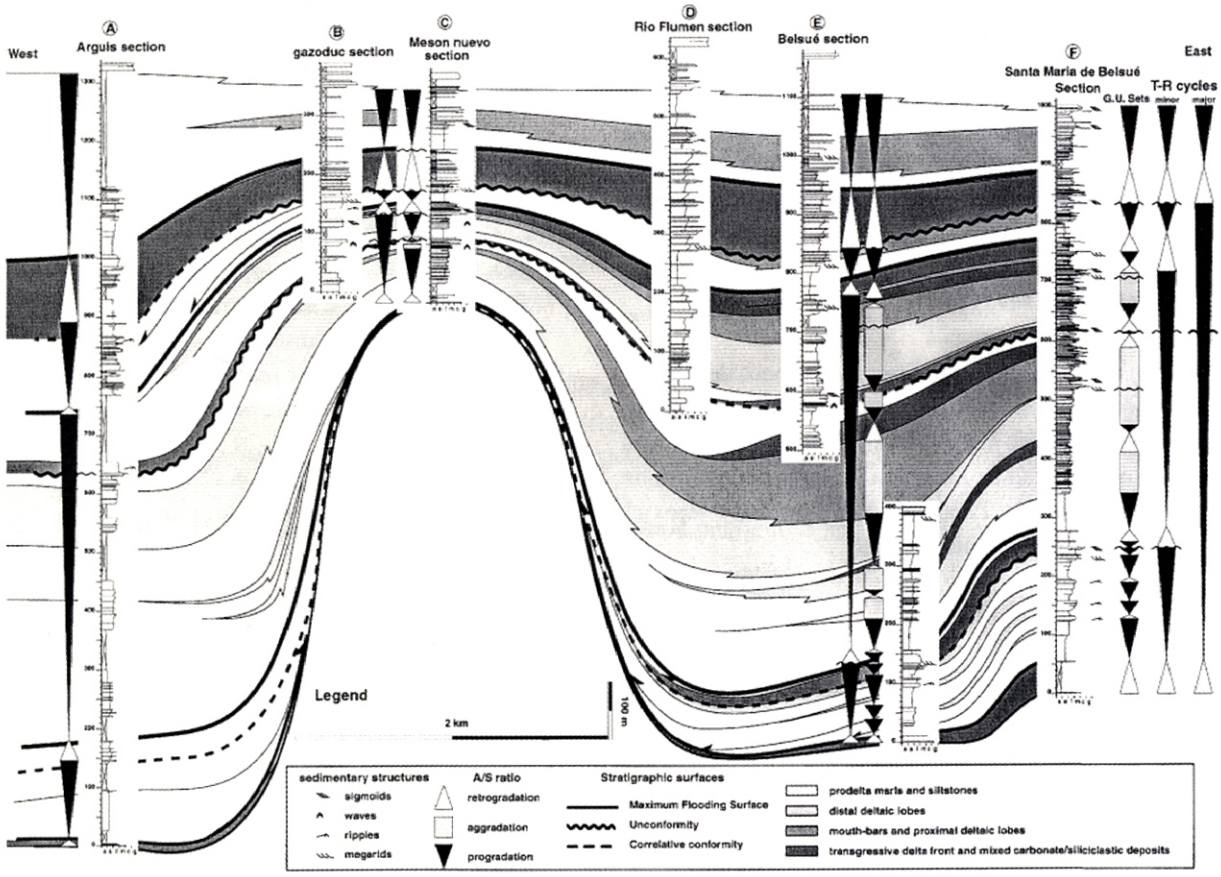


FIGURA 2.- *Arguis Anticline stratigraphic cross-section showing the sequence stratigraphic architecture of syntectonic deposits and principal groups of depositionnal environments.*

## DISCUSSION AND CONCLUSIONS

The field interpretation of the Arguis anticline syntectonic deposits shows evidences of a tectonically induced distorsion of stratigraphic cycles as predicted by our theorical approach. There is a higher factor reduction of the sedimentary thickness during progradation than retrogradation periods. The intuitive conclusion which follows this study is that during progradation periods, the sedimentary input is higher than accommodation and can only settle down where space is available (for example in both synclines), whereas while retrogradation times, the sedimentary input is lower than accommodation so space is available everywhere and sedimentation can take place everywhere with the same probability. In addition, in the case of the Arguis anticline this distorsion is amplified because during retrogradation periods, there is a strong increase of the carbonate component, which become dominant. As a consequence, the sedimentation tends to be much more homogeneous at the scale of the fold, during those retrogradation periods. However, the field study also shows that this distorsion is not so clear for each cycle so the main question which arises from this work is: how is the sedimentary influx distributed during progradation and retrogradation times in the case of a short wave-lenght tectonically induced topography ? This also lead to the problem of reverse modelling of such a tectonic structure (Poblet & Hardy, 1995), because we have shown that with a constant rate of development, a non-uniform variation of the thickness of the syntectonic units can occur, depending on the period of the stratigraphic cycle which is taken in account.

## ACKNOWLEDGEMENTS

We thank the "Parque de la Sierra y Cañones de Guara" (Provincia de Huesca) for their permission to do this work. We thank also Antonio Casas, Teresa Roman-Berdiel, and the staff of universidad de Zaragoza for helpful discussions and accommodation in Zaragoza. We thank also Renaud Bourroulec for week-end discussions.

## REFERENCES

Cross, T A. (1988): Controls on coal distribution in transgressive-regressive cycles. In: Sea-level Changes: an Integrated Approach (Wilgus C.K., Hastings B.S., Kendall C.G.St.C., Posamentier H.W., Ross C.A., Van Wagoner J.C., eds.). Soc. Econ. Paleontol. Mineral. Spec. Publ., 42: 371-380.

Guillocheau, F. (1995): Nature, rank and origin of Phanerozoic sedimentary cycles. C. R. Acad. Sci. Paris, II, 320: 1141-1157.

Homewood, P., Guillocheau, F., Eschard R., Cross, T.A. (1992): Corrélations haute résolution et stratigraphie génétique: une démarche intégrée. Bull. Cent. Rech. Explor.-Prod. Elf-Aquitaine, 16: 357-381.

Millán, H., Aurell, M., Melendez, A. (1994): Synchronous detachment folds and coeval sedimentation in the Prepyrenean External Sierras (Spain): a case study for a tectonic origin of sequences and systems tracts. Sedimentology, 41: 1001-1024.

Poblet, J., Hardy, S. (1995): Reverse modellig of detachment folds ; application to the Pico del Aguila anticline in the South Central Pyrenees (Spain). J. Struct. Geol., 17 (12): 1707-1724.

Posamentier, H.W., Jervey, M.T., Vail, P.R. (1988): Eustatic control on clastic deposition I – Conceptual Framework. En: Sea-level Changes: an Integrated Approach (Wilgus C.K., Hastings B.S., Kendall C.G.St.C., Posamentier H.W., Ross C.A., Van Wagoner J.C., eds.). Soc. Econ. Paleontol. Mineral. Spec. Publ., 42: 109-124.

Rey, J. (1995): Tectonic control in the boundaries of the genetic units: an example in the Dogger of the External Zones of the Betic Cordillera (province of Murcia and Almeria, Spain). Sediment. Geol., 95: 57-68.

Schlager, W. (1993): Accommodation and supply, a dual control on stratigraphic sequences. Sediment. Geol., 86: 111-136.

Suppe, J., Chou, G.T., Hook, S.C. (1992): Rates of folding and faulting determined from growth strata. In: Thrust tectonics (K.R. McClay, ed.). Chapman & Hall: 105-121.

## 2.1.3. La sédimentologie et les foraminifères bartoniens et priaboniens des coupes d'Arguis (Prépyrénées aragonaises, Espagne). Incidence sur la corrélation des biozones à la limite Bartonien/Priabonien

---

Article :

## Bartonian and priabonian foraminifera from Arguis sections (prepyrenean external sierras, Spain). Impact on the correlation of biozones at the Bartonian/Priabonian boundary

Karoly Sztrakos[1] et Sébastien Castelltort[2]

[1] 35 Rue Savier, F-92240 - France

[2] Géosciences Rennes, Campus de Beaulieu, 35042 Rennes cedex - France

*Revue de Micropaléontologie (2001)*

---

REVUE DE MICROPALÉONTOLOGIE
Vol. 44, n° 3, septembre 2001, pp. 233-247

# LA SÉDIMENTOLOGIE ET LES FORAMINIFÈRES BARTONIENS ET PRIABONIENS DES COUPES D'ARGUIS (PRÉPYRÉNÉES ARAGONAISES, ESPAGNE). INCIDENCE SUR LA CORRÉLATION DES BIOZONES À LA LIMITE BARTONIEN/PRIABONIEN

# *BARTONIAN AND PRIABONIAN FORAMINIFERA FROM ARGUIS SECTIONS (PREPYRENEAN EXTERNAL SIERRAS, SPAIN). IMPACT ON THE CORRELATION OF BIOZONES AT THE BARTONIAN/ PRIABONIAN BOUNDARY*

**par Károly SZTRÁKOS* et Sébastien CASTELLTORT****

RÉSUMÉ. – L'étude sédimentologique de l'anticlinal d'Arguis dans le Bassin de Jaca a montré la progradation d'un système deltaïque qui le recouvre progressivement, à partir du Bartonien. Les Marnes d'Arguis et la Formation de Belsué-Atarés qui correspondent à ces dépôts comptent 206 espèces de foraminifères benthiques et sont représentatifs des milieux circalittoraux à infralittoraux. Les foraminifères planctoniques définissent les zones à *Morozovella lehneri* (avec un doute), *Truncorotaloides rohri* s. l., *Dentoglobigerina eocaena* et à *Globigerinatheka semiinvoluta*. Les corrélations interrégionales mettent en évidence un décalage important des apparitions et disparitions de nummulites à l'échelle de la Téthys. En Europe centrale et occidentale, comme à Arguis, *N. fabianii* et *N. garnieri*, marqueurs du Priabonien apparaissent probablement en même temps que *G. semiinvoluta*. En Egypte, cet événement est plus tardif et s'effectue dans la zone éponyme. Dans la première région, les nummulites bartoniennes (*N. perforatus*, *N. millecaput*, etc.) disparaissent avant cette zone, tandis qu'en Arménie, elles semblent coexister avec *N. fabianii*. Ces incertitudes montrent que la définition de la limite Bartonien/Priabonien doit être précédée par la révision de nombreuses coupes, afin de mieux asseoir la corrélation des biozones de ces étages.

ABSTRACT. – The sedimentological study of Arguis anticline in the Jaca basin (south-central Pyrenees, Spain), has shown the overall progradation of a deltaic system, which progressively overlap the structure since Bartonian. The Arguis Marl and Belsué-Atarés Formation which correspond to these sediments contain 206 species of benthic foraminifera. They represent outer and inner shelf depositional environments. Planktonic foraminifera define *Morozovella lehneri* (with uncertainty), *Truncorotaloides rohri* s. l., *Dentoglobigerina eocaena* and *Globigerinatheka semiinvoluta* zones. Interregional correlations put forward substantial differences between different regions of the Tethys. In central and western Europe as well as in the Arguis sections, *N. fabianii* and *N. garnieri*, which mark Priabonian, probably appear coevally with *G. semiinvoluta*. In Egypt, this event occurs later in the same zone. In the first region, bartonian nummulites (*N. perforatus*, *N. millecaput*, etc.) disappear before that zone, whereas in Armenia they seem to coexist with *N. fabianii*. These uncertainties show that the definition of the Bartonian/Priabonian boundary should be preceded by the revision of numerous sections, in order to better establish the correlation of biozones of these stages.

**Mots clés :** Espagne – Bartonien – Priabonien – Biostratigraphie – Foraminiferida.

**Key-words :** Spain – Bartonian – Priabonian – Biostratigraphy – Foraminiferida.

* K. Sztrákos, 35 rue Savier, F-92240 Malakoff, France.

** S. Castelltort, Géosciences Rennes, Equipe Bassins Sédimentaires, Campus de Beaulieu, 35, avenue du Général-Leclerc, F-35042 Rennes cedex, France.

## INTRODUCTION

L'anticlinal d'Arguis se situe dans les Pyrénées aragonaises (Espagne), à mi-chemin entre les villes de Huesca et Sabiñanigo et fait partie d'une succession de structures jalonnant la partie méridionale du bassin de Jaca. Les liens entre la structuration et la sédimentation, ainsi que la biostratigraphie des formations paléogènes affleurantes sont bien connus.

La reprise de l'étude de ces coupes est justifiée par deux raisons. Premièrement, les petits foraminifères benthiques sont peu connus dans cette partie du bassin de Jaca, malgré la richesse de la faune. Nous allons donc tenter d'en dresser l'inventaire, de les utiliser pour estimer des paléoprofondeurs de dépôt et de préciser ainsi l'interprétation sédimentologique. Deuxièmement, des problèmes de corrélation existent entre les nannofossiles calcaires, les foraminifères planctoniques et les grands foraminifères benthiques à la limite Bartonien/Priabonien. La qualité des coupes de la région d'Arguis permet de corréler directement les biozones basées sur ces organismes. Ceci nous amène à affiner la biostratigraphie de cette région de l'avant-pays sud-pyrénéen, et à apporter des contraintes supplémentaires aux événements qui se sont déroulés prés de cette limite, à l'échelle de la Téthys occidentale.

## CADRE GÉOLOGIQUE

Le bassin de Jaca est le sous-bassin transporté (piggy-back) situé le plus à l'Ouest de l'avant-pays sud-pyrénéen. Son développement s'est effectué principalement au cours du Paléogène, en réponse à l'avancée vers le Sud du front de déformation (Séguret, 1972 ; Lafont, 1994). La bordure sud du bassin de Jaca est marquée par une série de structures d'orientation nord-sud qui constitue un relief caractéristique du front sud-pyrénéen appelé « Sierras exteriores », et qui souligne la limite avec le bassin de l'Èbre peu déformé (Millàn *et al.*, 1994). Ces structures forment une succession d'anticlinaux et de synclinaux dont l'amplitude et l'âge diminuent vers l'Ouest et qui se sont développés pendant le Paléogène dans des conditions de sédimentation deltaïque.

Les séries étudiées dans ce travail appartiennent à l'enregistrement syntectonique de l'anticlinal d'Arguis, qui est une de ces structures.

L'architecture antétectonique de ce pli est constituée d'une centaine de mètres de calcaires crétacés, de 70 mètres de grès garumniens et de 800 mètres de calcaires lutétiens de plate-forme peu profonde du bombement externe (Calcaires de Guara à alvéolines). Cette épaisseur de strates compétentes est décollée au dessus d'une unité incompétente composée de 600 mètres d'évaporites, marnes et dolomites du Trias du faciès Keuper (Millàn *et al*, 1994).

Le développement de l'anticlinal d'Arguis commence dès la fin du Lutétien, et les premières géométries syntectoniques sont observables dans les dernières strates des Calcaires de Guara. Ensuite la croissance du pli s'effectue dans des conditions de sédimentation marine deltaïque mixte siliciclastique/carbonatée. Les premiers dépôts deltaïques distaux (Formation des Marnes d'Arguis) sont en onlap sur les flancs de l'anticlinal, puis progressivement, les faciès plus proximaux de la formation des grès bartoniens de Belsué-Atarés passent au dessus de la charnière anticlinale. Les dernières géométries syntectoniques s'enregistrent dans la formation alluviale des conglomérats priaboniens de Campodarbe.

## SÉDIMENTOLOGIE

De nombreuses études ont porté sur la sédimentologie et la stratigraphie des séries syntectoniques de l'anticlinal d'Arguis, parmi lesquelles on peut citer Puygdefàbregas (1975), Delfaud (1984), Medjadj (1985), Nuñez del Prado (1986), Toledo (1990, 1991), Lafont (1994), et Millàn *et al.* (1994). Toutes ces études s'accordent sur le caractère deltaïque des séries mais diffèrent sur plusieurs points comme les influences relatives des marées et des tempêtes, et sur la reconnaissance et l'interprétation des carbonates.

Les faciès rencontrés ont été classés en six groupes :

Groupe 1 : il s'agit de marnes bleues et grises et de silts très bioturbés (ichnofaciès *cruziana*), pauvres en fossiles, et qui correspondent aux environnements distaux d'un système deltaïque.

Groupe 2 : ce groupe est constitué de silts et sables fins intensément bioturbés (ichnofaciès *cruziana* et *skolithos*), mal classés, pauvres en fossiles, à rides de courant qui suggèrent un environnement de prodelta à front de delta distal.

Groupe 3 : il s'agit de grès fins à très grossiers, très mal classés, à stratifications obliques. La bioturbation est faible et limitée à quelques terriers d'*Ophiomorpha*. Ces grès sont caractéristiques du front de delta aux barres d'embouchures.

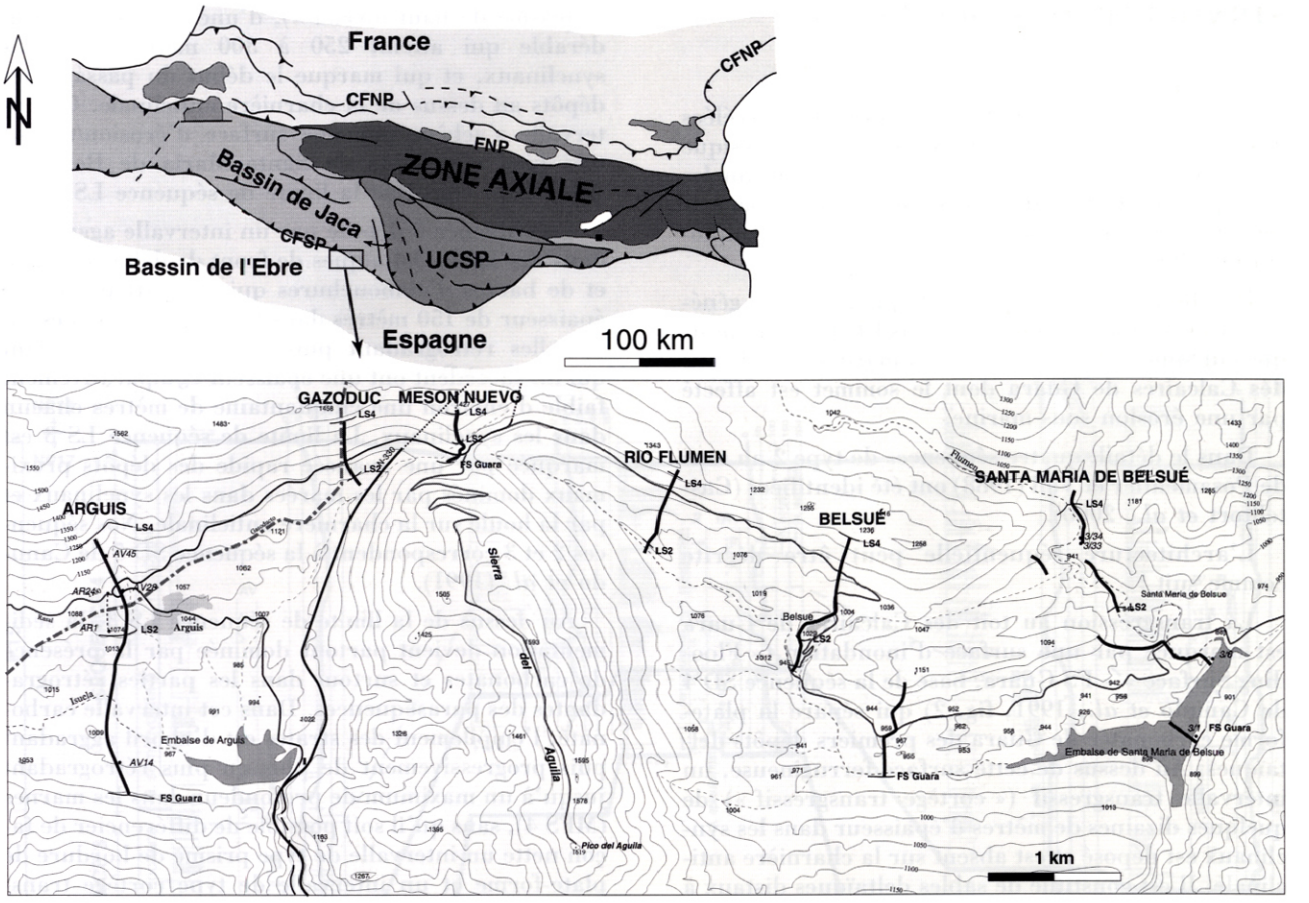


FIG. 1. – Plan de position des coupes étudiées. CFNP : chevauchement frontal Nord-Pyrénéen ; CFSP : Chevauchement Frontal Sud-Pyrénéen ; UCSP : Unité Centrale Sud-Pyrénéene.

*Location map of studied sections. CFNP : North-Pyrenean Frontal Thrust ; CFSP : South-Pyrenean Frontal Thrust ; UCSP : South-Central Pyrenean Unit.*

Groupe 4 : ces faciès sont des grès fins à très grossiers caractérisés par la présence de stratifications sigmoïdales à drapages argileux et attribués à des dunes subtidales et des dépôts subtidaux de front de delta distal.

Groupe 5 : il s'agit de grès fins à moyens très bien classés et à figures sédimentaires de houle (rides symétriques de petite échelle et litage oblique en mamelons). Ils sont caractéristiques de dépôts de tempêtes de plate-forme supérieure.

Groupe 6 : il s'agit de bancs bioclastiques à textures wackstone à packstone et plus rarement grainstone. La matrice est constituée principalement par des silts et des sables fins dans certains packstones, et par une boue carbonatée. Ces dépôts bioclastiques largement ignorés dans les précédentes études sont attribués aux tempêtes dans un environnement mixte, où coexistent les influences deltaïques et la production carbonatée.

La limite d'action des vagues permanentes n'a pas été identifiée.

Dans l'ensemble, les faciès des dépôts syntectoniques de l'anticlinal d'Arguis peuvent être positionnés sur un profil de type lobe deltaïque progradant, de la plate-forme silteuse aux barres d'embouchures, avec parfois prédominance de la houle ou des marées, et substitution possible en rampe de tempêtes carbonatée (Castelltort *et al*, 2000).

## STRATIGRAPHIE SÉQUENTIELLE

Les coupes sédimentologiques ont été corrélées grâce aux photographies aériennes, au suivi physique des bancs sur le terrain (Fig. 1), et en utilisant les concepts de la stratigraphie séquentielle (Posamentier et Vail, 1988 ; Homewood *et al.*, 1992 ; Guillocheau, 1995).

On observe dans l'ensemble la progradation générale d'un système deltaïque depuis l'Est vers l'ouest, qui fait suite à une transgression marquée au dessus des Calcaires de Guara dont le sommet est affecté par une érosion sous-marine.

Dans le détail, quatre séquences de type 2 au sens de Posamentier et Vail (1988) ont été identifiées (Castelltort *et al.*, 2000).

L'architecture séquentielle peut être décrite comme suit :

La transgression au toit des Calcaires de Guara est marquée par une surface d'inondation (« Flooding Surface » – FS Guara, base de la séquence SD 4 de Canudo *et al.*, 1991, fig. 2) qui sépare la plateforme carbonatée de Guara des premiers dépôts deltaïques. Au dessus de cette surface ferrugineuse, un intervalle transgressif (« cortège transgressif ») de quelques dizaines de mètres d'épaisseur dans les synclinaux est déposé et est absent sur la charnière anticlinale. Il est constitué de sables deltaïques distaux à glauconie arrangés en paraséquences granodécroissantes qui passent vers le haut à des marnes. L'intervalle marneux qui suit correspond à la première surface de maximum d'inondation (« Maximum Flooding Surface » – MFS 1).

Au dessus de la MFS 1, le système deltaïque va ensuite progader jusqu'à la limite de séquence LS 1 qui marque la fin de la première séquence. Cette première séquence voit son épaisseur varier d'environ 150 à 250 mètres d'Ouest en Est et n'est pas enregistrée sur la charnière anticlinale.

La deuxième séquence débute par un intervalle aggradant dans des faciès proximaux (« prisme de bordure de plate-forme ») de très faible épaisseur et qui n'est enregistré que sur les coupes de Belsué et Santa Maria de Belsué. Ensuite intervient une rétrogradation qui conduit sur toutes les coupes à une surface de maximum d'inondation (MFS 2, Fig. 2) bien marquée par un intervalle marneux d'une puissance supérieure à 50 mètres. Cette surface MFS 2 marque probablement aussi le maximum de profondeur atteint à l'échelle de toute la série syntectonique. Au dessus, un intervalle progradant/aggradant puis de plus en plus progradant est enregistré (« prisme de haut-niveau »), d'une puissance considérable qui atteint 250 à 300 mètres dans les synclinaux, et qui marque le début du passage des dépôts au dessus de la charnière anticlinale. Cet intervalle s'achève par une surface d'érosion/transit très bien corrélable de Santa Maria de Belsué à Arguis qui constitue la limite de séquence LS 2.

La séquence 3 débute par un intervalle aggradant dans des faciès deltaïques de front de delta proximal et de barres d'embouchures qui peut atteindre une épaisseur de 150 mètres dans le synclinal est. Les intervalles rétrogradant puis à nouveau progradant qui lui succèdent ont une épaisseur comparativement faible d'environ une cinquantaine de mètres chacun dans les synclinaux. La limite de séquence LS 3 est marquée par une avancée rapide des dépôts proximaux dominés par les marées dans les synclinaux et par la houle sur la charnière anticlinale. Nos séquences 2 et 3 correspondent à la séquence SD 5 de Canudo *et al.* (1991).

Au dessus de la limite de séquence LS 3, la sédimentation devient partout dominée par la présence de carbonates et surtout dans les parties rétrogradantes des paraséquences. Dans cet intervalle carbonaté, l'empilement des strates est d'abord aggradant puis progressivement de plus en plus rétrogradant jusqu'à un maximum de profondeur dans les marnes (MFS 4), sans qu'il soit possible de différencier de façon nette un intervalle de type prisme de bordure de plate-forme et un intervalle de type cortège transgressif. La progradation reprend ensuite jusqu'à la limite de séquence majeure LS 4 qui marque le passage à des faciès nettement dominés par l'action des marées et beaucoup plus proximaux (plaine côtière et conglomérats de la Formation de Campodarbe). Cette séquence est équivalente de la partie inférieure de la séquence SD 6 de Canudo *et al.* (1991).

## LES PETITS FORAMINIFÈRES BENTHIQUES ET LES PALÉOENVIRONNEMENTS

La microfaune des Marnes d'Arguis est mal conservée et fortement recristallisée. Par ce fait, les espèces de petite taille sont souvent méconnaissables. Malgré ces difficultés, nous avons pu déterminer 206 espèces de petits foraminifères benthiques. Leur liste figure dans le tableau 1, où elles ont été regroupées par biozones de foraminifères planctoniques. Les espèces de cette faune sont toutes connues des Marnes de la Côte des Basques à Biarritz (Bartonien-Priabo-

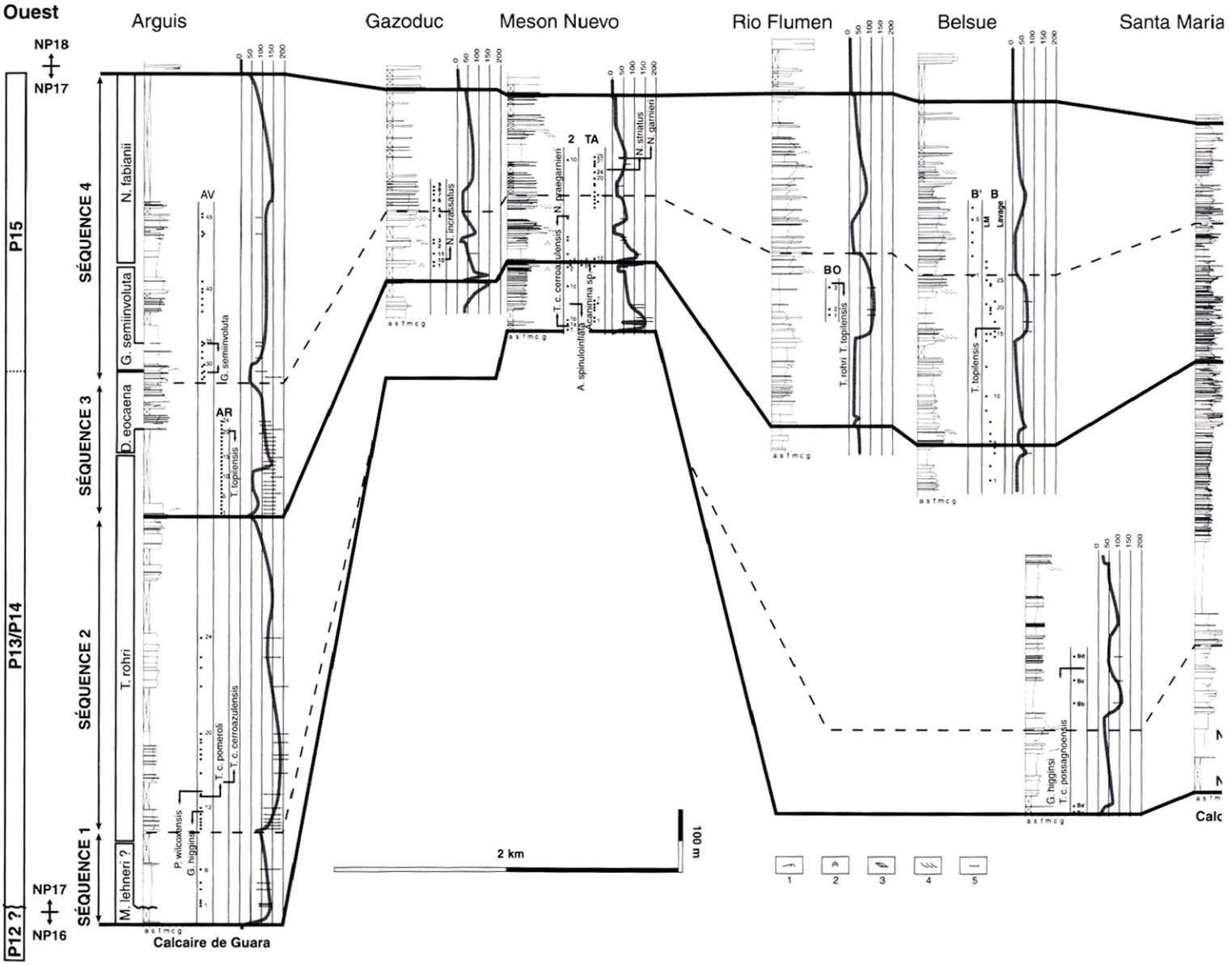


FIG. 2. – Lithologie, séquences de dépôt et événements biostratigraphiques dans les coupes éocènes d'Arguis. a – argile silteuse ; s – silt ; f – sable fin ; m – sable moyen conglomérat. LS : limite de séquence ; MFS : surface de maximum d'inondation. 1 : rides de vagues ; 2 : rides de courant ; 3 : megarides de courant ; 4 : megarides à léoprofondeur estimée par la microfaune.

*Lithology, depositional sequences and biostratigraphic events in the Eocene Arguis sections. a – argilaceous siltstone ; s – siltstone ; f – fine-grained sandstone ; m - stone ; c – coarsely-grained sandstone ; g – gravelly-grained sandstone. LS – sequence boundary ; MFS : maximum flooding surface. 1 : wave ripples ; 2 : small-sc trough-cross bedding ; 4 : sigmoidal cross bedding ; 5 : paleodepth estimated using microfauna.*

nien) et ont été figurées par Mathelin et Sztràkos (1993). Si la faune est plus pauvre (les associations de Biarritz comptent environ 500 espèces), c'est à cause d'une profondeur plus faible et d'une sédimentation plus détritique, deux facteurs défavorables à la diversification. Cet appauvrissement se manifeste également dans le nombre d'espèces présentes dans chacun des échantillons. Dans les environs d'Arguis, cette diversité ne dépasse qu'exceptionnellement 50, tandis qu'à Biarritz, elle atteint souvent 100 à 150.

Le milieu de dépôt influe sur la microfaune, déterminant la fréquence de certains genres et espèces qui constituent les associations.

L'association la plus distale, indiquant une paléoprofondeur entre 100 et 200 m, s'observe dans la zone à *Truncorotaloides rohri* et est confinée à la partie occidentale de la région étudiée. Les grands foraminifères sont absents, ainsi que les formes habitant l'étage épibathyal, comme *Reticulophragmium*, *Repmanina*, *Pleurostomella*, *Osangularia*. Les genres *Ammodiscus* et *Martinottiella* qui apparaissent à partir de 100 m de profondeur (Mathelin et Sztràkos, 1993) sont représentés par quelques individus dans les échantillons. Les formes les plus fréquentes sont les suivantes : *Cylindroclavulina pyrenaica*, *Spirorutilus pectinataformis*, *Uvigerina eocaena*, *Globobulimina pyrula*, *Cibicidoides alleni*, *Riminopsis rotulus* et *Gyroidinoides girardanus*.

Les paléoprofondeurs entre 80 et 100 à 130 m sont indiquées par la fréquence des bryozoaires, discocyclines et *Operculina*. Les petits foraminifères dominants sont les mêmes que dans l'association précédente auxquels s'ajoute *Nonion commune*, abondant dans la coupe de Santa Maria de Belsué. Cette faune est présente dans les sections d'Arguis et Meson Nuevo, ainsi qu'à la base des coupes de Belsué et Santa Maria de Belsué.

Avec la diminution de la profondeur de la mer, les nummulites puis les alvéolines deviennent plus fréquentes, indiquant l'étage infralittoral. La présence des genres *Cassidulina* et *Uvigerina* permet de différencier les associations qui habitaient les profondeurs supérieures à 50 m (Mathelin et Sztràkos, 1993). *Asterigerina rotula*, *Sphaerogypsina globula*, *Fabiania cassis* et les miliolidés sont fréquents dans les couches carbonatées, tandis que *Nonion commune* domine dans les niveaux gréseux. Ces associations caractérisent les Calcaires de Guara (éch. 2/1 et 3/1), la partie supérieure des coupes de Meson Nuevo, Rio Flumen, Belsué et Santa Maria de Belsué.

L'étage circalittoral prédomine à l'Ouest de l'anticlinal d'Arguis, tandis que les faciès infralittoraux sont plus fréquemment rencontrés au-dessus de l'anticlinal et dans la région située plus à l'Est. La succession de ces associations décrit les variations de paléoprofondeurs au cours du Bartonien et Priabonien (Fig. 2). On observe une augmentation rapide, de l'ordre de 100 à 150 m à la base des Marnes d'Arguis, puis une période stable dans la partie inférieure de la zone à *Truncorotaloides rohri* (base de la séquence 2), quand le remplissage sédimentaire et la subsidence étaient proches de l'équilibre. La paléoprofondeur décroît à partir de la partie supérieure de cette zone et se poursuit dans la zone à *Globigerinatheka semiinvoluta*, jusqu'à l'apparition des faciès continentaux (Canudo *et al.*, 1988). Des fluctuations surviennent à la limite des séquences, l'intervalle transgressif se déposant dans un milieu plus profond que le prisme de haut niveau. Ceci est difficile à déceler à l'aide de la microfaune, l'amplitude des variations de profondeur n'étant pas suffisante pour modifier les associations de foraminifères.

Les écarts visibles sur la figure 2 entre la paléobathymétrie moyenne donnée par les environnements de dépôts et la paléobathymétrie donnée par les associations de foraminifères sont dus à l'échantillonnage qui a été effectué dans les intervalles marneux (donc les plus profonds) des paraséquences.

Le schéma paléobathymétrique décrit est en accord avec les travaux de Molina *et al.* (1988) et de Canudo *et al.* (1993).

## BIOSTRATIGRAPHIE

### Les données bibliographiques

Les Calcaires de Guara sont surmontés par quelques mètres de marnes sableuses, glauconieuses, représentant un niveau de faible vitesse de sédimentation à la base des Marnes d'Arguis (Millán *et al.*, 1994). Ces marnes ont été placées dans la zone à *Morozovella lehneri* (P 12, Canudo *et al.*, 1988). Les dépôts sus-jacents ont été datés des zones à *Orbulinoides beckmanni* et *Truncorotaloides rohri* (P 13-P 14). La séparation de ces deux zones de foraminifères planctoniques n'est pas possible dans cette région à cause des conditions paléoclimatiques défavorables pour *Orbulinoides beckmanni*. Canudo et Molina (1992) ont créé une nouvelle zone pour cet intervalle, la « zone à *Truncorotaloides rohri* ». Plus haut dans la coupe d'Arguis, il existe 80 m de sédiments entre la disparition de *T. rohri* et l'apparition de *Globigerinatheka semiinvoluta*. Canudo et Molina (1992) ont nommé cet intervalle « zone à *Dentoglobigerina eocaena* » et corrélé avec la partie inférieure

de la zone à *Globigerinatheka semiinvoluta*, dans le sens de Toumarkine et Luterbacher (1985) qui ont défini la base de cette zone par la disparition de *T. rohri*. *G. semiinvoluta* a été trouvée dans la partie sommitale des Marnes d'Arguis (Canudo *et al.*, 1988). Les foraminifères planctoniques sont absents dans la partie supérieure des coupes, à cause de l'installation des milieux infralittoraux.

Les Calcaires de Guara appartiennent à la zone à *Nummulites aturicus* près de leur sommet (Canudo *et al.*, 1988), selon la zonation de Schaub (1981), ou à la zone SBZ 16, d'après le travail de Serra-Kiel *et al.* (1998). Schaub (1981) a noté *N. perforatus* (SBZ 17) dans la partie inférieure des Marnes d'Arguis et *N. striatus*, *N. boulangeri*, *N. discorbinus* et *N.* cf. *garnieri* dans les dernières couches marines « indiquant un niveau de passage du Biarritzien au Priabonien ». Canudo *et al.* (1988) ont observé *N. striatus*, *N. incrassatus ramondiformis* et *N.* aff. *cyrenaicus* (SBZ 18) dans les niveaux correspondant à la zone à *Dentoglobigerina eocaena*. Ils signalent une faune riche priabonienne des calcaires sommitaux : *N. boulangeri*, *N. incrassatus incrassatus*, *N. chavannesi*, *N. garnieri*, *N. pulchellus*, *N. stellatus* (zone à *N. fabianii*, SBZ 19).

Les nannofossiles calcaires montrent que les marnes glauconieuses à la base des Marnes d'Arguis appartiennent à la zone NP 16. Leur épaisseur atteint 50 m dans la coupe de Santa Maria de Belsué et quelques mètres dans la coupe d'Arguis (Toledo, 1990). Le restant de cette formation et une partie de la Formation de Belsué-Atarés ont été placés dans la zone NP 17. *Chiasmolithus oamaruensis*, marqueur de la zone NP 18 apparaît dans des niveaux priaboniens situés peu après la limite de séquence LS4 (Toledo, 1990 ; Canudo *et al.*, 1988) et non analysés dans cette étude.

## LES NOUVEAUX ÉLÉMENTS BIOSTRATIGRAPHIQUES

L'étude de la faune de la partie basale, glauconieuse des Marnes d'Arguis, appartenant à la zone P 12 n'a pas été reprise ici.

Dans les Marnes d'Arguis datées de la zone NP 17, nous avons observé quelques foraminifères planctoniques qui se limitent à l'Yprésien et au Lutétien : *Turborotalia griffinae*, *Subbotina inaequispira*, et *Pseudohastigerina wilcoxensis*, accompagnés par des foraminifères benthiques bathyaux, comme *Repmanina charoides*, *Haplophragmoides walteri* et *Spiroplectammina spectabilis* (tableau 1). Leur fréquence diminue en montant dans les coupes, mais on les retrouve très rarement encore dans la zone à *Dentoglobigerina eocaena*. La source de ces éléments se trouve probablement au sein des marnes bathyales ypréso-lutétiennes qui affleurent actuellement près de Mediano, au Nord-Ouest de Huesca (Teixell et Barnolas, 1995). Il est possible qu'elles aient occupé un domaine plus vaste au Nord, dans la direction de l'actuelle zone axiale des Pyrénées et que leur érosion ait alimenté la sédimentation deltaïque du Bartonien.

Les espèces suivantes, signalées dans l'horizon glauconieux et attribuées à la zone à *Morozovella lehneri* (=P 12) et NP 16 (Canudo *et al.*, 1988), ont été observées dans les marnes sus-jacentes, appartenant aux zones à *Truncorotaloides rohri* s. l. (= P 13-P 14) et NP 17 : *Turborotalia cerroazulensis frontosa*, *T. cerroazulensis possagnoensis*, *Guembelitrioides higginsi*. La disparition de ces espèces a été proposée pour définir la limite des zones à *Morozovella lehneri* et *Orbulinoides beckmanni*, en l'absence de cette dernière espèce dans les régions à climat chaud tempéré (Toumarkine et Luterbacher, 1985 ; Canudo et Molina, 1992).

On ne peut considérer avec certitude que ces espèces soient remaniées. Leur présence à des niveaux plus élevés a été signalé dans d'autres bassins. Gonzalvo et Molina (1996) mentionnent *Turborotalia cerroazulensis frontosa* de la zone à *Orbulinoides beckmanni* des Cordillères bétiques. Krasheninnikov (1974) et Krasheninnikov *et al.* (1985) ont observé cette espèce dans la zone à *H. alabamensis* en Arménie que nous corrélons ici avec les zones à *Orbulinoides beckmanni* et *Truncorotaloides rohri*. Berggren *et al.* (1995) notent sa présence jusqu'à la partie médiane de la dernière zone. *T. cerroazulensis possagnoensis* a été observée dans la zone à *Globigerinatheka semiinvoluta* par Canudo et Molina (1992), mais nous pensons qu'il pourrait s'agir dans ce cas de remaniements. *Guembelitrioides higginsi* a été signalé dans la partie inférieure de la zone à *Truncorotaloides rohri* dans la coupe de Monte Cagnero (Italie, Parisi *et al.*, 1988). Cette espèce a été retrouvée dans une carotte du sondage Gourbera 1 du Bassin d'Aquitaine, appartenant à la zone NP 17. La disparition quasi-simultanée des trois espèces dans la coupe de Miretrain du même bassin est liée aux conditions tectono-sédimentaires : cet horizon est probablement tronqué et surmonté par un niveau glauconieux, riche en éléments remaniés, comme des silex sénoniens (Sztràkos *et al.*, 1998).

Ces éléments jettent un doute sur la datation P 12 de l'horizon glauconieux qui se trouve à la base des

TABLEAU 1. – Répartition des foraminifères dans les coupes éocènes d'Arguis. TR – zone à *Truncorotaloides rohri* ; DE – zone à *Dentoglobigerina eocaena* ; GS – zone à *Globigerinatheka semiinvoluta* ; R – remaniement.

*Distribution of foraminifers in the Eocene sections of Arguis.*

| | T.R. | D.E. | G.S. |
|---|---|---|---|
| Sous-ordre : TEXTULARIINA | | | |
| | | | |
| Bathysiphon cf. taurinensis SACCO, 1893 | | | |
| Silicobathysiphon sp. | | | |
| Rhabdammina cf. eocenica CUSHMAN et HANNA, 1927 | | | |
| Rhabdammina sp. | | | |
| Ammodiscus sp. | | | |
| Repmanina charoides (JONES et PARKER, 1860) | R | | |
| Reophax duplex GRZYBOWSKI, 1896 | | | |
| R. cf. pilulifera BRADY, 1884 | | | |
| Haplophragmoides latidorsatus (BORNEMANN, 1855) | | | |
| H. tumidus (HALKYARD, 1919) | | | |
| H. walteri (GRZYBOWSKI, 1898) | R? | | |
| Ammobaculites agglutinans (d'ORBIGNY, 1846) | | | |
| Ammomarginulina cf. hockleyensis (CUSHMAN et APPLIN, 1926) | | | |
| Recurvoides ? sp. | | | |
| Haddonia intermedia (HALKYARD, 1919) | | | |
| Reticulophragmium sp. | | | |
| Spiroplectammina spectabilis (GRZYBOWSKI, 1898) | R | | |
| Vulvulina haeringensis (GÜMBEL, 1870) | | | |
| Trochammina quadriloba ( GRZYBOWSKI, 1896) | | | |
| Gerochammina cf. conversa (GRZYBOWSKI, 1901) | | | |
| Plectina dalmatina (SCHUBERT, 1911) | | | |
| Dorothia fallax HAGN, 1954 | | | |
| D. traubi (HAGN,1956) | | | |
| Eggerella polymorphinoides (HALKYARD, 1919) | | | |
| Martinottiella cocoaensis (CUSHMAN, 1936) | | | |
| Spirorutilus dalmatinus (v. BELLEN, 1941) | | | |
| S. pectinataformis (BALAKHMATOVA, 1964) | | | |
| Textularia adalta CUSHMAN, 1926 | | | |
| T. crookshanki HAQUE, 1956 | | | |
| T. lontensis LALICKER, 1935 | | | |
| Karrerotextularia olianensis (COLOM et RUIZ de GAONA, 1950) | | | |
| Pseudogaudryina ? difformis (HALKYARD, 1919) | | | |
| P.? gardnerae (CUSHMAN, 1926) | | | |
| P.? glabrata (CUSHMAN, 1922) | | | |
| Cylindroclavulina pyrenaica (COLOM et RUIZ de GAONA, 1950) | | | |
| | | | |
| Sous-ordre : SPIRILLININA | | | |
| | | | |
| Spirillina sp. | | | |
| Patellina sp. | | | |
| | | | |
| Sous-ordre : MILIOLINA | | | |
| | | | |
| Spiroloculina canaliculata d'ORBIGNY, 1846 | | | |
| Cycloforina lippa (LE CALVEZ, 1947) | | | |
| Quinqueloculina cf. carinata d'ORBIGNY, 1905 | | | |
| Pyrgo sp. | | | |
| Triloculina angularis d'ORBIGNY, 1905 | | | |
| T. gibba d'ORBIGNY, 1846 | | | |
| Sigmoilinita tenuis (CZJZEK, 1848) | | | |
| Sigmoilopsis bartoniensis (COLOM et RUIZ de GAONA, 1950) | | | |
| Pentellina pseudosaxorum SCHLUMBERGER, 1905 | | | |
| Alveolina sp. | | | |
| | | | |
| Sous-ordre : LAGENINA | | | |
| | | | |
| Chrysalogonium ewaldi (REUSS, 1851) | | | |
| C. lanceolum CUSHMAN et JARVIS, 1934 | | | |
| C. resupinatum (GÜMBEL, 1870) | | | |
| C. tenuicostatum CUSHMAN et BERMUDEZ, 1936 | | | |
| D. albatrossi (CUSHMAN, 1923) | | | |
| D. fissicostata GÜMBEL, 1870 | | | |
| Grigelis hispidus (SOLDANI, 1791) | | | |
| G. semirugosus (d'ORBIGNY, 1846) | | | |
| Laevidentalina cooperensis (CUSHMAN, 1933) | | | |
| L. cf. mucronata (NEUGEBOREN, 1856) | | | |
| L. neugeboreni (SCHWAGER, 1866) | | | |
| Nodosaria soluta (REUSS, 1851) | | | |
| Pseudonodosaria brevis (d'ORBIGNY, 1846) | | | |
| P. discreta (REUSS, 1850) | | | |
| P. inflata (BORNEMANN, 1855) | | | |
| Pyramidulina latejugata (GÜMBEL, 1870) | | | |

| | T.R. | D.E. | G.S. |
|---|---|---|---|
| P. sp. | | | |
| Svenia bulbosa (HALKYARD, 1919) | | | |
| Lenticulina alabamensis (CUSHMAN, 1944) | | | |
| L. cf. alatolimbata (GÜMBEL, 1870) | | | |
| L. depauperata (REUSS, 1851) | | | |
| L. dumblei (WEINZIERL et APPLIN, 1929) | | | |
| L. inornata (d'ORBIGNY, 1846) | | | |
| L. limbosa (REUSS, 1863) | | | |
| L. magnifica (TOULMIN, 1941) | | | |
| L. platyptera (REUSS, 1870) | | | |
| L. princeps (REUSS, 1865) | | | |
| L. pseudovortex (COLE, 1927) | | | |
| Percultazonaria fragaria (GÜMBEL, 1870) | | | |
| Saracenaria boettcheri (REUSS, 1863) | | | |
| S. hantkeni CUSHMAN, 1933 | | | |
| Frondovaginulina tenuissima (HANTKEN, 1875) | | | |
| Hemirobulina hantkeni (BANDY, 1949) | | | |
| H. inconspicua (HUSSEY, 1949) | | | |
| H. pediformis (BORNEMANN, 1855) | | | |
| H. tenuis (BORNEMANN, 1855) | | | |
| H. tumida (REUSS, 1851) | | | |
| Marginulina behmi (REUSS, 1866) | | | |
| M. multiplicata BERGQUIST, 1942 | | | |
| M. porvaensis (HANTKEN, 1875) | | | |
| M. propinqua HANTKEN, 1883 | | | |
| Vaginulinopsis cumulicostatus (GÜMBEL, 1870) | | | |
| V. minutus (HANTKEN, 1875) | | | |
| V. robustus (HALKYARD, 1919) | | | |
| Spirolingulina acutimargo (HALKYARD, 1919) | | | |
| Lagena altahumifera COPELAND, 1964 | | | |
| L. gracilicosta REUSS, 1858 | | | |
| L. sp. 4. SZTRAKOS, 2000 | | | |
| Pygmaeoseistron vulgaris (WILLIAMSON, 1858) | | | |
| Globulina gibba gibba (d'ORBIGNY, 1846) | | | |
| G. gibba myristiformis (WILLIAMSON, 1858) | | | |
| Guttulina communis (d'ORBIGNY, 1826) | | | |
| G. hantkeni CUSHMAN et OZAWA, 1930 | | | |
| Pyrulina thouini (d'ORBIGNY, 1865) | | | |
| Ramulina kittlii RZEHAK, 1885 | | | |
| Favulina geometrica (REUSS, 1863) | | | |
| Homalohedra cf. bifurcata (LEROY, 1944) | | | |
| Glandulina glans (d'ORBIGNY, 1865) | | | |
| | | | |
| Sous-ordre : ROBERTININA | | | |
| | | | |
| Ceratocancris sp. | | | |
| Robertina germanica CUSHMAN et PARKER, 1938 | | | |
| | | | |
| Sous-ordre : GLOBIGERININA | | | |
| | | | |
| Laterostomella sp. | | | |
| Turborotalia bolivariana (PETTERS, 1954) | | | |
| T. cerroazulensis cerroazulensis (COLE, 1928) | | | |
| T. cerroazulensis frontosa (SUBBOTINA, 1953) | | | |
| T. cerroazulensis pomeroli (TOUMARKINE et BOLLI, 1970) | | | |
| T. cerroazulensis possagnoensis (TOUMARKINE et BOLLI, 1970) | R | R | |
| T. griffinae (BLOW, 1979) | R | | |
| Acarinina bullbrooki (BOLLI, 1957) | | | |
| A.? medizzai (TOUMARKINE et BOLLI, 1975) | | | |
| A. spinuloinflata (BANDY, 1949) | | | |
| Morozovella spinulosa (CUSHMAN, 1927) | | | |
| Truncorotaloides rohri BRÖNNIMANN et BERMUDEZ, 1953 | | | |
| T. topilensis (CUSHMAN, 1925) | | | |
| Globorotaloides carcosellensis TOUMARKINE et BOLLI, 1975 | | | |
| G. suteri BOLLI, 1957 | | | |
| Guembelitrioides higginsi (BOLLI, 1957) | R | R | |
| Subbotina eocaena eocaena (GÜMBEL, 1870) | | | |
| S. eocaena cryptomphala (GLAESSNER, 1937) | | | |
| S. hagni (GOHRBANDT, 1967) | | | |
| S. inaequispira (SUBBOTINA, 1953) | R | R | |
| S. linaperta (FINLAY, 1939) | | | |
| Pseudohastigerina micra (COLE, 1927) | | | |
| P. wilcoxensis (CUSHMAN et PONTON, 1932) | R | | |
| Globigerina cf. ouachitaensis gnaucki BLOW et BANNER, 1962 | | | |

| | T.R. | D.E. | G.S. |
|---|---|---|---|
| Globigerinatheka index (FINLAY, 1939) | | | |
| G. index rubriformis (SUBBOTINA, 1953) | ? | | |
| G. mexicana barri BRÖNNIMANN, 1952 | | | |
| G. mexicana mexicana (CUSHMAN, 1925) | | | |
| G. semiinvoluta (KEIJZER, 1945) | | | |
| | | | |
| Sous-ordre : ROTALIINA | | | |
| | | | |
| Bolivina budensis (HANTKEN, 1875) | | | |
| B. crenulata CUSHMAN,1936 | | ? | |
| B. cf. elongata HANTKEN, 1875 | | | |
| B. nobilis HANTKEN, 1875 | | | |
| B. semistriata HANTKEN, 1868 | | | |
| B. striatocarinata CUSHMAN, 1936 | | | |
| B. vaceki SCHUBERT, 1902 | | | |
| Latibolivina janoscheki (GOHRBANDT, 1962) | | | |
| Nodobolivinella sp. | | | |
| Globocassidulina globosa (HANTKEN, 1875) | | | |
| G. subglobosa (BRADY, 1884) | | | |
| Sporobulimina eocaena BYKOVA, 1959 | | | |
| Sagrinopsis aspera (TERQUEM, 1882) | | | |
| Bulimina rostrata BRADY, 1884 | | | |
| Globobulimina pyrula (d'ORBIGNY, 1846) | | | |
| Uvigerina topilensis CUSHMAN, 1925 | | | |
| U. eocaena GÜMBEL, 1870 | | | |
| U. gracilis REUSS, 1851 | | | |
| Uvigerinella abbreviata abbreviata (TERQUEM, 1882) | | | |
| U. abbreviata tubulifera (KAASSCHIETER, 1961) | | | |
| U. ? sp. | | | |
| Angulogerina globosa (STOLTZ, 1925) | | | |
| A. muralis (TERQUEM, 1882) | | | |
| Dymia labrum (SUBBOTINA, 1953) | | | |
| Kolesnikovella elongata (HALKYARD, 1919) | | | |
| Trifarina budensis (HANTKEN, 1868) | | | |
| Reussella elongata (TERQUEM, 1882) | | | |
| R. recurvata (HALKYARD, 1919) | | | |
| R. terquemi CUSHMAN, 1945 | | | |
| Fursenkoina halkyardi (CUSHMAN, 1936) | | | |
| Caucasina eocaenica CHALILOV, 1958 | | | |
| Drepaniota lorifera (HALKYARD, 1919) | | | |
| Siphonodosaria annulifera (CUSHMAN et BERMUDEZ, 1936) | | | |
| S. camerani (DERVIEUX, 1894) | | | |
| Baggina dentata HAGN, 1956 | | | |
| Cancris auriculus primitivus CUSHMAN et TODD, 1942 | | | |
| C. subconicus (TERQUEM, 1882) | | | |
| Valvulineria cf. complanata (d'ORBIGNY, 1846) | | | |
| Eponides polygonus LE CALVEZ, 1949 | | | |
| Stomatorbina torrei (CUSHMAN et BERMUDEZ, 1937) | | | |
| Discorbis ? baconicus (HANTKEN, 1875) | | | |
| D. perplexus LE CALVEZ, 1949 | | | |
| D. propinquus (TERQUEM, 1882) | | | |
| Neoeponides navarraensis (COLOM et RUIZ de GAONA, 1950) | | | |
| N. schreibersii (d'ORBIGNY, 1846) | | | |
| Neoconorbina circularis (SIDEBOTTOM,1918) | | | |
| Glabratella cf. neumannae RAHAGHI, 1976 | | | |
| Planoglabratella biarritzensis SZTRAKOS, 1993 | | | |
| P. elegans (HALKYARD, 1919) | | | |
| Siphonina advena eocenica CUSHMAN et APPLIN, 1926 | | | |
| Cibicidoides alleni (PLUMMER,1927) | | | |
| C. bionus (SHUTSKAYA, 1963) | | | |
| C. cf. mauricensis (HOWE et ROBERTS, 1939) | | | |
| C. praelopjanicus MYATLYUK, 1970 | — | | |
| Planulina costata (HANTKEN, 1875) | | | |
| P. pseudowuellerstorfi (COLE, 1927) | | | — |
| Cibicides westi HOWE, 1939 | | | |
| Falsoplanulina ammophila (GÜMBEL, 1870) | | | |
| Lobatula carinata (TERQUEM, 1882) | | | |
| L. lobatula (WALKER et JACOB, 1798) | | | |
| Stichocibicides moravicus POKORNY, 1956 | | | |
| Cycloloculina eocenica (TERQUEM, 1882) | | | |
| Fabiania cassis (OPPENHEIM, 1896) | | | |
| Halkyardia minima (LIEBUS, 1911) | | | |
| Gyroidinella magna LE CALVEZ, 1949 | ? | | |
| Korobkovella sublobatula (GÜMBEL, 1870) | | | |

| | T.R. | D.E. | G.S. |
|---|---|---|---|
| Acervulina dudarensis HORVATH-KOLLANYI, 1988 | | | |
| Sphaerogypsina globula (REUSS, 1848) | | | |
| Asterigerinata pustulosa GOHRBANDT, 1962 | | | |
| Asterigerina rotula (KAUFMANN, 1867) | | | |
| Nonion commune (d'ORBIGNY, 1846) | | | |
| Nonionella cf. humelincki (PIJPERS, 1933) | | | |
| Melonis pompilioides (FICHTEL et MOLL, 1798) | | | |
| Pullenia quinqueloba (REUSS, 1851) | | | |
| Almaena epistominoides (MARIE, 1950) | | | |
| Allomorphina trigona REUSS, 1850 | | | |
| Chilostomella cf. ovoidea REUSS, 1850 | | | |
| Quadrimorphina petrolei (ANDREAE, 1884) | | | |
| Alabamina wilcoxensis TOULMIN, 1941 | | | |
| Globorotalites granulatus POZARYSKA et SZCHECHURA, 1968 | | | |
| Charltonina budensis (HANTKEN, 1875) | | | |
| Oridorsalis umbonatus (REUSS, 1851) | | | |
| Heterolepa eocaena (GÜMBEL, 1870) | | | |
| Loisthostomata ilbarritzensis SZTRAKOS, 1993 | | | |
| Gyroidinoides batjesi (HAUSMANN, 1964) | | | |
| G. girardanus (REUSS, 1851) | | | |
| G. hannai (GARRETT, 1939) | | | |
| G. octocameratus (CUSHMAN et HANNA, 1927) | | | |
| Anomalinulla byramensis (CUSHMAN et TODD, 1946) | | | |
| Gavelinella acuta (PLUMMER, 1927) | | | |
| Hansenisca poignantae SZTRAKOS, 1993 | | | |
| Hanzawaia producta (TERQUEM, 1882) | | | |
| Riminopsis rotulus (d'ORBIGNY, 1846) | | | |
| Paralabamina eocaenica SZTRAKOS, 1993 | | | |
| P. toulmini (BROTZEN, 1948) | | | |
| Neorotalia lecalvezae (BOULANGER et POIGNANT, 1971) | | | |
| N. lithothamnica (UHLIG, 1886) | | | |
| Pararotalia armata (d'ORBIGNY, 1865) | | | |
| P. audouini (d'ORBIGNY, 1906) | | | |
| P. spinigera (TERQUEM, 1882) | | | |
| Elphidium laeve (d'ORBIGNY, 1826) | | | |
| Nummulites chavannesi de la HARPE, 1883 | | | |
| N. garnieri de la HARPE, 1911 | | | |
| N. incrassatus de la HARPE, 1883 | — | | |
| N. praegarnieri SCHAUB, 1981 | | | |
| N. striatus (BRUGUIERE, 1872) | | | |
| Operculina alpina DOUVILLE, 1916 | | | |

marnes : il pourrait être (tout au moins en partie) équivalent de la zone à *Orbulinoides beckmanni*, dont la base se situe encore dans la zone NP 16 (Berggren *et al.*, 1995).

*Turborotalia cerroazulensis pomeroli* et *T. cerroazulensis cerroazulensis* apparaissent dans la partie médiane de la zone à *T. rohri* dans la coupe d'Arguis située dans le synclinal, environ 200 m au-dessus du toit des Calcaires de Guara. Au sommet de l'anticlinal d'Arguis, *T. cerroazulensis cerroazulensis* est présente dès la base des marnes, soulignant ainsi l'importance de la tectonique à l'origine de la lacune entre les deux formations (Fig. 2).

La transition entre les zones à *Truncorotaloides rohri* et *Dentoglobigerina eocaena* a été étudiée en détail dans une coupe qui suit un ravin à l'Ouest d'Arguis, entre le point côté 1014 et la route de Bentué de Rasal (AR 1 à 24, Fig. 1, 2). La faune de foraminifères planctoniques y est très pauvre et le nombre d'espèces ne dépasse pas sept dans l'ensemble des échantillons (tableau 1). Les globorotalidés épineux sont extrêmement rares. Le dernier représentant de ces formes, un spécimen de *Truncorotaloides topilensis* a été trouvé dans l'échantillon AR 20. Les corrélations montrent que le niveau de disparition de cette espèce et de celle de *T. rohri* se trouve dans la même séquence dans les autres coupes, comme dans celle du Rio Flumen ou de Belsué (Fig. 2). *Globigerinatheka semiinvoluta* représentée par les formes typiques, apparaît dans l'échantillon AV 28, 80 m plus haut que le dernier *Truncorotaloides*, et disparaît au-dessus de l'échantillon AV 33. Sa disparition est liée au changement de faciès.

Certains niveaux sont riches en nummulites (déterminations effectuées par A. Blondeau). *N. incrassatus* est présent dès la partie supérieure de la zone à *Truncorotaloides rohri* (coupe du gazoduc, AM 11, fig. 2). Dans la coupe de Meson Nuevo voisine, *N. praegarnieri* persiste jusqu'au sommet de cette zone (éch. 2/9), comme à Santa Maria de Belsué, où cette espèce, ainsi que *N. striatus* et *N. chavannesi* coexistent (éch. 3/30). *N. garnieri* apparaît dans un niveau qui correspond à la base de la zone à *Globigerinatheka semiinvoluta* (Meson Nuevo, éch. TA 25, fig. 2). Les nouvelles observations montrent que la faune de la zone SB 18 de Serra-Kiel *et al.* (1998) est associée aux foraminifères planctoniques de la zone à *Truncorotaloides rohri* et *N. garnieri*, espèce priabonienne, à ceux de la zone à *G. semiinvoluta*.

Ces éléments ne clarifient pas la position stratigraphique de la zone à *Dentoglobigerina eocaena*. Les données de Canudo *et al.* (1988) montrent la présence de *N.* cf. *cyrenaicus* 30 m au-dessous des premiers *N. garnieri*, horizon qui se situe dans la zone de foraminifères planctoniques mentionnée. Comme *N. cyrenaicus* se limite à la zone SBZ 18 et coexiste avec les nummulites de l'Eocène moyen, la zone à *Dentoglobigerina eocaena* doit être placée dans le Bartonien.

## CORRÉLATION DES BIOZONES À LA LIMITE BARTONIEN/PRIABONIEN

Berggren *et al.* (1995) et Serra-Kiel *et al.* (1998) ont situé l'apparition de *Nummulites fabianii* (base de la zone SBZ 19 et limite Bartonien/Priabonien) au milieu de la zone à *Globigerinatheka semiinvoluta*. La révision bibliographique de Sztrákos (2000) a souligné la fragilité de cette corrélation dans le cas des coupes d'Europe centrale et occidentale, où l'absence des foraminifères planctoniques dans les calcaires à grands foraminifères et celle des nummulites dans les marnes pélagiques ont rendu impossible une corrélation directe entre les deux types de biozonation. La révision des coupes d'Arguis a montré que les apparitions de *G. semiinvoluta* et de *Nummulites garnieri*, espèce considérée priabonienne de la zone SBZ 19 se situent dans des niveaux très proches, à la base de la séquence 4 (Fig. 2). En revanche, les incertitudes persistent concernant la corrélation de la zone à *Dentoglobigerina eocaena* avec les biozones planctoniques standard. En effet, cet intervalle peut correspondre à la partie sommitale de la zone à *Truncorotaloides rohri* de Toumarkine et Luterbacher (1985) par suite de la disparition précoce du marqueur en Europe, ou être l'équivalent de la zone P 15 de Berggren *et al.* (1995), par suite de l'apparition tardive de *Globigerinatheka semiinvoluta* dans les régions septentrionales. Bien entendu, la combinaison des deux causes reste également possible.

Blow (1979) et Berggren et Miller (1988) ont constaté la coexistence de *Globigerinatheka semiinvoluta* avec *Truncorotaloides rohri* dans les mers tropicales, parfois avec *Morozovella spinulosa* (Berggren *et al.*, 1995). Dans de nombreuses régions d'Afrique du Nord et d'Europe, *G. semiinvoluta* apparaît plus tardivement, surmontant directement les associations à globorotalidés épineux (Alpes maritimes, Italie) ou bien après un intervalle dépourvu des formes mentionnées (Krasheninnikov et Ptukhian, 1986 ; Haggag, 1990 ; Canudo et Molina, 1992 ; Mathelin et Sztràkos, 1993 ; Gonzalvo et Molina, 1996).

En Aquitaine, où la zone à *Dentoglobigerina eocaena* a également été signalée (zone EPA 14 : Sztrákos, 2000), elle contenait encore quelques

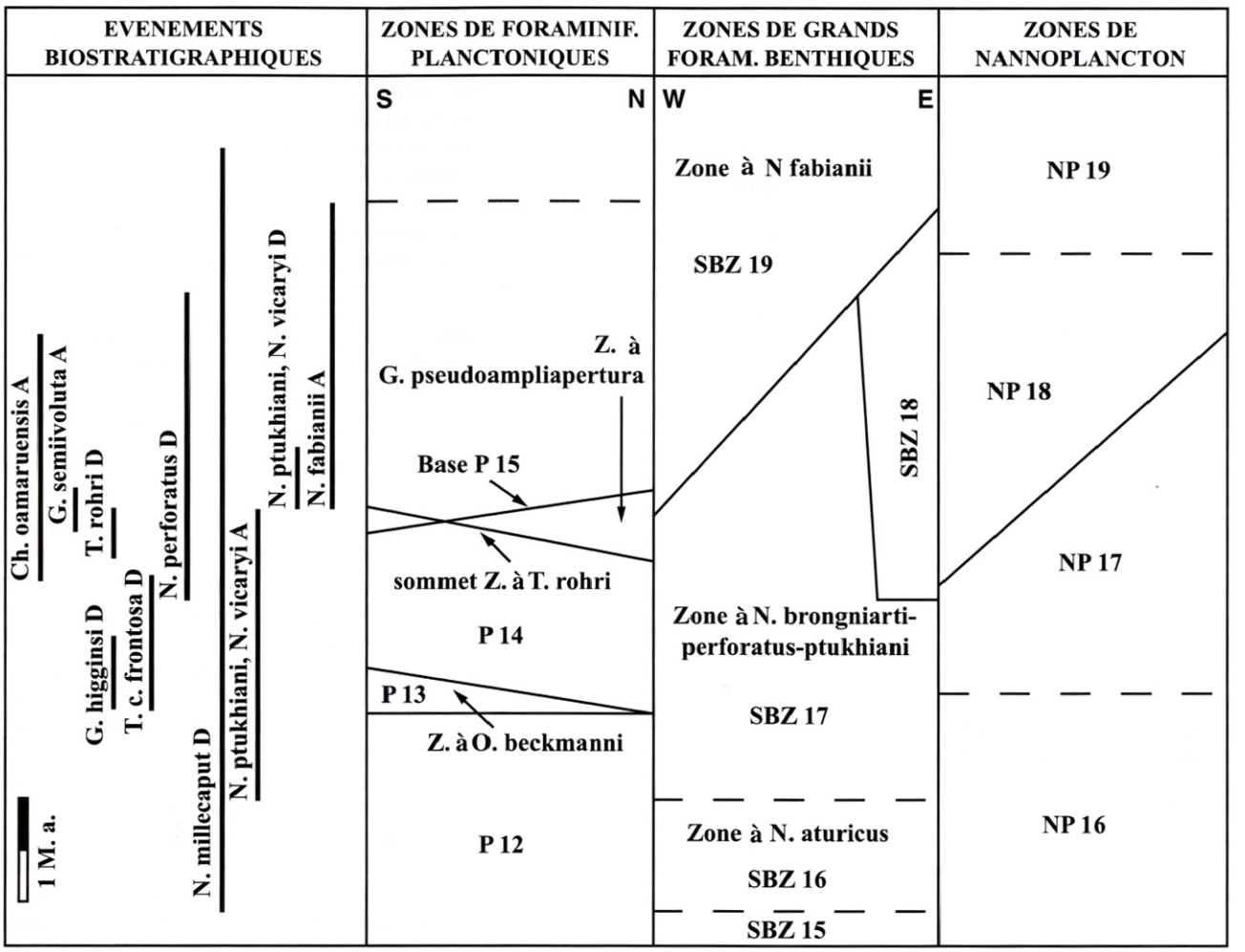


FIG. 3. – Apparitions et disparitions de quelques espèces d'importance stratigraphique près de la limite Bartonien/Priabonien. Incidence sur la limite des biozones dans la Téthys. A – apparition ; D – disparition.

*Appearances and disappearances of some species of stratigraphic importance near Bartonian/Priabonian boundary. Impact on biozonal boundaries in the Tethysian realm. A – appearance ; D – disappearance.*

exemplaires de *Planorotalites pseudoscitulus*, *Acarinina spinuloinflata* et *Morozovella spinulosa*, interprétés comme remaniés de l'Eocène moyen (tableau 1 *in* Mathelin et Sztràkos, 1993).

Haggag (1990) a retrouvé le même intervalle, nommé zone à *Globigerina pseudoampliapertura* dans les coupes d'Egypte, représenté par quelques mètres de marnes entre les derniers *Truncorotaloides rohri* et les premières *Globigerinatheka semiinvoluta*. Elle a remarqué que toutes les espèces de cette unité apparaissent dans la zone à *T. rohri* et que des petites acarinines persistent localement dans la partie inférieure de la zone.

La zone à *Globigerina turcmenica* surmonte celle à *Hantkenina alabamensis* en Arménie (Krasheninnikov *et al.*, 1985). Cette dernière correspond à la zone à *Orbulinoides beckmanni* et à la partie inférieure de la zone à *Truncorotaloides rohri* d'après nos corrélations. Compte tenu de sa position stratigraphique, la zone à *G. turcmenica* est l'équivalent de la zone à *Dentoglobigerina eocaena*. La rareté du genre *Acarinina* et *T.* aff. *rohri* les rapproche également. La présence de ces globorotalidés épineux montre son appartenance au Bartonien, même si la majorité des taxons présents dans cette unité franchit la limite Bartonien/Priabonien. En plus de

l'Arménie, la zone à *G. turcmenica* a été reconnue dans le bassin de Varna (Bulgarie), en Crimée et aux alentours du Caucase, où elle est représentée par les dépôts de l'horizon de Kuma (Krasheninnikov *et al.*, 1985). Elle pourrait exister aussi en Syrie (Bolli et Krasheninnikov, 1977).

Il faut noter que l'extension stratigraphique de cette zone est très différente d'une région à l'autre, en terme de nannofossiles calcaires : NP 16 – NP 18 basale en Crimée (Shcherbina, 2000) et dans le Caucase (Gavrilov *et al.*, 2000) et NP 17 sommitale-NP 18 basale en Arménie (Krasheninnikov et Ptukhian, 1986).

Ces exemples montrent que les apparitions et disparitions des foraminifères planctoniques ne sont pas isochrones entre les différentes régions. L'utilisation des grands foraminifères benthiques, tels que les nummulites, pose les mêmes problèmes à l'échelle de la Téthys.

Ainsi, l'apparition de *N. fabianii* semble hétérochrone : les formes proches de *N. fabianii* peuvent coexister avec *N. cyrenaicus*, *N. ptukhiani*, *N.* cf. *biarritzensis* comme à Girona en Espagne (Schaub, 1981). Dans les Alpes maritimes et en Savoie, les niveaux à *N. fabianii* surmontent directement les calcaires à *N. perforatus* (Blondeau *et al.*, 1968 ; Campredon, 1977 ; Schaub, 1981). Il est déjà présent à la base de la coupe-type à Priabona, dans la zone NP 18 (Barbin, 1988) et apparaît plus tardivement en Egypte, dans la partie supérieure de la zone citée, correspondant à la zone NP 19, mais pour des raisons faciologiques.

Strougo (1992) a observé une faune bartonienne, composée de *N. bullatus decroueze*, *N. beaumonti*, *N. lyelli*, *N. cyrenaicus* dans la zone à *Globigerina pseudoampliapertura* d'Egypte. Deux autres espèces bartoniennes, *N. ptukhiani* et *N. vicaryi* n'apparaissent que dans sa partie sommitale, après la disparition des espèces citées et persistent à la base de la zone à *Globigerinatheka semiinvoluta*. Il faut remarquer que l'apparition de *N. ptukhiani* est plus précoce dans d'autres localités, où cette espèce coexiste avec l'association à *N. lyelli* d'Egypte, comme en Tunisie (Schaub, 1981) ou avec *N. perforatus*, comme en Aquitaine (Sztràkos *et al.*, 1998).

Krasheninnikov *et al.* (1985) ont noté que *N. fabianii* apparaît dans la partie supérieure la zone à *Hantkenina alabamensis* en Arménie. Compte tenu de ce qui précède, ces formes peuvent correspondre à *N.* aff. *fabianii* de Schaub (1981), décrit dans la coupe bartonienne de Girona ou bien à *N. ptukhiani*. Il est donc probable que ces auteurs, ainsi que Krasheninnikov et Nemkov (1975) utilisent *N. fabianii* dans un sens plus large qu'en Europe centrale et occidentale. Dans la même région, Krasheninnikov et Ptukhian (1986) ont observé *N. biedai*, *N. perforatus*, *N. lyelli* et *N. millecaput* dans les zones à *Globigerinatheka semiinvoluta* et NP 18. D'après cette publication, *N. millecaput* disparaît dans les zones à *Turborotalia cerroazulensis* (P 16) et NP 18 du Priabonien moyen. Ces nummulites sont faciles à reconnaître grâce à leurs caractéristiques morphologiques. Nous pensons donc que leur présence dans les zones de foraminifères planctoniques mentionnées ne peut être remise en cause.

Pour conclure sur la corrélation des biozones de foraminifères planctoniques et des grands foraminifères près de la limite Bartonien/Priabonien, il ne semble pas possible de trouver une solution globale. Les coupes des Alpes maritimes suggèrent l'équivalence de la zone SBZ 18 avec la zone à *Truncorotaloides rohri*. En Espagne, dans la coupe d'Arguis, les foraminifères planctoniques appartenant aux zones à *T. rohri* et à *Dentoglobigerina eocaena* coexistent avec une faune de nummulites de type Bartonien. Les nummulites priaboniennes (*N. garnieri*) apparaissent en même temps que *Globigerinatheka semiinvoluta*. En Egypte et en Arménie, les nummulites bartoniennes de grande taille montent plus haut et s'observent encore dans la zone à *G. semiinvoluta*, associées à *N. fabianii*. L'apparition des nummulites priaboniennes, comme *N. fabianii* et *N. garnieri* semble être un événement hétérochrone entre la partie septentrionale et méridionale de la Téthys, plus précoce au Nord (à la base de la zone à *G. semiinvoluta* en Europe) qu'au Sud (au milieu de cette zone en Egypte). En Europe centrale et occidentale, ces espèces remplacent des associations bartoniennes à *N. perforatus* – *N. millecaput* (Schaub, 1981 ; Kecskeméti, 1987) dans un niveau qui correspond à la base de la zone à *G. semiinvoluta*. En Arménie, il existe un intervalle à la base de cette zone, où les deux associations coexistent. En Egypte, *N. ptukhiani* et *N. vicaryi*, espèces bartoniennes et *N. fabianii* se succèdent, le changement se situant dans la partie inférieure de la biozone mentionnée. Les incertitudes concernant les apparitions et disparitions des espèces-guides bartoniennes et priaboniennes sont reportées sur la figure 3.

En ce qui concerne les nannofossiles calcaires, la révision bibliographique de Sztrákos (2000) a montré que l'apparition de *Chiasmolithus oamaruensis*, marqueur de la limite NP 17/NP 18 était hétérochrone, s'échelonnant entre la partie médiane de la zone à *Truncorotaloides rohri* et celle de la zone à *Globigerinatheka semiinvoluta*. Ce décalage dans le temps est plus lié à sa rareté qu'aux variations climatiques, puisque *Chiasmolithus oamaruensis* apparaît

dans la zone à *T. rohri* en Aquitaine (Mathelin et Sztràkos, 1993) et dans la zone à *G. semiinvoluta* au Sud des Pyrénées (Canudo *et al.*, 1988 ; Toledo, 1990). Les données de Krasheninnikov et Ptukhian (1986, Arménie) ; Shcherbina, (2000, Crimée) ; Gavrilov *et al.* (2000, Caucase) et de Strougo (1992, Egypte) montrent également son apparition dans les zones à G. turcmenica et G. pseudoampliapertura de l'Eocène moyen.

## CONCLUSIONS

L'étude sédimentologique des coupes autour de l'anticlinal d'Arguis a mis en évidence la progradation d'un système deltaïque depuis l'Est vers l'Ouest, représenté par les Marnes d'Arguis et la Formation de Belsué-Atarés, qui recouvre progressivement l'anticlinal. La faune de foraminifères benthiques est constituée des espèces connues des dépôts du même âge du Bassin d'Aquitaine. Le nombre plus faible d'espèces (206) est en relation avec la sédimentation deltaïque, peu favorable au développement de ce groupe. Les associations permettent de définir l'épaisseur de la tranche d'eau et son évolution au cours du Bartonien et du Priabonien. Celle-ci varie entre l'étage circalittoral et infralittoral, avec une tendance générale à la diminution de l'accomodation vers le haut.

La datation de la partie basale des Marnes d'Arguis est incertaine, l'extension stratigraphique de certaines espèces considérées comme marqueurs de la limite des zones *Morozovella lehneri* et *Orbulinoides beckmanni* étant plus large : *Turborotalia cerroazulensis frontosa*, *T. cerroazulensis possagnoensis*, *Guembelitrioides higginsi* persistent localement jusqu'à la partie médiane de la zone à *Truncorotaloides rohri*. La position de la zone à *Dentoglobigerina eocaena* (Canudo et Molina, 1992), définie comme intervalle entre la disparition de *T. rohri* et l'apparition de *Globigerinatheka semiinvoluta*, a été revue : d'après la faune de nummulites, elle se place dans le Bartonien.

Cette zone est connue dans d'autres parties de la Téthys : en Egypte, elle a été décrite sous le nom « zone à *Globigerina pseudoampliapertura* » (Haggag, 1990) et entre la Bulgarie et la partie orientale du Caucase, elle est appelée « zone à *Globigerina turcmenica* » (Krasheninnikov et Muzylöv, 1975 ; Krasheninnikov et Bolli, 1977).

Les corrélations biostratigraphiques montrent que l'extension des nummulites varie d'Ouest en Est et du Nord au Sud au sein de la Téthys. Les espèces bartoniennes disparaissent en Europe centrale et occidentale à la limite inférieure de la zone à *Globigerinatheka semiinvoluta*, tandis qu'en Arménie et en Egypte, elles la franchissent. De même, l'apparition de *N. garnieri* et du groupe de *N. fabianii* est proche de cette limite en Europe et en Arménie et elle est plus tardive en Egypte.

Ces quelques éléments montrent qu'il serait indispensable de reprendre l'étude des coupes qui traversent la limite Bartonien/Priabonien en Europe et en Arménie, en calant des événements biostratigraphiques bassin par bassin, par le plus grand nombre de méthodes possibles et de les comparer sans les à priori des échelles de corrélation actuellement en vigueur. Cette comparaison pourrait mettre en évidence l'influence des variations paléoclimatiques et paléogéographiques sur l'évolution de la faune. Une telle démarche ne peut se concevoir sans l'intervention de la stratigraphie séquentielle qui permet de préciser les lacunes et les niveaux condensés ou d'autres éléments sédimentologiques ayant une influence sur les interprétations faunistiques. Compte tenu des incertitudes recensées, cette démarche est indispensable pour fixer la limite Bartonien/Priabonien d'une façon plus fiable.

### REMERCIEMENTS

Nous remercions vivement M. Alphonse Blondeau pour la détermination des nummulites et M. Jean-Pierre Gély (Gaz de France) pour ses conseils.

## BIBLIOGRAPHIE

BARBIN V. (1988) : Le Priabonien dans sa région-type (Vicentin, Italie du Nord). Stratigraphie, micropaléontologie, essai d'intégration dans l'échelle chronostratigraphique. *Mém. Sci. de la Terre Univ. P. et M. Curie*, Paris, vol. 86-29, 281 p.

BERGGREN W. A., KENT D. V., SWISHER C. C. et AUBRY M. P. (1995) : A revised Cenozoic geochronology and chronostratigraphy. *SEPM Spec.Publ.*, Tulsa, Okl., vol. 54, p. 129-212.

BERGGREN W. A. et MILLER K.G. (1988) : Paleogene tropical planktonic foraminiferal biostratigraphy and magnetochronology. *Micropaleontology*, New York, vol. 35, n° 4, p. 308-320.

BLONDEAU A., BODELLE J., CAMPREDON R., LANTEAUME M. et NEUMANN M. (1968) : Répartition stratigraphique des grands foraminifères de l'Eocène dans les Alpes-Maritimes (franco-italiennes) et les Basses-Alpes. Colloque sur l'Eocène, Paris, mai 1968. *Mém. du B.R.G.M.*, Paris., vol. 58, p. 13-26.

BLOW W. H. (1979) : The Cainozoic Globigerinida. A study of the morphology, taxonomy, evolutionary relationships and the

stratigraphical distribution of some Globigerinida (mainly Globigerinacea). E. J. Brill, Leiden, vol. 1-3, 1413 p., 264 pl.

BOLLI H. M. et KRASHENINNIKOV V. A. (1977) : Problems in Paleogene and Neogene correlations based on planktonic foraminifera. *Micropaleontology*, New York, vol. 23, n° 4, p. 436-452.

CAMPREDON R. (1977) : Les formations paléogènes des Alpes maritimes franco-italiennes. *Mém. hors sér. N° 9, Soc. géol. France*, Paris, 199 p.

CANUDO J. I., GONZALVO C. et MOLINA E. (1993) : Los foraminíferos planctónicos del tránsito Eoceno medio-superior en la cuenca de Jaca (Huesca, Pirineo) : implicationes bioestratigráficas y paleoceanográficas. Communicationes de la IX Jornadas de Paleontología, Málaga, p. 37-42.

CANUDO J. I., MALAGON J., MELENDEZ A., MILLAN H., MOLINA E. et NAVARRO J. J. (1991) : Las secuencias deposicionales del Eoceno medio y superior de las Sierras exteriores (Prepirineo meridional aragonés). *Geogaceta*, Madrid, vol. 9, p. 81-84.

CANUDO J. I. et MOLINA E. (1992) : Biostratigrafía con foraminíferos planctónicos del Paleógeno del Pirineo. *Neues Jahrbuch Geol. Paläont.Abh.*, Stuttgart, vol. 186, n° 1-2, p. 97-135.

CANUDO J. I., MOLINA E., RIVELINE J., SERRA-KIEL J. et SUCUNZA M. (1988) : Les événements biostratigraphiques de la zone prépyrénéenne d'Aragon (Espagne), de l'Eocène moyen à l'Oligocène inférieur. *Rev. Micropaléont.*, Paris, vol. 31, n° 1, p. 15-29.

CASTELLTORT S., GUILLOCHEAU F., NALPAS T., ROUBY D., ROBIN C., DE URREIZTIETA M. et COUTAND I. (2000) : Tectonically induced distorsion of stratigraphic cycles – Example of the Arguis anticline in the south-central Pyrenees (Spain). IV Congreso del Grupo Español del Terciario, *Geotemas* 1 (2), Madrid, p. 55-58.

DELFAUD (1984) : Organisation du complexe deltaïque de Jaca (Aragon, Espagne). 5e Congrès Européen de Géologie, Marseille.

GAVRILOV Y. O., SHCHERBINA E. A. et MUZILÖV N. G. (2000) : Paleogene sequence in central North Caucasus : a response to paleoenvironmental changes. *GFF*, Stockholm, vol. 122, p. 51-53.

GONZALVO C. et MOLINA E. (1996) : Bioestratigrafía y chronoestratigrafía del tránsito Eoceno medio-Eoceno superior en la Cordillera Bética. *Rev. esp. Micropal.*, Madrid, vol. 28, n° 2, p. 25-44.

GUILLOCHEAU F. (1995) : Nature, rank and origin of Phanerozoic sedimentary cycles. *C. R. Acad. Sci.*, Paris, vol. 320, p. 1141-1157.

HAGGAG M. A. (1990) : Globigerina pseudoampliapertura zone, a new late Eocene planktonic foraminiferal zone (Fayoum area, Egypt). *Neues Jahrbuch Geol. Paläont.*, Stuttgart, Monatshefte, vol. 5, p. 295-307.

HOMEWOOD P., GUILLOCHEAU F., ESCHARD R. et CROSS T. (1992) : Corrélation haute résolution et stratigraphie génétique : une démarche intégrée. *Bull. Centres Rech. Explor.-Prod. Elf Aquitaine*, Pau, vol. 16, p. 375-381.

KECSKEMÉTI T. (1987) : Contributions to the phylogenetic connections of *Nummulites* species. *Ann. Hist. Nat. Mus. Nat. Hung.*, Budapest, vol. 79, p. 61-75.

KRASHENINNIKOV V. A. (1974) : Some species of planktonic foraminifera from the Eocene and Oligocene deposits of South Armenia.*Voprosy Mikropaleontologii*, Leningrad-Moskva, vol. 17, p. 95-135 (en russe).

KRASHENINNIKOV V. A. et MUZYLÖV N. G. (1975) : Relationship between the zonal scales based on planktonic foraminifers and nannoplankton in Paleogene sections of the North Caucasus. *Voprosy Mikropaleontologii*, Leningrad-Moskva, vol. 18, p. 212-224 (en russe).

KRASHENINNIKOV V. A., MUZYLÖV N. G et PTUKHIAN A. E. (1985) : Stratigraphical subdivision of Paleogene deposits of Armenia by planktonic foraminifers , nannoplankton and nummulites. (Pt. I. Reference paleogene sections of Armenia). *Voprosy Mikropaleontologii*, Leningrad-Moskva, vol. 27, p. 130-169 (en russe).

KRASHENINNIKOV V. A. et NEMKOV G. I. (1975) : Relationship between the faunas of planktonic foraminifers and Nummulites in Paleogene deposits of Syria. *Voprosy Mikropaleontologii*, Leningrad-Moskva, vol. 18, p. 179-211 (en russe).

KRASHENINNIKOV V. A. et PTUKHIAN A. E. (1986) : Stratigraphical subdivision of Armenian Paleogene deposits by planktonic microfossils and *Nummulites* (regional stratigraphy, zonal scales by planktonic and benthic microfossils, their correlation). *Voprosy Mikropaleontologii*, Leningrad-Moskva, vol. 28, p. 60-99 (en russe).

LAFONT F. (1994) : Influences relatives de la subsidence et de l'eustatisme sur la localisation et la géométrie des réservoirs d'un système deltaïque. Exemple de l'Eocène du bassin de Jaca (Pyrénées espagnoles). *Thèse doct.*, Univ. Rennes I., 258 p.

MATHELIN J.C. et SZTRÁKOS K. (1993) : L'Eocène de Biarritz (Pyrénées Atlantiques, SW France). Stratigraphie et paléoenvironnement. Monographie des foraminifères. *Cah. Micropal.*, Paris, n. sér., vol. 8, n° 1, p. 5-85, 48 pl.

MEDJADJ F. (1985) : Une zone de confluence deltaïque en domaine compressif : le delta paléogène de Jaca dans le secteur de Sabiñanigo. *Thèse doct.*, Univ. Pau, 417 p.

MILLÁN H., AURELL M. et MELENDEZ A. (1994) : Synchronous detachment folds and coeval sedimentation in the Prepyrenean External Sierras (Spain) : a case study for tectonic origin of sequences and system tracts. *Sedimentology*, Amsterdam, vol. 41, p. 1001-1024.

MOLINA E., ORTIZ N. et SERRA-KIEL J. (1988) : Implicaciones paleoecológicas de los foraminíferos en el Eoceno del Prepirineo oscense (sector de Arguis). *Rev. esp. Micropal.*, Madrid, vol. 3, p. 45-57.

NUÑEZ DEL PRADO H. (1986) : Systèmes de dépôt et évolution sédimentaire des séries de transition marin-continental dans le synclinorium du Rio Guargua. *Thèse doct.*, Univ. Pau, 350 p.

PARISI G., GUERRERA F., MADILE M., MAGNONI G., MONACO P., MONECHI S. et NOCCHI M. (1988) : Middle Eocene to Early Oligocene calcareous nannofossil and foraminiferal biostratigraphy in the Monte Cagnero section, Piobbico (Italy). Internat. Subcomm. Paleog. Strat. E/O Meeting, Ancona, oct. 1987. Spec. Publ. 2, p. 119-135.

POSAMENTIER H.W. et VAIL P.R. (1988) : Eustatic controls on clastic deposition II. Sequence and systems tract models. C.K. Wilgus (Editeur), Sea level changes – An integrated approach. *SEPM Spec. Publ.*, Tulsa, Okl., 42, p.126-154.

PUYGDEFÁBREGAS C. (1975) : La sedimentación molasica en la cuenca de Jaca. *Monografias del Instituto de Estudios Pirenaïcos*, Jaca, vol. 104, 204 p.

SCHAUB H. (1981) : Nummulites et assilines de la Téthys paléogène. *Mém. suisses Paléont.*, Basel, vol. 104-106, 227 p.

SHCHERBINA E. A. (2000) : Middle Eocene nannofossils and geological events of the northeastern peri-Tethys. *GFF*, Stockholm, vol. 122, p. 143-145.

SEGURET M. (1972) : Etude tectonique des nappes et séries décollées de la partie centrale du versant sud des Pyrénées. *Publ.*

*Univ. Sci. et Techn. du Languedoc, Sér. Géologie Structurale*, Montpellier, vol. 2, 155 p.

SERRA-KIEL J., HOTTINGER L., CAUS E., DROBNE K., FERRANDEZ C., JAUHRI A. K., LESS G.Y., PAVLOVEC R., PIGNATTI J., SAMSO J. M., SCHAUB H., SIREL E., STROUGO A., TAMBAREAU Y., TOSQUELLA J. et ZAKREVSKAYA E. (1988) : Larger foraminiferal biostratigraphy of the Tethyan Paleocene and Eocene. *Bull. Soc. géol. France*, Paris, vol. 169, n° 2, p. 281-299.

STROUGO A. (1992) : The Middle Eocene/Upper Eocene transition in Egypt reconsidered. *Neues Jahrbuch Geol. Paläont.*, Stuttgart, Abhandl., vol. 186, n° 1-2, p. 71-89.

SZTRÁKOS K. (2000) : Les foraminifères de l'Eocène du Bassin de l'Adour (Aquitaine, France) : biostratigraphie et taxinomie. *Rev. Micropaléont.*, Paris, vol. 43, n° 1-2, p. 71-172.

SZTRÁKOS K., GÉLY J.P., BLONDEAU A. et MÜLLER C. (1998) : L'Eocène du Bassin sud-aquitain : lithostratigraphie,biostratigraphie et analyse séquentielle. *Géologie de la France*, Orléans-Paris, vol. 4, p. 57-105.

TEIXELL A. et BARNOLAS A. (1995) : Significado de la discordancia de Mediano en relación con las estructuras adyacentes (Eoceno, Pirineo Central). *Geogaceta*, Madrid, vol. 18, p. 34-37.

TOLEDO M. J. (1990) : Séquences de dépôts et cyclicité tectonique dans l'Eocène du bassin de Jaca (Espagne). *Mém. ENSPM* (Inst. Fr. Pétr.), Rueil-Malmaison, 156 p.

TOLEDO M. J. (1991) : Secuencias deposicionales y fases tectónicas en el Eoceno de la cuenca de Jaca. I. Congr. del Grupo Esp. Terciario, Vic (Barcelona), communic., p. 329-333.

TOUMARKINE M. et LUTERBACHER J.P. (1985) : Paleocene and Eocene planktic foraminifera. *In* : Bolli H. M., Saunders J. B. et Perch-Nielsen K. : Plankton stratigraphy. Cambridge University Press, Cambridge, p. 87-154.

## 2.2. Implications pour l'interprétation des strates de croissance

L'étude de terrain du chapitre précédent a mis en évidence la distorsion des séquence haute-fréquence par la déformation. Cet effet est dû au fait que les strates enregistrent de manière différente une déformation même continue selon le type de sédimentation en cours. Nous développons ce point car les cycles stratigraphiques haute-fréquence sont les briques élémentaires de toutes les accumulations sédimentaires.

Dans les contextes de sédimentation syntectonique, ces cycles induisent une alternance entre des processus qui comblent ou drapent les topographies d'origine tectonique, et les dépôts vont ainsi être alternativement épaissis et isopaques au passage des structures de croissance même si celles-ci se développent de manière continue. Deux implications majeures en découlent :

1) les études à haute-résolution de la cinématique des plis et failles de croissance qui font l'hypothèse d'une sédimentation comblant instantanément les topographies créées par la déformation courrent le risque de confondre la cyclicité naturellement présente dans l'enregistrement sédimentaire pour une cyclicité tectonique, i.e. une alternance de phases d'activité et de quiescence, alors que la tectonique est continue;
2) dans le cas où les structures de croissance se développent de manière continue, les alternances de strates épaissies et non épaissies témoignent de périodes de sédimentation dynamique et non dynamique respectivement, permettant ainsi de déterminer au premier ordre la répartition des sables et des argiles à partir d'un profil sismique.

## 2.2.1. Strates de croissance et cinématique à court-terme de la déformation (10's à 100's ka)

---

Article :

## How reliable are growth strata in interpreting short-term (10's to 100's ka) growth structures kinematics?

Sébastien Castelltort, Stéphane Pochat and Jean Van Den Driessche

Géosciences Rennes, Campus de Beaulieu, 35042 Rennes cedex - France

*Submitted to Comptes Rendus Géosciences (Comptes Rendus de l'Académie des Sciences - Series IIA - Earth and Planetary Science*).

---

## Abstract

**High-frequency stratigraphic cycles (10's to 100's ka), often show, at a specific location, an alternance of "dynamic" (proximal-energetic), and "non-dynamic" (distal-pelagic) processes with time. When sedimentation is syn-deformation, these processes tend respectively to fill-up tectonically-induced topography or to drape it. As a consequence, growth strata are alternatively thickened and isopach across the growth structure. High-resolution kinematic studies of growth structures (folds and faults), which assume that sedimentation always fill-up topographies ("fill-to-the-top" model), may therefore mistake sedimentary cyclicity for tectonic cyclicity. We adress this problem with one example of growth anticline in the spanish Pyrenees, and we discuss the fill-to-the-top model.**

## Résumé

**Les cycles stratigraphiques haute-fréquence (10s-100s ka) montrent souvent une alternance de processus dynamiques (proximaux-énergétiques) et non-dynamiques (distaux-pelagiques). Lorsque la sédimentation est syn-déformation, ces processus comblent ou drapent respectivement les topographies d'origine tectonique, les dépôts sont ainsi alternativement épaissies et isopaques au passage des structures de croissances. Les études à haute-résolution de la cinématiques des plis et failles synsédimentaires faisant l'hypothèse d'une sédimentation comblant toujours les topographies (modèle « fill-to-the-top »), risquent de confondre cyclicité sédimentaire et cyclicité tectonique. Nous analysons ce problème sur l'exemple d'un pli synsédimentaire dans les Pyrénées espagnoles, et discutons l'hypothèse du modèle « fill-to-the-top ».**

*Version française abrégée*

## 1. Introduction

Nous savons d'après l'observation des séismes que les failles ont des mouvements discontinus sur des courtes périodes (< 10 ka). Cependant, leurs comportements sur des périodes plus grandes(> 10 ka) reste problématique. La déformation peut-elle être considérée comme continue ou discontinue sur des échelles de temps de l'ordre de la dizaine à plusieurs centaines de ka ? Des études néotectoniques récentes penchent en faveur de l'hypothèse continue (e.g. [26, 28]). Au contraire, à partir de l'analyse des strates de croissances sur des failles ou des plis synsédimentaires, de nombreux travaux invoquent une tectonique épisodique sur ces mêmes échelles de temps (e.g. [1, 3, 15, 16]). Cette cyclicité tectonique est basée sur l'alternance existant entre des dépôts épaissis et isopaques.

Dans ce travail, à partir de l'analyse des relations entre déformation et sédimentation sur un exemple de pli syn-sédimentaire (Pico del Aguila, Pyrénées espagnoles), nous discutons ces conclusions qui, selon nous, ne prennent pas en compte la nature variable de la sédimentation, en particulier à haute-fréquence (10's à 100's ka).

## 2. L'exemple de l'anticlinal du Pico del Aguila

L'anticlinal du Pico del Aguila, d'axe N-S, est situé à la limite entre les bassins de l'Ebre et de Jaca dans le nord de l'Espagne (fig.1). Il affecte des séries crétacé/éocène inférieur sur un décollement situé dans les évaporites du trias, et se développe de la fin du Lutétien au début du Priabonien contemporainement à la progradation d'Est en Ouest d'un appareil deltaïque [17]. Les dépôts synsédimentaires sont fortement épaissis dans le synclinal (1200 m) par rapport au sommet de l'anticlinal (300 m). L'architecture séquentielle est constituée de six cycle régressif-transgressif (cycles 1 à 6, fig. 2) de durées comprises entre 90 et 850 ka [5], qui sont eux-même composés de séquences à plus haute fréquence de durée de l'ordre de 100 ka (paraséquences). Ces séquences correspondent à des phases d'avancé/recul du delta [5, 13] et sont parfois corrélées à l'échelle du bassin [13], ce qui leur confère une origine de longueur d'onde supérieure au pli (e.g. eustatisme, tectonique, climat).

Les phases de progradation sont marquées par une sédimentation terrigène sableuse et toujours plus épaisses que les phases de rétrogradation qui sont caractérisées par des dépôts plus marneux et carbonatés (fig. 3). Dans l'ensemble, les paraséquences sont plus épaisses vers le synclinal que sur son sommet. Cependant, les phases de fin de progradation/aggradation, plus sableuses (dépôts proximaux), sont plus épaissies, alors que

les phases de début de progradation/rétrogradation, qui sont plus marneuses et carbonatées (dépôts distaux), montrent pas ou peu d'épaississement.

Deux interprétations existent : soit (1) la croissance du pli est épisodique et donne lieu à des épaississements pendant les phases d'activité, et à des strates isopaques pendant les phases de quiescence, soit (2) le pli étant controllé à la base par un décollement, il se comporte globalement de manière ductile, sa croissance est continue, et la configuration des strates de croissance est le résultat de la superposition d'une sédimentation variable sur un taux de croissance constant [4, 5].

Pendant la progradation, la sédimentation est « dynamique », i.e. sableuse, et est préférentiellement piégée dans les creux topographiques (synclinaux) créés par la déformation. Pendant la rétrogradation la sédimentation est « non-dynamique », i.e. plus pélagique et carbonatée, et nappe la topographie sans épaississement vers les synclinaux .

**3. Discussion-conclusion**

Des travaux récents (e.g. [1, 3, 15, 16]) ont interprété le même type d'observations comme résultant d'une tectonique discontinue (fig. 4A), en prenant pour hypothèse que la sédimentation remplit toujours la topographie créée par la tectonique, ou modèle « fill-to-the-top » [10].

Nous contestons ce modèle car l'enregistrement stratigraphique est, par nature, constitué de cycles à toutes les échelles de temps et d'espace, liés à des facteurs tels que l'eustatisme, la tectonique ou le climat (e.g. [11, 22]). En particulier, les variations climatiques induisent des cycles stratigraphiques à haute fréquence (10's à 100's ka), ou paraséquences. Ces cycles s'expriment fréquement, au cours du temps, par l'alternance entre des processus dynamiques (courants, vagues, marées), et non-dynamiques (décantation).

Les études ayant pour but, de déterminer la cinématique des structures de croissances doivent prendre en compte le fait que les strates de croissances enregistrent au moins la superposition de deux signaux : (1) la cyclicité sédimentaire inhérente à l'enregistrement stratigraphique, et (2) la subsidence différentielle locale due à la déformation.

En particulier, l'occurrence périodique de processus non-dynamiques (pélagique) peut conduire à la préservation d'escarpement topographiques d'origine tectonique [18, 20, 27, 29].

De ce fait, les travaux utilisant les variations d'épaisseurs selon le modèle "fill-to-the-top" et concluant à un fonctionnement épisodiques des failles, avec la même périodicité que les cycles stratigraphiques peuvent aussi bien être considérés comme mettant en évidence un

déplacement continu (fig. 4B) sur ces échelles de temps (10’s to 100’s ka). Cette interprétation est plus en accord avec les études néotectoniques récente qui mettent en évidence un taux de fonctionnement constant des failles crustales sur des périodes supérieures à 100 ka [26, 28].

*English version*

## 1. Introduction

It is a currently observable and historically documented fact through earthquakes that movements on faults are episodic on short time scales (< 10 ka). However, less is known for time scales of more than 10 ka, i.e. beyond historical documentation. The key problem is: is deformation a continuous or a discontinuous process over time scales ranging from 10's to 100's of thousands years? Neotectonics studies, by surface dating of crustal strike-slip faults offsets, have recently evidenced constant slip rates over such periods (e.g. [26, 28]), which would best support the continuous hypothesis. By contrast, in sedimentary basins, numerous works have argued for episodic development of intra-basin growth structures (faults and folds) with periods of 10's to 100's of thousands years (e.g. [1, 3, 15, 16]). These are based on the observation of growth strata which are alternatively thickened and of equal thickness across structures.

In this paper, we propose that such a pattern can instead be interpreted as the result of a continuous growth (of fault or fold) superimposed on variable sedimentation. To do this, we first examine the relation between growth strata thickness variations and the nature of sedimentation in the case of a growth detachment-fold. Then, we discuss the "fill-to-the-top" model, which consists in assuming that sedimentation always fill the topographies created by growth structures, and its application to fault and fold kinematics reconstruction.

## 2. The Pico del Aguila anticline example

The Pico del Aguila anticline is situated on the South-Pyrenean Frontal-Thrust (SPFT), at the separation between the Jaca and the Ebro basins in northern Spain (Fig. 1). It is a ~5 km wide anticline which is one of a series of N-S trending folds called the "Sierras marginales" which developed during middle to late Eocene times in response to the southward advance of the South-Central Pyrenean Unit (SCPU). The deformation affects a pretectonic sedimentary layer composed mainly of ~800 m of Lutetian limestones which are detached over a 600 to 800 m ductile unit dominated by triassic evaporites.

From end Lutetian to early Priabonian, the anticline developed in a subsiding basin which was coevally filled by a delta prograding from East to West. As a consequence, during its development the fold was progressively buried by sediments which now exhibit progressive unconformities on both sides of the anticline and thickness variations from ~1200 m in the

synclines to ~300 m on the hinge (Fig. 2). The current attitude of the anticline which plunges ~30° to the North and its intersection with the topography result today in a good exposure of the growth strata. This allows to follow them physically across the fold from Arguis syncline to Belsue syncline (Fig. 2). Sedimentary facies are mainly terrigenous and reflect the westward progradation of the delta [17]. They range from prodelta marls to mouth-bar coarse sandstones, some of these showing evidences of tides and storms influences. In addition carbonates are also present, probably due to the destruction and redistribution by storms of a carbonate platform situated southward and of nummulites patch reefs developing in protected (from siliciclastic input) areas as also evidenced in the eastern part of the south-Pyrenean foreland during Bartonian times [14].

The sequence stratigraphic framework of these deposits is made of six fourth-order regressive-transgressive cycles (cycles 1 to 6, fig. 2) of duration ranging between 90 and 850 ka [4, 5]. They are themselves composed of stacked high frequency regressive-transgressive cycles (called parasequences in the following), of durations on the order of 100 ka or less.

### 2.1 Parasequences

As a whole, the expression of parasequences can be summarized as follows: progradation phases are markedly terrigenous and always thicker than retrogradation phases which are more carbonated and marly. This results from the volumetric partitionning [7] of sediments in a marine deltaic setting: the detritic supply is mainly stocked in the marine realm (delta) during progradation, whereas it is trapped landward during retrogradation, which allows the expression of carbonates seaward. These parasequences therefore record high-frequency cycles of advance and retreat of the delta. As shown in [13] and [4, 5], they can often be followed across the fold and sometimes at basin scale. The parasequences are therefore controlled by a phenomena of broader extent than the structure, i.e. eustatic, basin-scale tectonics or sediment input variations.

In this work, we focus on the expression of parasequences (Fig. 3) of cycle 5 (Fig. 2) situated between the hinge of the anticline and the western syncline, because they can be particularly well followed there.

As a whole, parasequences are thicker toward the syncline and condensated on the hinge of the anticline because accommodation space increases toward synclines. More in detail, we observe that most of the thickness expansion takes place during end-progradation and aggradation periods, when deposits are proximal and more sandy in proportion. This is expressed by the time equivalence of proximal delta-front facies on the west flank with a by-

pass/erosive surface on the hinge. By contrast, retrogradation and early progradation, are far less affected by the growth of the fold, and are nearly of equal thickness on the hinge and in the syncline.

**2.2 Interpretation**

Two main interpretations are possible: (1) the fold growth could have been episodic (discontinuous) with periods of activity during end-progradation/aggradation periods explaining the thickening at this moment, and periods of quiescence during retrogradation/early-progradation periods, explaining the isopach layer at this moment, (2) alternatively, the fold growth could also have taken place as a continuous process, with this pattern of thickened and isopachs sedimentary layers being only the result of variable sedimentation superimposed on a constant rate of fold growth [4, 5].

The second interpretation is favoured here because the Pico del Aguila anticline is a detachment fold [17, 23], i.e. developed over a ductile basal decollement. This strongly suggests that the fold has grown continuously as long as no strain accumulation is possible in the ductile layer. The fold growth may therefore be entirely controlled by the decollement, and behave as a whole in a ductile manner. However, this only means that fold growth should be continous rather than episodic. Indeed, [5] have shown that fold growth has taken place with a variable rate over timescales of several 100's of thousands years.

With this hypothesis of a continous growth, why are end-progradation/aggradation periods thickened toward the syncline, and retrogradation/early-progradation of more equal thickness across the fold?

During retrogradation and early progradation periods the sedimentation is distal (marls) and dominated by particle settling (decantation), carbonates production and redistribution by storms. This induces almost equal sedimentary thicknesses on highs and lows. By contrast during end-progradation, sedimentation processes are more "dynamic" (i.e. energetic), and are preferentially trapped in topographic lows [25]. Moreover, the lowering of base-level imposes for sedimentation to take place only in structural lows, i.e.toward synclines. Indeed, the hinge of the anticline, where by-pass or erosion surfaces are recorded, may be aerial or subaerial during progradation.

The important point which is put forward through this example is the first-order dichotomy between "dynamic" (energetic) and "non-dynamic" (decantation) sedimentary processes with regard to the syntectonic thicknesses. Non-dynamic sedimentary processes drape topography

with a homogeneous thickness of sediments, while dynamic processes preferentially fill-up topographic lows before highs.

### 3. The "fill-to-the-top" model: discussion

Recent works [1, 3, 15, 16, 19] have used similar observations to argue for the episodic development of growth faults and folds, with periods in the range of 10's to 100's ka. In those studies, it is assumed that thickened strata reflect tectonic activity, whereas strata with equal thickness across structures reflect tectonic quiescence. Actually, those studies make the strong assumption that sedimentation always fill-up the topography created by tectonic movement, or "fill-to-the-top" assumption [9]. Moreover, certain authors, such as [1, 3, 15] note that the periodicity of fault activity is correlated with the cyclic stratigraphy. In particular, quiescence is in phase with retrogradation (fine-grained) periods and activity corresponds to progradation (more coarse-grained) periods. This leads them to invoke a coupling between fault activity and sediment loading in a gravity driven context, and even, for periods such as the cenozoic, an astronomic control on fault activity [15]. However, we should point out that, because the fill-to-the-top model implies a constant filling of the topography created by the fault, the load should never diminishes and should therefore maintain fault activity, unless fault scarps are developed which is in contradiction with the model statement. By this way, using the fill-to-the-top model requires to consider implicitly that deformation is controlled by sedimentation. Also, we note that the loading/unloading mechanism, that is supposed to be responsible for the cyclic activity of growth faults, remains to be quantified.

As explained above, in the case studied herein, the same observations lead us to rather different conclusions because the Pico del Aguila anticline is linked to a basal decollement and due to compression [2, 23, 24]. This means that the fold is not associated to a gravity instability and is therefore not sensitive to small-scale cycles of sediment loading/unloading. Also, as long as parasequences are of broader origin than the fold, there is no reason that fold activity should occur during progradation periods, and fold quiescence during retrogradation. Also, similar growth strata patterns have been documented in other compressive [10] and extensive [12, 21] settings, without being interpreted as alternative phases of tectonic activity and quiescence. In consequence, for growth folds as for growth faults, the alternance between thickness expansion and continuity across structures needs not being related to a cyclic tectonic activity. Rather, it should simply be related to cyclically varying sedimentary processes superimposed on a continuous structure growth. Indeed, the fill-to-the-top model, imply that sedimentary processes are uniform throughout the deformation (Fig. 4A), i.e. on

time scales of more than 10's ka. However, it has been known for a long time that due to numerous factors, such as eustasy, tectonics, or climate, the stratigraphic record is, by nature, made of cycles at all time and space scales (e.g. [11, 22]). In particular, climate acts on eustasy and sediment supply to produce stratigraphic cycles with periods on the order of 10's to 100's ka (parasequences). At a given location in a basin this is expressed by a variation with time of the type of sedimentation and sedimentary processes. In marine deltaic parasequences for example, the volumetric partitionning of sediments induces, schematically, an alternance of large input of coarse materials supplied dynamically (currents, waves, tides) during progradation, and smaller input of finer particles mainly deposited at low energy (settling) during retrogradation [7]. Generally speaking, in all depositional settings, the sedimentation is characterized by such alternances between energetic/dynamic and calm/non-dynamic periods. These different processes react differently to differential subsidence due to growth faulting or folding. Non-dynamic (pelagic) sedimentation can be distributed homogeneously across structures [3, 15] without being diffused to topographic lows on time scales of 10's to 100's ka [18, 29]. This leads to the creation of fault- or fold-induced topography (e.g. [20, 27]) when structures are active during non-dynamic sedimentation (Fig. 4B). Along with deformation, sedimentation is likely to be made of processes which alternatively fill-up and drape topography with periods of 10's to 100's ka. This is why the "fill-to-the-top" assumption may not be valid for most natural cases, and in particular during periods of strong climatic variations.

Kinematic analysis based on this assumption are therefore likely to mistake sedimentation cycles for tectonic activity cycles.

The same conclusions are also applicable for studies based on seismic profiles, because boundaries between sedimentary units depicted from seismics are likely to represent changes of lithologies and sedimentary processes. This also induces a potential bias in relating syntectonic strata thickness variations to growth structures kinematics from seismic data.

Eventually, it can be pointed out that, using sedimentary cycles to infer tectonic cyclicity and concluding on a causal relationship between sedimentation and tectonics should be made with caution to avoid any circular reasonning.

## 4. Conclusion

Studies attempting to infer the kinematics of intra-basin faults and folds should be aware that growth strata always record the superimposition of at least two signals: (1) the sedimentary

cyclicity inherent to the stratigraphic record and (2) the local differential subsidence due to growth faulting or folding.

In particular the periodic occurrence of non-dynamic (pelagic) processes can lead to fault- or fold-induced topographies. This underscores the need for quantification of synsedimentary topographies and the search for accurate paleobathymetric indicators, and potential sedimentary processes disturbances.

At the moment, works that have used growth strata with simple "fill-to-the-top" assumptions and concluded on the episodic development of faults and folds with the same periodicities as stratigraphic cycles, could as well be taken as evidences of constant slip rates on time scales of 10's to 100's ka. This would be more in line with recent neotectonics studies using cosmogenic radionuclides which have evidenced constant slip rates on crustal faults over periods of up to 110 ka [26, 28].

Our reasonning also raises questions regarding growth strata thickness variations and episodicity of tectonics on greater times scales of $10^6$-$10^7$ a (e.g. [6]) as long as stratigraphic cycles also naturally exist at those time scales.

**References**

[1] Bhattacharya J.P., Davies R.K., Growth faults at the prodelta to delta-front transition, Cretaceous Ferron sandstone, Utah, Mar. Petr. Geol. 18 (2001) 525-534.

[2] Blin B., Mitouard P., Le frond sud-pyrénéen: bordure sud du bassin de Jaca - tectonique et modélisation analogique, pp. 141, Rap. Int. ENSPM (Institut Francais du Petrole), 1990.

[3] Cartwright J., Bouroullec R., James D. , Johnson H., Polycyclic motion history of some Gulf Coast growth faults from high-resolution displacement analysis, Geology 26 (9) (1998) 819-822.

[4] Castelltort S., Guillocheau F., Nalpas T., Rouby D., Robin C., De-Urreiztieta M. , Coutand I., Tectonically induced distorsion of stratigraphic cycles - Example of the Arguis anticline in the south-central Pyrenees (Spain)., Geotemas 2 (2000) 55-58.

[5] Castelltort S., Guillocheau F., Robin C., Rouby D., Nalpas T., Lafont F., Eschard R., Fold control on the stratigraphic record: a quantified sequence stratigraphic study of the Pico del Aguila anticline in the South-western Pyrenees (Spain), Basin Res. (submitted)

[6] Contreras J., Anders M.H. , Scholz C.H., Growth of a normal fault system: observations from the Lake Malawi basin of the east African rift, J. Struct. Geol. 22 (2000) 159-168.

[7] Cross T.A. , Lessenger M.A., Sediment volume partitioning: rationale for stratigraphic model evaluation and high-resolution stratigraphic correlation, in: Sequence Stratigraphy - Concepts and Applications, F.M. Gradstein, K.O. Sandvik and N.J. Milton, eds., Norwegian Petroleum Society (NPF) Special Publications 8, pp. 171-195, Elsevier, 1998.

[8] ECORS Pyrenees Team., The ECORS deep reflection seismic survey across the Pyrenees, Nature 331 (6156) (1988) 508-511.

[9] Gawthorpe R., Hardy S., Extensional fault-propagation folding and base-level change as controls on growth-strata geometries, Sediment. Geol. 146 (2002) 47-56.

[10] Gawthorpe R.L., Hall M., Sharp I. , Dreyer T., Tectonically enhanced forced regressions: examples from growth folds in extensional and compressional settings, the Miocene of the Suez rift and the Eocene of the Pyrenees, in: Sedimentary Responses to Forced Regressions, D. Hunt and R.L. Gawthorpe, eds., Geological Society of London Special Publications 172, pp. 177-191, 2000.

[11] Guillocheau F., Nature, rank and origin of Phanerozoic sedimentary cycles, C. R. Acad. Sci. Paris 320 (1995) 1141-1157.

[12] Hiscott R.N., Depositional sequences controlled by high rates of sediment supply, sea-level variations, and growth faulting: the Quaternary Baram Delta of northwestern Borneo, Mar. Geol. 175 (2001) 67-102.

[13] Lafont F., Influences relatives de la subsidence et de l'eustatisme sur la localisation et la géometrie des reservoirs d'un système deltaique. Exemple de l'Eocene du bassin de Jaca (Pyrenees espagnoles), PhD Thesis, University of Rennes, France, 1994.

[14] Lopez-Blanco M., Stratigraphy and sedimentary development of the Sant-Llorenç del Munt fan-delta complex (Eocene, southern Pyrenean foreland basin, northeast Spain), in: Tectonic Controls and Signatures in Sedimentary Successions, L.E. Frostick and R.J. Steel, eds., International Association of Sedimentologists (IAS) Special Publications 20, pp. 67-88, Blackwell, 1993.

[15] Lowrie A., Model for fine-scaled movements associated with climate and sea-level changes along Louisiana shelfbreak growth faults, Gulf Coast Association of Geological Societies Transactions 36 (1986) 497-509.

[16] Masaferro J.L., Bulnes M., Poblet J. , Eberli G.P., Episodic folding inferred from syntectonic carbonate sedimentation: the Santaren anticline, Bahamas foreland, Sediment. Geol. 146 (2002) 11-24.

[17] Millán H., Aurell M. , Meléndez A., Synchronous detachment folds and coeval sedimentation in the Prepyrenean External Sierras (Spain): a case study for a tectonic origin of sequences and systems tracts, Sedimentology 41 (1994) 1001-1024.

[18] Mitchell N.C., Creep in pelagic sediments and potential for morphologic dating of marine fault scarps, Geophys. Res. Lett. 23 (1996) 483-486.

[19] Morley C.K., Vanhauwaert P. , De Batist M., Evidence for high-frequency cyclic fault activity from high-resolution seismic reflection survey, Rukwa Rift, Tanzania, J. Geol. Soc. London 157 (2000) 983-994.

[20] Morris S.A., Alexander J., Kenyon N.H. , Limonov A.F., Turbidites around an active fault scarp on the Lower Valencia Fan, northwest Mediterranean, Geo-Mar. Lett. 18 (1998) 165-171.

[21] Newell A.J., Fault activity and sedimentation in marine rift basin (Upper Jurassic, Wessex Basin, UK), J. Geol. Soc. London 157 (2000) 83-92.

[22] Nystuen J.P., History and development of sequence stratigraphy, in: Sequence Stratigraphy - Concepts and Applications, F.M. Gradstein, K.O. Sandvik and N.J. Milton, eds., Norwegian Petroleum Society (NPF) Special Publications 8, pp. 31-116, Elsevier, 1998.

[23] Poblet J. , Hardy S., Reverse modelling of detachment folds; application to the Pico del Aguila anticline in the South Central Pyrenees (Spain), J. Struct. Geol. 17 (12) (1995) 1707-1724.

[24] Seguret M., Etude tectonique des nappes et séries décollées de la partie centrale du versant sud des Pyrénées. Caractère synsédimentaire, rôle de la compression et de la gravité., 155 pp., Publ. Univ. Sci. Tech. Languedoc, Montpellier, France, 1972.

[25] Shaw J.H., Novoa E. , Connors C.D., Structural controls on growth stratigraphy, in: Thrust Tectonics, K. McClay, ed., pp. 80-82, London, 1999.

[26] Tapponnier P., Ryerson F.J., VanDerWoerd J., Meriaux A.-S. , Lasserre C., Long-term slip rates and characteristic slip: keys to active fault behaviour and earthquake hazard, C. R. Acad. Sci. Paris, Sciences de la Terre 333 (2001) 483-494.

[27] Thornburg T.M., Kulm L.D. , Hussong D.M., Submarine-fan development in the southern Chile Trench: A dynamic interplay of tectonics and sedimentation, Geol. Soc. Am. Bull. 102 (1990) 1658-1680.

[28] Van der Woerd J., Ryerson F.J., Tapponnier P., Meriaux A.-S., Gaudemer Y., Meyer B., Finkel R.C., Caffee M.W., Guoguang Z. , Zhiqin X., Uniform Slip-Rate along the Kunlun Fault: Implications for seismic behaviour and large-scale tectonics, Geophys. Res. Lett. 27 (16) (2000) 2353-2356.

[29] Webb H.F. , Jordan T.H., Pelagic sedimentation on rough seafloor topography 1. Forward Model, J. Geophys. Res. 106 (B12) (2001) 30433-30449.

**Figures captions/Légende des figures**

Figure 1.

Simplified structural map of the Pyrenees (modified from [8]) with location of the Pico del Aguila anticline (black star). SPFT: South-Pyrenean Frontal Thrust. SCPU: South-Central Pyrenean Unit. The grey colour delineates the hercynian basement.

Carte structurale simplifiée des Pyrénées (modifiée d'après [8]) montrant la localisation de l'anticlinal du Pico del Aguila (étoile noire). SPFT : chevauchement frontal sud-pyrénéen. SCPU : unité central sud-pyrénéene. Le grisé délimite le socle hercynien.

Figure 2.

East-West cross-section of the Pico del Aguila anticline showing large-scale sequence-stratigraphic framework (cycles 1 to 6) and facies (modified from [5]). The parasequences grossly represent the small-scale lithology variations on the sedimentologic vertical cross-sections.

Coupe Est-Ouest de l'anticlinal du Pico del Aguila montrant l'architecture séquentielle générale (cycles 1 à 6) et les faciès (modifiée d'après [5]). Les parasequences représentent grossièrement les variations de lithologie à petite échelle sur les coupes sédimentologiques verticales.

Figure 3.

Illustration showing the variable expression of a parasequence between the hinge of the anticline (S3) and the western flank (S2) during cycle 5. Sandy facies of end-progradation/aggradation phase are thickened toward the syncline, whereas marls and carbonates of early-progradation/retrogradation phase are nearly of equal thickness across the fold.

Illustration mettant en évidence l'expression variable d'un exemple de paraséquence entre le sommet de l'anticlinal (S3) et son flanc ouest (S2), pendant le cycle 5. Les faciès les plus sableux de fin de progradation/aggradation s'épaississent vers le synclinal, alors que les faciès marneux et les carbonates gardent une épaisseur égale sur toute la structure.

Figure 4.

Sketch illustrating the two opposed end-members hypotheses discussed in this work: both lead to the same final growth strata pattern. A) Discontinuous deformation and "fill-to-the-top" sedimentation. Fault growth occurs only during intervals 0-1, 2-3, and 4-5. Sedimentation always fill-up topography. B) Continuous deformation and variable sedimentation. The fault is always active, but topography is alternatively filled-up and draped by dynamic and non-dynamic processes respectively.

Schéma illustrant l'opposition entre les deux hypothèses discutées dans cette étude : elles aboutissent toutes les deux à la même configuration finale. A) déformation discontinue at sédimentation « fill-to-the-top ». La croissance de la faille n'a lieu que pendant les intervalles 0-1, 2-3, et 4-5. La sédimentation comble toujours la topographie. B) Déformation continue et sédimentation variable. La faille est toujours active, mais la topographie est alternativement comblée et drapée par des processus respectivement dynamiques et non-dynamiques.

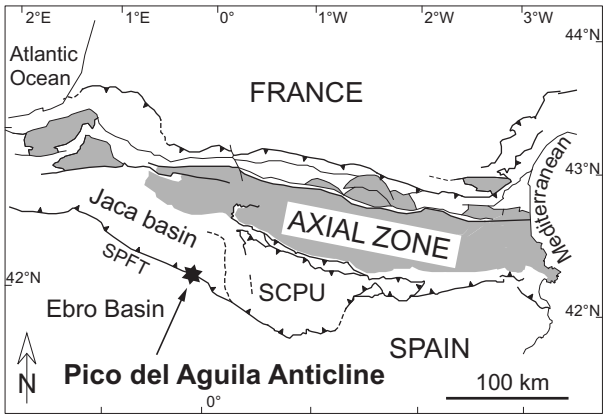
2°E
1°E
0°
1°W
2°W
3°W
44°N
43°N
42°N
42°N
0°
Atlantic
Ocean
FRANCE
AXIAL ZONE
Jaca basin
SPFT
SCPU
Ebro Basin
Mediterranean
SPAIN
Pico del Aguila Anticline
N
100 km

FIGURE 1

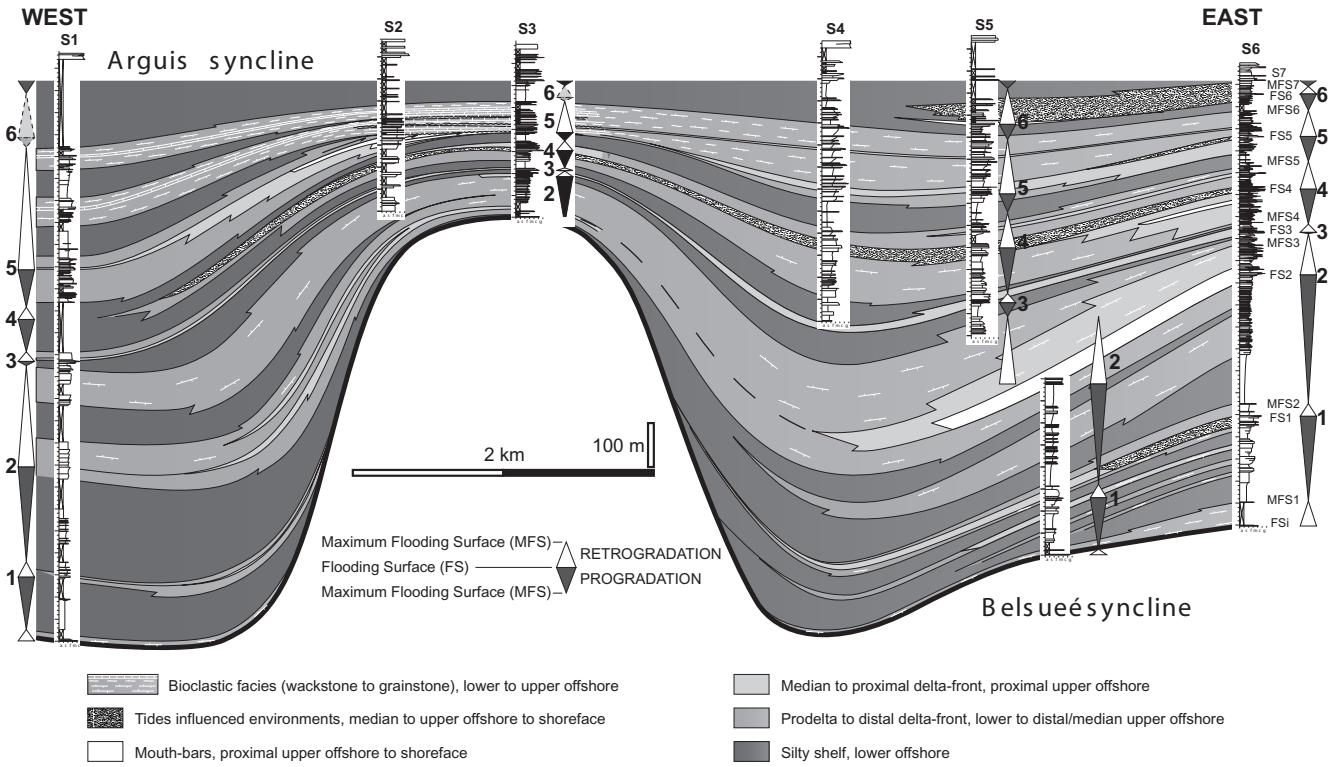
WEST
EAST
S1
S2
S3
S4
S5
S6
S7
Arguis syncline
Belsueé syncline
2 km
100 m
Maximum Flooding Surface (MFS)
Flooding Surface (FS)
Maximum Flooding Surface (MFS)
RETROGRADATION
PROGRADATION
MFS7
FS6
MFS6
FS5
MFS5
FS4
MFS4
FS3
MFS3
FS2
MFS2
FS1
MFS1
FSi
Bioclastic facies (wackstone to grainstone), lower to upper offshore
Tides influenced environments, median to upper offshore to shoreface
Mouth-bars, proximal upper offshore to shoreface
Median to proximal delta-front, proximal upper offshore
Prodelta to distal delta-front, lower to distal/median upper offshore
Silty shelf, lower offshore

FIGURE 2

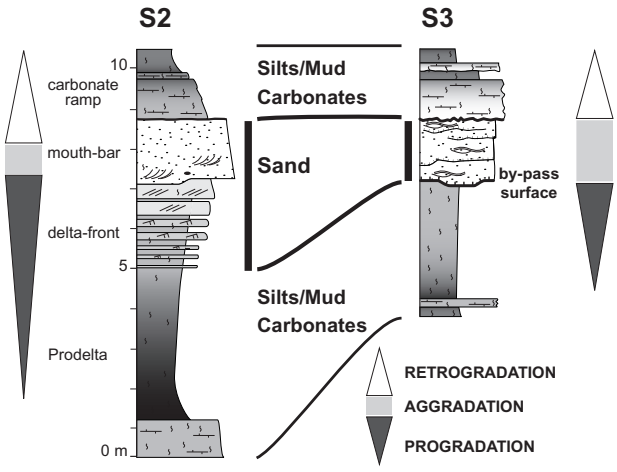
S2
S3
10
carbonate ramp
mouth-bar
delta-front
5
Prodelta
0 m
Silts/Mud Carbonates
Sand
Silts/Mud Carbonates
by-pass surface
RETROGRADATION
AGGRADATION
PROGRADATION

FIGURE 3

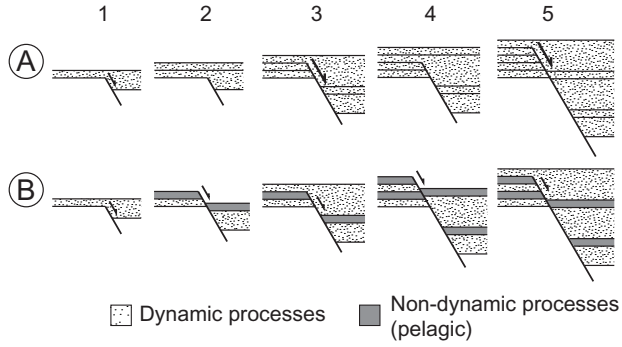


FIGURE 4

## 2.2.2. Méthode de détermination des variations lithologiques à partir des strates de croissance

---

Article :

## Using T-Z plots as a graphical method to infer lithological variations from growth strata

Sébastien Castelltort, Stéphane Pochat and Jean Van Den Driessche

Géosciences Rennes, Campus de Beaulieu, 35042 Rennes cedex - France

*Submitted to Journal of Structural Geology*

---

## Abstract

**The "T-Z plot" method has been initially developed for the analysis of growth fault kinematics from seismic data. A brief analytical examination of such plots shows that they can provide valuable informations not only about fault activity but also about fault topography evolution. When growth is a continuous process, periods of topography creation and filling are related to non-dynamic (draping) and dynamic sedimentation respectively. In this case, the T-Z plot analysis becomes a powerful additional tool to predict, at first sight, major lithological variations on seismic profiles in faulted settings.**

## Keywords

Growth fault, growth strata, fault topography, fault kinematics, net-to-gross ratio.

## 1. Introduction

The analysis of syntectonic strata (growth strata) is widely used to infer the kinematics of growth structures (fold and faults) at various degrees of resolution. The graphical method called “T-Z plot” initially developed for the seismic analysis of growth structures consists in plotting, for each horizon, the stratigraphic (vertical) throw of the considered marker versus its depth (Bischke 1994, Tearpock & Bischke 1991).

This method can be used to constrain the slip history of growth faults by always assuming a “fill-to-the-top” sedimentation (i.e., sedimentation always fill-up fault-induced topography) (e.g., Cartwright et al. 1998, Mansfield & Cartwright 1996)

However, several studies have evidenced sedimentation disturbances induced by fold- and fault topographies on the sea floor, which means that the “fill-to-the-top” assumption is not always valid (e.g., Anderson et al. 2000, Bornhauser 1959, Edwards 1976, Hodgetts et al. 2001, Hooper et al. 2002, Morris et al. 1998, Ravnas & Steel 1997, Shaw et al. 1999, Soreghan et al. 1999, Thornburg et al. 1990)**.**

This paper is a brief study of the significance of T-Z plots for both opposed end-members: (1) a “fill-to-the-top” sedimentation with variable slip rate, and (2) a more general model that combines variable displacement and occurrence of topographies.

The implications of both models are examined and lead us to propose T-Z plots as a graphical tool to infer the lithologies of growth strata from subsurface data.

## 2. Construction and interpretation of T-Z plots

Let us consider the case of a normal growth fault in which *n* stratigraphic horizons can be correlated across the fault (Fig.1a). In the following, the younger horizon at $i=0$ is the first post-faulting stratigraphic surface, and the older $i=n$ is the younger pre-faulting horizon (i.e. the older faulted surface) (Fig.1a). If palaeotopography and the age of each horizon are known, fault slip rates and topography evolution are known directly. However, in the absence of such data, which is generally the case, only the growth strata thicknesses can provide informations about fault kinematics.

The construction of the corresponding T-Z plot (Fig. 1b) consists in plotting the vertical throw *Ti* of each horizon versus the associated depth *Zi* in the hanging-wall.

The problem is to interpret the slope variations which occur on the T-Z plot.

In the general case, the throw contains the displacement and the pre-existing topography (if any) (Fig. 2). Therefore, the expression of the throw $\tau_i$ on the first increment of deposition (interval *[i; i-1]*) after time i (Fig. 2) is:

$$\tau_i = d_i + e_i \quad (1)$$

where $d_i$ is the vertical displacement on the fault between *i* and *i-1*, and $e_i$ is the topography at time *i* (Fig. 2). All the subsequent increase in throw is only due to the displacement on the fault, and the expression of the final throw $T_i$ of horizon *i* at instant *0* is:

$$T_i = \sum_{i}^{0} d_i + e_i \quad (2)$$

where $\sum_{i}^{0} d_i$ represents the total displacement due to fault growth from time *i* up to the end of fault activity (time *0*).

If no data on paleotopography at each instant is available, two end-members models can be considered in order to interpret the T-Z plots: (1) the “fill-to-the-top” model, and (2) the variable displacement/topography model.

### *2.1. The fill-to-the-top model*

In some cases, the sedimentation can be considered as always filling-up fault-induced topography, which is known as the “fill-to-the-top model” (e.g., Gawthorpe et al. 2000, Masaferro et al. 2002). In such cases, the topography at each instant is zero ($e_i=0 \ \forall i$ , cf. Fig. 3). Therefore, removing topography from Eq. (2) gives the expression of the final throw and throw variations in the fill-to-the-top model :

$$\tau_i = d_i = Sh_i - Sf_i \quad (3)$$

$$T_i = \sum_{i}^{0} d_i \quad (4)$$

$$T_i - T_{i-1} = \sum_{i}^{0} d_i - \sum_{i-1}^{0} d_i = d_i \quad (5)$$

The slope $\alpha_i$ on each interval (Fig. 1b) is then given by:

$$\alpha_i = \frac{T_i - T_{i-1}}{Z_i - Z_{i-1}} = \frac{d_i}{Sh_i} \quad (6)$$

where $Sh_i$ is the thickness of sediments deposited between *i* and *i-1* in the hanging-wall. Then as long as time is not known and only thicknesses are available, the slope only indicates the slip rate relative to the sedimentation rate on each interval:

$$\alpha_i = \frac{d_i / t_i}{Sh_i / t_i} \quad (7)$$

where $t_i$ is the duration of interval *[i; i-1]*. In other words even if sedimentation rate exceeds the vertical component of displacement (i.e. fill-to-the-top model), the slope variations on the T-Z plot cannot be linked in a straightforward way to fault activity. For example, Eq. (7) shows that with a constant displacement rate, variations in the sedimentation rate only, will induce slope variations on the T-Z plot.

Therefore, while throw variations give the absolute magnitude of vertical displacement (Fig. 1b) and can be interpreted as such, the slope variations should be interpreted carefully unless time is known, by taking into consideration the variations of thickness.

Also, the slope can be expressed in terms of strata thickness variation by using Eq (3) and (5) which give $T_i - T_{i-1} = Sh_i - Sf_i$ (Fig. 1a and 3):

$$\alpha_i = \frac{T_i - T_{i-1}}{Z_i - Z_{i-1}} = \frac{Sh_i - Sf_i}{Sh_i} = 1 - EI^{-1} \quad (8)$$

with $EI = \frac{Sh_i}{Sf_i}$ is the Expansion Index defined by Thorsen (1963).

In this way, the additional information displayed by T-Z plots, that lacks in the expansion index method of Thorsen (1963) is the absolute magnitude of vertical displacement on fault (Cartwright et al. 1998).

However, intervals of zero slope (i.e. intervals with no throw variation) necessarily indicate periods of fault inactivity in the fill-to-the-top model, i.e. expansion indexes of 1. This has been used, for example, in the analysis of a set of normal growth faults from the Gulf of Mexico to put forward their polycyclic activity (Cartwright et al. 1998).

Similarly a negative slope would imply a negative displacement, i.e. an inversion of the movement on the fault. In an alternative explanation, Mansfield & Cartwright (1996) proposed that negative slope may be associated with overlap and linkage processes due to fault propagation.

*2.2. The variable displacement/topography model*

As mentioned above, several studies have evidenced the presence of fault- or fold-induced topographies in currently active settings or for fossilized growth structures. Also, it is known that pelagic sedimentation can drape topography and leave equivalent sediment thicknesses in the hanging-wall and on the footwall (Cartwright et al. 1998). In such cases, the topography $e_i$ at each instant can be different from zero (Fig. 2), and can not be further neglected. It follows that throw variations do no longer represent only displacement but a combination of displacement and topography as shown by Eq. (2).

We propose here to conciliate both the fill-to-the-top model and the occurrence of fault-induced topographies.

The general expression of slope on any interval *[i; i-1]* from Eq.(1) is:

$$\alpha_i = \frac{T_i - T_{i-1}}{Sh_i} = \frac{\left(\sum_{n=i}^{n=0} d_n - e_i\right) - \left(\sum_{n=i-1}^{n=0} d_n - e_{i-1}\right)}{Sh_i} \quad (9)$$

$$\alpha_i = \frac{d_i - \Delta e_i}{Sh_i} \quad (10)$$

where $\Delta e_i$ is the variation of topography between *i* and *i-1* (i.e., $\Delta e_i = e_i - e_{i-1}$) (Fig. 1b and 2b). For a constant displacement $d_i$, the slope increases when topography diminishes from *i* to *i-1*. As a consequence, on a T-Z plot, the points $[T_i;Z_i]$ which follow the stronger slopes may be interpreted with confidence as representing low to zero topography. By contrast, between two of such points, the other points follow lower or even negative slopes and result from the creation of topography. Moreover, the first (*i=0*) and the last (*i=n*) points of the T-Z plots do not record any topography. Indeed, there is no reason that a topography exists before faulting occurred (*i=n*). Also, the last horizon (*i=0*) represents the first post-faulting horizon , i.e. which is not deformed and may be horizontal.

Therefore, on any T-Z plots, *m* segments between the points of assumed low topography can be drawn, starting from *j=0,* at the origin of the T-Z plot, to *j=m* (for the older horizon) (Fig. 4). The slope of each of these segment represents the mean displacement rate relative to the sedimentation rate on the considered interval, and the deviations of the T-Z curve with respect

to these segments represent creation of fault-induced topography (shadowed areas on Fig. 4). In this way, a fill-to-the-top sedimentation is implicitly assumed to work at the resolution of the chosen segments, and topographies occur at a higher frequency due to sedimentation changes. The only condition to respect when choosing intervals of steady growth is that there should be no point $[T_i;Z_i]$ of any interval *[j; j-1]* situated below the corresponding segment *j*. Indeed, such a situation would imply a negative topography at time of deposition of horizon *i* (i.e., horizon *i* topographically higher in the hanging-wall than on the footwall), which would be unlikely.

The expression of the throw $T_i$ of each horizon *i* in any interval *[j; j-1]* becomes:

$$T_i = T_{j-1} + \frac{T_j - T_{j-1}}{Z_j - Z_{j-1}}\left(Z_i - Z_{j-1}\right) + e_i \quad (11)$$

$$T_i = T_{j-1} + \alpha_j\left(Z_i - Z_{j-1}\right) + e_i \quad (12)$$

where $\alpha_j$ is the slope of the segment *j*, and represents the mean displacement rate (relative to the mean sedimentation rate) on this interval. With this method, the T-Z contains the magnitude of the displacement on the fault at the segment resolution (intervals *j*), and the evolution of topography at each instant *i* by the deviation of the curve from the segments. Segments should be chosen, by comparison with well log data, as the scale at which slope variations on the T-Z plot can no longer be associated to lithological changes. More important than the magnitudes which are function of the chosen segments, the T-Z plot used in this way provides the relative evolution of fault-induced topography which is possibly linked to sedimentation evolution.

## 3. Conclusion

Both end-members models lead to fundamentally different interpretations. In the fill-to-the-top model, the slope variations on a T-Z plot are associated to displacement variations on the fault. Therefore, in the fill-to-the-top model, there is *a priori* neither lithological nor sediment flux variations, which implies that sedimentation be always dynamic. On the contrary, in the variable displacement / topography model, the slope variations are interpreted as topography creation or filling linked to sediment flux variations superimposed on a constant displacement signal over given time steps. These sediment flux variations are likely linked to changes in sedimentation dynamics and lithology. For example, pelagic type sedimentation will leave equivalent thicknesses across a fault and therefore induce the creation of a topography during fault activity. Inversely, dynamic sedimentation (sands) will more likely tend to fill fault-induced topographies.

An obvious way to choose between the two models is to compare T-Z plots with sedimentary well logs data. If no major lithological variation is observed, then T-Z slope variations are rather related to variable fault activity. However, if slope variations can be correlated with lithological variations, then the T-Z plot may indicate sedimentation changes. In this way, it can be proposed as an additional tool, in particular in petroleum geology, for the prediction of growth strata lithologies and the correlation of sand-shale successions (net-to-gross ratio) inside a basin and across growth structures where well log data are not available.

**References**


Anderson, J. E., Cartwright, J., Drysdall, S. J. & Vivian, N. 2000. Controls on turbidite sand deposition during gravity-driven extension of a passive margin: examples from Miocene sediments in Block 4, Angola. *Marine and Petroleum Geology* **17**, 1165-1203.

Bischke, R. E. 1994. Interpreting sedimentary growth structures from well log and seismic data (with examples). *American Association of Petroleum Geologists Bulletin* **78**(6), 873-892.

Bornhauser, M. 1959. Depositional and structural history of Northwest Hartburg Field, Newton County, Texas. *American Association of Petroleum Geologists Bulletin* **44**(4), 458-470.

Cartwright, J., Bouroullec, R., James, D. & Johnson, H. 1998. Polycyclic motion history of some Gulf Coast growth faults from high-resolution displacement analysis. *Geology* **26**(9), 819-822.

Edwards, M. B. 1976. Growth faults in Upper Triassic deltaic sediments. *American Association of Petroleum Geologists Bulletin* **60**(3), 341-355.

Gawthorpe, R. L., Hall, M., Sharp, I. & Dreyer, T. 2000. Tectonically enhanced forced regressions: examples from growth folds in extensional and compressional settings, the Miocene of the Suez rift and the Eocene of the Pyrenees. In: *Sedimentary Responses to Forced Regressions* (edited by Hunt, D. & Gawthorpe, R. L.). *Geological Society [London] Special Publications* **172**, 177-191.

Hodgetts, D., Imber, J., Childs, C., Flint, S., Howell, J., Kavanagh, J., Nell, P. & Walsh, J. 2001. Sequence stratigraphic responses to shoreline-perpendicualr growth faulting in shallow marine reservoirs of the Champion field, offshore Brunei Darussalam, South China Sea. *American Association of Petroleum Geologists Bulletin* **85**(3), 433-457.

Hooper, J. R., Fitzsimmons, R. J., Grant, N. & Vendeville, B. C. 2002. The role of deformation in controlling depositional patternes in the south-central Niger Delta, West Africa. *Journal of Structural Geology* **24**, 847-859.

Mansfield, C. S. & Cartwright, J. A. 1996. High resolution displacment mapping from 3-D seismic data. *Journal of Structural Geology* **18**, 249-263.

Masaferro, J. L., Bulnes, M., Poblet, J. & Eberli, G. P. 2002. Episodic folding inferred from syntectonic carbonate sedimentation: the Santaren anticline, Bahamas foreland. *Sedimentary Geology* **146**, 11-24.

Morris, S. A., Alexander, J., Kenyon, N. H. & Limonov, A. F. 1998. Turbidites around an active fault scarp on the Lower Valencia Fan, northwest Mediterranean. *Geo-Marine Letters* **18**, 165-171.

Ravnas, R. & Steel, R. J. 1997. Contrasting styles of Late Jurassic syn-rift turbidite sedimentation : a comparative study of the Magnus and Oseberg areas, northern North Sea. *Marine and Petroleum Geology* **14**(4), 417-449.

Shaw, J. H., Novoa, E. & Connors, C. D. 1999. Structural controls on growth stratigraphy. In: *Thrust Tectonics* (edited by McClay, K.), London, 80-82.

Soreghan, M. J., Scholz, C. A. & Wells, J. T. 1999. Coarse-grained, deep-water sedimentation along a border fault margin of Lake Malawi, Africa: Seismic stratigraphic analysis. *Journal of Sedimentary Research* **69**, 832-846.

Tearpock, D. & Bischke, R. E. 1991. *Applied Subsurface Geological Mapping*. Prentice-Hall, New-York.

Thornburg, T. M., Kulm, L. D. & Hussong, D. M. 1990. Submarine-fan development in the southern Chile Trench: A dynamic interplay of tectonics and sedimentation. *Geological society of America Bulletin* **102**, 1658-1680.

Thorsen, C. E. 1963. Age of growth faulting in Southeast Louisiana. *Transactions. Gulf Coast Association of Geological Societies* **13**, 103-110.

**Figure captions**

Figure 1

Principle of T-Z plot construction. A) example of correlated stratigraphic markers across a normal growth fault. B) corresponding T-Z plot.

Figure 2

General relationships between vertical throw ($\tau_i$), displacement ($d_i$), stratigraphic thicknesses ($Sh_i$ and $Sf_i$) and fault topography ($e_i$ and $e_{i-1}$) during one step of fault growth.

Figure 3

Relationships between stratigraphic thicknesses, throw and displacement in the "fill-to-the-top" case.

Figure 4

T-Z plot interpretation of the fault of Fig. 1a in the case of variable displacement/topography model. The segments represent intervals of constant displacement (with $\alpha_j$ the mean displacement rate), and the shadowed areas denote periods of topography creation. The upper and lower two curves represent different choices of segments, which involve different topography magnitudes (see text).

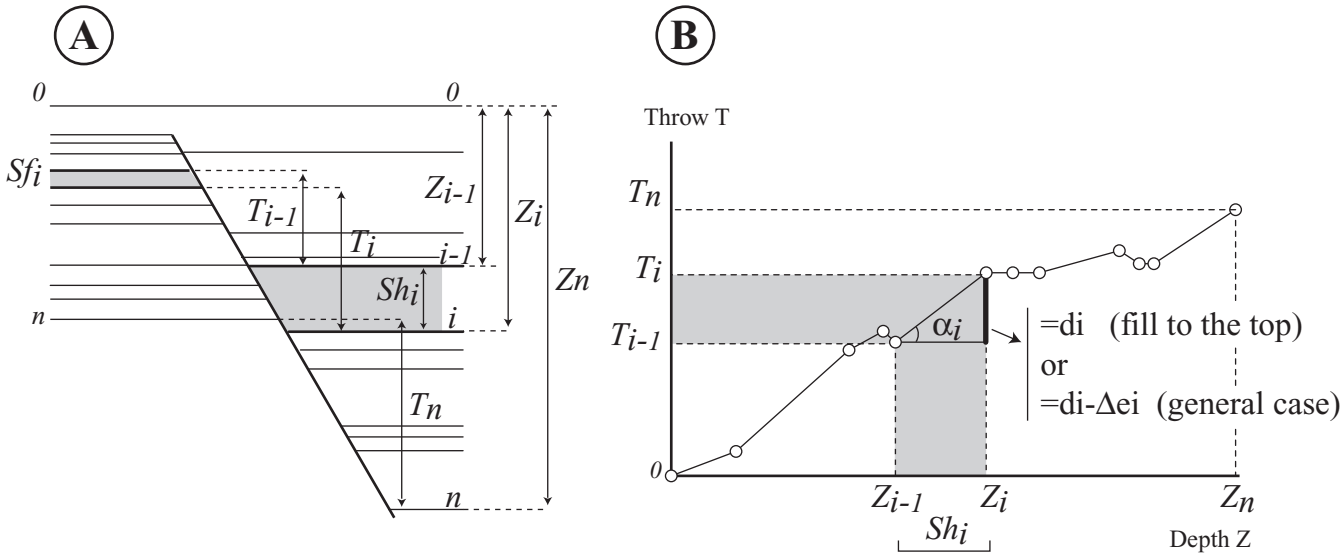
A
0
0
Sfi
Ti-1
Ti
Zi-1
Zi
Zn
i-1
Shi
i
n
Tn
n
B
Throw T
Tn
Ti
Ti-1
αi
=di (fill to the top)
or
=di-Δei (general case)
0
Zi-1
Zi
Zn
Shi
Depth Z

**FIGURE 1**

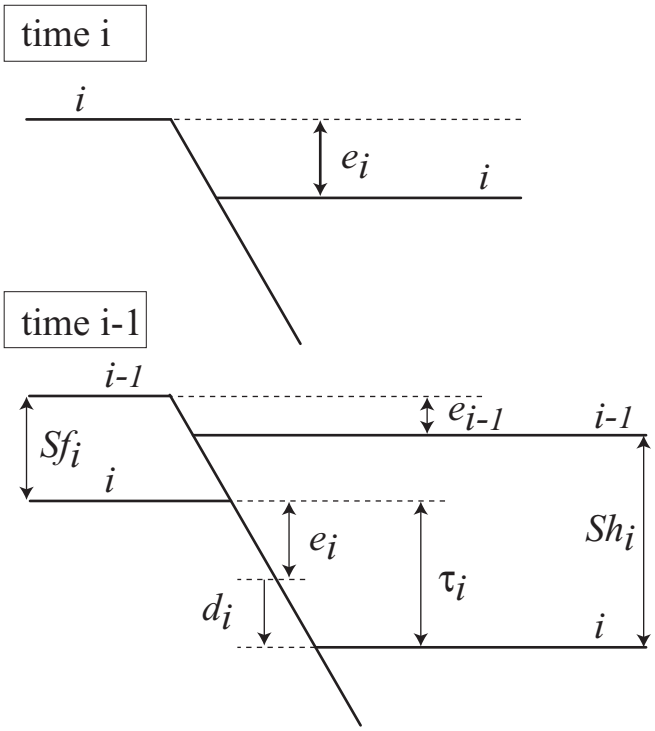


**FIGURE 2**

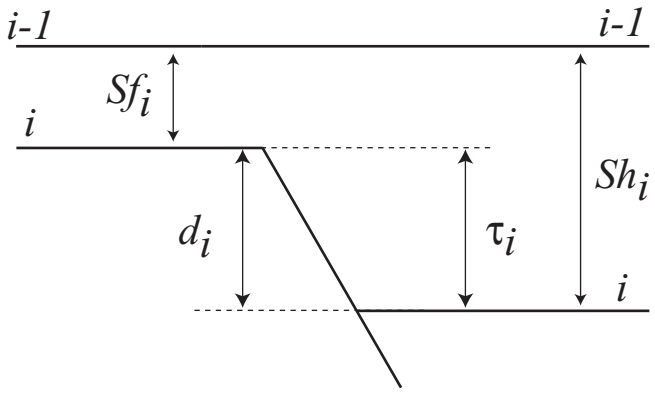


**FIGURE 3**

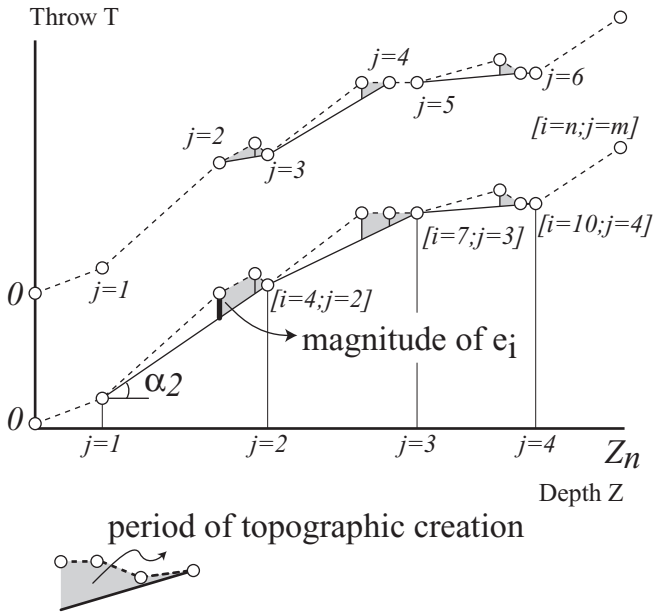
Throw T
j=4
j=6
j=5
[i=n;j=m]
j=2
j=3
[i=10;j=4]
[i=7;j=3]
0
j=1
[i=4;j=2]
magnitude of e_i
α2
0
j=1
j=2
j=3
j=4
Z_n
Depth Z
period of topographic creation

**FIGURE 4**

# 3. RÔLE DU FLUX SÉDIMENTAIRE TERRIGÈNE DANS L'ORIGINE DES CYCLES STRATIGRAPHIQUES

## Importance de la zone en transfert (rivières).

Dans la partie précédente nous avons examiné l'effet des variations locales d'accommodation sur l'enregistrement sédimentaire car il est reconnu que les variations régionales ou globales d'accommodation peuvent *créer* des cycles stratigraphiques.

L'importance du flux sédimentaire en tant que facteur de contrôle majeur a été clairement mise en évidence depuis la dernière décennie (e.g., Lawrence 1993), mais ses variations restent encore mal connues et mal comprises ainsi que son rôle dans la création des cycles stratigraphiques. En effet, le flux sédimentaire, et en particulier le flux particulaire, est difficile à mesurer à partir des accumulations sédimentaires en raison d'un enregistrement trop souvent incomplet et de données éparses (Métivier, 2002), ainsi que des problèmes que posent la diagénèse et la compaction.

Certaines études ont pu cependant montrer que le flux sédimentaire aux bassins pouvait être variable à basse fréquence (> 1 Ma) à partir de mesures du flux dans l'ancien (e.g., Galloway and Williams 1991 ; Liu and Galloway 1997 ; Peizhen et al. 2001). En revanche, des études récentes ont suggéré des variations à haute fréquence (10's à 100's ka) du flux sédimentaire (e.g., Perlmutter and Matthews, 1989; Weltje and de Boer, 1993; Weltje et al., 1996; Burns et al., 1997; Tiedemann and Franz, 1997; Perlmutter et al., 1998; Lopez-Blanco et al., 2000; Marzo and Steel, 2000; Van der Zwan, 2002). Dans ces études, il est implicitement considéré que le flux varie directement en fonction de changements climatiques ou tectoniques dans l'aire source. Un tel lien direct est basé sur les nombreuses corrélations existantes entre différents paramètres climatiques (moyenne ou total des précipitations, variations de température…) et géographiques (pente, altitude maximale, altitude moyenne, aire de drainage…), d'une part, et le flux sédimentaire actuel à la sortie des systèmes fluviatiles, d'autre part (e.g., Fournier, 1960; Milliman and Meade, 1983; Pinet and Souriau, 1988; Milliman and Syvitski, 1992; Summerfield and Hulton, 1994; Mulder and Syvitski, 1996; Hovius, 1998). Ceci pose le problème suivant : *si ces corrélations sont considérées comme des lois d'érosion, cela impose de considérer le système comme étant en équilibre avec les différents facteurs invoqués, hypothèse qui n'est pas démontrée*. On peut en conséquence questionner la réalité de ces variations du flux à haute fréquence.

En fait, il existe une grande diversité de facteurs qui peuvent intervenir dans les variations de flux (voir par exemple, Einsele 2000 ; Jones and Frostick 2002), et cette diversité implique aussi différentes échelles de temps auxquelles le flux sédimentaire peut varier.

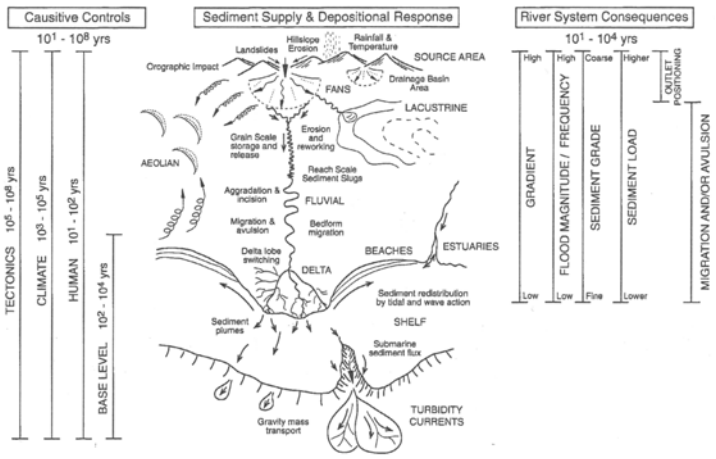


Illustration de la diversité des causes, réponses, et conséquences des variations de flux sédimentaire au bassin (Frostick & Jones, 2002).

Pour comprendre les variations du flux sédimentaire sans se perdre dans la complexité et la diversité des nombreux cas de figures et facteurs de contrôle, il est nécessaire d'adopter une approche holistique du problème *en considérant le système sédimentaire dans son ensemble*.

Dans les chapitres suivants nous nous sommes donc appuyés sur la notion de *système sédimentaire qui englobe les zones en érosion, transfert et dépôt*. Le flux sédimentaire est produit en grande majorité par les versants et dans une moindre mesure par l'incision fluviatile (Hovius, 1998). Il est ensuite transmis par les rivières (zone de transfert) jusqu'aux bassins où il se dépose.

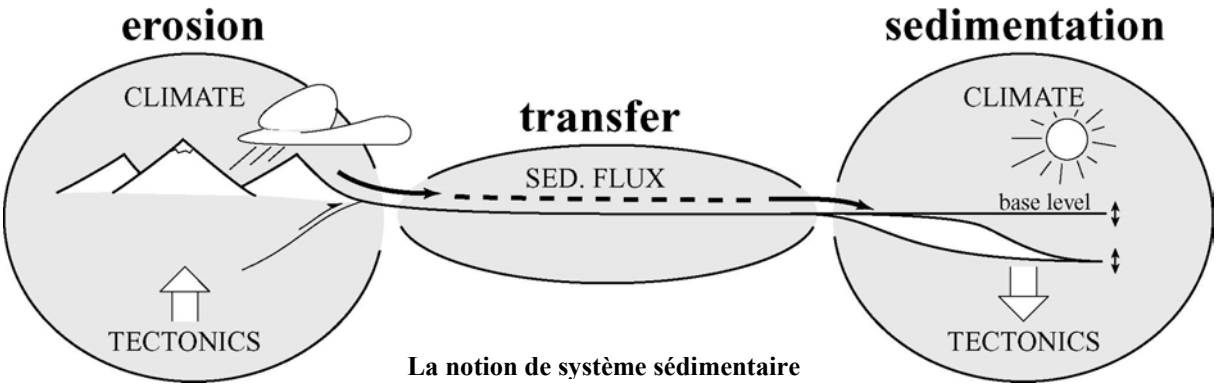


**La notion de système sédimentaire**

Une notion commune à la géomorphologie et à la stratigraphie est la *notion d'équilibre* (e.g., « graded stream profile » de Davis, « shoreface profile » de Bruun…etc ; Swift et al.

1991 ; Paola 1992 ; Galloway 1998 ; Paola, 2000). Pourtant, *la notion de temps d'équilibre*, ou *de temps de réponse* (temps nécessaire au système pour qu'il retrouve l'équilibre après une perturbation, Beaumont 2000), qui accompagne naturellement celle d'équilibre, est généralement négligée par les stratigraphes. *Or, dans la perspective du système sédimentaire, il apparaît que le temps d'équilibre est un paramètre crucial des différentes entités qui produisent et transportent le flux sédimentaire (versants, chenaux)*. En effet, selon la valeur du temps d'équilibre de ces différentes entités, des changements des facteurs externes avec une périodicitée donnée, vont donner lieu, ou non, à une réponse en termes de flux sédimentaire.

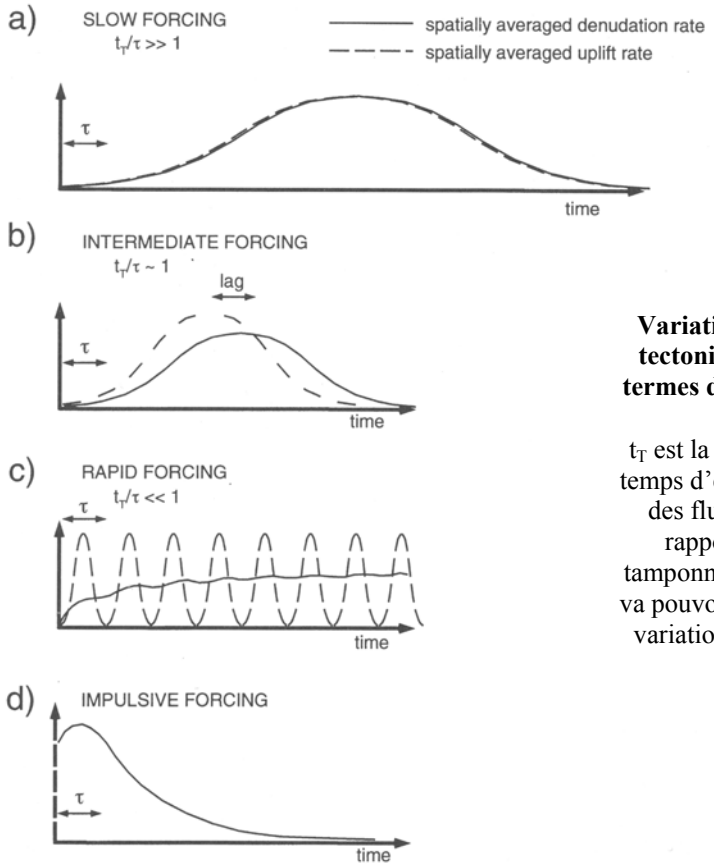


**Variation d'un facteur externe (ici la tectonique) et réponse du système en termes de flux sédimentaire (Beaumont et al., 2000).**
$t_T$ est la périodicité du forçage, et τ est le temps d'équilibre du système. On voit que des fluctuations haute-fréquence (par rapport au temps d'équilibre) sont tamponnées par le système (c), alors qu'il va pouvoir répondre « en équilibre » à une variation lente des facteurs externes (a).

Si les temps d'équilibre peuvent être bien contraints pour la zone en érosion à partir des récents développements en géomorphologie, beaucoup moins d'études se sont concentrées sur la zone en transfert. Dans ce qui suit notre démarche a été de modéliser, afin de mieux l'appréhender, le comportement de cette zone qui est crucial pour comprendre les variations du flux sédimentaire et la signification de l'enregistrement stratigraphique.

## 3.1. Echelles de temps des variations du flux sédimentaire terrigène aux bassins

Ce chapitre tente de quantifier les échelles de temps possibles des variations du flux sédimentaire terrigène à l'entrée des bassins sédimentaires. Notre approche est basée sur le concept de système sédimentaire qui résume les systèmes naturels à fondamentalement trois zones dominées par des processus différents : la zone en érosion, la zone en transfert, et la zone en sédimentation. Nous examinons des résultats récents de la géomorphologie qui montrent que des changements climatiques fréquents peuvent induire des variations haute-fréquence du flux sédimentaire à la sortie de la zone en érosion. Le rôle crucial de la zone en transfert est ensuite mis en avant car, selon son comportement, elle va transmettre ou ne pas transmettre les variations de flux depuis la zone en érosion jusqu'à la zone en dépôt. En appliquant un modèle diffusif à un certain nombre de rivières à travers le monde, nous étendons aux grandes rivières (>1000 km) et aux rivières intermédiaires (>300 km) le résultat déjà démontré pour les grandes plaines alluviales d'Asie (e.g., Métivier 1999*), à savoir que le système en transfert joue le rôle de « tampon » pour les variations de flux sédimentaire haute-fréquence (10's à 100's ka). Cela implique que les cycles stratigraphiques haute-fréquence enregistrés dans des bassins sédimentaires alimentés par des systèmes de drainage de grande dimension et de dimension intermédiaire ne peuvent probablement pas être associés à des variations du flux sédimentaire à ces fréquences*.

---

Article :

### How plausible are high-frequency sediment supply-driven cycles in the stratigraphic record ?

Sébastien Castelltort and Jean Van Den Driessche

Géosciences Rennes, Campus de Beaulieu, 35042 Rennes cedex - France

*Sedimentary Geology (2003)*

---

Available online at www.sciencedirect.com
SCIENCE DIRECT®
Sedimentary Geology 157 (2003) 3–13
Sedimentary Geology
www.elsevier.com/locate/sedgeo

ExpresSed

# How plausible are high-frequency sediment supply-driven cycles in the stratigraphic record?

Sébastien Castelltort*, Jean Van Den Driessche

*Géosciences Rennes, Université de Rennes 1, UMR 6118 du CNRS, Campus de Beaulieu, 35042 Rennes, France*

Received 8 November 2002; received in revised form 17 December 2002; accepted 18 December 2002

**Abstract**

This paper is an attempt to quantify the plausible time scales of clastic sediment supply variations at the entrance of sedimentary basins. Our approach is based on the sedimentary system concept, which simplifies natural systems by dividing them into three zones of dominant processes: the erosion, the transfer, and the sedimentation subsystems. We examine recent results from geomorphology, which show that frequent climate changes can induce high-frequency sediment flux variations at the outlet of the source area. We put forward the crucial role of the transfer subsystem, which conveys sediment from the erosion zone to the basin. By applying a diffusive model to a number of worldwide rivers, we extend from large (>1000 km) to intermediate (>300 km) rivers the previous finding that the transfer subsystem acts as a buffer for short periods sediment pulses (tens to hundreds of kiloyears). This implies that high-frequency stratigraphic cycles in clastic accumulations fed by large drainage systems are unlikely to reflect sediment supply cycles of tens to hundreds of thousands of years of periodicities.


*Keywords:* Cycles; Sequences; Sediment supply; Sedimentary system; Geomorphology

## 1. Introduction

At first order, the stratigraphic record is made of sedimentation changes that encompass a large range of time scales (Einsele et al., 1991) from a few seconds (laminations) to several tens of million years or more (major global changes). The most commonly studied of those variations are basin scale repetitive packages of strata called sequences or cycles, with periods ranging from tens of thousands of years to several million years. In siliciclastic successions, such cycles can be recognized by tracking the movements of a stratigraphic indicator as, for instance, the gravel–sand transition or the shoreline in continental or marine deposits, respectively (Marr et al., 2000; Paola et al., 1992; Swenson et al., 2000). These movements indicate changes of the shape of the entire depositional system in the search for an equilibrium with changing boundary conditions. The goal of stratigraphy is to read this stratigraphic record of changing external factors. A crucial question then is: what is the origin of those cycles?

Since Sloss (1962) and the subsequent advances brought by sequence stratigraphy (e.g., Cross, 1988; Jervey, 1988; Posamentier et al., 1988; Schlager, 1993; Shanley and McCabe, 1994; Muto and Steel,

* Corresponding author. Fax: +33-2-23-23-61-00.
*E-mail address:* sebastien.castelltort@univ-rennes1.fr (S. Castelltort).

0037-0738/03/$ - see front matter © 2003 Elsevier Science B.V. All rights reserved.
doi:10.1016/S0037-0738(03)00066-6

1997, 2000; Blum and Törnqvist, 2000), it is now generally accepted that stratigraphic cycles are somehow governed by changes in the ratio between space available for sedimentation or accommodation (A) and sediment supply (S) to this space. In this way, all factors that can affect accommodation and/or sediment supply are virtually able to produce cycles in the stratigraphic record. Eustasy, or another base level in continental areas, basin tectonics, and sediment supply have all been claimed to be variable at all time scales and responsible for creating stratigraphic cycles.

There is broad agreement that climate-induced base-level oscillations with Milankovitch periodicities of tens to hundreds of thousands of years are responsible for creating high-frequency stratigraphic cycles (fourth- and higher-order cycles) with the same periodicities (e.g., Van Wagoner et al., 1990; Plint et al., 1992; Nystuen, 1998; Gale et al., 2002). Also, some recent studies (e.g., Perlmutter and Matthews, 1989; Weltje and de Boer, 1993; Weltje et al., 1996; Burns et al., 1997; Tiedemann and Franz, 1997; Perlmutter et al., 1998; Lopez-Blanco et al., 2000; Marzo and Steel, 2000; Van der Zwan, 2002) have suggested that the sediment flux to basins could vary with those periodicities due to climate changes or vertical movements (tectonics) in the source area, and should therefore have direct control over the high-resolution stratigraphic record. This idea is mainly influenced by the correlations found between various climatic (mean precipitation, total precipitation, temperature range, etc.) and geographic (drainage area, relief, maximum height, etc.) factors and the present-day sediment output at the mouth of rivers (e.g., Fournier, 1960; Milliman and Meade, 1983; Milliman and Syvitski, 1992; Pinet and Souriau, 1988; Summerfield and Hulton, 1994; Mulder and Syvitski, 1996; Hovius, 1998). Such correlations can be considered as erosion laws, but this requires the assumption that the system is at equilibrium with those factors.

In this paper, we put in question the high-frequency variability of sediment flux to basins (with tens to hundreds of thousands of years periods) and its link with climate and vertical movement changes in the source domain.

We first investigate how the sedimentary system concept, rooted in the earlier work of Schumm (1977), clarifies our questioning of the variability of sediment flux. In particular, this highlights the crucial role of the transfer zone, which conveys sediments from the source area to the basin. Then, we put constraints on the plausibility of high-frequency sediment flux variations to the basin by (1) examining the response times of the source area to climate and vertical movement changes, in light of recent results from geomorphology, and (2) analysing the first-order response time of some worldwide rivers to sediment input variations coming from the source area.

## 2. The sedimentary system

Following Schumm (1977) and Allen (1997), let us consider a sedimentary system (Fig. 1) as a closed domain at the lithosphere/atmosphere interface, composed of three subsystems each characterized by a dominant process: erosion, transfer (the balance between erosion and sedimentation), and sedimentation subsystems. This is valid at any space and time scales for which such distinct zones of dominant processes can be identified. Here we consider only

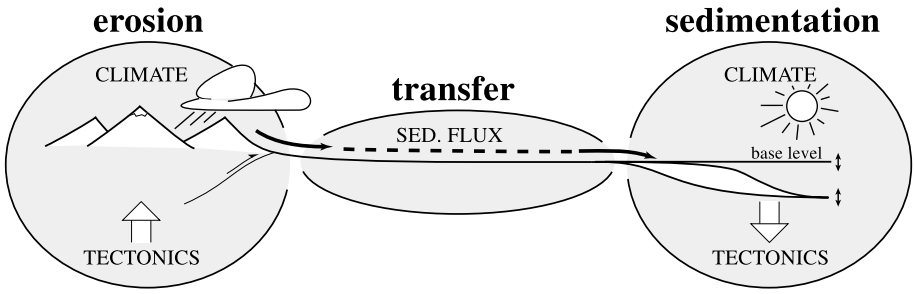


Fig. 1. Idealized cartoon of a mountain–river–delta sedimentary system showing the three elementary subsystems of erosion, transfer, and sedimentation.

macroscale sedimentary systems (e.g., schematic mountain–river–delta or catchment–fan systems) on geological time scales. This concept is aimed at distilling the first-order characteristics and dynamics of real systems from their natural complexity.

The erosion subsystem is composed schematically of hillslopes, which are the main sediment feeders, and channels, which incise and drain sediment downstream. It is controlled by vertical movements with respect to a reference level defined at its outlet, either due to tectonics or associated with base-level changes, and by climate.

The transfer subsystem is made up of rivers transporting the sedimentary flux leaving the erosion subsystem to the sedimentation subsystem. The length of the transfer subsystem varies from zero in catchment–fan systems to several thousands of kilometers in the largest current systems. At its upstream boundary, it is then subjected to sediment flux variations coming from the erosion subsystem, and to base-level changes at its downstream boundary.

The sedimentation subsystem (basin) stores the sediment flux in a variety of depositional environments whether continental and/or marine. It is subject, on one hand, to sediment flux variations at its boundary with the preceding subsystem (erosion or transfer) and, on the other hand, to base-level changes and basin tectonics, both of which modify the space available for sedimentation.

This raises a fundamental difference between accommodation modifying factors and sediment supply modifying factors: while base-level variations and basin tectonics apply directly to the sedimentation subsystem, the sediment flux appears to be a complex derivative of the effects of external forcing on the erosion zone and of their transmission by the transfer subsystem. Each subsystem has an intrinsic response time (or equilibrium time), which is the time needed to return to equilibrium after a change in boundary conditions (Paola et al., 1992; Beaumont et al., 2000). A system with stable boundary conditions is at equilibrium (with these conditions) when its shape does not evolve with time. If boundary conditions evolve slowly compared to the response time, the subsystem will respond in a quasi-equilibrium manner (i.e., at each time in equilibrium with its new conditions). On the contrary, if they vary rapidly compared to the response time, the response will not be in equilibrium with the forcing (i.e., out-of-phase with the forcing and of different amplitude). Therefore, sediment flux variations at the sedimentation subsystem entrance may not necessarily be tied in a straightforward way to allogenic changes in the erosion zone, depending on the response times of the erosion and transfer subsystems compared with the periodicities of allogenic forcing.

In the following, we do not address the response of the transfer subsystem to base-level changes (see, e.g., Paola et al., 1991; Burns et al., 1997) since the production and transport of sediments may be mostly upstream-controlled (Blum and Törnqvist, 2000). The understanding of the variability of sediment flux to sedimentary basins in relation with upstream allogenic controls therefore requires determining (1) the response time of the erosion zone to climate changes and vertical movements (tectonics/base level) and (2) the response time of the transfer subsystem to sediment flux variations coming from the erosion subsystem.

## 3. Constraints from geomorphology

### *3.1. The erosion subsystem*

A number of recent works in geomorphology address the response of erosion to climate and tectonics.

A first important qualitative result, although not explicitly stated, is that the response to vertical movements will always take longer than the response to climate because the tectonic signal must propagate up the drainage network whereas climate can impact the entire drainage basin at once (Whipple, personal communication; e.g., Fernandes and Dietrich, 1997).

Secondly, the response times have been assessed by the field evidence of landscape adjustment to new conditions, and computed by the calibration of models on natural cases. The minimum response times to tectonics are on the order of 100 ka in small (10 km) catchment–fan systems (Allen and Densmore, 2000) and coastal drainage basins (3–10 km; Snyder et al., 2000), and best comprised between 0.25 and 2.5 Ma in drainage basins of medium size (20–40 km; Whipple, 2001). This suggests minimum response times to tectonics ranging from hundreds of thousands of years to 1 Ma, or more in larger drainage basins (Tucker and Slingerland, 1996; Whipple, 2001).

The response to climate in terms of sediment flux is different because there is an initial near-immediate response (i.e., on the order of 1 ka to several thousands of years, when erosivity is increased). This mostly reflects a release of the sediments stored in hillslope soils that affects the entire drainage area (Fernandes and Dietrich, 1997; Tucker and Slingerland, 1997). However, the ability of hillslopes to produce significant regolith depends on the dominant climate. For instance, Bull (1991) notes that during the last 130 ka, only three aggradation events are recorded in the arid San Gabriel Mountains and Mojave Desert, whereas the marine record yields 11 highstand terraces for the same interval. This suggests that initial response times can reach several tens of thousands of years in particular environments. In addition to the initial response time, over the long term, sustained climate shifts (greater than hundreds of thousands of years) can modify channel long profiles with the same response times as for responses to tectonic changes (i.e., on the order of hundreds of thousands of years or more) (Whipple, 2001).

In conclusion, the erosion subsystem will filter high-frequency tectonic events (<100 ka) and take more than 100 ka to adjust to sustained climate shifts and tectonic disturbances. By contrast, because of the initial response due to the interaction between channels and hillslopes, the erosion subsystem has the potential to respond immediately to frequent climate changes, and therefore to produce high-frequency sediment flux oscillations at its outlet (Tucker and Slingerland, 1997).

### 3.2. The transfer subsystem

In the transfer subsystem, rivers convey sediments from the upstream source area down to the sedimentation subsystem. Following Allen and Densmore (2000), one can consider, at first order, its behaviour as diffusive (Paola et al., 1992; Humphrey and Heller, 1995; Dade and Friend, 1998; Métivier, 1999; Métivier and Gaudemer, 1999). In that case, the response time $T$ of the transfer subsystem is of the form:

$$T = L^2/K \tag{1}$$

with $L$ as the length of the subsystem and $K$ as its coefficient of diffusivity. The larger the transfer subsystem, the longer its response time, and the more diffusive it is, the shorter its response time. Note that we do not investigate here the fate of sediment waves supplied kinematically to channels, which can quickly deliver sediment downstream. These are short-term events for which the transfer subsystem may no longer be considered as a simple diffusive entity (see, e.g., Cui et al., submitted for publication; Lisle et al., 1997).

In natural systems, Dade and Friend (1998) have calculated river diffusivities by using the water flux per unit width and a sediment mobility parameter, which embodies the effects of bedload and suspended load in transport. They find response times of 65, 85, 21, 2.4, 74, and 5.5 ka for the Mississippi, Brahmaputra, Indus, Savannah, North Platte, and Cheyenne rivers, respectively (i.e., in the range of 1 ka to tens of thousands of years). Although the physical ground of this calculation is attractive, it is difficult to apply it to other rivers in the world because accurate data as bedload proportion and median grain size are usually not available. Also, those response times do not reflect the buffering effect of large Asian rivers for high-frequency sediment input variations, as evidenced by the correlation between currently measured sediment flux at their mouth and the average filling rates of their marine depocentres over the last 2 Ma, despite strong climatic variations (Métivier et al., 1999).

Métivier (1999) and Métivier and Gaudemer (1999) show that the diffusivity coefficient of a river approaching equilibrium conditions scales with its output sediment flux Qst, width $W$, and mean slope $\langle \partial z/\partial x \rangle$:

$$K = \frac{\mathrm{Qst}}{W\left\langle \frac{\partial z}{\partial x} \right\rangle} \tag{2}$$

With this relation and relation (1), they derive first-order response times in the range of $10^5$–$10^6$ years for some large Asian river floodplains, which explains their strong buffering action for high-frequency sediment input variations (Métivier, 1999; Métivier and Gaudemer, 1999).

We apply relations (1) and (2) to the dataset of Hovius (1998) to further investigate the magnitude of the buffer effect for a greater variety of intermediate and large drainage basins worldwide (>$2.5 \times 10^4$ km$^2$; Table 1).

Table 1
Response times for 93 rivers of the Hovius (1998) database

| River [units] | Stream length,[a] Lr [km] | Drainage area,[a] $A$ [km$^2$] | Maximum height,[a] $H_{max}$ [m] | Sediment flux,[a] Qst (with sediment density = 2700 kg/m$^3$) [10$^6$ m$^3$/a] | Mean slope,[a] $S$ ($S=H_{max}$/Lr) [10$^{-3}$] | Minimum estimated width, $W$ ($W=cA^b$ with $c=0.001$ and $b=0.5$) [m] | Diffusivity coefficient, $K$ ($K=$Qst/$WS$) [10$^6$ m$^2$/a] | Response time, $T$ ($T=L^2/K$ with Qst = suspended and dissolved loads) [ka] | Response time,[b] Tb (Tb = $T$/2 with Qstb = 2Qst) [ka] |
|---|---|---|---|---|---|---|---|---|---|
| Nile | 6670 | 2,715,000 | 5110 | 53 | 0.8 | 1648 | 42 | 1060 | 530 |
| Amazon | 6299 | 6,150,000 | 6768 | 508.5 | 1.1 | 2480 | 190.8 | 208 | 104 |
| Mississippi | 5985 | 3,344,000 | 4400 | 194.4 | 0.7 | 1829 | 144.6 | 248 | 124 |
| Ob | 5570 | 2,500,000 | 4506 | 24.4 | 0.8 | 1581 | 19.1 | 1623 | 812 |
| Yenisey | 5550 | 2,580,000 | 3492 | 28.9 | 0.6 | 1606 | 28.6 | 1078 | 539 |
| Yangtze | 5520 | 1,940,000 | 6800 | 261.5 | 1.2 | 1393 | 152.4 | 200 (170–330)[c] | 100 |
| Yellow (Huang He) | 4670 | 980,000 | 5500 | 52.6 | 1.2 | 990 | 45.1 | 483 (970) | 242 |
| Mekong | 4500 | 810,000 | 6000 | 81.5 | 1.3 | 900 | 67.9 | 298 | 149 |
| Parana | 4500 | 2,600,000 | 6720 | 62.2 | 1.5 | 1612 | 25.8 | 784 | 392 |
| Amur | 4416 | 1,855,000 | 2499 | 26.7 | 0.6 | 1362 | 34.6 | 564 | 282 |
| Lena | 4400 | 2,430,000 | 2579 | 37 | 0.6 | 1559 | 40.5 | 478 | 239 |
| Zaire | 4370 | 3,700,000 | 4507 | 25.5 | 1 | 1924 | 12.8 | 1487 | 743 |
| Mackenzie | 4240 | 1,448,000 | 3955 | 70 | 0.9 | 1203 | 62.4 | 288 | 144 |
| Niger | 4160 | 1,112,700 | 2918 | 15.6 | 0.7 | 1055 | 21 | 823 | 412 |
| Kolyma | 3513 | 647,000 | 3147 | 2.2 | 0.9 | 804 | 3.1 | 4002 | 2001 |
| Murray | 3490 | 910,000 | 2239 | 14.4 | 0.6 | 954 | 23.6 | 516 | 258 |
| Volga | 3350 | 1,350,000 | 1638 | 38.1 | 0.5 | 1162 | 67.1 | 167 | 84 |
| Indus | 3180 | 960,000 | 8611 | 107.8 | 2.7 | 980 | 40.6 | 249 (440) | 124 |
| Salween | 3060 | 325,000 | 6070 | 37 | 2 | 570 | 32.8 | 286 | 143 |
| St. Lawrence | 3060 | 1,185,000 | 1917 | 23.3 | 0.6 | 1089 | 34.2 | 274 | 137 |
| Yukon | 3000 | 855,000 | 6194 | 34.8 | 2.1 | 925 | 18.2 | 494 | 247 |
| Rio Grande | 2870 | 670,000 | 4295 | 11.9 | 1.5 | 819 | 9.7 | 851 | 426 |
| Danube | 2860 | 815,000 | 3087 | 48.1 | 1.1 | 903 | 49.4 | 166 | 83 |
| Brahmaputra | 2840 | 610,000 | 7736 | 215.2 | 2.7 | 781 | 101.1 | 80 (90) | 40 |
| Sao Francisco | 2800 | 640,000 | 1800 | 2.2 | 0.6 | 800 | 4.3 | 1814 | 907 |
| Shatt al Arab | 2760 | 1,050,000 | 4168 | 44.8 | 1.5 | 1025 | 29 | 263 | 132 |
| Orinoco | 2740 | 945,000 | 5493 | 70 | 2 | 972 | 35.9 | 209 | 105 |
| Zambezi | 2660 | 1,400,000 | 2606 | 23.3 | 1 | 1183 | 20.1 | 352 | 176 |
| Amudar'ya | 2620 | 309,000 | 7459 | 44.8 | 2.8 | 556 | 28.3 | 242 | 121 |
| Ganges | 2510 | 980,000 | 8848 | 221.9 | 3.5 | 990 | 63.6 | 99 (470) | 50 |
| Ural | 2430 | 237,000 | 1000 | 2.2 | 0.4 | 487 | 11.1 | 532 | 266 |
| Colorado (Cal) | 2333 | 640,000 | 4730 | 61.1 | 2 | 800 | 37.7 | 144 | 72 |
| Irrawaddy | 2300 | 410,000 | 5881 | 130.4 | 2.6 | 640 | 79.6 | 66 | 33 |
| Syrdar'ya | 2210 | 219,000 | 5880 | 8.9 | 2.7 | 468 | 7.1 | 684 | 342 |
| Dnepr | 2200 | 504,000 | 325 | 4.9 | 0.1 | 710 | 46.3 | 105 | 52 |
| Xi Jiang | 2129 | 464,000 | 2500 | 78.5 | 1.2 | 681 | 98.2 | 46 | 23 |
| Columbia | 1950 | 670,000 | 3748 | 18.5 | 1.9 | 819 | 11.8 | 323 | 162 |
| Don | 1870 | 422,000 | 367 | 7.4 | 0.2 | 650 | 58.1 | 60 | 30 |
| Orange | 1860 | 1,020,000 | 3482 | 38.1 | 1.9 | 1010 | 20.2 | 171 | 86 |
| Pechora | 1810 | 322,000 | 1894 | 4.9 | 1 | 567 | 8.2 | 401 | 200 |
| Indigirka | 1726 | 360,000 | 3147 | 5.9 | 1.8 | 600 | 5.4 | 550 | 275 |
| Limpopo | 1600 | 440,000 | 2322 | 12.2 | 1.5 | 663 | 12.7 | 202 | 101 |
| Volta | 1600 | 394,000 | 500 | 8.1 | 0.3 | 628 | 41.5 | 62 | 31 |
| Magdalena | 1530 | 260,000 | 5493 | 91.9 | 3.6 | 510 | 50.2 | 47 | 23 |

(continued on next page)

Table 1 (*continued*)

| River [units] | Stream length,[a] Lr [km] | Drainage area,[a] $A$ [km$^2$] | Maximum height,[a] $H_{max}$ [m] | Sediment flux,[a] Qst (with sediment density = 2700 kg/m$^3$) [10$^6$ m$^3$/a] | Mean slope,[a] $S$ ($S=H_{max}/Lr$) [10$^{-3}$] | Minimum estimated width, $W$ ($W=cA^b$ with $c=0.001$ and $b=0.5$) [m] | Diffusivity coefficient, $K$ ($K=Qst/WS$) [10$^6$ m$^2$/a] | Response time, $T$ ($T=L^2/K$ with Qst = suspended and dissolved loads) [ka] | Response time,[b] Tb (Tb = $T/2$ with Qstb = 2Qst) [ka] |
|---|---|---|---|---|---|---|---|---|---|
| Godavari | 1500 | 287,000 | 1300 | 63 | 0.9 | 536 | 135.6 | 17 | 8 |
| Colorado (Tex) | 1450 | 100,000 | 1440 | 6.7 | 1 | 316 | 21.2 | 99 | 50 |
| Senegal | 1430 | 441,000 | 1000 | 1.1 | 0.7 | 664 | 2.3 | 884 | 442 |
| Brazos | 1400 | 114,000 | 950 | 12.6 | 0.7 | 338 | 55 | 36 | 18 |
| Chari | 1400 | 880,000 | 3071 | 2.6 | 2.2 | 938 | 1.3 | 1556 | 778 |
| Rufiji | 1400 | 178,000 | 2959 | 6.3 | 2.1 | 422 | 7.1 | 278 | 139 |
| Kura | 1360 | 188,000 | 4480 | 15.2 | 3.3 | 434 | 10.6 | 174 | 87 |
| Rhein | 1360 | 225,000 | 4158 | 6.6 | 3.1 | 474 | 4.5 | 409 | 204 |
| Dnestr | 1350 | 72,100 | 2058 | 2.4 | 1.5 | 269 | 5.9 | 310 | 155 |
| Liao He | 1350 | 170,000 | 2029 | 15.2 | 1.5 | 412 | 24.5 | 74 | 37 |
| Krishna | 1290 | 256,000 | 1892 | 24.1 | 1.5 | 506 | 32.4 | 51 | 26 |
| Chao Phraya | 1200 | 160,000 | 2300 | 5.2 | 1.9 | 400 | 6.8 | 213 (1400) | 106 |
| Red (Song Koi) | 1200 | 120,000 | 3000 | 45.6 | 2.5 | 346 | 52.6 | 27 | 14 |
| Kizil Irmak | 1151 | 75,800 | 3916 | 8.5 | 3.4 | 275 | 9.1 | 146 | 73 |
| Elbe | 1110 | 148,000 | 1603 | 0.3 | 1.4 | 385 | 0.6 | 2200 | 1100 |
| Fraser | 1110 | 220,000 | 4043 | 11.5 | 3.6 | 469 | 6.7 | 183 | 92 |
| Loire | 1110 | 120,000 | 1885 | 0.6 | 1.7 | 346 | 0.9 | 1305 | 652 |
| Kuskokwim | 1080 | 116,000 | 6194 | 2.8 | 5.7 | 341 | 1.4 | 820 | 410 |
| Mobile | 1064 | 57,000 | 1360 | 2.3 | 1.3 | 239 | 7.6 | 148 | 74 |
| Vistula | 1014 | 198,000 | 2499 | 5.7 | 2.5 | 445 | 5.2 | 196 | 98 |
| Rio Colorado (Arg) | 1000 | 65,000 | 6960 | 2.6 | 7 | 255 | 1.4 | 694 | 347 |
| Rio Grande Santiago | 960 | 125,000 | 4577 | 0.4 | 4.8 | 354 | 0.2 | 4194 | 2097 |
| Ebro | 930 | 86,800 | 3404 | 7.8 | 3.7 | 295 | 7.2 | 120 | 60 |
| Meuse | 925 | 29,000 | 692 | 0.3 | 0.7 | 170 | 2 | 420 | 210 |
| Oder | 909 | 112,000 | 1603 | 2.6 | 1.8 | 335 | 4.5 | 185 | 92 |
| Apalachicola | 880 | 51,800 | 1458 | 0.4 | 1.7 | 228 | 1.1 | 674 | 337 |
| Jana | 872 | 238,000 | 3000 | 1.5 | 3.4 | 488 | 0.9 | 861 | 431 |
| Sanaga | 860 | 135,000 | 2000 | 2.2 | 2.3 | 367 | 2.6 | 289 | 145 |
| Mahanadi | 858 | 133,000 | 1027 | 22.2 | 1.2 | 365 | 50.9 | 14 | 7 |
| Sepik | 825 | 81,000 | 4500 | 29.6 | 5.5 | 285 | 19.1 | 36 | 18 |
| Rhone | 810 | 99,000 | 4810 | 22.2 | 5.9 | 315 | 11.9 | 55 | 28 |
| Seine | 780 | 78,600 | 902 | 4.9 | 1.2 | 280 | 15 | 41 | 20 |
| Fly | 744 | 64,400 | 3993 | 25.9 | 5.4 | 254 | 19 | 29 | 15 |
| Susquehanna | 733 | 72,500 | 950 | 0.7 | 1.3 | 269 | 1.9 | 281 | 141 |
| Rio Negro (Arg) | 729 | 130,000 | 4800 | 4.8 | 6.6 | 361 | 2 | 262 | 131 |
| Weser | 724 | 46,000 | 1142 | 0.1 | 1.6 | 214 | 0.4 | 1451 | 725 |
| Tana | 720 | 91,000 | 5200 | 11.9 | 7.2 | 302 | 5.4 | 95 | 48 |
| Po | 691 | 75,000 | 4810 | 10.4 | 7 | 274 | 5.4 | 88 | 44 |
| Burdekin | 680 | 131,000 | 1277 | 1.1 | 1.9 | 362 | 1.6 | 283 | 141 |
| Colville | 662 | 60,900 | 2320 | 2.6 | 3.5 | 247 | 3 | 146 | 73 |
| Garonne | 650 | 86,000 | 3308 | 0.8 | 5.1 | 293 | 0.5 | 774 | 387 |
| Haiho | 650 | 50,800 | 2870 | 30 | 4.4 | 225 | 30.1 | 14 | 7 |
| Terek | 623 | 43,200 | 5642 | 10 | 9.1 | 208 | 5.3 | 73 | 37 |
| Sacramento | 610 | 73,000 | 3187 | 9.3 | 5.2 | 270 | 6.6 | 57 | 28 |
| Kemijoki | 600 | 37,800 | 807 | 0.1 | 1.3 | 194 | 0.2 | 1695 | 847 |

Table 1 (*continued*)

| River [units] | Stream length,[a] Lr [km] | Drainage area,[a] $A$ [km$^2$] | Maximum height,[a] $H_{max}$ [m] | Sediment flux,[a] Qst (with sediment density = 2700 kg/m$^3$) [10$^6$ m$^3$/a] | Mean slope,[a] $S$ ($S=H_{max}$/Lr) [10$^{-3}$] | Minimum estimated width, $W$ ($W=cA^b$ with $c=0.001$ and $b=0.5$) [m] | Diffusivity coefficient, $K$ ($K=$Qst/$WS$) [10$^6$ m$^2$/a] | Response time, $T$ ($T=L^2/K$ with Qst = suspended and dissolved loads) [ka] | Response time,[b] Tb (Tb = $T$/2 with Qstb = 2Qst) [ka] |
|---|---|---|---|---|---|---|---|---|---|
| San Joaquin | 560 | 80,100 | 4420 | 0.7 | 7.9 | 283 | 0.3 | 946 | 473 |
| Delaware | 518 | 22,900 | 1360 | 0.6 | 2.6 | 151 | 1.6 | 171 | 86 |
| Susitna | 454 | 50,300 | 6190 | 9.3 | 13.6 | 224 | 3 | 68 | 34 |
| Copper | 360 | 61,800 | 5952 | 25.9 | 16.5 | 249 | 6.3 | 21 | 10 |

[a] All the rivers in the Hovius (1998) database are used, less the Mahakam, Ord, Sevemaya Dvina, and Uruguay rivers for which the lengths are not given.

[b] Tb is the response time computed with a sediment flux two times larger than given in Hovius (1998) in order to take into account a maximum of 50% bedload contribution.

[c] For comparison, the values computed by Métivier (1999) for some large Asian rivers are given between parentheses.

The total sediment flux output Qst of these rivers is given by the sum of the total annual suspended and solute loads (Table 1). Taking into account the bedload contribution, usually considered to be on the order of 10% (Hovius, 1998), and trying to avoid sediment flux underestimations, we increase sediment flux Qst by a factor of two (Qstb). This is based on Paleogene sediment volume measurements in the North Sea basin, which have shown an average proportion of up to 50% sand (Liu and Galloway, 1997).

The estimate of the river width $W$ at its mouth is based on the classic hydraulic geometry relation (Leopold and Maddock, 1953):

$$W = cA^b$$

where $A$ is the drainage area, and $c$ and $b$ are two positive coefficients. We use $b=0.5$ to respect the classic square root relationship between width and discharge for alluvial channels (Leopold and Maddock, 1953; Knighton, 1998). Although the coefficient $c$ is naturally specific for each river, we use the same $c=0.001$ for all rivers because it is a minimum coefficient observed on natural alluvial reaches (Montgomery and Gran, 2001), and in the hope that this would therefore provide a minimum width (Table 1).

The mean river gradient $\langle \partial z/\partial x \rangle$ ($S$ in Table 1) is calculated by dividing the maximum elevation $H_{max}$ in the drainage basin by the stream length Lr.

The obtained response times (Table 1, Fig. 2) range between a maximum $T$ calculated with only suspended and dissolved loads, and a minimum Tb calculated with a sediment flux at river mouths two times larger to account for 50% of bedload sediment transport.

The comparison of our results with the response times of Métivier and Gaudemer (1999) (Table 1) shows that even our maximum response times may be large underestimations of real ones, and may therefore strongly minimize the buffering action of rivers. This is mainly due to the underestimation of river widths by about one order of magnitude compared with certain real values (Penn, 2001). In the minimum case (Tb), 58% of those rivers have response times of more than 100 ka, 78% of more than 40 ka, and 91% of more than 20 ka. Therefore, even intermediate rivers, compared to large Asian rivers, can have a strong buffering effect for high-frequency sediment input disturbances.

By analogy with the skin distance in heat diffusion problems (e.g., Turcotte and Schubert, 1982), we have plotted (Fig. 2) a "buffer distance" Bd for sediment flux oscillations with periods of 20, 40, and 100 ka (Fig. 2B–D respectively):

$$\mathrm{Bd} = \sqrt{\frac{K\lambda}{\pi}}$$

This buffer distance is the distance over which sediment flux disturbances of period $\lambda$ are lessened by one

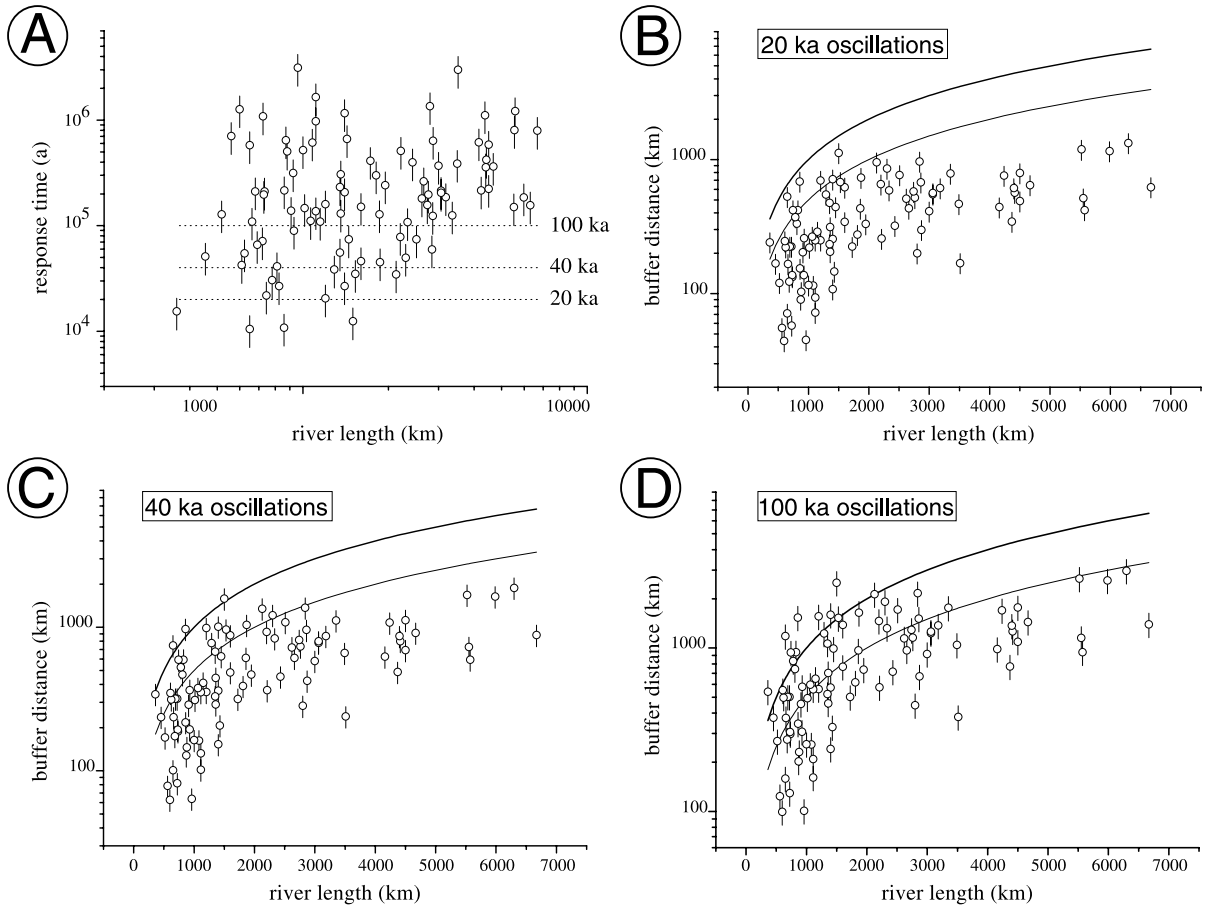


Fig. 2. Response times and buffer distances of some modern rivers (data from Hovius, 1998) as a function of their length, considering a diffusive behaviour for the transfer of sediments by rivers. For each point, the vertical line represents the uncertainty associated with a more or less 50% of bedload contribution to the total sediment load. (A) Response times versus river lengths: a majority of response times reach values of more than 100 ka. (B–D) Buffer distances versus river lengths for 20, 40, and 100 ka sediment flux disturbances, respectively. The bold and tight curves represent river and half-river lengths, respectively.

third of their initial amplitude. After the distance Bd, the disturbances are phase-delayed by 1 rad (i.e., by about 0.16 $\lambda$) (Turcotte and Schubert, 1982). For most rivers, sediment flux disturbances of 20 and 40 ka periodicities are attenuated by one third of their initial amplitude over distances of less than half their length (Fig. 2B and C). This is less well defined for 100 ka disturbances (Fig. 2D), although it remains valid for a majority of rivers.

Note that a drawback of this model is that it assumes a constant diffusivity with time. In particular, the influence of water discharge variations (due to climate change), which are expected to accompany sediment input variations to the transfer subsystem, is not accounted for by this model. This means that the model only investigates the response time of the transfer subsystem to sediment input variations.

Taking into account that we have computed minimum estimates, it appears that not only large but also intermediate rivers (>300 km) can act as a strong buffer for high-frequency ( $\leq$ 100 ka) sediment input variations to the transfer subsystem. For most natural rivers and for disturbances with periodicities between 20 and 100 ka, the buffer effect induces a significant signal attenuation over a distance of less than half the river length.

## 4. Discussion

There is no debate as to whether the sediment input is a fundamental variable in controlling the stratigraphic record (e.g., Galloway, 1989; Lawrence, 1993; Schlager, 1993). The debate is about the time scales of this control. By focusing on the depositional area, stratigraphers have often assumed that sediment flux was comparable to relative sea level in terms of variability (i.e., that sediment flux variations to the basin were directly tied to climate or tectonic disturbances in the source area). In the light of the sedimentary system concept, however, it appears that (1) the sediment flux is a derivative of tectonic and climatic changes in the source area and (2) then has to be transported from its production zone to the deposition zone, which is unlikely to be instantaneous. This last point is usually neglected (e.g., Perlmutter et al., 1998; Van der Zwan, 2002). The sedimentary system concept therefore puts forward that the first-order controls on the time scales of variation of the sediment flux to the basin are the response times of the erosion and transfer subsystems.

The analysis provided here by using a simple diffusive model for fluvial entities shows that intermediate and large transfer subsystems (>300 km) will buffer high-frequency ($\leq 100$ ka) sediment input disturbances coming from the erosion subsystem. This is in agreement with the buffering action evidenced for large Asian floodplains facing potential high-frequency climate-induced sediment flux variations during the last 2 Ma (Métivier, 1999; Métivier and Gaudemer, 1999). The transfer subsystem therefore plays a crucial role in the final stratigraphic record of allogenic forcings.

A strong implication is that stratigraphic studies interested in clastic successions should always be aware of the first-order dimensions of the erosion and transfer subsystems in order to assess the plausibility of high-frequency sediment flux variations. In sedimentary systems with short (perhaps less than 300 km) to negligible transfer subsystems, such as catchment–fan systems, high-frequency variations of sediment flux to the sedimentation subsystem can occur in equilibrium with climate changes in the source area. In such systems, if the influences of basin factors, which combine with the sediment flux to yield the final stratigraphy, can be unraveled, the stratigraphic record may therefore provide valuable information about short-term climatic and tectonic changes in the source zone. In detrital accumulations fed by way of intermediate to large transfer subsystems, as in the case of large deltas for example, high-frequency (100 ka) sediment flux oscillations may not occur in equilibrium with allogenic changes in the source area. Therefore, high-frequency stratigraphic cycles cannot be an equilibrium response to such allogenic changes. In these accumulations, only over the long term (i.e., of more than hundreds of thousands of years) can sediment supply variations in equilibrium with climate or tectonic changes in the source area be detected, as evidenced in several studies (e.g., Sloss, 1979; Raymo et al., 1988; Hay et al., 1988; Galloway and Williams, 1991; Nott and Roberts, 1996; Liu and Galloway, 1997; Peizhen et al., 2001), and have a possible influence on the stratigraphic record. The high-resolution stratigraphic record of basins fed by intermediate to large transfer subsystems can provide information about high-frequency variations of basin factors as eustasy or basin tectonics, but not about high-frequency climatic or tectonic changes in the upstream zones. Note that we do not argue here that high-frequency sediment supply variations at the outlet of the transfer subsystem do not occur. We only put forward that they will not be in equilibrium with the forcing if the transfer length is intermediate to large. In this way, our conclusions do not preclude rich stratigraphic responses of alluvial basins to rapidly changing sediment supply or diffusivity (Paola et al., 1992).

A weakness of our analysis is that it is based on modern river data and on assumptions, such as the square root relationship between drainage area and river width, which may be different in ancient sedimentary systems (Paola, 2000). Also, the problem of approximating the transfer of sediments by linear diffusion should be further addressed.

Therefore, our conclusions underscore the need for future research on the behaviour of the transfer subsystems and of the sedimentary system in general.

## Acknowledgements

We are indebted to D. Lague and K. Whipple for decisive discussions in the writing of this paper. Also,

we are grateful to an anonymous reviewer for helpful and constructive remarks. It is a pleasure to thank C. Anderson-Cambefort, P. Anderson-Cambefort, K. Besnard, P. Davy, F. Guillocheau, and N. Loget for their assistance and encouragement at various stages of this work. Carol Anderson-Cambefort kindly corrected the English.

## References

Allen, P.A., 1997. Earth Surface Processes. Blackwell, Oxford. 404 pp.

Allen, P.A., Densmore, A.L., 2000. Sediment flux from an uplifting fault block. Basin Res. 12, 367–380.

Beaumont, C., Kooi, H., Wilett, S., 2000. Coupled tectonic-surface process models with applications to rifted margins and collisional orogens. In: Summerfield, M.A. (Ed.), Geomorphology and Global Tectonics. Wiley, New York, pp. 29–55.

Blum, M.D., Törnqvist, T.E., 2000. Fluvial responses to climate and sea-level change: a review and look forward. Sedimentology 47 (Suppl. 1), 2–48.

Bull, W.B., 1991. Geomorphologic Responses to Climate Change. Oxford Univ. Press, New York. 326 pp.

Burns, B.A., Heller, P.L., Marzo, M., Paola, C., 1997. Fluvial response in a sequence stratigraphic framework: example of the Montserrat fan delta, Spain. J. Sediment. Res. 67 (2), 311–321.

Cross, T.A., 1988. Controls on coal distribution in transgressive–regressive cycles. Upper Cretaceous, Western Interior, USA. In: Wilgus, C.K., et al. (Eds.), Sea-Level Changes: An Integrated Approach. Soc. Econ. Paleontol. Mineral. Spec. Publ., vol. 42, pp. 47–70. Tulsa.

Cui, Y., et al. Sediment pulses in mountain rivers: Part 1. Experiments. Water Resour. Res., submitted for publication.

Dade, W.B., Friend, P.F., 1998. Grain-size, sediment-transport regime, and channel slope in alluvial rivers. J. Geol. 106, 661–675.

Einsele, G., Ricken, W., Seilacher, A. (Eds.), 1991. Cycles and Events in Stratigraphy. Springer-Verlag, Berlin.

Fernandes, N.F., Dietrich, W.E., 1997. Hillslope evolution by diffusive processes: the timescale for equilibrium adjustments. Water Resour. Res. 33 (6), 1307–1318.

Fournier, F., 1960. Climat et erosion: la relation entre l'erosion du sol par l'eau et les precipitations atmospheriques. Presses Universitaires de France, Paris.

Gale, A.S., et al., 2002. Global correlation of Cenomanian (Upper Cretaceous) sequences: evidence for Milankovitch control on sea level. Geology 30 (4), 291–294.

Galloway, W.E., 1989. Genetic stratigraphic sequences in basin analysis: I. Architecture and genesis of flooding-surface bounded depositional systems. Am. Assoc. Pet. Geol. Bull. 73, 125–142.

Galloway, W.E., Williams, T.A., 1991. Sediment accumulation rates in time and space: Paleogene genetic stratigraphic sequences of the northwestern Gulf of Mexico basin. Geology 19, 986–989.

Hay, W.W., Sloan II, J.L., Wold, C.N., 1988. Mass/age distribution and composition of sediments on the ocean floor and the global rate of sediment subduction. J. Geophys. Res. 93 (B12), 14933–14940.

Hovius, N., 1998. Controls on sediment supply by large rivers. In: Shanley, K.W., McCabe, P.J. (Eds.), Relative Role of Eustasy, Climate and Tectonism in Continental Rocks. Soc. Econ. Paleontol. Mineral. Spec. Publ., vol. 59, pp. 3–16. Tulsa.

Humphrey, N.F., Heller, P.L., 1995. Natural oscillations in coupled geomorphic systems: an alternative origin for cyclic sedimentation. Geology 23 (6), 499–502.

Jervey, M.T., 1988. Quantitative geological modeling of siliciclastic rock sequences and their seismic expressions. In: Wilgus, C.K., et al. (Eds.), Sea-Level Change: An Integrated Approach. Soc. Econ. Paleontol. Mineral. Spec. Publ., vol. 42, pp. 47–69. Tulsa.

Knighton, D., 1998. Fluvial Forms and Processes. Arnold, London.

Lawrence, D.T., 1993. Evaluation of eustasy, subsidence, and sediment input as controls on depositional sequence geometries and the synchroneity of sequence boundaries. In: Weimer, P., Posamentier, H. (Eds.), Siliciclastic Sequence Stratigraphy: Recent Developments and Applications. Am. Assoc. Pet. Geol. Mem., vol. 58, pp. 337–367.

Leopold, L.B., Maddock, T., 1953. The hydraulic geometry of streams channels and some physiographic implications. Prof. Pap.-Geol. Surv. (U. S.) 252, 57.

Lisle, T.E., Pizzuto, J.E., Ikeda, H., Iseya, F., Kodama, Y., 1997. Evolution of a sediment wave in an experimental channel. Water Resour. Res. 33 (8), 1971–1981.

Liu, X., Galloway, W.E., 1997. Quantitative determination of Tertiary sediment supply to the North Sea basin. Am. Assoc. Pet. Geol. Bull. 81 (9), 1482–1509.

Lopez-Blanco, M., Marzo, M., Piña, J., 2000. Transgressive–regressive sequence hierarchy of foreland, fan–delta clastic wedges (Montserrat and Sant Llorenç del Munt, Middle Eocene, Ebro Basin, NE Spain). Sediment. Geol. 138, 41–69.

Marr, J.G., Swenson, J.B., Paola, C., Voller, V.R., 2000. A two-diffusion model of fluvial stratigraphy in closed depositional basins. Basin Res. 12, 381–398.

Marzo, M., Steel, R.J., 2000. Unusual features of sediment supply-dominated, transgressive–regressive sequences: Paleogene clastic wedges, SE Pyrenean foreland basin, Spain. Sediment. Geol. 138, 3–15.

Métivier, F., 1999. Diffusive-like buffering and saturation of large rivers. Phys. Rev., E Stat. Phys. Plasmas Fluid Relat. Interdiscip. Topics 60 (5), 5827–5832.

Métivier, F., Gaudemer, Y., 1999. Stability of output fluxes of large rivers in South and East Asia during the last 2 million years: implications on floodplain processes. Basin Res. 11, 293–303.

Métivier, F., Gaudemer, Y., Tapponnier, P., Klein, M., 1999. Mass accumulation rates in Asia during the Cenozoic. Geophys. J. Int. 137, 280–318.

Milliman, J.D., Meade, R.H., 1983. World-wide delivery of river sediment to the oceans. J. Geol. 91 (1), 1–21.

Milliman, J.D., Syvitski, J.P.M., 1992. Geomorphic/tectonic control of sediment discharge to the ocean: the importance of small mountainous rivers. J. Geol. 100 (5), 525–544.

Montgomery, D.R., Gran, K.B., 2001. Downstream variations in

the width of bedrock channels. Water Resour. Res. 37 (6), 1841–1846.
Mulder, T., Syvitski, J.P.M., 1996. Climatic and morphologic relationships of rivers: implications of sea-level fluctuations on river loads. J. Geol. 106, 509–523.
Muto, T., Steel, R.J., 1997. Principle of regression and transgression: the nature of the interplay between accommodation and sediment supply. J. Sediment. Res. 67 (6), 994–1000.
Muto, T., Steel, R.J., 2000. The accommodation concept in sequence stratigraphy: some dimensional problems and possible redefinition. Sediment. Geol. 130, 1–10.
Nott, J., Roberts, R.G., 1996. Time and process rates over the past 100 m.y.: a case for dramatically increased landscape denudation rates during the late Quaternary in northern Australia. Geology 24 (10), 883–887.
Nystuen, J.P., 1998. History and development of sequence stratigraphy. In: Gradstein, F.M., Sandvik, K.O., Milton, N.J. (Eds.), Sequence Stratigraphy—Concepts and Applications. Norwegian Petroleum Society (NPF) Special Publications. Elsevier, Amsterdam, pp. 31–116.
Paola, C., 2000. Quantitative models of sedimentary basin filling. Sedimentology 47, 121–178.
Paola, C., Heller, P.L., Angevine, C.L., 1991. The response distance of river systems to variations in sea level. Geol. Soc. Am. Abstr. Programs 23, A170–A171.
Paola, C., Heller, P.L., Angevine, C.L., 1992. The large-scale dynamics of grain-size variation in alluvial basins: I. Theory. Basin Res. 4 (2), 73–90.
Peizhen, Z., Molnar, P., Downs, W.R., 2001. Increased sedimentation rates and grain sizes 2–4 Myr ago due to the influence of climate change on erosion rates. Nature 410, 891–897.
Penn, J.R., 2001. Rivers of the World : A Social, Geographical, and Environmental Sourcebook. ABC-CLIO, Santa Barbara, CA.
Perlmutter, M.A., Matthews, M.D., 1989. Global cyclostratigraphy—a model. In: Cross, T.A. (Ed.), Quantitative Dynamic Stratigraphy. Prentice-Hall, Englewood Cliffs, pp. 233–260.
Perlmutter, M.A., Radovic, B.J., Matthews, M.D., Kendall, M.D., 1998. The impact of high-frequency sedimentation cycles on stratigraphic interpretation. In: Gradstein, F.M., Sandvick, K.O., Milton, N.Y. (Eds.), Sequence Stratigraphy, Concepts and Applications. NPF Special Publications. Elsevier, Amsterdam, pp. 141–170.
Pinet, P., Souriau, M., 1988. Continental erosion and large-scale relief. Tectonics 7 (3), 563–582.
Plint, A.G., Eyles, N., Eyles, C.H., Walker, R.G., 1992. Control of sea level change. In: Walker, R.G., James, N.P. (Eds.), Facies Models: Response to Sea Level Change. Geological Association of Canada, St. John's, pp. 15–25.
Posamentier, H.W., Jervey, M.T., Vail, P.R., 1988. Eustatic control on clastic deposition: I. Conceptual framework. In: Wilgus, C.K., et al. (Eds.), Sea-Level Change: An Integrated Approach. Soc. Econ. Paleontol. Mineral. Spec. Publ., vol. 4, pp. 109–124. Tulsa.
Raymo, M.E., Ruddiman, W.F., Froelich, P.N., 1988. Influence of late Cenozoic mountain building on ocean geochemical cycles. Geology 16, 649–653.
Schlager, W., 1993. Accommodation and supply—a dual control on stratigraphic sequences. In: Cloetingh, S., Sassi, W., Horvath, P., Puigdefabregas, C. (Eds.), Basin Analysis and Dynamics of Sedimentary Basin Evolution. Sediment. Geol., pp. 111–136.
Schumm, 1977. The Fluvial System. Wiley, New York.
Shanley, K.W., McCabe, P.J., 1994. Perspectives on the sequence stratigraphy of continental strata. Am. Assoc. Pet. Geol. Bull. 78 (4), 544–568.
Sloss, L.L., 1962. Stratigraphic Models in Exploration. Am. Assoc. Pet. Geol. Bull. 46 (7), 1050–1057.
Sloss, L.L., 1979. Global sea level changes: a view from the Craton. In: Watkins, J.S., Montadert, L., Dickerson, P.W. (Eds.), Am. Assoc. Pet. Geol. Mem., vol. 29, pp. 461–467.
Snyder, N.P., Whipple, K.X., Tucker, G.E., Merrits, D.J., 2000. Landscape response to tectonic forcing: digital elevation model analysis of stream profiles in the Mendocino triple junction region, northern California. Geol. Soc. Am. Bull. 112 (8), 1250–1263.
Summerfield, M.A., Hulton, N.J., 1994. Natural controls of fluvial denudation rates in major world drainage basins. J. Geophys. Res. 99 (B7), 13871–13883.
Swenson, J.B., Voller, V.R., Paola, C., Parker, G., Marr, J.G., 2000. Fluvio-deltaic sedimentation: a generalized Stefan problem. Eur. J. Appl. Math. 11, 1–20.
Tiedemann, R., Franz, S.O., 1997. Deep-water circulation chemistry and terrigenous sediment supply in the equatorial Atlantic during the Pliocene, 3.3–2.6 Ma and 5–4.5 Ma. In: Shackleton, N.J., Curry, W.B., Richter, C., Brawlower, T.J. (Eds.), Proc. Ocean Drill. Program Sci. Results, pp. 299–318.
Tucker, G.E., Slingerland, R., 1996. Predicting sediment flux from fold and thrust belts. Basin Res. 8, 329–349.
Tucker, G.E., Slingerland, R., 1997. Drainage basin response to climate change. Water Resour. Res. 33 (8), 2031–2047.
Turcotte, D.L., Schubert, G., 1982. Geodynamics. Wiley, New York.
Van der Zwan, C.J., 2002. The impact of Milankovitch-scale climatic forcing on sediment supply. Sediment. Geol. 147, 271–294.
Van Wagoner, J.C., Mitchum, R.M., Campion, K.M., Rahmanian, V.D. (Eds.), 1990. Siliciclastic sequence stratigraphy in well logs, cores and outcrops: concepts for high-resolution correlation of time and facies. Am. Assoc. Pet. Geol., Methods Explor. Ser., vol. 7. 55 pp.
Weltje, G.J., de Boer, P.L., 1993. Astronomically induced paleoclimatic oscillations reflected in Pliocene turbidite deposits on Corfu (Greece): implications for the interpretation of higher order cyclicity in ancient turbidite systems. Geology 21, 307–310.
Weltje, G.J., VanAnsenwoude, S.O.K.J., DeBoer, P.L., 1996. High-frequency detrital signals in Eocene fan–delta sandstones of mixed parentage (south-central Pyrenees, Spain): a reconstruction of chemical weathering in transit. J. Sediment. Res. 66 (1), 119–131.
Whipple, K.X., 2001. Fluvial landscape response time: how plausible is steady-state denudation? Am. J. Sci. 301, 313–325.

## 3.2. Modélisation de la dynamique des systèmes fluviatiles

Cette partie concerne la simulation du comportement des rivières alluviales au moyen du modèle numérique EROS conçu et développé à Rennes par Philippe Davy et Alain Crave pour l'étude de la dynamique de l'érosion. Le but recherché est de contraindre le rôle du système fluviatile dans la transmission du flux sédimentaire depuis la zone en érosion jusqu'aux bassins. Le modèle EROS utilise l'approche des automates cellulaires (appelés precipitons dans le modèle) pour simuler les systèmes complexes dynamiques à l'aide d'un nombre restreint de lois physiques simples. Les precipitons sont des éléments d'eau qui se déplacent de cellule en cellule et qui transportent les sédiments en fonction du bilan entre les deux processus d'érosion et de sédimentation traités de manière indépendante dans le modèle. L'érosion est une fonction du flux d'eau et de la pente. La sédimentation est définie comme une fraction $1/l_d$ de la charge sédimentaire en transport, $l_d$ étant un paramètre qui caractérise la longueur de transport des sédiments. Comme dans le modèle de rivières en tresses de Murray & Paola (1994), une loi d'érosion latérale a été incorporée pour permettre l'érosion des bordures de chenal nécessaire aux avulsions et migrations latérales des chenaux.

Différents aspects ont été analysés dans les simulations.

1. Nous montrons d'abord que *la variété des formes fluviales en tresses, droites et sinueuses, est reliée à l'écart du système par rapport à sa pente d'équilibre pour des conditions de flux d'eau et de sédiment fixés (nature et quantité)*. Les systèmes en tresses s'installent toujours pendant les phases d'aggradation vers la pente d'équilibre, alors que les systèmes sinueux ne sont présents qu'à l'équilibre, et les systèmes droits en incision et à l'équilibre.
2. Nous avons réalisé ensuite une série d'expériences pour examiner les relations entre temps d'équilibre caractéristique et longueur des systèmes fluviatiles simulés, de manière à tester l'hypothèse diffusive adoptée dans le chapitre précédent. *Dans l'ensemble les rivières simulées se comportent comme des systèmes diffusifs tant que la longueur de transport reste inférieure à la longueur du système*. Ceci confirme la prédiction selon laquelle les rivières peuvent être considérées comme des entités diffusives, et renforce l'idée *qu'elles jouent le rôle de filtre pour les variations haute-fréquence du flux sédimentaire venant de l'aire source*.
3. Enfin, ces simulations montrent que *des cycles de flux sédimentaire à la sortie du système fluviatile peuvent être produits par sa propre dynamique interne (autocyclicité) en raison du couplage non-linéaire entre les processus d'érosion et sédimentation*. Ces cycles pourraient être alors confondus avec des cycles allogéniques pour un observateur situé dans le bassin.

Article :

## Sediment flux to basins: some insights from a numerical river model

Sébastien Castelltort, Philippe Davy and Jean Van Den Driessche

Géosciences Rennes, Campus de Beaulieu, 35042 Rennes cedex - France

*To be submitted*

# SEDIMENT FLUX TO BASINS: SOME INSIGHTS FROM A NUMERICAL RIVER MODEL

SÉBASTIEN CASTELLTORT, PHILIPPE DAVY AND JEAN VAN DEN DRIESSCHE

*Géoscience Rennes, UMR 6118 du CNRS, Campus de Beaulieu, 35042 Rennes, FRANCE*

## Abstract

**Building on the numerical model of landscape evolution Eros, this study is an attempt to simulate river patterns and to understand the role of fluvial systems in transmitting sediment flux from source areas to basins. The simulator uses the precipiton approach to simulate complex dynamics with a small number of simple physical rules. The precipitons represent unit volumes of water flowing from cell to cell and transporting sediments according to erosion and deposition which are treated independently. Erosion is a function of local slope and water flux. Deposition is defined as a proportion of $1/l_d$ of the sediment load in transport, with $l_d$ a parameter characterizing the transport length of sediments. Also, following Murray and Paola's model (1994), a lateral erosion rule has been added which allows erosion of bed banks, avulsion and lateral migration of channels. Different aspects of the simulated rivers are analysed. Firstly, it is shown that a variety of fluvial forms from multiple-thread braided to single-thread sinuous arises as a function of the deviation of the system from its equilibrium slope for fixed flow conditions of water and sediment flux (quantity and transport length). Braided systems occur always during aggradation toward equilibrium slope while single-thread sinuous or straigth systems only take place at equilibrium. Secondly, a series of experiments have been carried out to investigate the scaling relationships between equilibrium time (time to reach equilibrium after a disturbance) of the simulated systems and their length. The simulated rivers behave diffusively as a whole but approach an advective behaviour when the transport length is close to the system's length or larger. This confirms the prediction that rivers can be considered as diffusive entities, and reinforces the idea that they act as a buffer for high-frequency sediment flux variations coming from the source area. Lastly, the simulations show autogenic cycles of sediment output flux as a result of the non-linear coupling of erosion and deposition rules. These can be mistaken for allogenic cycles from the basin perspective.**

### INTRODUCTION

One of the first and most extensively studied feature of sedimentary successions is the presence of stratigraphic cycles at nearly all time scales from several 10's of thousand years to several million years (Einsele et al. 1991). These are cycles of advance and retreat of the whole sedimentary landscape which are classicaly attributed, for terrigenous successions, to three main variables: eustasy (or an other base level in continental areas), deformation of the

basin floor, and sediment input to the basin. While the timescales of variation of eustasy and tectonics have been fairly adressed in past works, a fondamental problem remains with regards to the timescales of variation of sediment input to basins. Indeed, quantification of past solid fluxes have been done by a few researchers due to an often partial sedimentary record and other difficulties as diagenetic and compaction processes. It has been clearly shown, however, that sediment flux could be variable at low frequencies of about 1 Ma and more (Galloway and Williams 1991; Liu and Galloway 1997; Peizhen et al. 2001; Sloss 1978). Recently, the measure of terrigenous input to basins fed by large Asian rivers has been shown to be averagely constant over the last million years, despite strong climatic fluctuations (Métivier and Gaudemer 1999). This suggests a buffering action of those river systems for high-frequency sediment flux variations with periodicities of 10's to 100's ka (Métivier 1999), which supports the idea that river systems can be considered at first order as diffusive entities (Allen and Densmore 2000; Dade and Friend 1998; Paola et al. 1992). The transfer subsystem (rivers) has therefore a crucial role in transmitting sediment flux from the source area to basins. However, although a number of numerical models readily simulate the erosion of continents and the deposition in basins, comparatively few models have tried to capture the large-scale dynamics of the transfer subsystem (Murray and Paola 1994; Murray and Paola 1997).

The present work builds on the cellular automata model of landscape evolution Eros (Crave and Davy 2001; Davy and Crave 2000) in order to simulate some of the main feature of river dynamics and implications for the sediment flux to basins. An attempt is drawn to relate the first order channel pattern (single- or mutiple-threads) to the state of the system with regards to aggradation, incision or equilibrium. Then, to test the validity of assuming a diffusive behaviour for rivers, experiments are performed to explore the scaling relationships between system's equilibrium time and system's length.

#### BRIEF BACKGROUND ON FLUVIAL EROSION-DEPOSITION MODELLING

There is currently two main types of numerical models that simulate the macroscopic evolution of the earth surface: (1) those models interested in simulating relief evolution as resulting from the coupled action of hillslopes and rivers in response to climate and tectonics, or "surface-processes models" (SPMs, Beaumont et al. 2000), and (2) those which simulate the dynamics of sedimentation in response to subsidence, base level, sediment input and physiographic factors, or "quantitative stratigraphic models" (Paola 2000). A gap exists

between these two end-members because, apart from very specific numerical simulations of meandering rivers, only few models have attempted to capture river dynamics which make the link between the erosion zone as modelled in SPMs and the sedimentation zone of stratigraphic models. To our knowledge, only recently did the cellular automata model of Murray and Paola (1994; 1997) filled in this gap. By contrast, one can note that the contrary occurs in the experimental research realm where, until recently, there has been much more investigation of river dynamics than of erosion processes or basin stratigraphy.
However, most fluvial processes have been formalised for the needs of SPMs because fluvial dynamics are an essential component of the landscape evolution. In the following we briefly report the different approaches of fluvial processes as employed in SPMs, only in order to put forward the Eros model specificities. This part is based upon Lague (2001) to which the reader is referred for a more exhaustive review.

Natural observations classicaly yield two main river types : *bedrock* and *alluvial* channels. Channels which are bedrock-floored detach particles from their cohesive bed because the transport capacity of the flow exceeds the available sediment load. On the contrary, alluvial channels are floored with a thickness of unconsolidated sediments, sourced by the upstream (and/or local) detachment and hillslope production, which are available for loading the flow up to its transport capacity. This distinction has naturally lead to the development of *detachment-limited* and *transport-limited* end-members models of landscape evolution in which the channel bed elevation is dominated by detachment and transport respectively. Eventually, *mixed alluvial-bedrock* models give a more general representation of natural landscapes as long as they allow both processes to develop contemporaneously.

**Detachment-limited models.**—Detachment rate $\varepsilon_b$ (bedrock incision in $L.T^{-1}$) is usually described (Howard and Kerby 1983; Whipple and Tucker 1999) as a function of the shear stress $\tau$ (or a unit stream power $\tau \cdot V$ with $V$ the mean flow velocity) exerted in the channel by the dominant discharge, a threshold shear stress $\tau_c$ for incision to begin, and the bedrock properties via an erodibility coefficient $K_b$ :

$$\varepsilon_b = \frac{\partial z}{\partial t} = -K_b(\tau - \tau_c)^{\zeta}$$

with $\zeta$ a positive exponent. This can be simplified, for a steady uniform flow, by using relations between the drainage area $A$, the local stream gradient $S$, the geometry of the

channel (width and depth), and dynamic parameters as water discharge and flow velocity (Howard 1994; Whipple and Tucker 1999):

$$\varepsilon_b = K\left(A^g S^h - \tau_c\right)^\zeta$$

with $K$, $g$, $h$ as constants. If the threshold is ignored, as it is often the case, because incision is likely to occur during the most important discharge events (when $\tau >> \tau_c$), the relation can be recast to the classic power law of drainage area and slope:

$$\varepsilon_b = KA^m S^n$$

The determination of the exponents $m$ and $n$ has been the subject of numerous work. The theoretical approach of Whipple and Tucker (1999) yields values of $n$ comprised between 2/3 and as much as 7/3 depending on the shear stress exponent $\zeta$ ($1 < \zeta < 7/2$) values for which there is still much uncertainty, and restricts the $m/n$ ratio to a 0.35-0.6 range. Calibration on natural streams shows values of $n$ from 0 to 2, and of $m$ from 0.1 to 0.5.

**Transport-limited models.**—In such models the transport capacity is assumed to be always satisfied, which means that bed sediment is always available for transport. Thus, sediment bed elevation change $\varepsilon_t$ can be defined as the divergence of sediment flux $q_s$ (sediment transport rate per unit channel width):

$$\varepsilon_t = -\nabla \cdot q_s$$

and sediment flux $q_s$ equals transport capacity $q_c$ which is usually described by a generic shear stress formula similar in form to that for detachment rate (Howard 1994):

$$q_c = K_t\left(\tau^* - \tau_c^*\right)^\upsilon$$

with $K_t$ a transport coefficient, $\upsilon$ a positive exponent of about 3, $\tau^*$ a dimensionless shear stress, and $\tau_c^*$ a threshold to initiate grain movement. Because it would be difficult to define the transport threshold for each grain size, a characteristic grain size $D_g$ is used as representative of the total transport and the dimensionless shear stress is defined as:

$$\tau^* = \frac{\tau}{(\rho_s - \rho)gD_g}$$

with $\rho_s$ the density of grains and $g$ the gravity. Substituting with the same relations as above, linking drainage area and flow characteristics, gives a function of the same type as for detachment:

$$q_c = K_c\left(A^{g'}S^{h'} - \tau_c^*\right)^p$$

with $K_c$ the bed sediment erodibility (different from the bedrock erodibility $K$), and $g'$, and $h'$ positive coefficients. Again, if the threshold is neglected:

$$q_c = K_c A^{m'} S^{n'}$$

The parameters $m'$ and $n'$ have been set to 1 in a number of studies for simplicity reasons, (Densmore et al. 1998; Kooi and Beaumont 1994)but are generally thought to be of more than 2 in alluvial rivers (Kirkby 1971; Murray and Paola 1997).

**Mixed models.**—If detachment- and transport-limited models impose by themselves the way they have to be simulated, different modelling approaches exist for mixed models.

First, the detachment rate can be limited by the transport capacity. This means that only stream power in excess of the available load will be used for bedrock detachment (e.g., Allen and Densmore 2000; Densmore et al. 1998; Tucker and Slingerland 1996).

Second, the variation of sediment load in a particular node is proportional to the deviation between entering sediment flux and actual transport capacity (degree of disequilibrium), via a reaction time $t_s$ (e.g., Kooi and Beaumont 1994):

$$\frac{dq_s}{dt} = \frac{1}{t_s}\left(q_c - q_s\right)$$

From a fixed viewpoint:

$$\frac{dq_s}{dt} = \frac{\partial q_s}{\partial t} + v_s \cdot \nabla q_s$$

with $v_s$ as the advection velocity of sediment flux. If sediment flux is constant over $\Delta t$, then $dq_s/dt = v_s dq_s/dx$, and the continuity equation gives:

$$\frac{\partial h}{\partial t} = -\frac{dq_s}{dx} = -\frac{1}{l_s}\left(q_c - q_s\right)$$

with $l_s = v_s t_s$ is a material property for constant $v_s$. If the transport capacity does not vary, a solution of this equation is:

$$q_s(x) = q_c\left(1 - e^{-\frac{x}{l_s}}\right)$$

Therefore, $l_s$ can be viewed as a characteristic erosion-deposition length, for which the deviation from transport capacity is reduced to $1/e$. A small $l_s$, i.e. a short reaction time, represents an easily detachable material for which the deviation is quickly reduced and the sediment load nears the transport capacity. This is thus close to the transport-limited case. On

the contrary, when $l_s$ increases, $q_s$ keeps small compared to $q_c$, and the evolution of the channel bed is closer to the detachment-limited case.

The third philosophy (Crave and Davy 2001), which is the one used in the present study, explicitly express the channel bed elevation changes as the net result of a detachment flux $\varepsilon(w,S)$ from the bed to the water phase, and a deposition flux $\delta(w,S)$ from the water phase to the bed :

$$\frac{\partial h}{\partial t} = -\varepsilon(w,S) + \delta(w,S)$$

The detachment flux $\varepsilon$ is described as a generic stream power law of water discharge $w$ and stream gradient $S$ ($\varepsilon = Kw^m S^n$), and the deposition flux $\delta$ is proportional to the sediment load in transport $q_s$ via a characteristic deposition length $l_d$ :

$$\delta = \frac{q_s}{l_d}$$

Therefore, the sediment flux variation along flow (along $l$) is :

$$\frac{dq_s}{dl} = \varepsilon - \frac{q_s}{l_d} = \frac{1}{l_d}\left(\varepsilon \cdot l_d - q_s\right)$$

The term $\varepsilon \cdot l_d$ is similar to the transport capacity $q_c$ in the model of Kooi and Beaumont (1994). By tuning the sole paramater $l_d$, all conditions can be simulated: (1) when $l_d \to 1$, the deposition flux increases and the channel nears transport-limited conditions, (2) when $l_d \to +\infty$, the deposition flux is always negligible and the channel elevation changes are detachment-limited, and (3) when $l_d$ is of the order of the system size, conditions are mixed detachment/transport-limited.

**THE EROS MODEL**

Eros (Crave and Davy 2001; Davy and Crave 2000) is based on cellular automata modelling of dynamical systems. In such models, the physics of the modelled phenomena is incorporated in a series of simple rules that specify how the network cells interact with each other. With those simple interactions they can create complex auto-organized spatial patterns and are therefore particularly well adapted for modelling the complex spatial and temporal

organization of erosional landforms (e.g., Chase 1992) and fluvial systems (Murray and Paola 1994; Murray and Paola 1997).

In Eros, the evolution of topography results from the action of discrete elements called "precipitons" (Chase 1992). Precipitons each have their own variables as discharge and sediment load which evolve along the precipiton path, and which combine with the local variables, as slope for example, to induce erosion and deposition. This scheme intuitively simulates the action of a moving elementary flow on the topography.

In its original form Eros is aimed at simulating landscape evolution at continental to sub-continental scales, and thus include a number of processes acting on hillslopes which have been described elsewhere (Crave and Davy 2001; Davy and Crave 2000). Here Eros is described as it has been employed for the simulation of river systems for the purposes of the present study, and it is compared to the model of (Murray and Paola 1994; Murray and Paola 1997).

***Method***

**Simulation grid.—**Precipitons move on a grid of square cells (pixels), defined by their elevation. For river modelling purposes, the grids employed usually are rectangular, with lengths of the order of 100 to 2000 pixels, widths ranging from 10 to 300 pixels and an initial uniform slope from the first row to the downstream end. The flow is constrained between both sides. At each iteration, precipitons are dropped randomly at an average rate on the first row of the grid, and represent a unit quantity of water (constant) with a user defined initial sediment load $[s]_p^i$ with values from 0 to 1 (concentration, or "stock"). They then follow the slope and exit the model at the last (lower) row. With time the flow can erode in, or aggrade on the initial slope which adjusts itself to the flow conditions (stream power, sediment load and deposition length).

**Walking rules.**—At each step along their walk, precipitons are free to go from one pixel to one of the height nearest neighbours, and have therefore a 360° freedom. The probability $p$ to go to a pixel of higher elevation, i.e. to follow a negative slope, is always zero:

$$S<0 \Rightarrow p(S)=0$$

When slope is positive the probability of the path depends on the slope value with two flow models:

(1) flow model 1: the “Steepest-slope condition” states that the precipiton always choose the lower nearest pixel

$$p(S)=S^{+\infty}$$

(2) flow model 2: to introduce a stochastic character to the flow direction, a second model allows the choice of other pixels than the lowest :

$$p(S_i)=\frac{S_i}{\sum_{S>0} S_i}$$

The probability that a precipiton choose the lowest pixel is still stronger but other are different from zero.

**Discharge.**—Each precipiton routes a unit water volume $v_p$ which is a constant. Therefore, the elementary water flux associated to a precipiton is a function of the duration of the precipiton event $dt_p$ :

$$w_p=\frac{v_p}{dt_p}$$

To attribute some stochasticity to the water flux values, the calculation consists in measuring, at each pixel, the time $\Delta t_p$ associated to the passage of a fixed number $k$ of precipitons. The water flux is then expressed in precipiton volume per unit time:

$$w_p=\frac{k}{\Delta t_p}$$

By tuning the parameter $k$, various water flux distributions can be predicted : when $k$ increases, water flux tend to average around the mean, whereas when $k$ decreases, water flux are more dependent on the arrival time of precipitons, which allow to increase the contribution of strong events.

**Mass conservation.**—When a precipiton walks through a pixel *M*, it both carries to, and extracts matter from this pixel. The carried matter is decribed as a depositional input flux $q_s^{in}$ from the water phase to the bed which is a function of the water flux $w_p$, the slope $S$ and the sediment stock $[s]_p$ in the precipiton :

$$q_s^{in} = \delta_p\left(w_p, S, [s]_p\right)$$

The erosion flux in turn is described as an output flux from the bed to the precipiton water phase, only depending on discharge and slope (stream power):

$$q_s^{out} = \varepsilon_p \left( w_p, S \right)$$

After the action of a number *P* of precipitons on the pixel *M*, the mass balance is:

$$dh(M) = \sum_P \left( \delta_p dt_p - \varepsilon_p dt_p \right)$$

**Fluvial processes.**—Eros uses a generic expression for sediment flux delivered from one pixel to the following, i.e. a function of the water flux $w$ and the local gradient $S$ with exponents $m$ and $n$:

$$q_s = K w^m S^n$$

Varying the exponent $m$ is a mean to simulate various erosion laws with regards to incision instabilities (Davy and Crave 2000). In Eros, values of the flow exponent $m$ less than 1 are used to represent hillslope processes, and $m > 1$ is used to represent fluvial processes assumed as non-linear transport processes.

As outlined in the preceding section on fluvial modelling, Eros explicitly differentiates erosion and deposition, and modulate the entering depositional flux by a deposition length $l_d$. On a single pixel :

$$\frac{\partial h}{\partial t} = \frac{q_s^{in}}{l_d} - q_s^{out}$$

When $l_d$ is small compared to the observed zone, the depositional flux is close to the erosion flux, as is the case in alluvial channels (transport-limited). For example, if $l_d = 1$, conditions are purely transport-limited :

$$\frac{\partial h}{\partial t} = q_s^{in} - q_s^{out} = -\nabla \cdot q_s$$

When $l_d$ is much larger than the observed zone, the deposition flux can be negligible compared to the erosion flux, and the channel becomes bedrock floored (detachment-limited):

$$\frac{\partial h}{\partial t} = -q_s^{out}$$

When $l_d$ is of the order of the system size, both comportments can take place contemporaneously in different zones of the model.

**Lateral erosion.**—Lateral erosion, i.e. sediment flux between pixels in a direction perpendicular to the flow, has been noted by Murray and Paola (1994; 1997) as a crucial parameter in keeping a constantly evolving channel system with time. This component of erosion-deposition rules is aimed at simulating the erosion of channel banks. In their model,

the lateral erosion $Q_{sl}$ of a pixel $M_l$ induced by the water flow on the pixel $M$ is proportional to the lateral slope $S_l$ between $M_l$ and $M$, and to the quantity of sediment $Q_{sM}$ leaving the pixel M:

$$Q_{sl} = K_l S_l Q_{sM}$$

$K_l$ is adjusted such as $Q_{sl}$ is of the order of some percents of $Q_{sM}$.

Following those authors a lateral erosion rule has been included in Eros (Fig. 1). For reasons of simplicity, in a preliminary step lateral erosion $\varepsilon_p^l$ is defined as a fixed percentage $\gamma$ ($0 \le \gamma \le 1$) of the vertical erosion in the pixel $M$ as :

$$\varepsilon_p^l = \gamma \cdot \varepsilon_p$$

**Topographic sinks.**—When a precipiton reaches a topographic sink, i.e. a pixel whose all neighbours are highers and constitute barriers, three cases are possible depending on the stock of sediment in the precipiton: (1) if the sediment stock is lower than the smaller barrier, all the stock is deposited and the precipiton vanishes (case 1 small load, Fig. 2), (2) if the sediment stock in larger than the smallest barrier and lower than the second smallest barrier, all the stock is deposited and the precipiton continues its path without sediment load (case 2, medium load, Fig. 2), and (3) if the sediment stock is higher than the second smallest barrier (case 3, large load, Fig. 2), the maximum deposition can fill in the sink up to the second smallest barrier $h'_{\min}$ :

$$\delta_p^{\max} = [s]_p - h'_{\min}$$

and the precipiton can then be routed downslope with the residual stock.

**Model outputs.**—A number of grid variables as topography, water flux, or sediment stock are recorded over user-defined time intervals. In this study, a 3D grid visualisation software called GridVisual developed by Philippe Davy is used to display graphic results. Also, the sediment flux at the entrance and outlet of the river are recorded at each iteration.

***Comparison with the Murray and Paola's model***

The model of Murray and Paola (1994; 1997) is aimed at simulating the topographic evolution of braided rivers. As Eros, it is a cellular automata model in which elements of

water and sediment move on a grid of cells whose elevation vary with erosion-deposition. However, it differs from Eros in some ways that are examined here.

**Introduction of sediments and river slope.**—In the Murray and Paola's model, the introduction of sediments at the entrance of the river system is indirect because only water elements are introduced and the sediment flux actually results from the erosion of the first row. To keep sediment available the elevation of the first row is kept constant during the simulations. As a consequence, the input sediment flux is not a user defined variable, and the slope of the model cannot adapt itself fully to flow conditions.
This may be a strong difference with Eros which allows the slope to adjust itself to the flow regime, as a natural river may adjust its profile in response to external factor changes.

**Walking rules and water flux.**—Walkers in the Murray and Paola's model, equivalent to precipitons in Eros, move always from one row to the following. Therefore, a walker can only move from one pixel down to its three downstream neighbours. This restricts the freedom degree of walkers compared to Eros. An other difference is that walkers have a variable water volume. At each step, the water volume $Q_0$ on the pixel $M_0$ can be distributed to the three downstream neighbours $M_i$ depending on the slopes between $M_0$ and $M_i$ :

$$Q_i = \frac{S_i^n}{1/\sum_i (S_i)^n} Q_0$$

Also, water can move uphill if no downstream path is available. Indeed, in natural streams water can flow on short distance over negative bed slope as long as stream surface slope is positive. This can also be viewed as the effect of some flow inertia. For negative slopes, the water flux is expressed as:

$$Q_i = \frac{S_i^{-n}}{1/\sum_i (S_i)^{-n}} Q_0$$

Therefore, even if walkers have less net freedom of movement, their model may allow for more flux divergence due to the water routing procedure. However, a similar effect may be obtained by using the flow model 2 in Eros.

**Fluvial processes.**—Murray and Paola (1997) have tested six different transport rules which all are based on the stream power definition of sediment flux: $q_s = K[wS]^m$.
These allow to:

(1) avoid the dependence on slope:

$$q_s = Kw^m$$

(2) add a constant $C$ for allowing sediment flux on flat surfaces:

$$q_s = K\left[w(S+C)\right]^m$$

(3) add an erosion threshold $Th$ :

$$q_s = K\left[w(S+C) - Th\right]^m$$

(4) add a term for simulating the effect of flow inertia on sediment flux as a function of the upslope stream power from the $j$ upstream pixels:

$$Q_{si} = K\left[ Q_i S_i + \varepsilon \sum_{j=1}^{3} Q_{uj} S_{uj} \right]^m$$

From those tests, it appears that the most fundamental aspects to produce braiding are the presence of an exponent higher than 1 on the water discharge, necessary to produce excess scour and fill at flow convergences and divergences respectively, a slope dependence to fill in the holes and destroy the highs, and a lateral erosion rule to avoid the concentration and stabilisation of the flow on the long term (Murray and Paola 1994; Murray and Paola 1997). In the end, the main difference with Eros lies in the fact that the elevation change of a cell in the Murray and Paola's model is expressed as $\frac{\partial h}{\partial t} = q_s^{in} - q_s^{out}$ , i.e. always transport-limited.

**MODEL RESULTS**

The first objective of this study is to see if rivers can be considered in some way as diffusive entities. Rivers therefore need first to be modelled. How one can say that a model river behaves as a real one is a crucial issue, though not adressed here. Methods such as state-space plots (Murray and Paola 1996) clearly provide future opportunities for investigations in this field. However, the scientific philosopher Gaston Bachelard can be quoted at that point: "the quantity does not matter if the quality stays obvious! Even all the qualities do not matter when some of them are characteristic!" (Bachelard 1934). Therefore, in the present work, models are considered as "rivers" when the flow (water and sediments) is localised in one or more channels that can always evolve in space (laterally and longitudinally) and time.

In the following, the parameters needed for the system to organize in such a way are presented along with the variations of river pattern. Then, the problem of the response time of those systems is adressed.

***Parameters***

**Exponents.**—As predicted by Smith and Bretherton (1972) and shown in Davy and Crave (2000), differential incision, i.e. channelization (or incision instability), develops when the flow exponent $m$ is larger than 1. The condition $m>1$ is therefore the first requirement for simulating rivers as defined above, i.e. with channels. Also, as illustrated in Murray and Paola (1997), an other consequence is that when $m>1$, the sediment flux produced at a convergence between two channels is larger than the sum of sediment flux produced individually by those channels. The contrary occurs at water flux divergences where deposition takes place. This therefore induces the formation of scour zones at convergences, and deposition zones at divergences. The sediments eroded in scour zones are deposited downstream where the flow diverges, therefore leading to even more divergence, leading itself again to scouring downstream, and the phenomenon repeats itself in a sort of periodic way downstream. This coupling between flow organization (convergence-divergence) and channel bed evolution (scour and deposition) has long been recognized as a fondamental aspect of the initial development and long-term evolution of braided flows (e.g., Ashmore 1982).

A second requirement to produce a realistic pattern is the presence of a slope dependence. Indeed, Murray and Paola (1997) have shown that without such a slope dependence, stream power and hence sediment flux have no reason to increase with increasing slope. Therefore, this can eventually lead to an irealistic topography made of alternating deep scours and high hills. A slope dependence with $n \geq 1$ allow to smooth the topography by eroding the highs and filling the holes.

Therefore, channels can be obtained as long as $m > 1$ and $n \geq 1$. Based on Ashmore's (1982) experimental data, Murray and Paola (1997) set the exponent values to $m = n = 2.5$.

In the present work, for computation time and simplicity reasons, the flow exponent has been set to $m = 2$, and the slope exponent to $n = 1$ as in a number of other studies (e.g., Allen and Densmore 2000; Davy and Crave 2000; Kooi and Beaumont 1994).

Figure 3 illustrates an example of braided pattern obtained with these exponents. Although no quantitative comparisons with real streams has been done (e.g., Murray and Paola 1996) such a pattern seems to realistically simulate natural braided channels. The flow width varies along river course depending on the number of channels. Also, the model respects the convergence/divergence mechanisms as shown by the sediment concentration in the river (fig.

3B) which increases at convergences where scouring may take place, and decreases with deposition in divergent zones.

**Lateral erosion.**—With Eros, as also demonstrated in Murray and Paola (1997), when an equilibrium slope is reached, the absence of lateral erosion leads to flow concentration in a single frozen channel (fig. 4A), i.e. which pattern does not evolve further. This does not preclude the presence of a multi-thread changing pattern in the early stages of the system evolution, but doesn't allow a dynamic equilibrium pattern to be eventually reached.
The second consequence of lateral erosion is that it provides a certain width to the flow. As it is defined in Eros (a fixed percentage of vertical erosion), an increase in the lateral erosion parameter $\gamma$ induces a wider flow (figs. 4B, 4C, 4D). Along the stream, this therefore accounts for the presence of alternating wide and narrow zones depending on local erosion rates.
Figure 5 illustrates how avulsion occurs naturally in the model as a consequence of lateral erosion. The erosion of the channel bank (black circle) between t1 and t2 allows the flow to change its path toward a lower zone which becomes the main channel at t3.

***Equilibrium and channel patterns***

An important feature of the simulations made in this work is that the fluvial network can be in aggradation, degradation or in equilibrium. This is a consequence of the fact that the slope is a result of the model. Only the initial slope is imposed as an initial condition. For a given initial slope and depending on the flow conditions in terms of sediment load and deposition length, the model will aggrade or degrade its bed until an equilibrium slope is reached. Figure 6 shows an example of slope aggradation. Two phenomena characterize the system when it is in equilibrium: (1) the average slope (topography) of the system is constant, and (2) the sediment ouput flux equals the sediment input flux. In other words, when equilibrium is reached, the system neither aggrades nor degrades its bed. It is therefore important to note that the fundamental concept of equilibrium widely used in stratigraphy and geomorphology arises naturally from the incorporation of simple physical rules in the model.
A second important observation is that channel patterns and sediment output flux are different depending on the state of the system with regards to equilibrium, i.e. aggradation, incision or equilibrium. With the same conditions different channel patterns appear for different states

with respect to equilibrium. This could reinforce and complete the idea of a continuum of channel patterns as suggested by Leopold and Wolman (1957).

Braiding always takes place when the system aggrades under the equilibrium slope. This is recorded at the outlet of the system by a highly variable sediment flux without variable input (figs. 7A, 7B, 7C). Indeed, when the slope does not provide sufficient stream power to carry all the sediment load, deposition occurs. This does not occur as sheet-like deposition which would build-up the whole bed with the same rate everywhere. Instead, as explained above, the flow is channelized because of the flow exponent $m > 1$. Until the equilibrium slope is reached for the whole bed, the topography stays irregular, and local slope diminutions induce sediment accumulations which then divert the flow and produce a braided pattern by the divergence/convergence scour and fill mechanism. This occurs with any transport length as long as the system aggrades (figs. 8A, 8B, 9A, 10A). This can also be seen by looking at the sedimentary load in the flow which decreases downstream during aggradation because sediments are gradually deposited from upstream to downstream (figs. 8A, 8B, 9A, 10A).

During incision (figs. 11, 12), the flow is always concentrated in a single stable low-sinuosity channel, with no or little lateral migration. Even if the channel may search its course during the early stages of incision, when the topography is still smooth enough to allow flow divagation, it rapidly concentrates in a single channel configuration. Then, due to its confined nature, the single-channel configuration doesn't allow subsequent channel changes.

At equilibrium, the system is mostly constituted of a single channel with an average constant sediment load along flow (figs. 8C, 8D, 9B, 10B, 11C). Indeed, because at equilibrium the average slope is constant and the output sediment flux equals the input sediment flux, the system may be self-organised in a way such that the amount of sediment in transport be constant along the flow. To respect this, the water discharge may be averagely constant along flow, i.e. with a main single channel. However, channel patterns at equilibrium are different depending on whether the equilibrium is reached after a period of aggradation or a period of incision, and on the transport length.

First, when the equilibrium slope is reached after a period of aggradation, the whole plain has been leveled and smoothed, and two more cases arise depending on the transport length:

(1) with diminishing transport length the channel patterns at equilibrium migrate laterally constantly, and are sinuous. Indeed, when the transport length is small compared to the system's length, the sediments are temporarily deposited in the system (even if there is

still an exact balance between erosion and deposition to respect equilibrium state). Because the channel bed slope is everywhere at or near equilibrium, any small deposition immediately forces the channel to migrate lateraly toward a lower area, or divert the flow. However, divergences never persist a long time in the system because the stream power of a diverted channel, i.e. with a lower discharge, immediately lead to deposition and abandonment of the diverted channel. The sinuosity is therefore associated to temporary deposition, and is reflected in the strong variability of equilibrium output flux at the outlet of systems with low transport length (figs. 7A, 7B, and associated figs. 8C, 8D and 9B). Note that when the system's width increases, it seems that some sections of the river may temporarily become braided due to autogenic disturbances of the single-thread pattern. With increasing system's width, flow divergences can persist longer even at equilibrium. This phenomenom can produce well developed autogenic cycles which will be explained below.

(2) with increasing transport length the sinuosity of equilibrium channel diminishes, and its stability increases. With a transport length of the order of the system's size or more, the equilibrium channel is more straight and stable. This follows from a shorter residence time of sediments (longer transport length) which means that they are no longer deposited in the system and thus can not disturb the flow path. With an intermediate transport length of 10 (fig. 10B), the equilibrium channel is only slightly sinuous, which is expressed by a lower variability of output sediment flux on figure 7C (by comparison with low-transport length systems).

Second, when equilibrium is reached after a period of incision, the system is characterized by a single channel with a generally straight (fig. 11C) or slightly sinuous planform shape. This can be seen in the output sediment flux which is almost constant after incision (fig. 7D). In fact, the final shape of a channel after incision depends better on the ratio between sinuosity at the beginning of incision and the rate of incision, or the deviation from equilibrium. At equilibrium, the vertical erosion rate is null, and so is the lateral erosion due to the definition used in this work. Therefore, if equilibrium is reached quickly after the onset of incision, the sinuosities can not be smoothed by lateral erosion (fig. 12). It perhaps would not be the case for short transport lengthssystems in which sediments are constantly stored and removed in the system. This would indeed imply transient and local periods of vertical and associated lateral erosion which do not occur in large transport length systems. More research would therefore be needed to test the influence of different lateral erosion descriptions during channel incision.

***Equilibrium time***

When alluvial systems are considered as diffusive entities (Paola et al. 1992), the elevation of the channel bed is described by the linear diffusion equation of the form:

$$\frac{\partial h}{\partial t} \sim K \frac{\partial^2 h}{\partial x^2}$$

with $K$ as the system's diffusivity. By scaling this equation, Paola et al. (1992) put forward that such systems therefore own an intrinsic equilibrium time of the form:

$$Teq \sim \frac{L^2}{K}$$

with $L$ as the characteristic system's diffusivity.

As a difference with the linear diffusive case, deriving the analytical expression of the equilibrium time from the transport equations used in Eros is complicated by the presence of a flow exponent larger that 1, the incorporation of the transport length $l_d$, and a slope dependence $n$ which can be different from 1. Even when $n$ and $l_d$ are set equal to 1 which is the simplest case, the effects of the flow exponent larger than 1, which induces longitudinal and cross-sectional discharge variations, are unknown. Numerical resolution is one way to adress this problem.

A series of experiments has been performed to observe the evolution of equilibrium time with system length for transport lengths of 1, 10 and 100. In these runs, the equilibrium time is the time needed for the system after the onset of an experiment to reach the state at which sediment output flux equals sediment input. A problem is in defining accurately the time to reach equilibrium as long as the sediment output curves exponentially approach the input value. A mean to avoid this problem is to consider other characteristic times as for example the time needed to achieve a fraction of 1-1/e of the sediment input flux (Beaumont et al. 2000). The time defined in this way is quantitatively different from the exact equilibrium time, but is qualitatively also characteristic of the system. In this study, two characteristic times have been used: $Teq1$ and $Teq2$ which are the times for which the output flux equals 90% and 1-1/e of the input flux respectively.

The equilibrium slope of large transport length systems is much lower than for low transport lengths because there is less deposition. Therefore, starting from the same initial slope, equilibrium is attained more quickly for large transport lengths. In this way, the initial slope must be small enough in order that large transport length systems do not reach equilibrium

instantly or even incise their bed. A slope of $10^{-5}$ has been choosed and is the same for all runs in order to apply the same initial conditions. Also, because computation time is a direct function of grid size, all runs have been done with a small width of 14 pixels. This has imposed a low lateral erosion of 4% to avoid too wide flows compared to system width. A second control on computation time is linked with transport length: the smaller the transport length, the longer the computation time. Therefore, a run with a small transport length can only be done with a comparatively small system length to preserve a reasonnable computation time. This explains why runs with $l_d$=1 were performed with $L$ ranging from 32 to 192 pixels, whereas runs with $l_d$=100 could have been performed with much larger system lengths up to 1536 pixels. As explained in the parameters section, the flow exponent was set to $m=2$, the slope dependence to $n=1$, and the sediment input concentration to $[s]_i=0.05$ for all runs.

The figure 13 represents the equilibrium times obtained for all experiments. Regression analysis of equilibrium times versus river lengths always gives good regression coefficients $R$ larger than 0.98. The equilibrium times *Teq1* for $l_d$=1 and $l_d$=10, and *Teq2* for $l_d$=10, scale exponentially with system lengths with exponents of 2.01983, 2.07125 and 1.90887 respectively. However, equilibrium times *Teq2* for $l_d$=1, and *Teq1* and *Teq2* for $l_d$=100 show less dependence with system lengths with exponents of 1.76075, 1.76006 and 1.75532 respectively. Therefore, the modelled river systems seem to behave diffusively for transport lengths of 1 and 10. The low $L$ exponent on *Teq2* for $l_d$=1 may be due to a problem with the adjacent averaging smoothing of output flux curve, and accurate picking of equilibrium times. Indeed, the points for low $L$ and $l_d$=1 show significant departure from the regression line. However, the less than diffusive component for transport length of 100 seems to be a robust feature.

To overcome this problem, the data can be synthesized by normalizing the equilibrium times and system lengths by the transport length $l_d$ as shown on figure 14. This again strongly suggests that the modelled systems can be considered at first order as diffusive entities with system length exponents of 2.14509 and 2.12613 for *Teq1* and *Teq2* respectively. However, regression analysis can be performed over different ranges of normalized length. This put forward that equilibrium time is much less dependent on system length when transport length nears system's length ($L/ld<5$). In this case the system behaviour is closer to an advective behaviour. In this way, it can be postulated that for $L/l_d<1$, i.e. large transport lengths compared to the system's size, the equilibrium time may loose its dependence with system length.

In conclusion, the normalization gives the following scaling relationship between equilibrium time *Teq*, system length *L* and deposition length $l_d$:

$$T_* \sim L_*^{\alpha} \Leftrightarrow Teq \sim \frac{L^{\alpha}}{l_d^{\alpha-1}}$$

Therefore, when the system is diffusive ($\alpha$=2), the diffusion coefficient *K* may be linearly proportional to transport length $l_d$.

The diffusive approximation therefore seems to be appropriate for simulating the behaviour of alluvial systems as has been done in a number of studies (e.g., Métivier 1999; Paola et al. 1992), i.e. for systems which may have a large ratio L/*ld* because they accumulate sediments. For example, large Asian floodplains which are alluvial systems, have been shown to buffer high-frequency (10's to 100's ka) sediment supply cycles due to such a diffusive behaviour. (Métivier 1999; Métivier and Gaudemer 1999; Métivier et al. 1999). Also, by assuming rivers as diffusive entities, Castelltort and Van Den Driessche (2003) have shown that a majority of intermediate and large current rivers have equilibrium times of more than 100 ka, and should act as a buffer for sediment flux variations coming from the source area with periodicities of less than 100 ka. This has implications for the stratigraphic record because it would imply that high-frequency stratigraphic cycles cannot find their origin in sediment flux variations.

However, this underscores the need to better stress the behaviour of the transfer subsystem and in particular the role of non-linear aspects. Further research will have, for example, to adress the response time of river systems to spike functions of sediment flux disturbing the system from equilibrium.

***Autocyclicity***

A major observation from the simulations is that sediment output flux often varies cyclically around the average sediment input flux when the system is in equilibrium (dynamic equilibrium) and also in the way to equilibrium (fig. 7). These sediment output flux cycles occur without any change of boundary conditions and can therefore be referred to as autocycles. Figure 15 illustrates a well developed autocycle during which the river evolution can be followed. In this example, the river pattern alternates between straigth and braided. When the pattern is straigth, the system is more efficient at evacuating sediments and the channel slope diminishes due to erosion. When a critical low slope is reached, then sediments again accumulate in the system due to the low transport length and a braided pattern arises. The braided pattern persists until a critical higher slope is reached which trigger incision and a

straigth channel can again take place. These autocycles therefore reflect the non-linear interaction between erosion and deposition which are treated separately in the model. This is somewhat analoguous to the cutting and filling oscillations obtained by Humphrey and Heller (1995) when a bedrock incision model for the mountain zone is coupled to a diffusion model (transport-limited) for the alluvial realm.

In consequence, in addition to the coupling of different geomorphic entities (Humphrey and Heller 1995), the coupling of processes like erosion and deposition in the alluvial system itself can produce autogenic cycles. These cycles may be preserved in the stratigraphic record of alluvial basins and be mistaken with allogenetic (tectonics, climate) cycles. Moreover, they may be transmitted downstream and become an external input for the sedimentation subsystem (as a marine delta for example), i.e. an allocycle.

More generally, the behaviour of low transport length systems (compared to system's length) always exhibit a strong variability of sediment output flux even at equilibrium (fig. 7A, 7B). It seems that the width of the system controls whether the pattern is sinuous single-thread or alternates between straigth and braided at equilibrium. This may imply different output flux cycles frequencies that it would be useful to study.

The development of such autocycles therefore put forward the necessity to better understand the non-linear aspects of the transfer subsystem in order to distinguish their record from the signature of allogenic controls (climate, tectonics, base level) in stratigraphic data.

**CONCLUSION**

The stochastic model of landscape evolution Eros (Crave and Davy 2001; Davy and Crave 2000), in which a simple set of rules are used as an abstraction of water, sediment and gravity, seems to capture the essential qualities of river systems. Even if tortuous meanders with specific features such as oxbow lakes, chute-and neck-cutoffs could not be simulated, the variety of fluvial forms which appears in the experiments, can be explained by the combinations of the deviation of the system from its equilibrium slope and the characteristic transport length of sediments (a proxy for residence time). Multiple-threads braided dynamics seem to be a characteristic of aggrading fluvial systems. Single stable channels whether straigth or sinuous are better encountered during incision. In contrast, at equilibrium, the system is constituted of a main channel mostly single after aggradation or incision, which sinuosity increases with diminishing transport length, and which can be occasionnaly (or cyclically) multiple over finite reaches due to temporary storage in low transport length

systems. This yields perspectives for explaining the various river patterns observed in nature in the context of river equilibrium. These results are preliminary and will make the subject of more systematic studies of the controls on channel patterns.

The equilibrium time in the experiments corresponds well to a diffusive behaviour of river systems when the system's length is greater than the transport distance of sediments, i.e. for alluvial channels. However, when they are both nearly of the same order, or even the transport distance is greater than system length, the behaviour of the river approaches advection. Therefore, the diffusive assumption often used for modelling alluvial systems behaviour may be well appropriate. River systems thus have a non-negligible equilibrium time and may act as a strong buffer for high-frequency sediment supply cycles. Implications for the stratigraphic record are that high frequency stratigraphic cycles found in basins fed by intermediate to large alluvial systems may not be the record of high-frequency disturbances (tectonic or climatic) in the upstream source areas.

The non-linear effects between erosion and deposition also put forward the necessity to consider the plausibility of sediment supply autocycles due to the internal dynamics of the fluvial system.

## REFERENCES


ALLEN, P.A., and DENSMORE, A.L., 2000, Sediment flux from an uplifting fault block: Basin Res., v. 12, p. 367-380.

ASHMORE, P.E., 1982, Laboratory modelling of gravel braided stream morphology: Earth Surf. Processes Landforms, v. 7, p. 201-225.

BACHELARD, G., 1934, Le nouvel esprit scientifique: Paris, Quadrige / Presses Universitaires de France.

BEAUMONT, C., KOOI, H., and WILETT, S., 2000, Coupled tectonic-surface process models with applications to rifted margins and collisional orogens, *in* Summerfield, M.A., ed., Geomorphology and Global Tectonics: New York, John Wiley & Sons, p. 29-55.

CASTELLTORT, S., and VAN DEN DRIESSCHE, J., 2003, How plausible are high-frequency sediment supply-driven cycles in the stratigraphic record?: Sediment. Geol., v. 157, p. 3-13.

CHASE, C.G., 1992, Fluvial landsculpting and the fractal dimension of topography: Geomorphology, v. 5, p. 39-57.

CRAVE, A., and DAVY, P., 2001, A stochastic "precipiton" model for simulating erosion/sedimentation dynamics: Computers & Geosciences, v. 27, p. 815-827.

DADE, W.B., and FRIEND, P.F., 1998, Grain-size, Sediment-Transport Regime, and Channel Slope in Alluvial Rivers: J. Geol., v. 106, p. 661-675.

DAVY, P., and CRAVE, A., 2000, Upscaling Local-Scale Transport Processes in Large-Scale Relief Dynamics: Phys. Chem. Earth (A), v. 25, p. 533-541.

DENSMORE, A.L., ELLIS, M.A., and ANDERSON, R.L., 1998, Landsliding and the evolution of normal-fault-bounded mountains: J. Geophys. Res., v. 103, p. 15,203-15,219.

EINSELE, G., RICKEN, W., and SEILACHER, A., 1991, Cycles and Events in Stratigraphy: Berlin Heidelberg, Springer-Verlag, p. 955.

GALLOWAY, W.E., and WILLIAMS, T.A., 1991, Sediment accumulation rates in time and space: Paleogene genetic stratigraphic sequences of the northwestern Gulf of Mexico basin: Geology, v. 19, p. 986-989.

HOWARD, A.D., 1994, A detachment-limited model of drainage basin evolution: Water Resources Research, v. 30, p. 2261-2285.

HOWARD, A.D., and KERBY, G., 1983, Channel changes in badlands: GSA Bull., v. 94, p. 739-752.

HUMPHREY, N.F., and HELLER, P.L., 1995, Natural oscillations in coupled geomorphic systems: An alternative origin for cyclic sedimentation: Geology, v. 23, p. 499-502.

KIRKBY, M.J., 1971, Hillslope process-response models based on the continuity equation, Slopes: Forms and Processes: London, Institute of British Geographers Special Publications, p. 15-30.

KOOI, H., and BEAUMONT, C., 1994, Escarpment evolution on high-elevation rifted margins: Insights derived from a surface processes model that combines diffusion, advection, and reaction: J. Geophys. Res., v. 99, p. 12,191-12,209.

LAGUE, D., 2001, Dynamique de l'érosion continentale aux grandes échelles de temps et d'espace: modélisation expérimentale, numérique et théorique [unpublished PhD Thesis thesis]: University of Rennes I, Rennes, France, 151 p.

LEOPOLD, L.B., and WOLMAN, M.G., 1957, River Channel Patterns: Braided, Meandering and Straight: US Geol. Surv. Prof. Pap., v. 282-B, p. 39-85.

LIU, X., and GALLOWAY, W.E., 1997, Quantitative determination of Tertiary sediment supply to the North Sea basin: Am. Ass. Petr. Geol. Bull., v. 81, p. 1482-1509.

MÉTIVIER, F., 1999, Diffusivelike buffering and saturation of large rivers: Phys. Rev. E, v. 60, p. 5827-5832.

MÉTIVIER, F., and GAUDEMER, Y., 1999, Stability of output fluxes of large rivers in South and East Asia during the last 2 million years: implications on floodplain processes: Basin Res., v. 11, p. 293-303.

MÉTIVIER, F., GAUDEMER, Y., TAPPONNIER, P., and KLEIN, M., 1999, Mass accumulation rates in Asia during the Cenozoic: Geophys. J. Int., v. 137, p. 280-318.

MURRAY, A.B., and PAOLA, C., 1994, A cellular model of braided rivers: Nature, v. 371, p. 54-57.

MURRAY, A.B., and PAOLA, C., 1996, A new quantitative test of geomorphic models, applied to a model of braided streams: Water Resour. Res., v. 32, p. 2579-2587.

MURRAY, A.B., and PAOLA, C., 1997, Properties of a cellular braided-stream model: Earth Surface Processes and Landforms, v. 22, p. 1001-1025.

PAOLA, C., 2000, Quantitative models of sedimentary basin filling: Sedimentology, v. 47, p. 121-178.

PAOLA, C., HELLER, P.L., and ANGEVINE, C.L., 1992, The large-scale dynamics of grain-size variation in alluvial basins. I : Theory: Basin Res., v. 4, p. 73-90.

PEIZHEN, Z., MOLNAR, P., and DOWNS, W.R., 2001, Increased sedimentation rates and grain sizes 2-4 Myr ago due to the influence of climate change on erosion rates: Nature, v. 410, p. 891-897.

SLOSS, L.L., 1978, Global Sea Level Changes: A view from the Craton: Am. Ass. Petr. Geol. Bull., p. 461-467.

SMITH, T.R., and BRETHERTON, F.P., 1972, Stability and the conservation of mass in drainage basin evolution: Water Resour. Res., v. 8, p. 1506-1529.

TUCKER, G.E., and SLINGERLAND, R., 1996, Predicting sediment flux from fold and thrust belts: Basin Res., v. 8, p. 329-349.

WHIPPLE, K.X., and TUCKER, G.E., 1999, Dynamics of the stream-power river incision model: Implications for height limits of mountain ranges, landscape response timescales, and research needs: J. Geophys. Res., v. 104, p. 17661-17674.

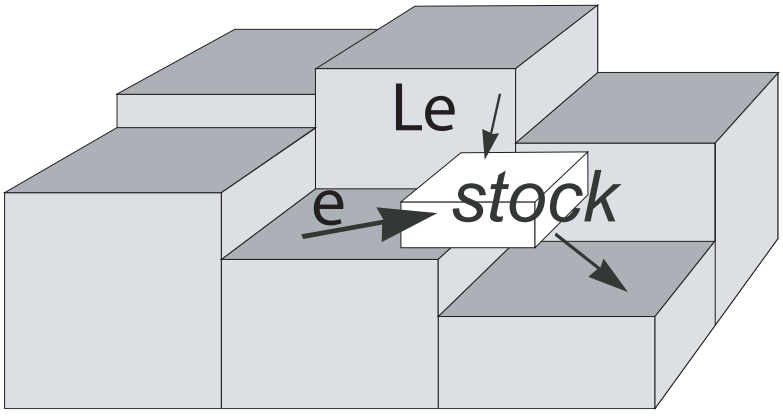


**Fig. 1. Lateral erosion rule.**
The sediment flux from lateral erosion Le to the precipiton stock is defined as a fixed percentage of the vertical erosion flux e.

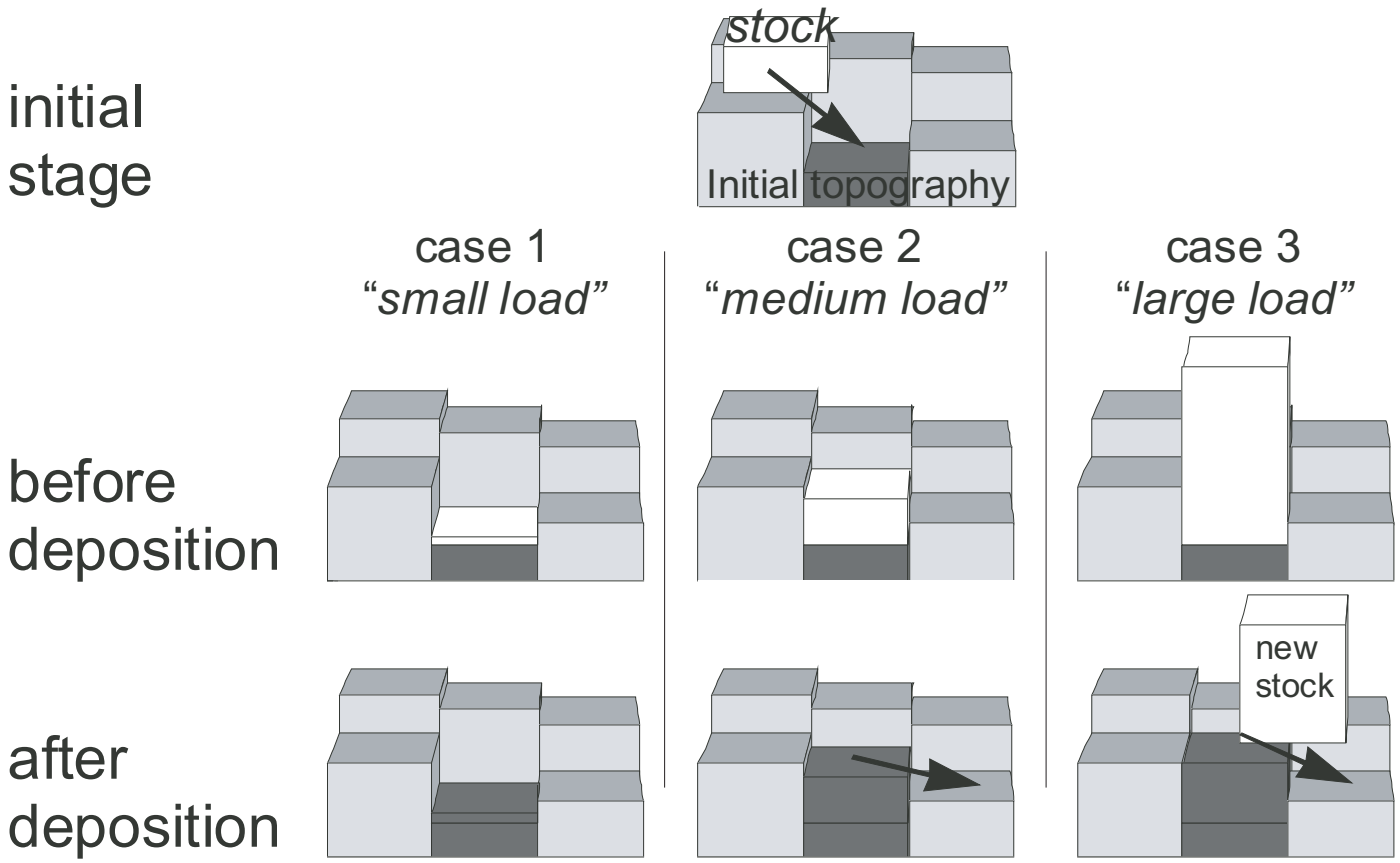


**Fig. 2. Sediment flux routing through topographic sinks.**

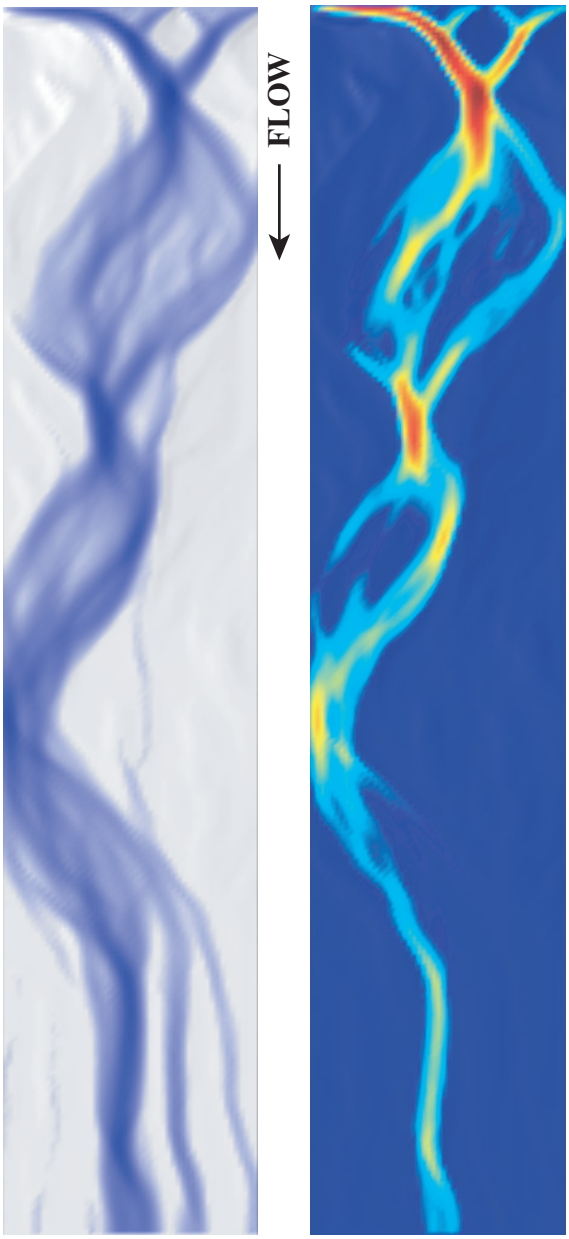


**Fig. 3. Example of a simulated braided pattern.**
Run largeur1Eroslat2, t=29 or 3.395E5 when rescaled to restorehope. Lateral erosion=0.1, transport length=4, width*length=64*256 pixels. A) The water flow follows single and multiple paths along its course. B) The sedimentary load increases at flow convergences (warm colors), and decreases at divergences (cold)

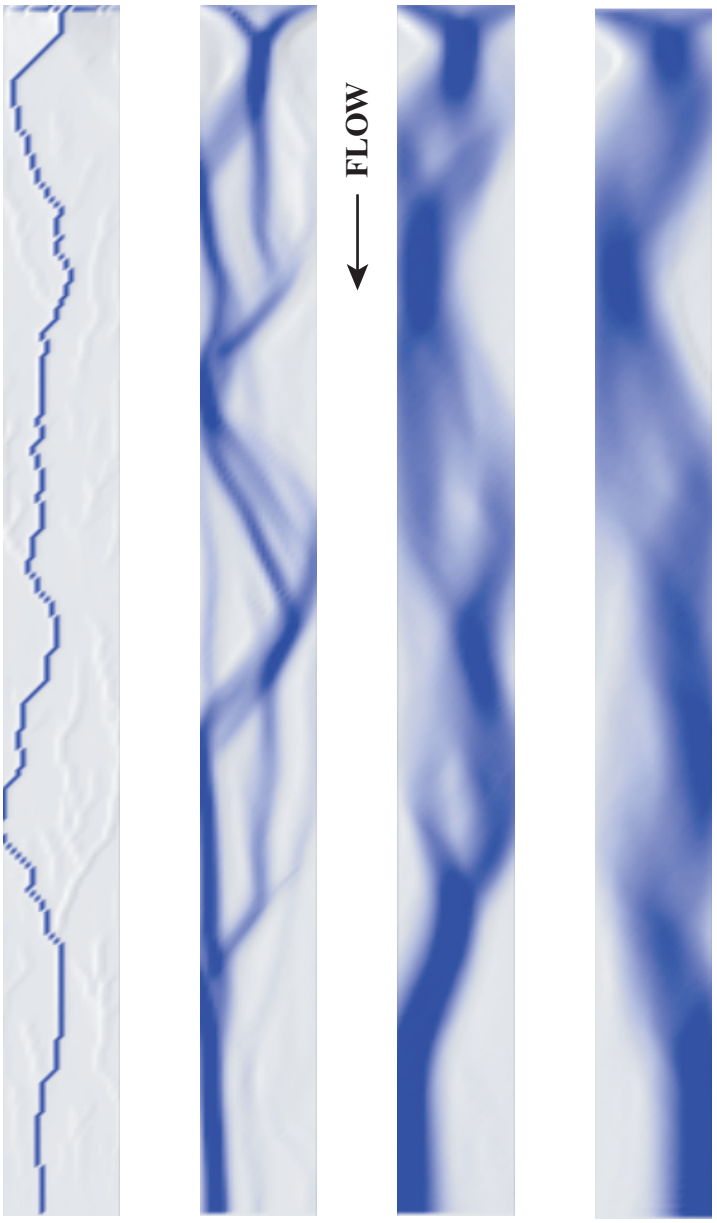


**Fig. 4. Influence of the lateral erosion parameters on the dynamics and width of modeled rivers.**

Run eroslat0, time rescaled to restorehope, le means lateral erosion (proportion of vertical erosion), transport length=4, width*length=32*256 pixels. A) When lateral erosion is not included in the transport laws, a single frozen (stable) channel of one-pixel width arises. B, C, D) The water flow path is not frozen when lateral erosion is different incorporated, and flow width increases with increasing lateral erosion.

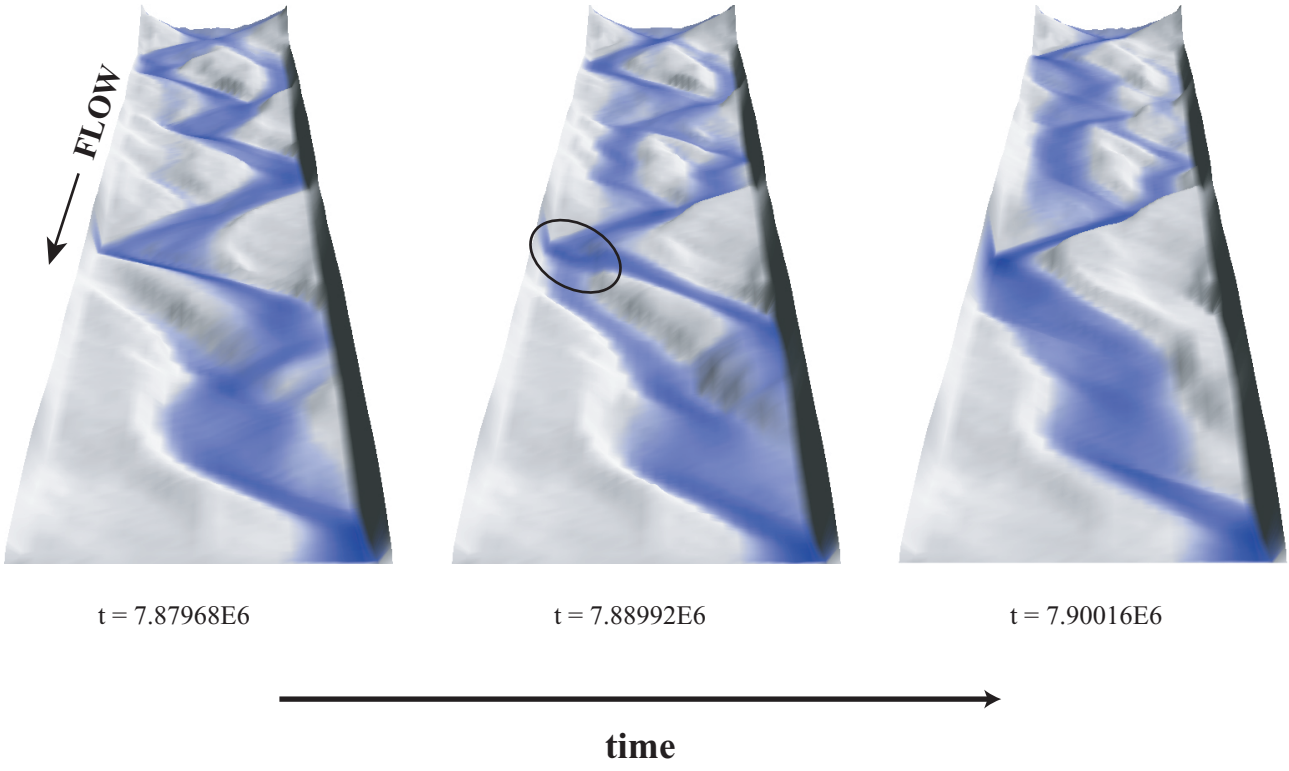


**Fig. 5. Illustration of the avulsion process due to lateral erosion.**
Bank cutting by lateral erosion (black circle) allows the flow to migrate lateraly to a topographically lower channel. Run newTL1, time rescaled to restorehope, transport length=1, width*length=28*256 pixels, 16x vertical exageration.

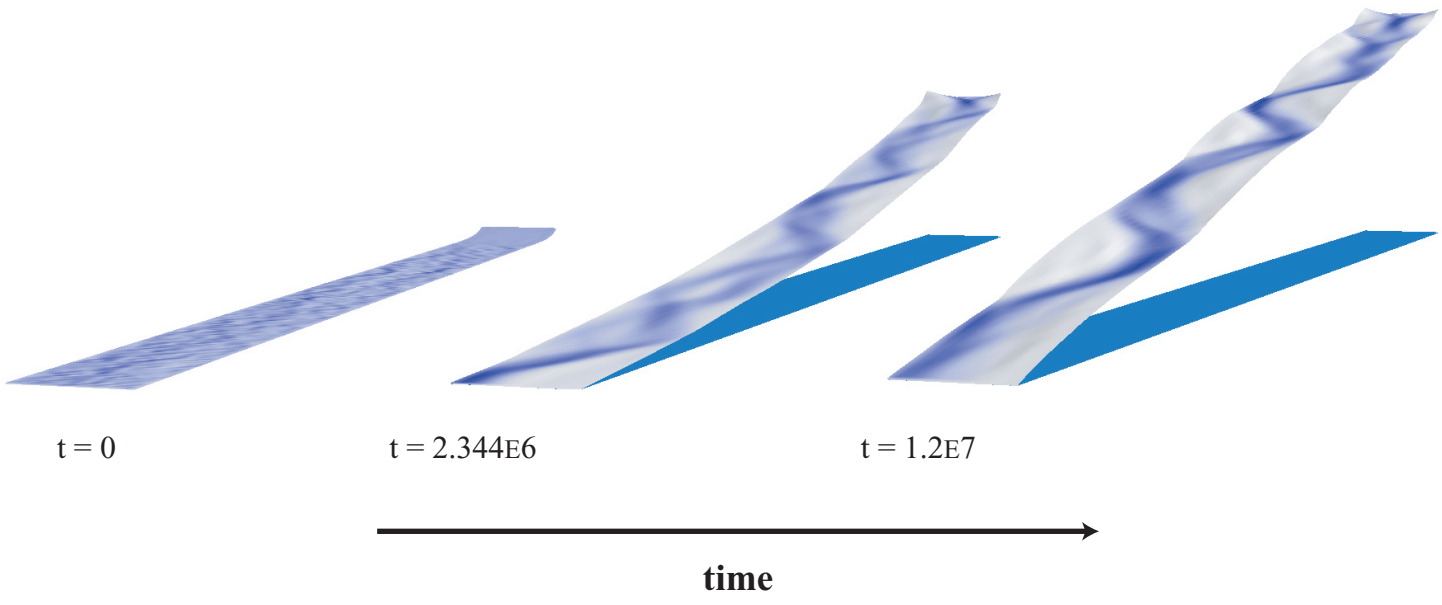


**Fig. 6. River profile aggradation toward equilibrium.**
Run TL1_192, time rescaled to restorehope, transport length=1, lateral erosion=0.04, width*length=14*192 pixels, 16x vertical exageration.

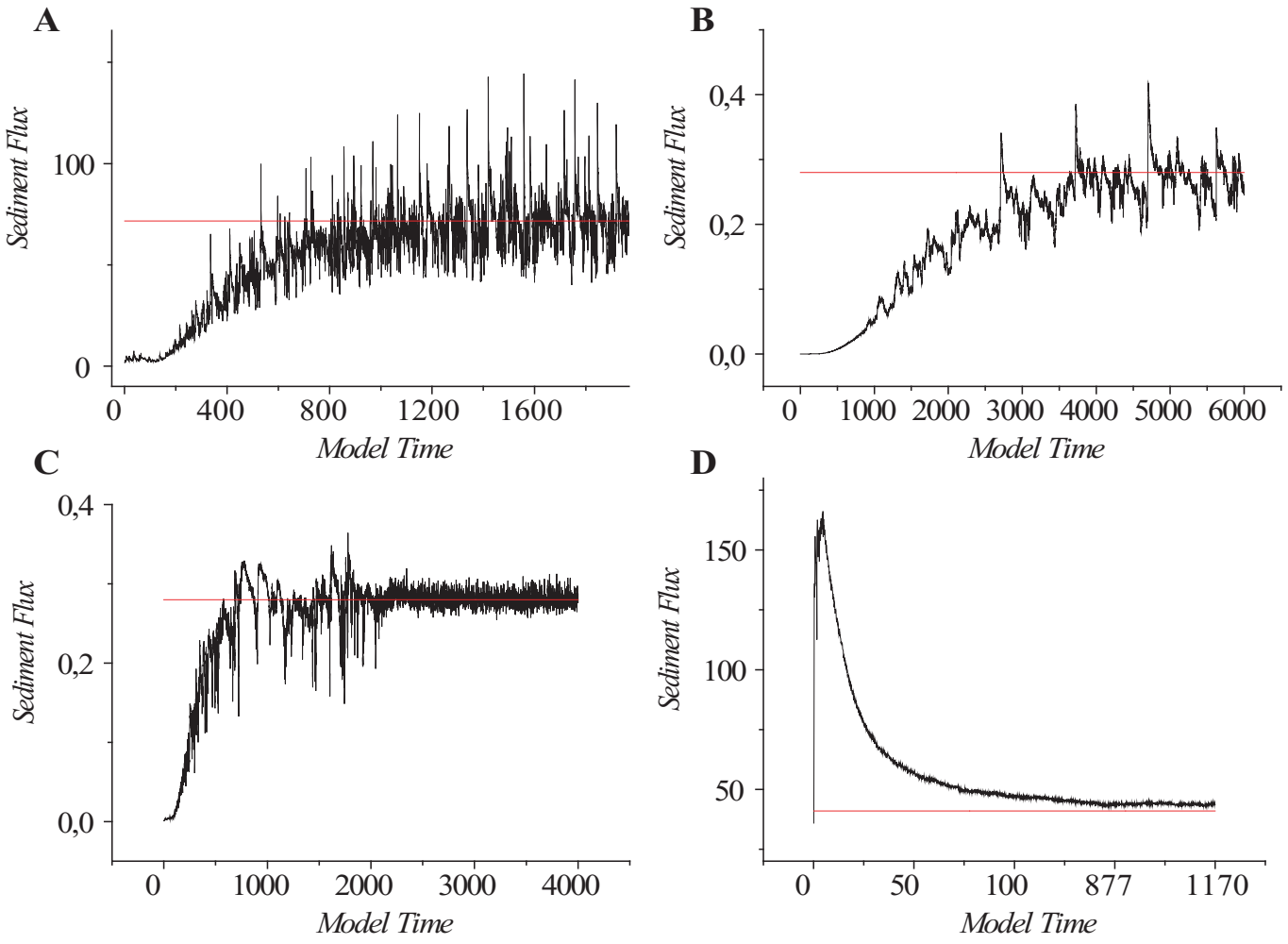


**Fig. 7. Examples of sediment output flux curves.**

The straigth line represents sediment input flux. The modeled systems aggrade (A, B, C) when the output flux is less than the input flux (sediment storage), and equilibrium is reached when output flux averages input flux. When ouput flux exceeds input flux, incision takes place in the system (D). Note the ouput flux variability for aggrading systems (A, B, C) and the low variability of output flux during incision (D).

A) Run newTL1_L256, transport length=1, lateral erosion=0.04, width*length=28*256 pixels. B) Run TL1_128, transport length=1, lateral erosion=0.04, width*length=14*128 pixels. C) Run New3TL10_256, transport length=10, lateral erosion=0.04, width*length=14*256 pixels. D) Run Basement1, transport length=4, lateral erosion=0.04, width*length=32*256 pixels.

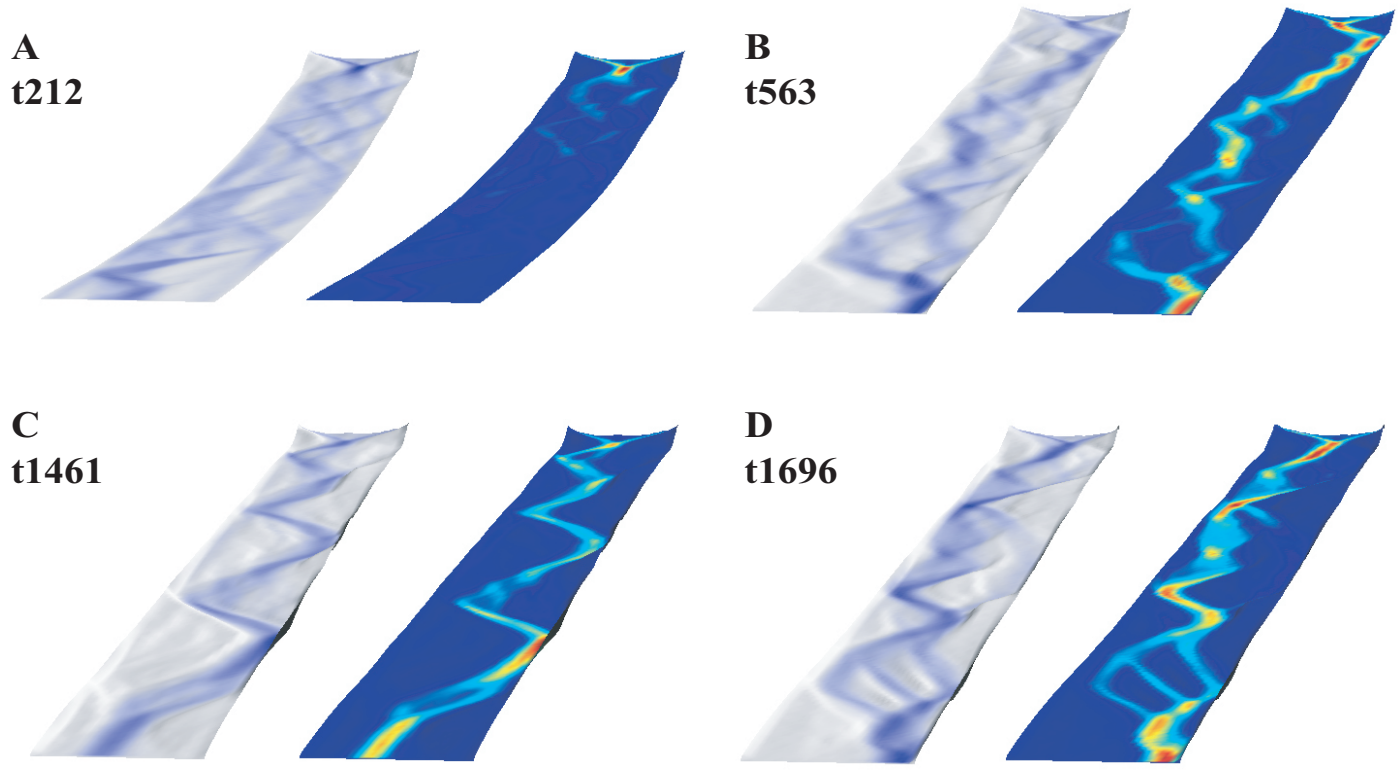


**Fig. 8. Low transport length system, evolution from braided to sinuous-braided.** Run newTL1_L256, transport length=1, lateral erosion=0.04, width*length=28*256 pixels. These snapshots of experiments correspond to the sediment ouput flux curve of fig.X5A. A) the system aggrades toward equilibrium with a braided pattern, and river load decreases downstream. Note the concave-up profile. B) Even if the profile is near graded, the flow is still braided which denotes that the system is not yet at equilibrium. C) The system is at equilibrium: the pattern is sinuous single-thread, and the river load is homogeneously distributed along flow path. D) Even during equilibrium, autogenic disturbances may produce temporary braided patterns, but the river load is still well distributed in the system.

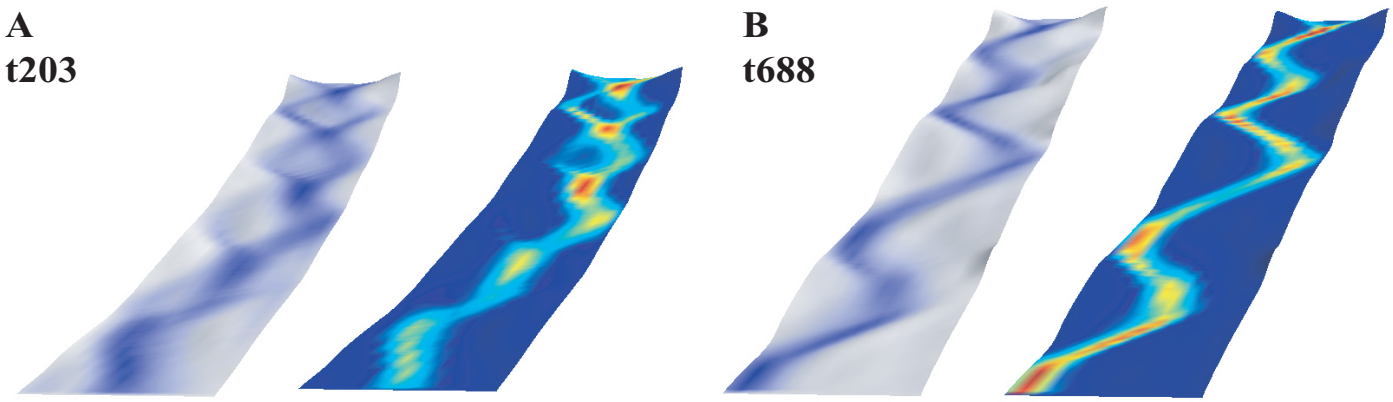


**Fig. 9. Low transport length, evolution from braided to single-thread sinuous.** Run TL1_128, transport length=1, lateral erosion=0.04, width*length=14*128 pixels. A) The river aggrades toward equilibrium, with a braided pattern made of an alternance of flow convergence and divergence zones, and river load decreases downstream. B) At equilibrium, the flow pattern is sinuous and the river load is homogeneously distributed in the system. The smaller system width compared to fig. X6 may account for the absence of braiding at equilibrium in this example.

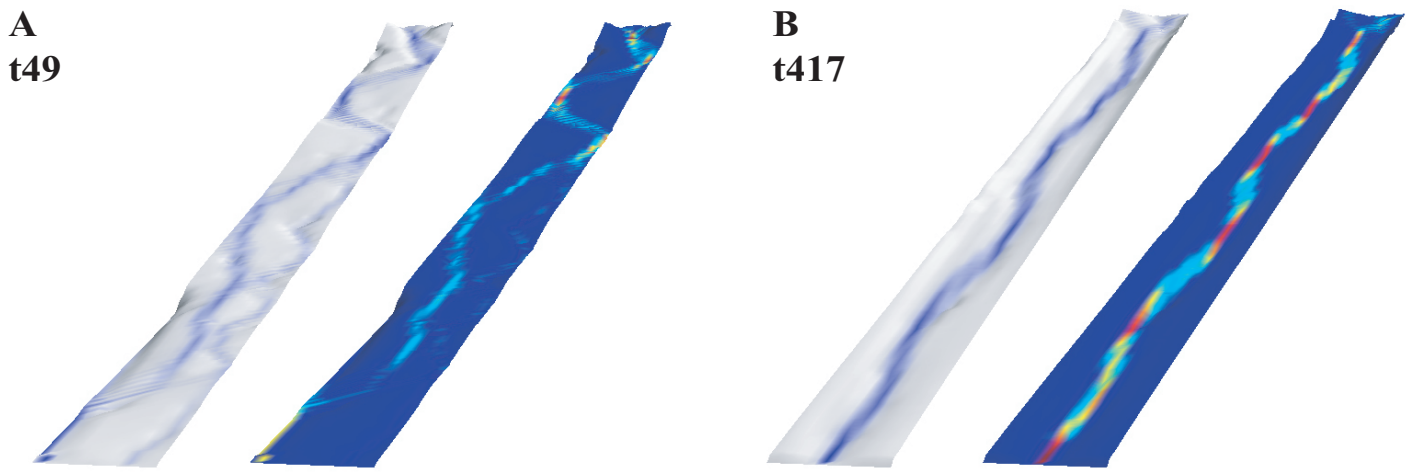


**Fig. 10. Low-sinuosity single-thread equilibrium channel due to larger transport length.** Run New3TL10_256, transport length=10, lateral erosion=0.04, width*length=14*256 pixels. As a difference with low transport length systems, the pattern at equilibrium in this example shows a low-sinuosity, near straigth, channel. This result from the lower residence time of sediments in the system due to the larger transport length.

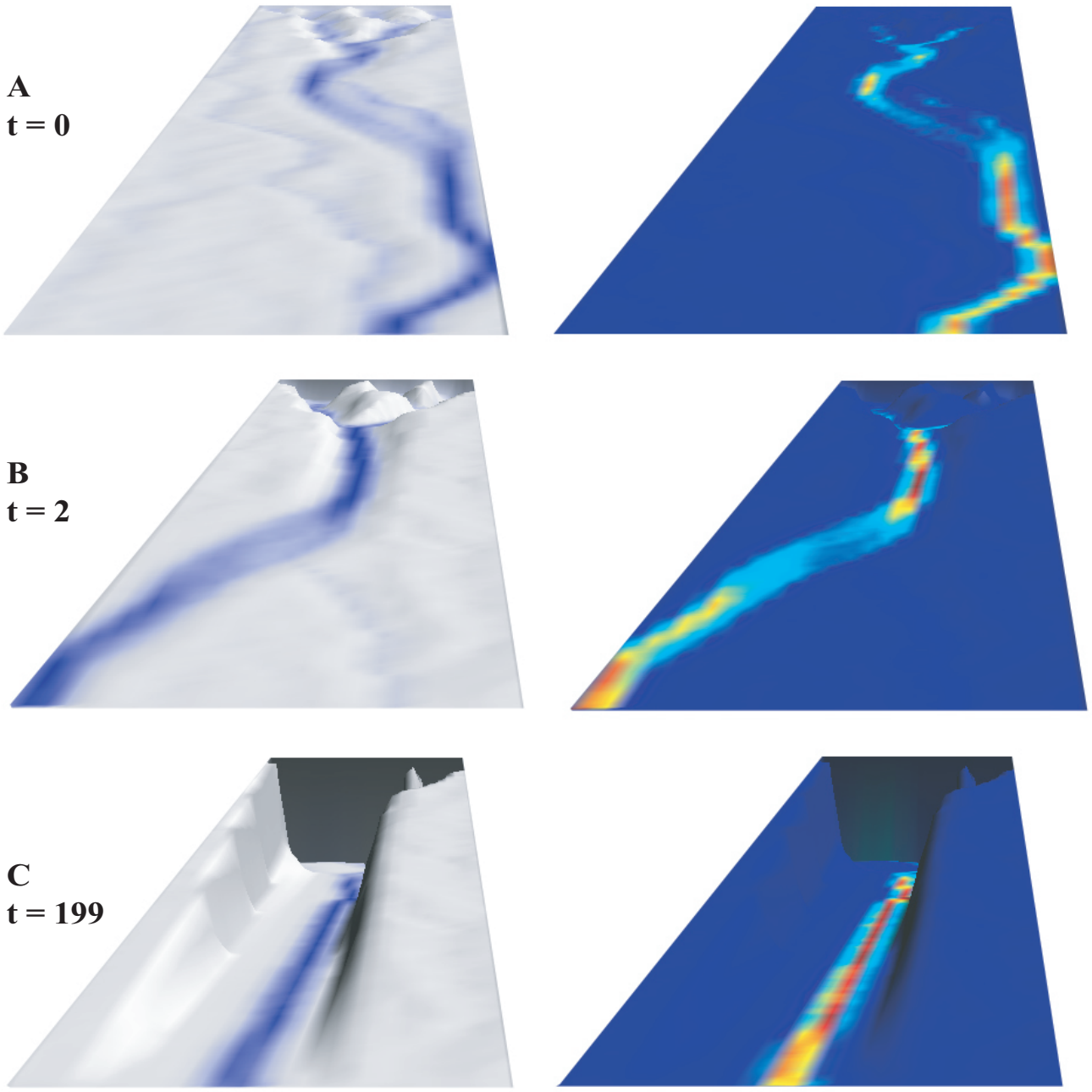


**Fig. 11. Example of river load and pattern during incision.**
Run Basement1, transport length=4, lateral erosion=0.04, width*length=32*256 pixels. Early after the onset of the experiment, the flow concentrates in a single erosive channel which becomes quickly straigth. The river load increases downstream due to the erosion of the upstream topography. Eventually, the river load is equally distributed in the equilibrium straigth single channel.

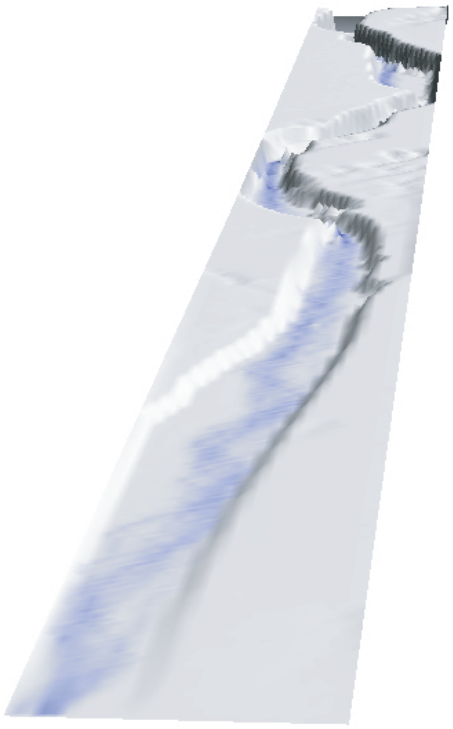

**Fig. 12. Example of a sinuous pattern obtained after incision.**
Run newTL6, t=600, transport length=100, lateral erosion=0.04, width*length=28*512 pixels. By contrast with fig. X9, the system was near equilibrium and reached it quickly after the onset of incision. The sinuosities therefore could not be removed by lateral erosion acting during incision.

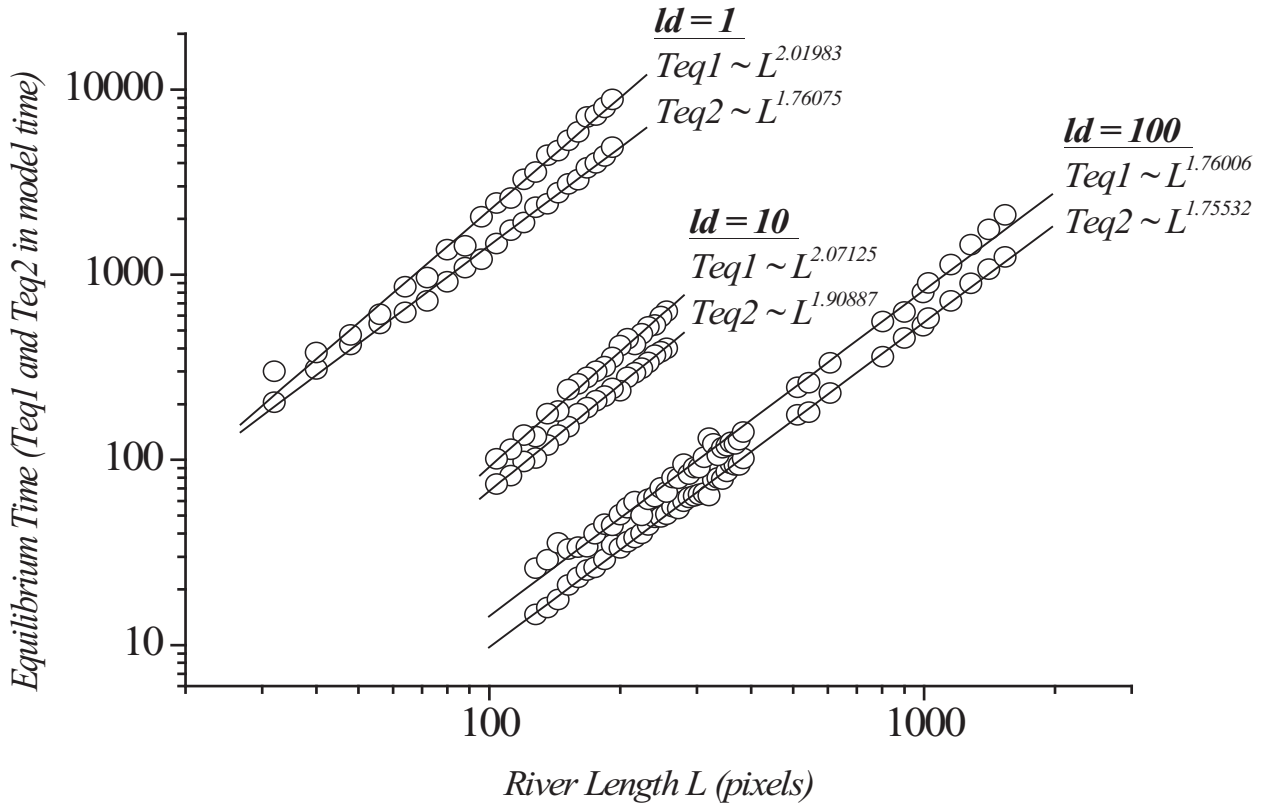


**Fig. 13. Equilibrium time versus river length for transport lengths of 1, 10 and 100.**

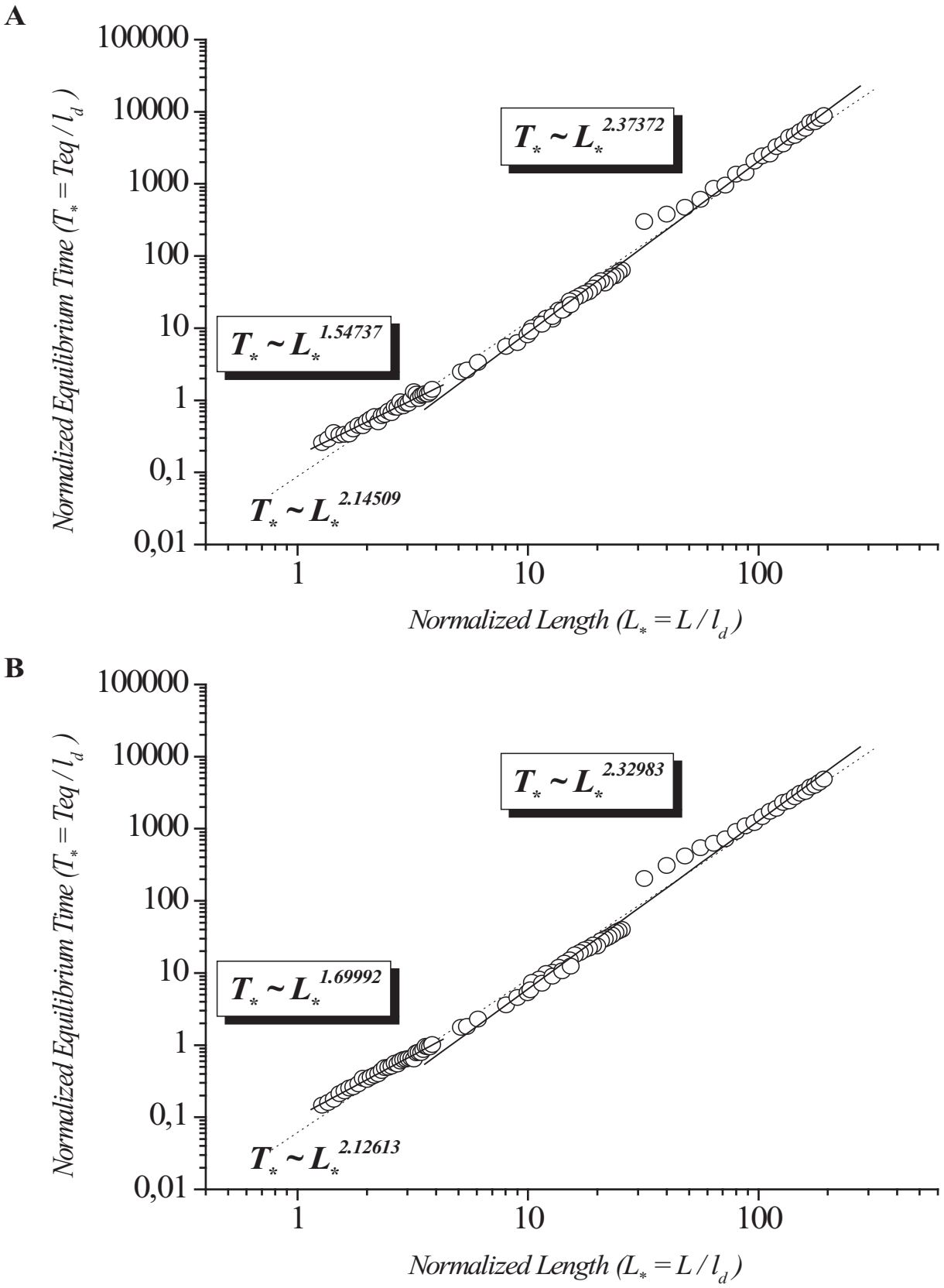


**Fig. 14. Scaling relationships between system equilibrium time *Teq* and length *L* normalized to transport length $l_d$.**
Relations for equilibrium time Teq1 (A) and Teq2 (B)

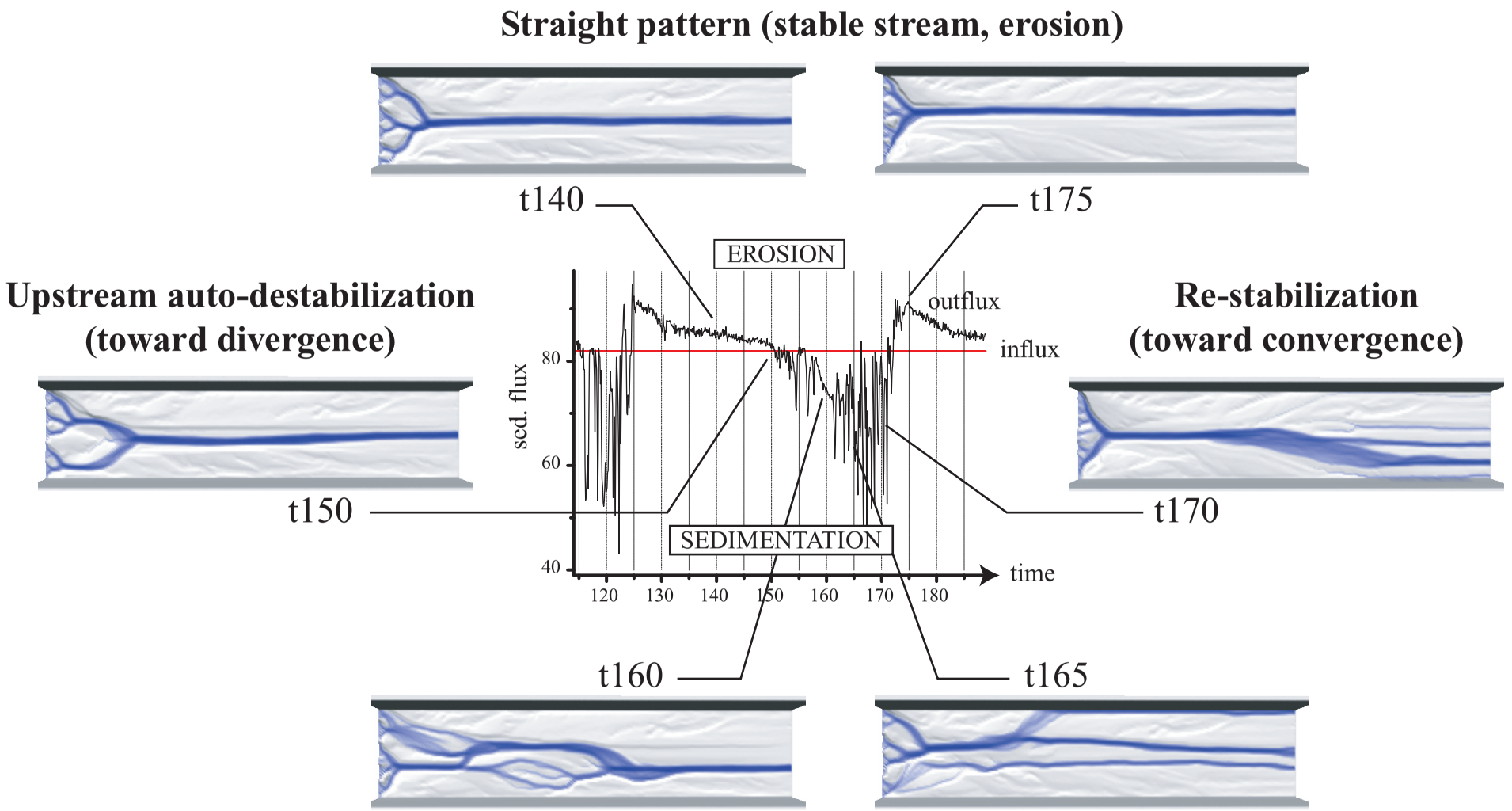


**Fig. 15. Illustration of an autogenic cycle.**
Run largeur1, transport length=4, lateral erosion=0.04, width*length=58*256 pixels, initial slope $s_i$=0.01. The non-linear interaction between deposition and erosion which are treated separately by the model produces the alternance of temporary periods of sediment storage and evacuation. This induces the alternance of braided and straigth patterns and a cyclic sediment output flux.

# 4. CONCLUSIONS

Deux problématiques principales ont été abordées dans ce travail à travers les deux paramètres principaux de contrôle de l'enregistrement stratigraphique que sont l'accommodation et le flux sédimentaire:

(1) l'influence des variations spatiales d'accommodation liées aux déformations intra-bassin (plis, failles, etc) sur les cycles stratigraphiques ;

(2) le contrôle par les systèmes fluviatiles des variations du flux sédimentaire terrigène aux bassins.

L'étude sédimentologique et stratigraphique détaillée des dépôts syntectoniques de l'anticlinal d'Arguis a révélé un fait très simple et qui finalement apparaît comme une évidence : *la déformation n'est pas enregistrée de la même manière dans les strates de croissance selon l'état stratigraphique pendant la sédimentation, i.e. en progradation, rétrogradation ou aggradation*. En effet, comme prédit par les concepts de la stratigraphie séquentielle, l'état stratigraphique contrôle non seulement la répartition de l'espace disponible en combinaison avec la tectonique locale, mais aussi le type de sédimentation (e.g., Systems Tracts).

Dans l'exemple d'Arguis, en rétrogradation et début de progradation, les dépôts argileux pélagiques et carbonatés vont avoir tendance à draper les structures tectoniques pendant leur fonctionnement à cause de leur nature non-dynamique et parce que l'espace disponible qui est peu perturbé par la tectonique locale dans ces états stratigraphiques permet le dépôt sur les hauts topographiques. Au contraire, en progradation, d'une part il n'y a pas d'espace pour la sédimentation sur les hauts topographiques créés par la tectonique, et d'autre part la sédimentation est dominée par des sables qui par nature se déposent préférentiellement dans les creux topographiques avant de sédimenter sur les hauts.

Il découle de cet aspect de l'enregistrement sédimentaire que lors d'un mouvement tectonique continu et constant, les strates syntectoniques vont montrer une alternance de cycles d'épaississement/non-épaississement uniquement liée aux cycles stratigraphiques.

Une première implication est qu'il faut prendre garde à ne pas confondre de telles relations tectonique/sédimentation avec la signature d'une tectonique épisodique. *Il est nécessaire de distinguer dans les dépôts syntectoniques la part de la cyclicité naturelle inhérente à l'enregistrement sédimentaire et la part des effets locaux*.

La deuxième implication, d'ordre plus pratique, est que ces relations particulières peuvent être mises à profit pour détecter rapidement (par exemple à partir de données sismiques) les variations de lithologies dans des contextes syntectoniques uniquement grâce aux variations d'épaisseur (méthode du T-Z plot).

Ainsi, c'est l'étude des perturbations de l'enregistrement sédimentaire (ici par la tectonique locale) qui permet de mettre en évidence différents aspects de sa nature. La déformation peut donc être utilisée comme un révélateur naturel de la sédimentation.

En ce qui concerne le flux sédimentaire, il apparaît que le problème réside actuellement dans les échelles de temps et les paramètres de contrôle de ses variations. Pour résoudre ce problème nous montrons qu'il est crucial de s'interesser au système sédimentaire dans son ensemble, c'est à dire constitué d'une zone en érosion, une zone en transfert, et une zone en sédimentation. *Le paramètre d'ordre 1 est le temps de réponse des différents composants de chaque zone aux variations des facteurs externes*. En prenant les plus efficaces des modèles d'érosion actuels et en supposant une adaptation immédiate des versants, il semble que les oscillations climatiques puissent produire des variations de flux sédimentaire à haute-fréquence (10's à 100's ka) à la sortie de la zone en érosion. *En considérant les cours d'eau comme des entités diffusives, nous estimons que les temps d'équilibre des rivières actuelles de longueur supérieures à 300 km sont majoritairement supérieurs à 100 ka*. Ainsi, des variations haute-fréquence du flux sédimentaire ne vont pas être transmises aux bassins par de telles rivières. *Il en résulte que des cycles stratigraphiques haute-fréquence enregistrés dans le bassin ne peuvent pas être l'expression de cycles climatiques ou tectoniques haute fréquence dans la zone en érosion si la zone de transfert est de taille supérieure à 300 km*.

Les simulations numériques réalisées montrent qu'à partir de lois simples qui décrivent le transport local de l'eau et des sédiments sans diffusion a priori, des systèmes fluviatiles émergent naturellement et ont effectivement un comportement diffusif à grande échelle. Ce comportement diffusif pourrait être lié à la distribution des sédiments par la divagation des chenaux dans le système.

La grande variété des formes fluviatiles décrites dans la littérature illustre probablement notre compréhension encore très limitée de ces systèmes. *La modélisation, qu'elle soit expérimentale ou numérique, montre que la complexité des systèmes naturels peut émerger spontanéement d'un nombre restreint de lois physiques simples.* Dans le présent travail, divers aspects des systèmes naturels tels que la divergence/convergence des flux d'eau, la variation

du nombre et de la largeur des chenaux, les phénomènes d'avulsion/migration latérale, et la sinuosité ont pu être simulés. *Ainsi, combiné aux analyses sédimentologiques classiques, ce type de modélisation ouvre la voie à une meilleure appréhension de la dynamique des systèmes fluviatiles à travers la stratigraphie et la géomorphologie.* Une telle approche devrait permettre à la stratigraphie de mieux saisir la signature des processus sédimentaires de premier ordre au sein de la multitude de détails qui composent l'enregistrement sédimentaire.

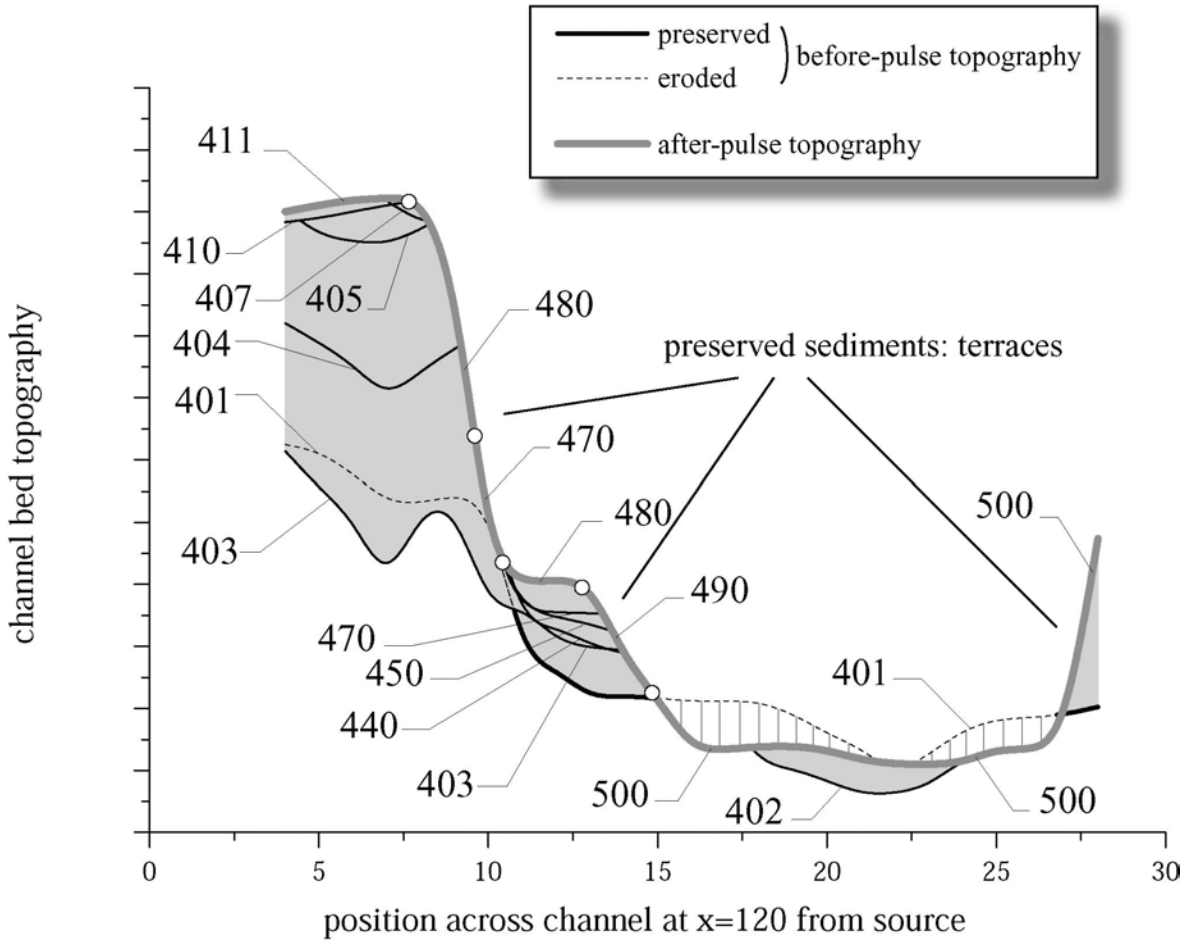


Cette illustration représente une coupe perpendiculaire à une simulation de plaine alluviale revenue à l'équilibre après le passage d'un pulse de sédiment. On observe plusieurs terrasses et surfaces d'érosion qui pourraient être interprétées comme résultant de plusieurs événements allogéniques. Ainsi, une cause unique et simple peut produire un enregistrement complexe.

L'approche qui consiste à prendre en compte le système sédimentaire dans son ensemble montre que la stratigraphie est naturellement impliquée dans les mêmes débats que la géomorphologie, la tectonique et la géochimie, tels que le rôle de l'érosion dans la

dynamique des chaînes de montagnes, et les couplages entre érosion, surrection et climat par exemple.

C'est en prenant part à ces débats plus larges que la stratigraphie pourra progresser sur elle-même.

# RÉFÉRENCES


Aigner, T., 1985, Storm depositional systems, Lecture Notes in Earth Sciences, Volume 3: Berlin, Springer, p. 174.

Allen, P.A., 1997, Earth Surface Processes: Oxford, Blackwell Science, 404 p.

Allen, P.A., and Densmore, A.L., 2000, Sediment flux from an uplifting fault block: Basin Res., v. 12, p. 367-380.

Anderson, J.E., Cartwright, J., Drysdall, S.J., and Vivian, N., 2000, Controls on turbidite sand deposition during gravity-driven extension of a passive margin: examples from Miocene sediments in Block 4, Angola.: Marine and Petroleum Geology, v. 17, p. 1165-1203.

Ashmore, P.E., 1982, Laboratory modelling of gravel braided stream morphology: Earth Surf. Processes Landforms, v. 7, p. 201-225.

Bachelard, G., 1934, Le nouvel esprit scientifique: Paris, Quadrige / Presses Universitaires de France.

Barnolas, A., and Teixell, A., 1994, Platform sedimentation and collapse in a carbonate-dominated margin of a foreland basin (Jaca basin, Eocene, southern Pyrenees): Geology, v. 22, p. 1107-1110.

Beaumont, C., Kooi, H., and Wilett, S., 2000, Coupled tectonic-surface process models with applications to rifted margins and collisional orogens, *in* Summerfield, M.A., ed., Geomorphology and Global Tectonics: New York, John Wiley & Sons, p. 29-55.

Berggren, W.A., Kent, D.V., Swisher, C.C., and Aubry, M.P., 1995, A revised Cenozoic geochronology and chronostratigraphy, *in* Berggren, W.A., Kent, D.V., Aubry, M.P., and Hardenbol, J., eds., Geochronology, time scales and global stratigraphic correlations, Volume 54: Spec. Publ. Soc. Econ. Palaeont. Miner.: Tulsa, SEPM, p. 129-212.

Bertram, G.T., and Milton, N.J., 1989, Reconstructing basin evolution from sedimentary thickness; the importance of palaeobathymetric control, with reference to the North Sea: Basin Res., v. 1, p. 247-257.

Bhattacharya, J.P., and Davies, R.K., 2001, Growth faults at the prodelta to delta-front transition, Cretaceous Ferron sandstone, Utah: Marine and Petroleum Geology, v. 18, p. 525-534.

Bhattacharya, J.P., and Walker, R.G., 1992, Deltas, *in* Walker, R.G., and James, N.P., eds., Facies Models, p. 157-177.

Bischke, R.E., 1994, Interpreting sedimentary growth structures from well log and seismic data (with examples).: American Association of Petroleum Geologists Bulletin, v. 78, p. 873-892.

Blin, B., and Mitouard, P., 1990, Le frond sud-pyrénéen: bordure sud du bassin de Jaca - tectonique et modélisation analogique, ENSPM (IFP), p. 141.

Blum, M.D., and Törnqvist, T.E., 2000, Fluvial responses to climate and sea-level change: a review and look forward: Sedimentology, v. 47 (Suppl. 1), p. 2-48.

Bornhauser, M., 1959, Depositional and structural history of Northwest Hartburg Field, Newton County, Texas.: American Association of Petroleum Geologists Bulletin, v. 44, p. 458-470.

Bull, W.B., 1991, Geomorphologic Responses to Climate Change: New York, Oxford University Press, 326 p.

Burbank, D., Meigs, A., and Brozovic, N., 1996, Interactions of growing folds and coeval depositional systems: Basin Res., v. 8, p. 199-223.

Burns, B.A., Heller, P.L., Marzo, M., and Paola, C., 1997, Fluvial response in a sequence stratigraphic framework: example from the Montserrat fan delta, Spain: J. Sed. Res., v. 67, p. 311-321.

Cande, S.C., and Kent, D.V., 1995, Revised calibrations of the geomagnetic polarity timescale for the late Cretaceous and Cenozoic: J. Geophys. Res., v. 100, p. 6093-6095.

Cartwright, J., Bouroullec, R., James, D., and Johnson, H., 1998, Polycyclic motion history of some Gulf Coast growth faults from high-resolution displacement analysis: Geology, v. 26, p. 819-822.

Castelltort, S., Guillocheau, F., Nalpas, T., Rouby, D., Robin, C., Urreiztieta, M.d., and Coutand, I., 2000, Tectonically induced distorsion of stratigraphic cycles - Example of the Arguis anticline in the south-central Pyrenees (Spain).: Geotemas, v. 2, p. 55-58.

Castelltort, S., Guillocheau, F., Robin, C., Rouby, D., Nalpas, T., Lafont, F., and Eschard, R., submitted, Fold control on the stratigraphic record: a quantified sequence stratigraphic study of the Pico del Aguila anticline in the South-western Pyrenees (Spain): Basin Res.

Castelltort, S., and Van Den Driessche, J., 2003, How plausible are high-frequency sediment supply-driven cycles in the stratigraphic record?: Sediment. Geol., v. 157, p. 3-13.

Catuneanu, O., Beaumont, C., and Waschbusch, P., 1997a, Interplay of static loads and subduction dynamics in foreland basins: Reciprocal stratigraphies and the "missing" peripheral bulge: Geology, v. 25, p. 1087-1090.

Catuneanu, O., Sweet, A.R., and Miall, A.D., 1997b, Reciprocal architecture of Bearpaw T-R sequences, uppermost Cretaceous, Western Canada sedimentary basin: Bull. Can. Petrol. Geol., v. 45, p. 75-94.

Chase, C.G., 1992, Fluvial landsculpting and the fractal dimension of topography: Geomorphology, v. 5, p. 39-57.
Cloetingh, S., and Kooi, H., 1989, intraplate stresses: a new perspective on QDS and Vail's third-order cycles, *in* Cross, T.A., ed., Quantitative Dynamic Stratigraphy: Englewood Cliffs, Prentice Hall, p. 127-148.
Cloetingh, S., McQueen, H., and Lambeck, K., 1985, On a tectonic mechanism for regional sea level variations: Earth Planet. Sci. Lett., v. 75, p. 157-166.
Coleman, J.M., and Gagliano, S.M., 1964, Cyclic sedimentation in the Mississippi River deltaic plain: Gulf Coast Assoc. Geol. Soc. Trans., v. 14, p. 67-80.
Coleman, J.M., and Prior, D., 1982, Deltaic environments of deposition, *in* Sholle, P.A.S., D., ed., Sandstone Depositional environments, Volume 31, Am. Ass. Petr. Geol., p. 139-178.
Contreras, J., Anders, M.H., and Scholz, C.H., 2000, Growth of a normal fault system: observations from the Lake Malawi basin of the east African rift: Journal of Structural Geology, v. 22, p. 159-168.
Crave, A., and Davy, P., 2001, A stochastic "precipiton" model for simulating erosion/sedimentation dynamics: Computers & Geosciences, v. 27, p. 815-827.
Cross, T.A., 1988a, Controls on coal distribution in transgressive-regressive cycles. Upper Cretaceous, Western Interior, USA, *in* Wilgus, C.K., Hastings, B.S., Kendall, C.G., Posamentier, H.W., Ross, C.A., and Van Wagoner, J.C., eds., Sea-Level Changes: An Integrated Approach, Volume 42: Spec. Publ. Soc. Econ. Palaeont. Miner.: Tulsa, SEPM, p. 371-380.
—, 1988b, Controls on coal distribution in transgressive-regressive cycles. Upper Cretaceous, Western Interior, USA, *in* Wilgus, C.K., Hastings, B.S., Kendall, C.G., Posamentier, H.W., Ross, C.A., and Van Wagoner, J.C., eds., Sea-level changes: an integrated approach, Volume 42: vol.42: Boulder, Soc. Econ. Paleontol. Mineral. Spec. Publ., p. 47-70.
Cross, T.A., and Lessenger, M.A., 1998, Sediment volume partitioning: rationale for stratigraphic model evaluation and high-resolution stratigraphic correlation, *in* Gradstein, F.M., Sandvik, K.O., and Milton, N.J., eds., Sequence Stratigraphy - Concepts and Applications, Volume 8: Norwegian Petroleum Society (NPF) Spec. Publ., Elsevier, p. 171-195.
Cui, Y., Parker, G., Lisle, T.E., Gott, J., Hansler, M.E., Pizzuto, J.E., Allmendinger, N.E., and Reed, J.M., submitted, Sediment Pulses in Mountain Rivers. Part 1. Experiments: Water Resour. Res.
Dade, W.B., and Friend, P.F., 1998, Grain-size, Sediment-Transport Regime, and Channel Slope in Alluvial Rivers: J. Geol., v. 106, p. 661-675.
Davy, P., and Crave, A., 2000, Upscaling Local-Scale Transport Processes in Large-Scale Relief Dynamics: Phys. Chem. Earth (A), v. 25, p. 533-541.
Delfaud, J., 1969, Essai sur la géologie dynamique du domaine aquitano-pyrénéen durant le Jurassique et le Crétacé inférieur [PhD Thesis thesis], University of Bordeaux, France.
den Bezemer, T., Kooi, H., and Cloetingh, S., 1999, Numerical modeling of fault-related sedimentation, *in* Harbaugh, J., Watney, L., Rankey, G., Slingerland, R., Goldstein, R., and Franseen, E., eds., Numerical Experiments in Stratigraphy: Recent Advances in Stratigraphic and Sedimentologic Computer Simulations, Volume 62: Spec. Publ. Soc. Econ. Palaeont. Miner.: Tulsa, SEPM, p. 177-196.
Densmore, A.L., Ellis, M.A., and Anderson, R.L., 1998, Landsliding and the evolution of normal-fault-bounded mountains: J. Geophys. Res., v. 103, p. 15,203-15,219.
ECORS, P.t., 1988, The ECORS deep reflection seismic survey across the Pyrenees: Nature, v. 331, p. 508-511.
Edwards, M.B., 1976, Growth faults in Upper Triassic deltaic sediments: American Association of Petroleum Geologists Bulletin, v. 60, p. 341-355.
Einsele, G., 2000, Sedimentary Basins: Evolution, Facies, and Sediment Budget. 2nd Edition: Berlin, Springer.
Einsele, G., Ricken, W., and Seilacher, A., 1991, Cycles and Events in Stratigraphy: Berlin Heidelberg, Springer-Verlag, p. 955.
Fernandes, N.F., and Dietrich, W.E., 1997, Hillslope evolution by diffusive processes: The timescale for equilibirum adjustments: Water Resources Research, v. 33, p. 1307-1318.
Ford, M., Williams, E.A., Artoni, A., Vergés, J., and Hardy, S., 1997, Progressive evolution of a fault-related fold pair from growth strata geometries, Sant Llorenç de Morunys, SE Pyrenees: J. Struct. Geol., v. 19, p. 413-441.
Fournier, F., 1960, Climat et erosion: la relation entre l'erosion du sol par l'eau et les precipitations atmospheriques: Paris, Presses Universitaires de France, 201 p.
Friend, P.F., Lloyd, M.J., McElroy, R., Turner, J., Van Gelder, A., and Vincent, S.J., 1996, Evolution of the central part of the northern Ebro basin, as indicated by its Tertiary fluvial sedimentary infill, *in* Friend, P.F., and Dabrio, C.J., eds., Tertiary basins of Spain, Cambridge Univ. Press, p. 166-171.
Frostick, L.E., and Jones, S.J., 2002, Impact of periodicity on sediment flux in alluvial systems: grain to basin scale, *in* Jones, S.J., and Frostick, L.E., eds., Sediment Flux to Basins: Causes, Controls and Consequences, Volume 191, Geological Society, London, Special Publications, p. 81-95.

Gale, A.S., Hardenbol, J., Hathway, B., Kennedy, W.J., Young, J.R., and Phansalkar, V., 2002, Global correlation of Cenomanian (Upper Cretaceous) sequences: Evidence for Milankovitch control on sea level: Geology, v. 30, p. 291-294.

Galloway, W.E., 1989, Genetic stratigraphic sequences in basin analysis I: architecture and genesis of flooding-surface bounded depositional systems: Am. Assoc. Petr. Geol. Bull., v. 73, p. 125-142.

Galloway, W.E., and Williams, T.A., 1991, Sediment accumulation rates in time and space: Paleogene genetic stratigraphic sequences of the northwestern Gulf of Mexico basin: Geology, v. 19, p. 986-989.

Galloway, W.E., 1998, Depositional processes, regime variables, and development of siliciclastic stratigraphic sequences, *in* Gradstein, F.M., Sandvik, K.O., and Milton, N.J., eds., Sequence Stratigraphy - Concepts and Applications, Volume 8: Norwegian Petroleum Society (NPF) Special Publications, Elsevier, p. 117-140.

Gawthorpe, R., and Hardy, S., 2002, Extensional fault-propagation folding and base-level change as controls on growth-strata geometries: Sediment. Geol., v. 146, p. 47-56.

Gawthorpe, R.L., Fraser, A.J., and Collier, R.E.L.L., 1994, Sequence stratigraphy in active extensional basins: implications for the interpretation of ancient basin-fills: Mar. Petrol. Geol., v. 11, p. 642-658.

Gawthorpe, R.L., Hall, M., Sharp, I., and Dreyer, T., 2000, Tectonically enhanced forced regressions: examples from growth folds in extensional and compressional settings, the Miocene of the Suez rift and the Eocene of the Pyrenees, *in* Hunt, D., and Gawthorpe, R.L., eds., Sedimentary Responses to Forced Regressions, Volume 172: Geol. Soc. London Spec. Publ., p. 177-191.

Gawthorpe, R.L., Hardy, S., and Ritchie, B., 2003, Numerical modelling of depositional sequences in half-graben rift basins: Sedimentology, v. 50, p. 169-185.

Gawthorpe, R.L., and Leeder, M.R., 2000, Tectono-sedimentary evolution of active extensional basins: Basin Res., v. 12, p. 195-218.

Gawthorpe, R.L., Sharp, I., McMurray, L., Underhill, J.R., and Gupta, S., 1997a, Variability of Systems Tracts, Sequence Boundaries and Flooding Surfaces, *in* Beauchamp, B., ed., Sedimentary Events & Hydrocarbon Systems: Calgary, CSPG-SEPM, p. 106.

Gawthorpe, R.L., Sharp, I., Underhill, J.R., and Gupta, S., 1997b, Linked sequence stratigraphic and structural evolution of propagating normal faults: Geology, v. 25, p. 795-798.

Guillocheau, F., 1990, Stratigraphie séquentielle des basins de plate-forme: l'exemple du Dévonien armoricain [Thèse d'état thesis], University of Strasbourg, France.

—, 1991, Stacking pattern of genetic sequences in a platform basin (Armorican Devonian): Nature and Distortion of the various orders of superimposed depositional sequences: Bull. Centres Rech. Explor. Prod. Elf Aquitaine, v. 15, p. 383-410.

—, 1995, Nature, rank and origin of Phanerozoic sedimentary cycles: C. R. Acad Sci. Paris, v. 320, p. 1141-1157.

Gupta, S., and Cowie, P., 2000, Processes and controls in the stratigraphic development of extensional basins: Basin Res., v. 12, p. 185-194.

Gupta, S., Cowie, P.A., Dawers, N.H., and Underhill, J.R., 1998, A mechanism to explain rift-basin subsidence and stratigraphic patterns through fault-array evolution: Geology, v. 26, p. 595-598.

Gupta, S., Underhill, J.R., Sharp, I.R., and Gawthorpe, R.L., 1999, Role of fault interactions in controlling synrift sediment dispersal patterns: Miocene, Abu Alaqa Group, Suez Rift, Sinai, Egypt: Basin Res., v. 11, p. 167-189.

Haq, B.U., Hardenbol, J., and Vail, P.R., 1987, Chronology of fluctuating sea level since the Triassic: Science, v. 235, p. 1156-1167.

Hardenbol, J., Thierry, J., Farley, M.B., Jacquin, T., DeGraciansky, P.C., and Vail, P.R., 1998, Mesozoic and Cenozoic Sequence Chronostratigraphic Framework of European Basins, Chart 1, *in* DeGraciansky, P.C., Hardenbol, J., Jacquin, T., and Vail, P.R., eds., Mesozoic and Cenozoic Sequence Stratigraphy of European Basins, Volume 60: Spec. Publ. Soc. Econ. Palaeont. Miner.: Tulsa, SEPM.

Hardy, S., and Gawthorpe, R.L., 1998, Effects of variations in fault slip rate on sequence stratigraphy in fan deltas: Insights from numerical modeling: Geology, v. 26, p. 911-914.

Hay, W.W., Sloan II, J.L., and Wold, C.N., 1988, Mass/Age Distribution and Composition of Sediments on the Ocean Floor and the Global Rate of Sediment Subduction: J. Geophys. Res, v. 93, p. 14933-14940.

Helland-Hansen, W., 1995, Sequence stratigraphy theory: remarks and recommendations, *in* Steel, R.J., Felt, V.L., Johannessen, E.P., and Mathieu, C., eds., Sequence Stratigraphy on the Northwest European Margin: Amsterdam, NPF Special Publications 5, Elsevier, p. 13-21.

Hiscott, R.N., 2001, Depositional sequences controlled by high rates of sediment supply, sea-level variations, and growth faulting: the Quaternary Baram Delta of northwestern Borneo: Marine Geology, v. 175, p. 67-102.

Hodgetts, D., Imber, J., Childs, C., Flint, S., Howell, J., Kavanagh, J., Nell, P., and Walsh, J., 2001, Sequence stratigraphic responses to shoreline-perpendicualr growth faulting in shallow marine reservoirs of the

Champion field, offshore Brunei Darussalam, South China Sea.: American Association of Petroleum Geologists Bulletin, v. 85, p. 433-457.
Hogan, P.J., and Burbank, D.W., 1996, Evolution of the Jaca piggyback basin and emergence of the External Sierras, southern Pyrenees, *in* Friend, P.F., and Dabrio, C.J., eds., Tertiary Basins of Spain, Cambridge Univ. Press, p. 153-160.
Homewood, P., Guillocheau, F., Eschard, R., and Cross, T.A., 1992a, Corrélations haute résolution et stratigraphie génétique : une démarche intégrée: Bull. Centres Rech. Explor. Prod. Elf-Aquitaine, v. 16, p. 357-381.
Homewood, P.W., Guillocheau, F., Eschard, R., and Cross, T., 1992b, Corrélation haute résolution et stratigraphie génétique: une démarche intégrée.: Bull. Centres Rech. Explor. Prod. Elf Aquitaine, v. 16, p. 375-381.
Homewood, P.W., Mauriaud, P., and Lafont, F., 2000, Best Practices in Sequence Stratigraphy, Volume Mémoire 25: Pau, Elf EP - Editions, p. 63 p.
Hooper, J.R., Fitzsimmons, R.J., Grant, N., and Vendeville, B.C., 2002, The role of deformation in controlling depositional patternes in the south-central Niger Delta, West Africa.: Journal of Structural Geology, v. 24, p. 847-859.
Hovius, N., 1998, Controls on sediment supply by large rivers, *in* Shanley, K.W., and McCabe, P.J., eds., Relative role of eustasy, climate and tectonism in continental rocks, Volume 59: Tulsa, Soc. Econ. Paleont. Min. Spec. Publ., p. 3-16.
Howard, A.D., 1994, A detachment-limited model of drainage basin evolution: Water Resources Research, v. 30, p. 2261-2285.
Howard, A.D., and Kerby, G., 1983, Channel changes in badlands: GSA Bull., v. 94, p. 739-752.
Humphrey, N.F., and Heller, P.L., 1995, Natural oscillations in coupled geomorphic systems: An alternative origin for cyclic sedimentation: Geology, v. 23, p. 499-502.
Jervey, M.T., 1988a, Quantitative geological modeling of siliciclastic rock sequences and their seismic expression, *in* Wilgus, C.K., Hastings, B.S., Kendall, C.G.S.C., Posamentier, H.W., Ross, C.A., and Van Wagoner, J.C., eds., Sea-Level Changes: An Integrated Approach, Volume 42: Spec. Publ. Soc. Econ. Palaeont. Miner.: Tulsa, SEPM, p. 47-69.
—, 1988b, Quantitative geological modeling of siliclastic rock sequences and their seismic expressions, *in* Wilgus, C.K., Hastings, B.S., Kendall, C.G., Posamentier, H.W., Ross, C.A., and Van Wagoner, J.C., eds., Sea-level change: an integrated approach, Volume 42: vol.42: Boulder, Soc. Econ. Paleont. Min. Spec. Publ., p. 47-69.
Jones, S.J., and Frostick, L.E., 2002, Introduction, *in* Jones, S.J., and Frostick, L.E., eds., Sediment Flux to Basins: Causes, Controls and Consequences, Volume 191, Geological Society, London, Special Publications, p. 1-4.
Jordan, T.E., and Flemings, P.B., 1991, Large-Scale Stratigraphic Architecture, Eustatic Variation, and Unsteady Tectonism: A Theoretical Evaluation: J. Geophys. Res., v. 96, p. 6681-6699.
Kirkby, M.J., 1971, Hillslope process-response models based on the continuity equation, Slopes: Forms and Processes, Volume 3: London, Institute of British Geographers Special Publications, p. 15-30.
Knighton, D., 1998, Fluvial forms and processes: London, Arnold.
Kooi, H., and Beaumont, C., 1994, Escarpment evolution on high-elevation rifted margins: Insights derived from a surface processes model that combines diffusion, advection, and reaction: J. Geophys. Res., v. 99, p. 12,191-12,209.
Lafont, F., 1994, Influences relatives de la subsidence et de l'eustatisme sur la localisation et la géometrie des reservoirs d'un système deltaique. Exemple de l'Eocene du bassin de Jaca (Pyrenees espagnoles) [PhD Thesis thesis], University of Rennes, France.
Lague, D., 2001, Dynamique de l'érosion continentale aux grandes échelles de temps et d'espace: modélisation expérimentale, numérique et théorique [PhD Thesis thesis]: Rennes, France, University of Rennes I.
Lawrence, D.T., 1993, Evaluation of eustasy, subsidence, and sediment input as controls on depositional sequence geometries and the synchroneity of sequence boundaries, *in* Weimer, P., and Posamentier, H., eds., Siliciclastic Sequence Stratigraphy: Recent Developments and Applications, Volume 58: American Association of Petroleum Geologists Memoir, p. 337-367.
Leeder, M.R., 1999, Sedimentology and sedimentary basins. From turbulence to tectonics: Oxford, Blackwell Science.
Leeder, M.R., and Gawthorpe, R.L., 1987, Sedimentary models for extensional tilt-block/half-graben basins, *in* Coward, M.P., Dewey, J.F., and Hancock, P.L., eds., Continental Extensional Tectonics, Volume 28: Geol. Soc. London Spec. Publ., p. 139-152.
Leopold, L.B., and Maddock, T., 1953, The hydraulic geometry of streams channels and some physiographic implications: US Geol. Surv. Prof. Pap., v. 252, p. 57.

Leopold, L.B., and Wolman, M.G., 1957, River Channel Patterns: Braided, Meandering and Straight: US Geol. Surv. Prof. Pap., v. 282-B, p. 39-85.
Lisle, T.E., Pizzuto, J.E., Ikeda, H., Iseya, F., and Kodama, Y., 1997, Evolution of a sediment wave in an experimental channel: Water Resour. Res., v. 33, p. 1971-1981.
Lister, G.S., Forster, M.A., and Rawling, T.J., 2001, Episodicity during orogenesis, *in* Miller, J.A., Holdsworth, R.E., Buick, I.S., and Hand, M., eds., Continental Reactivation and Reworking, Volume 184, Geological Society, London, Special Publications, p. 89-113.
Liu, X., and Galloway, W.E., 1997, Quantitative determination of Tertiary sediment supply to the North Sea basin: Am. Ass. Petr. Geol. Bull., v. 81, p. 1482-1509.
Lopez-Blanco, M., 1993, Stratigraphy and sedimentary development of the Sant-Llorenç del Munt fan-delta complex (Eocene, southern Pyrenean foreland basin, northeast Spain), *in* Frostick, L.E., and Steel, R.J., eds., Tectonic Controls and Signatures in Sedimentary Successions, Volume 20: International Association of Sedimentologists Special Publications, Blackwell, p. 67-88.
Lopez-Blanco, M., Marzo, M., and Piña, J., 2000, Transgressive-regressive sequence hierarchy of foreland, fan-delta clastic wedges (Montserrat and Sant Llorenç del Munt, Middle Eocene, Ebro Basin, NE Spain): Sediment. Geol., v. 138, p. 41-69.
Lowrie, A., 1986, Model for fine-scaled movements associated with climate and sea-level changes along Louisiana shelfbreak growth faults: Gulf Goast Association of Geological Societies Transactions, v. 36, p. 497-509.
Mansfield, C.S., and Cartwright, J.A., 1996, High resolution displacment mapping from 3-D seismic data.: Journal of Structural Geology, v. 18, p. 249-263.
Marr, J.G., Swenson, J.B., Paola, C., and Voller, V.R., 2000, A two-diffusion model of fluvial stratigraphy in closed depositional basins: Basin Res., v. 12, p. 381-398.
Marzo, M., and Steel, R.J., 2000, Unusual features of sediment supply-dominated, transgressive-regressive sequences: Paleogene clastic wedges, SE Pyrenean foreland basin, Spain: Sediment. Geol., v. 138, p. 3-15.
Masaferro, J.L., Bulnes, M., Poblet, J., and Eberli, G.P., 2002, Episodic folding inferred from syntectonic carbonate sedimentation: the Santaren anticline, Bahamas foreland: Sedimentary Geology, v. 146, p. 11-24.
McClay, K.R., and Ellis, P.G., 1987, Analogue models of extensional faults geometries, *in* Dewey, M.P., and Hancock, P.L., eds., Continental Extensional Tectonics, Volume 28: Geol. Soc. London Spec. Publ., p. 109-125.
Medjadj, F., 1985, Une zone de confluence deltaïque en domaine compressif: le delta paléogène de Jaca dans le secteur de Sabiñanigo [PhD Thesis thesis], University of pau, France.
Métivier, F., 1999, Diffusivelike buffering and saturation of large rivers: Phys. Rev. E, v. 60, p. 5827-5832.
Métivier, F., 2002, On the use of sedimentation rates in deciphering global change: Geophys. Res. Lett., v. In press, p. 1-4.
Métivier, F., and Gaudemer, Y., 1999, Stability of output fluxes of large rivers in South and East Asia during the last 2 million years: implications on floodplain processes: Basin Res., v. 11, p. 293-303.
Métivier, F., Gaudemer, Y., Tapponnier, P., and Klein, M., 1999, Mass accumulation rates in Asia during the Cenozoic: Geophys. J. Int., v. 137, p. 280-318.
Millán, H., Aurell, M., and Meléndez, A., 1994, Synchronous detachment folds and coeval sedimentation in the Prepyrenean External Sierras (Spain): a case study for a tectonic origin of sequences and systems tracts: Sedimentology, v. 41, p. 1001-1024.
Millán, H., Pueyo, E.L., Aurell, M., Luzon, A., Oliva, B., Martinez, M.B., and Pocovi, A., 2000, Actividad tectonica registrada en los depositos terciarios del frente meridional del Pirineo central: Rev. Soc. Geol. España, v. 13, p. 279-300.
Milliman, J.D., and Meade, R.H., 1983, World-Wide delivery of River Sediment to the Oceans: Journal of geology, v. 91, p. 1-21.
Milliman, J.D., and Syvitski, J.P.M., 1992, Geomorphic/Tectonic Control of Sediment Discharge to the Ocean: The Importance of Small Mountainous Rivers: Journal Of Geology, v. 100, p. 525-544.
Mitchell, N.C., 1996, Creep in pelagic sediments and potential for morphologic dating of marine fault scarps: Geophys. Res. Lett., v. 23, p. 483-486.
Molnar, P., and Lyon-Caen, H., 1988, Some simple physical aspects of the support, structure, and evolution of mountain belts: Geological Society of America, Special Paper, v. 218, p. 179-207.
Montgomery, D.R., and Gran, K.B., 2001, Downstream variations in the width of bedrock channels: Water Resources Research, v. 37, p. 1841-1846.
Morley, C.K., Vanhauwaert, P., and De Batist, M., 2000, Evidence for high-frequency cyclic fault activity from high-resolution seismic reflection survey, Rukwa Rift, Tanzania: Journal of the Geological Society of London, v. 157, p. 983-994.

Morris, S.A., Alexander, J., Kenyon, N.H., and Limonov, A.F., 1998, Turbidites around an active fault scarp on the Lower Valencia Fan, northwest Mediterranean: Geo-Marine Letters, v. 18, p. 165-171.
Mulder, T., and Syvitski, J.P.M., 1996, Climatic and Morphologic Relationships of rivers: Implications of Sea-Level fluctuations on river Loads: J. Geol., v. 106, p. 509-523.
Murray, A.B., and Paola, C., 1994, A cellular model of braided rivers: Nature, v. 371, p. 54-57.
—, 1996, A new quantitative test of geomorphic models, applied to a model of braided streams: Water Resour. Res., v. 32, p. 2579-2587.
—, 1997, Properties of a cellular braided-stream model: Earth Surface Processes and Landforms, v. 22, p. 1001-1025.
Muto, T., and Steel, R.J., 1997a, Principle of regression and transgression: the nature of the interplay between accommodation and sediment supply: J. Sedim. Res., v. 67, p. 994-1000.
—, 1997b, Principle of regression and transgression: the nature of the interplay between accommodation and sediment supply: J. Sed. Res., v. 67, p. 994-1000.
—, 2000, The accommodation concept in sequence stratigraphy: some dimensional problems and possible redefintion: Sediment. Geol., v. 130, p. 1-10.
Mutti, E., Tinterri, R., di Biase, D., Fava, L., Mavilla, N., Angella, S., and Calabrese, L., 2000, Delta-front facies associations of ancient flood-dominated fluvio-deltaic systems: Rev. Soc. Geol. España, v. 13, p. 165-190.
Nalpas, T., Györfi, I., Guillocheau, F., Lafont, F., and Homewood, P., 1999, Influence de la charge sédimentaire sur le développement d'anticlinaux synsédimentaires. Modélisation analogique et exemples de terrain (bordure sud du bassin de Jaca).: Bull. Soc. Géol. France, v. 170, p. 733-740.
Newell, A.J., 2000, Fault activity and sedimentation in marine rift basin (Upper Jurassic, Wessex Basin, UK): Journal of the Geological Society of London, v. 157, p. 83-92.
Nishikawa, T., 2001, Tectonic Control of Paleogeography Associated with a Barrier-Island System Documented in Late Pleistocene Paleo-Tokyo Bay, Japan, AAPG Annual Convention Abs.: Denver, Am. Ass. Petrol. Geol., p. A144.
Nishikawa, T., and Ito, M., 2000, Late Pleistocene barrier-island development reconstructed from genetic classification and timing of erosional surfaces, paleo-Tokyo Bay, Japan: Sediment. Geol., v. 137, p. 25-42.
Nott, J., and Roberts, R.G., 1996, Time and process rates over the past 100 m.y.: A case for dramatically increased landscape denudation rates during the late Quaternary in northern Australia: Geology, v. 24, p. 883-887.
Novoa, E., Suppe, J., and Shaw, J.H., 2000, Inclined-shear Restoration of growth folds: Am. Ass. Petrol. Geol. Bull., v. 84, p. 787-804.
Nuñez del Prado, H., 1986, Systèmes de dépôt et évolution sédimentaire des séries de transition marin-continental dans le synclinorium du Rio Guarga [PhD Thesis thesis], University of Pau, France.
Nystuen, J.P., 1998, History and development of sequence stratigraphy, *in* Gradstein, F.M., Sandvik, K.O., and Milton, N.J., eds., Sequence Stratigraphy - Concepts and Applications, Volume 8: Norwegian Petroleum Society (NPF) Spec. Publ., Elsevier, p. 31-116.
Ori, G.G., and Friend, P.F., 1984, Sedimentary basins formed and carried piggyback on active thrust sheets: Geology, v. 12, p. 475-478.
Paola, C., 2000, Quantitative models of sedimentary basin filling: Sedimentology, v. 47, p. 121-178.
Paola, C., Heller, P.L., and Angevine, C.L., 1991, The response distance of river systems to variations in sea level: Geol. Soc. Am. Abstracts with Programs, v. 23, p. A170-A171.
—, 1992, The large-scale dynamics of grain-size variation in alluvial basins. I : Theory: Basin Res., v. 4, p. 73-90.
Peizhen, Z., Molnar, P., and Downs, W.R., 2001, Increased sedimentation rates and grain sizes 2-4 Myr ago due to the influence of climate change on erosion rates: Nature, v. 410, p. 891-897.
Pemberton, S.G., MacEachern, J.A., and Frey, R.W., 1992, Trace Fossils Facies models: Environmental and Allostratigraphic Significance, *in* Walker, R.G., and James, N.P., eds., Facies Models, Geological Association of Canada, p. 47-71.
Penn, J.R., 2001, Rivers of the world : a social, geographical, and environmental sourcebook: Santa Barbara, California, ABC-CLIO.
Perlmutter, M.A., and Matthews, M.D., 1989, Global cyclostratigraphy-A model, *in* Cross, T.A., ed., Quantitative Dynamic Stratigraphy: Englewood Cliffs, Prentice Hall, p. 233-260.
Perlmutter, M.A., Radovic, B.J., Matthews, M.D., and Kendall, M.D., 1998, The impact of high-frequency sedimentation cycles on stratigraphic interpretation, *in* Gradstein, F.M., Sandvick, K.O., and Milton, N.Y., eds., Sequence Stratigraphy, Concepts and Applications, Volume 8, NPF Special Publications, p. 141-170.
Pinet, P., and Souriau, M., 1988, Continental erosion and large-scale relief: Tectonics, v. 7, p. 563-582.

Plint, A.G., Eyles, N., Eyles, C.H., and Walker, R.G., 1992, Control of sea level change, *in* Walker, R.G., and James, N.P., eds., Facies Models: Response to Sea Level Change: St. John's, Geological Association of Canada, p. 15-25.

Poblet, J., and Hardy, S., 1995a, Reverse modelling of detachment folds; application to the Pico del Aguila anticline in the South Central Pyrenees (Spain): J. Struct. Geol., v. 17, p. 1707-1724.

—, 1995b, Reverse modelling of detachment folds; application to the Pico del Aguila anticline in the South Central Pyrenees (Spain): Journal of Structural Geology, v. 17, p. 1707-1724.

Poblet, J., Muñoz, J.A., Travé, A., and Serra-Kiel, J., 1998, Quantifying the kinematics of detachment folds using three-dimensional geometry: Application to the Mediano anticline (Pyrenees, Spain): Geol. Soc. Am. Bull., v. 110, p. 111-125.

Posamentier, H.W., and Allen, G.P., 1993a, Siliciclastic sequence stratigraphic patterns in foreland ramp-type basins: Geology, v. 21, p. 455-458.

—, 1993b, Variability of the sequence stratigraphic model: effects of local basin factors: Sediment. Geol., v. 86, p. 91-109.

Posamentier, H.W., Jervey, M.T., and Vail, P.R., 1988, Eustatic control on clastic deposition I: Conceptual framework, *in* Wilgus, C.K., Hastings, B.S., Kendall, C.G., Posamentier, H.W., Ross, C.A., and Van Wagoner, J.C., eds., Sea-level change: an integrated approach, Volume 42: vol.42: Boulder, Soc. Econ. Paleont. Min. Spec. Publ., p. 109-124.

Pueyo-Morer, E.L., Parés i Casanova, J.M., Millán-Garrido, H., and Pocoví Juan, A., 1994, Evidencia magnetotectonica de la rotacion de las Sierras Exteriores Altoaragonesas, Comunicaciones del II Congreso del Grupo Español del Terciario: Jaca, p. 185-188.

Puigdefabregas, C., 1975, La sedimentación molásica en la cuenca de Jaca: Pirineos, v. 104, p. 1-188.

Puigdefàbregas, C., and Souquet, P., 1986, Tecto-sedimentary cycles and depositional sequences of the Mesozoic and Tertiary from the Pyrenees: Tectonophysics, v. 129, p. 173-203.

Ravnas, R., and Steel, R.J., 1997, Contrasting styles of Late Jurassic syn-rift turbidite sedimentation : a comparative study of the Magnus and Oseberg areas, northern North Sea.: Marine and Petroleum Geology, v. 14, p. 417-449.

Raymo, M.E., Ruddiman, W.F., and Froelich, P.N., 1988, Influence of late Cenozoic mountain building on ocean geochemical cycles: Geology, v. 16, p. 649-653.

Reineck, H.E., and Singh, I.B., 1980, Depositional Sedimentary Environments: Berlin, Springer-Verlag, 549 p.

Rey, J., 1995, Tectonic control in the boundaries of the genetic units: an example in the Dogger of the External Zones of the Betic Cordillera (province of Murcia and Almeria, Spain): Sediment. Geol., v. 95, p. 57-68.

Robin, C., 1997, Mesure stratigraphique de la déformation : application à l'évolution jurassique du Bassin de Paris [PhD Thesis thesis], University of Rennes, France.

Robin, C., Guillocheau, F., and Gaulier, J.M., 1996, Mesure des signaux eustatiques et tectoniques au sein de l'enregistrement sédimentaire d'un bassin intracratonique. Application au Lias du Bassin de Paris: C. R. Acad. Sci. Paris, v. 322, p. 1079-1086.

Schlager, W., 1993a, Accommodation and supply - a dual control on stratigraphic sequences, *in* Cloetingh, S., Sassi, W., Horvath, P., and Puigdefabregas, C., eds., Basin Analysis and Dynamics of Sedimentary Basin Evolution, Volume 86: Sediment. Geol., p. 111-136.

—, 1993b, Accommodation and supply - a dual control on stratigraphic sequences: Sediment. Geol., v. 86, p. 111-136.

Schumm, 1977, The Fluvial System, John Wiley & Sons, 338 p.

Sclater, J.G., and Christie, P.A.F., 1980, Continental stretching: an explanation of the mid-Cretaceous subsidence of the Central North Sea Basin: J. Geophys. Res., v. 85, p. 3711-3739.

Seguret, M., 1972, Etude tectonique des nappes et séries décollées de la partie centrale du versant sud des Pyrénées. Caractère synsédimentaire, rôle de la compression et de la gravité.: Montpellier, France, Publ. Univ. Sci. Tech. Languedoc, 155 p.

—, 1991, Paradox in tectonic dating: unconformities over thrusts do not date tectonic activity, south-pyrenean example, 3ème Congrès Français de Sédimentologie: Brest, France, ASF, p. 257-258.

Shanley, K.W., and McCabe, P.J., 1994, Perspectives on the Sequence Stratigraphy of Continental Strata: Am. Ass. Petrol. Geol. Bull., v. 78, p. 544-568.

Shaw, J.H., Novoa, E., and Connors, C.D., 1999, Structural controls on growth stratigraphy, *in* McClay, K., ed., Thrust Tectonics: London, p. 80-82.

Sloss, L.L., 1962, Stratigraphic Models in Exploration: Am. Ass. Petr. Geol. Bull., v. 46, p. 1050-1057.

—, 1978, Global Sea Level Changes: A view from the Craton: Am. Ass. Petr. Geol. Bull., p. 461-467.

Smith, T.R., and Bretherton, F.P., 1972, Stability and the conservation of mass in drainage basin evolution: Water Resour. Res., v. 8, p. 1506-1529.

Snyder, N.P., Whipple, K.X., Tucker, G.E., and Merrits, D.J., 2000, Landscape response to tectonic forcing: Digital elevation model analysis of stream profiles in the Mendocino triple junction region, northern California: GSA Bull., v. 112, p. 1250-1263.

Soreghan, M.J., Scholz, C.A., and Wells, J.T., 1999, Coarse-grained, deep-water sedimentation along a border fault margin of Lake Malawi, Africa: Seismic stratigraphic analysis.: Journal of Sedimentary Research, v. 69, p. 832-846.

Storti, F., and Poblet, J., 1997, Growth stratal architectures associated to decollement folds and fault-propagation folds. Inferences on fold kinematics: Tectonophysics, v. 282, p. 353-373.

Summerfield, M.A., and Hulton, N.J., 1994, Natural controls of fluvial denudation rates in major world drainage basins: J. Geophys. Res, v. 99, p. 13871-13883.

Suppe, J., Chou, C.T., and Hook, S.C., 1992, Rates of folding and faulting determined from growth strata., *in* McKlay, K.R., ed., Thrust Tectonics: London, Chapman & Hall, p. 105-121.

Swenson, J.B., Voller, V.R., Paola, C., Parker, G., and Marr, J.G., 2000, Fluvio-deltaic sedimentation: a generalized Stefan problem: European Journal of Applied Mathematics, v. 11, p. 1-20.

Swift, D.J.P., Oertel, G.F., Tillman, R.W., and Thorne, J.A., 1991, Shelf Sand and Sandstone Bodies, IAS Special Publications, Volume 14, Blackwell.

Sztràkos, K., and Castelltort, S., in press, La sédimentologie et les foraminifères bartoniens et priaboniens des coupes d'Arguis (Prépyrénées aragonaises, Espagne). Incidence sur la corrélation des biozones à la limite Bartonien/Priabonien.: Rev. Micropaléont., v. 44.

Tapponnier, P., Ryerson, F.J., VanDerWoerd, J., Meriaux, A.-S., and Lasserre, C., 2001, Long-term slip rates and characteristic slip: keys to active fault behaviour and earthquake hazard: C. R. Acad. Sci. Paris, Sciences de la Terre, v. 333, p. 483-494.

Tearpock, D., and Bischke, R.E., 1991, Applied Subsurface Geological Mapping: New-York, Prentice-Hall, 648 p.

Thornburg, T.M., Kulm, L.D., and Hussong, D.M., 1990, Submarine-fan development in the southern Chile Trench: A dynamic interplay of tectonics and sedimentation: Geological society of America Bulletin, v. 102, p. 1658-1680.

Thorsen, C.E., 1963, Age of growth faulting in Southeast Louisiana.: Transactions. Gulf Coast Association of Geological Societies, v. 13, p. 103-110.

Tiedemann, R., and Franz, S.O., 1997, Deep-water circulation chemistry and terrigenous sediment supply in the equatorial Atlantic during the Pliocene, 3.3-2.6 Ma and 5-4.5 Ma, *in* Shackleton, N.J., Curry, W.B., Richter, C., and Brawlower, T.J., eds., Proc. Ocean Drill. Program: Sci. Results, Volume 154, p. 299-318.

Toledo, M.J., 1990, Séquences de dépôt et cyclicité tectonique dans l'Eocène du bassin de Jaca, Espagne, ENSPM (IFP).

Tucker, G.E., and Slingerland, R., 1996, Predicting sediment flux from fold and thrust belts: Basin Res., v. 8, p. 329-349.

—, 1997, Drainage basin response to climate change: Water Resources Research, v. 33, p. 2031-2047.

Turcotte, D.L., and Schubert, G., 1982, Geodynamics, John Wiley & Sons.

Van der Woerd, J., Ryerson, F.J., Tapponnier, P., Meriaux, A.-S., Gaudemer, Y., Meyer, B., Finkel, R.C., Caffee, M.W., Guoguang, Z., and Zhiqin, X., 2000, Uniform Slip-Rate along the Kunlun Fault: Implications for seismic behaviour and large-scale tectonics: Geophys. Res. Lett., v. 27, p. 2353-2356.

Van der Zwan, C.J., 2002, The impact of Milankovitch-scale climatic forcing on sediment supply: Sediment. Geol., v. 147, p. 271-294.

Van Wagoner, J.C., Mitchum, R.M., Campion, K.M., and Rahmanian, V.D., 1990a, Siliciclastic sequence stratigraphy in well logs, cores and outcrops: Concepts for high-resolution correlation of time and facies, AAPG Methods in Exploration, Volume 7: Tulsa, Am. Ass. Petrol. Geol., p. 55.

—, 1990b, Siliciclastic sequence stratigraphy in well logs, cores and outcrops: Concepts for high-resolution correlation of time and facies, *in* Exploration, A.A.P.G.M.i., ed., Volume 7: Tulsa, p. 55.

Van Wagoner, J.C., Posamentier, H.W., Mitchum, R.M., Vail, P.R., Sarg, J.F., Loutit, T.S., and Hardenbol, J., 1988, An overview of the fundamentals of sequence stratigraphy and key definitions, *in* Wilgus, C.K., Hastings, B.S., Kendall, C.G.S.C., Posamentier, H.W., Ross, C.A., and Van Wagoner, J.C., eds., Sea-Level Change: An Integrated Approach, Volume 42: Spec. Publ. Soc. Econ. Palaeont. Miner.: Tulsa, SEPM, p. 39-45.

Vergès, J., Marzo, M., Santaeulària, T., Serra-Kiel, J., Burbank, D.W., Munoz, J.A., and Giménez-Montsant, J., 1998, Quantified vertical motions and tectonic evolution of the SE Pyrenean foreland basin, *in* Mascle, A., Puigdefàbregas, C., Luterbacher, H.P., and Fernàndez, M., eds., Cenozoic Foreland Basins of Western Europe, Volume 134: Geol. Soc. London Spec. Publ., p. 107-134.

Waschbusch, P.J., and Royden, L.H., 1992, Episodicity in foredeep basins: Geology, v. 20, p. 915-918.

Webb, H.F., and Jordan, T.H., 2001, Pelagic sedimentation on rough seafloor topography 1. Forward Model: J. Geophys. Res, v. 106, p. 30433-30449.

Weltje, G.J., and de Boer, P.L., 1993, Astronomically induced paleoclimatic oscillations reflected in Pliocene turbidite deposits on Corfu (Greece): implications for the interpretation of higher order cyclicity in ancient turbidite systems: Geology, v. 21, p. 307-310.

Weltje, G.J., VanAnsenwoude, S.O.K.J., and DeBoer, P.L., 1996, High-frequency detrital signals in eocene fan-delta sandstones of mixed parentage (south-central Pyrenees, Spain): a reconstruction of chemical weathering in transit: J. Sed. Res., v. 66, p. 119-131.

Whipple, K.X., 2001, Fluvial landscape response time: how plausible is steady-state denudation?: American Journal of Science, v. 301, p. 313-325.

Whipple, K.X., and Tucker, G.E., 1999, Dynamics of the stream-power river incision model: Implications for height limits of mountain ranges, landscape response timescales, and research needs: J. Geophys. Res., v. 104, p. 17661-17674.